DTIC FILE COPY

SECURITY CLASSIFICATION OF THIS PAGE

REPORT DOCUMENTATION PAGE

Form Approved OMB No. 0704-0188

1a. REPORT SECURITY CLASSIFICATION: UNCLASSIFIED	1b. RESTRICTIVE MARKINGS: NONE
2a. SECURITY CLASSIFICATION AUTHORITY	3. DISTRIBUTION/AVAILABILITY OF REPORT: APPROVED FOR PUBLIC RELEASE; DISTRIBUTION UNLIMITED.
AD-A217 925 (S)	5. MONITORING ORGANIZATION REPORT NUMBER(S): AFIT/CI/CIA-89-105
6a. NAME OF PERFORMING ORGANIZATION: AFIT STUDENT AT UNIV OF OK; 6b. OFFICE SYMBOL (If applicable)	7a. NAME OF MONITORING ORGANIZATION: AFIT/CIA
6c. ADDRESS (City, State, and ZIP Code)	7b. ADDRESS (City, State, and ZIP Code): Wright-Patterson AFB OH 45433-6583
8a. NAME OF FUNDING/SPONSORING ORGANIZATION; 8b. OFFICE SYMBOL (If applicable)	9. PROCUREMENT INSTRUMENT IDENTIFICATION NUMBER
8c. ADDRESS (City, State, and ZIP Code)	10. SOURCE OF FUNDING NUMBERS: PROGRAM ELEMENT NO. / PROJECT NO. / TASK NO. / WORK UNIT ACCESSION NO.

11. TITLE (Include Security Classification) (UNCLASSIFIED)

HYPERSONIC WAVERIDER CONFIGURATIONS FOR TRANS-ATMOSPHERIC VEHICLES

12. PERSONAL AUTHOR(S): WILLIAM P. MARTIN

13a. TYPE OF REPORT	13b. TIME COVERED	14. DATE OF REPORT (Year, Month, Day)	15. PAGE COUNT
THESIS/DISSERTATION X	FROM _____ TO _____	1989	186

16. SUPPLEMENTARY NOTATION: APPROVED FOR PUBLIC RELEASE IAW AFR 190-1
ERNEST A. HAYGOOD, 1st Lt, USAF
Executive Officer, Civilian Institution Programs

17. COSATI CODES			18. SUBJECT TERMS (Continue on reverse if necessary and identify by block number)
FIELD	GROUP	SUB-GROUP	

19. ABSTRACT (Continue on reverse if necessary and identify by block number)

20. DISTRIBUTION/AVAILABILITY OF ABSTRACT	21. ABSTRACT SECURITY CLASSIFICATION
☒ UNCLASSIFIED/UNLIMITED ☐ SAME AS RPT. ☐ DTIC USERS	UNCLASSIFIED

22a. NAME OF RESPONSIBLE INDIVIDUAL	22b. TELEPHONE (Include Area Code)	22c. OFFICE SYMBOL
ERNEST A. HAYGOOD, 1st Lt, USAF	(513) 255-2259	AFIT/CI

DD Form 1473, JUN 86 — Previous editions are obsolete. — SECURITY CLASSIFICATION OF THIS PAGE

AFIT/CI "OVERPRINT"

THE UNIVERSITY OF OKLAHOMA

GRADUATE COLLEGE

HYPERSONIC WAVERIDER CONFIGURATIONS FOR TRANS-ATMOSPHERIC VEHICLES

A THESIS SUBMITTED TO THE GRADUATE FACULTY

in partial fulfillment of the requirements for the

degree of

Master of Science

By

William P. Martin

Norman, Oklahoma

1989

HYPERSONIC WAVERIDER CONFIGURATIONS

FOR TRANS-ATMOSPHERIC VEHICLES

A THESIS APPROVED FOR THE SCHOOL OF

AEROSPACE AND MECHANICAL ENGINEERING

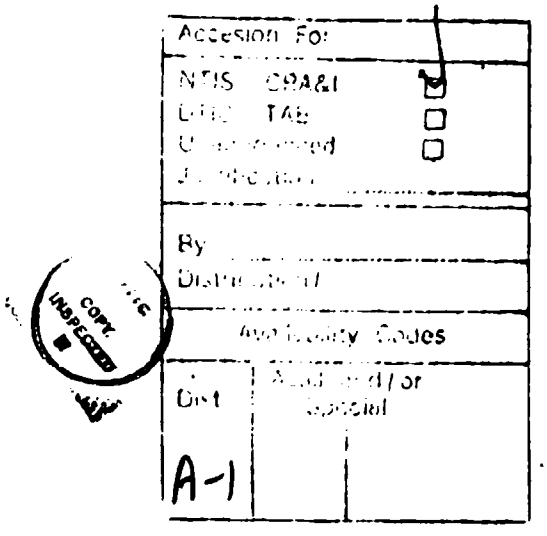

By M Rasmussen

E Emanuel

D Lee

ACKNOWLEDGEMENTS

I am extremely grateful to Dr. M. Rasmussen who guided me through this effort. His greatest task was to teach me to think. I hope he has succeeded.

No undertaking of any significance small or great is usually done alone. I owe much to the U.S. Air Force Institute of Technology for their financial support over a four and one half year period during which I completed two degrees at the University of Oklahoma. Also, I must thank Carl Adams and Mike Mould two colleagues who helped when I had problems and questions with the computer work. Their support helped to alleviate many headaches.

I would like to dedicate this work to my family--especially my wife Kathleen. Her emotional support and continual confidence in me was the force which kept me going. Her love has made it all worthwhile.

TABLE OF CONTENTS

LIST OF TABLES

TABLE

LIST OF ILLUSTRATIONS

FIGURE

Accompaniment to the Abstract

Author: William P. Martin

Title: HYPERSONIC WAVERIDER CONFIGURATIONS FOR TRANS-ATMOSPHERIC VEHICLES

Rank: 2ndLt. USAF

Date: 1989

Pages: 186

Degree Awarded: Master of Science in Aerospace Engineering

Institution: University of Oklahoma

ABSTRACT

This thesis describes the development of a catalogue of waverider shapes generated from axisymmetric conical flow. A simple but reliable method of calculating the viscous drag is presented and over one-hundred configurations are shown with various aerodynamic and pertinent geometric design factors. All of the configurations presented are based on Mach number of 10 and Reynolds number (based on the length of the waverider) of 10^6. However, the analysis presented here adapts itself to any Mach or Reynolds number. The lift-to-drag ratios presented range from 4.32 to 5.06 while the average skin friction coefficient ranged from 0.00176 to 0.00205. The volume to area ratio $V^{2/3}/S_p$ ranged from 0.224 to 0.153.

Nomenclature

A_b/A_{bi}	ratio of base areas of an arbitrary waverider with the idealized cone derived waverider
b/l_w	aspect ratio, base of waverider divided by the length of waverider
C_D	drag coefficient
$\overline{C_{fc}}$	average skin friction coefficient for the compression surface
C_{fe}	skin friction coefficient based on conditions just outside the boundary layer
$\overline{C_{ff}}$	average skin friction coefficient for the freestream surface
C_{fe}	average skin friction coefficient for the compression surface
$\overline{C_{ft}}$	average total skin friction coefficient
C_{ftav}	same as $\overline{C_{ft}}$
k_w	thermal conductivity at the wall
l	length of basic cone
l_w	length of waverider
$(L/D)_{vis}$	viscous lift to drag ratio
M_e	Mach number just outside the boundary layer
M_∞	Mach number at infinity or freestream

	conditions
Pr	Prandtl number
q	dynamic pressure
q_w	heat flux at the wall
r	distance from the origin of axis to a point on the waverider surface
R_{cb}	distance from origin to an arbitrary point on the the compression surface projected to the base plane
R_{exe}	Reynolds number based on conditions just out-side the boundary layer
R_{exo}	Reynolds number based on freestream conditions
R_{ob}	distance from origin to an arbitrary point on the freestream surface projected to the base plane
S_p/S_{pi}	ratio of planform areas of waverider to the idealized waverider
S_w/S_p	ratio of wetted area to planform area
SSD	shock standoff distance in the base plane
S_T	Stanton number
S_{wc}	wetted area of compression surface
S_{wf}	wetted area of freestream surface
T_{aw}	adiabatic wall temperature
T_w	temperature at the wall

V/V_i	volume ratio of waverider to idealized wave- rider
$V^{2/3}/S_p$	nondimensionalized volume to planform area ratio
β	half angle of shock cone
δ	half angle of basic cone
$\delta(x)$	boundary layer thickness
	boundary layer thickness in the transformed coordinates
Φ	angle between $-\Phi_1$ and Φ_1
Φ_1	dihedral angle of waverider in the base plane
Φ_z	dihedral angle of waverider at an arbitrary crossection
	ratio of specific heats
μ_e	viscosity coefficient just outside the boundary layer
μ_w	viscosity coefficient at the wall
σ	β/δ, radius of shock cone in the base plane of nondimensional coordinate system
σ_z	radius of shock cone at an arbitrary cross section of nondimensional coordinate system
τ_w	surface stresses at the wall

CHAPTER 1

Introduction

1.1 Introductory Remarks

Lifting-body configurations are currently of interest as a means for achieving long-range and high-performance hypersonic missile and aircraft characteristics. Semi-empirical methods used heretofore for calculating the flow fields and aerodynamics of blended wing-body shapes are not appropriate for modern hypersonic flight. Design requirements for hypersonic aircraft are discussed by Townend[1] and Stollery[2]. Elaborate computer codes have become necessary for predicting the characteristics of arbitrary configurations. Since these codes are still in evolutionary stages and are quite expensive as well as complex, a need for a simplified calculation scheme exists.

Waverider analysis provides one means for studying blended body configurations on a relatively simplified scale. The work presented here is well adapted to the personal computer. Shapes derived by this analysis yield flow fields and aerodynamic properties that are known for their particular on-design conditions, and allow for systematic variation of parameters pertinent to the design process.

An historical background on waveriders is provided by Kuchemann[3] and Hemsch and Nielsen[4] offer additional perspectives. Also, in recent times there have been several papers dealing with geometry variations, optimization, viscous effects, experimental verification, and applications.[5-15]

1.2 Primary Goals

This study has two primary goals. The first is essentially an extension of the work by Rasmussen and Stevens[14]. In this sense, this work is a catalog of many shapes and variations of waveriders (over 100 are presented) that can be generated by axisymmetric flow past a cone. Lift, drag, and friction coefficients as well as lift-to-drag ratios are calculated together with pertinent design factors such as projected planform area, base area, wetted surface area, volume ratio, and aspect ratio.

The other goal of this study is the calculation of the viscous drag in a simple but reliable fashion. The viscous drag has been calculated previously by an average skin friciton coefficient, such as outlined by reference 8, or by means of an elaborate integral boundary-layer method[13]. Here however, a new method is presented for laminar boundary layers that allows for variations in Mach number, Reynolds

numbers based on body length, and wall temperature conditions. The method involves simple quadratures associated with the wetted surface area of the waveriders.

It is hoped that we can present some configurations that heretofore were not envisaged using cone derived waveriders. None-the-less these perhaps unusual shapes still render flow fields that are known based on supersonic flow past a cone.

CHAPTER 2

Development of Waverider Shape

2.1 Introductory Remarks

We will start by defining a coordinate system and basic parameters. Then we will determine in a systematic way the waverider shape starting with the base plane view. Finally, we will present views at arbitrary cross sections and a view from overhead.

2.2 Coordinate System and Basic Definitions

To begin we will use the spherical coordinate system shown below in figure 2-1.

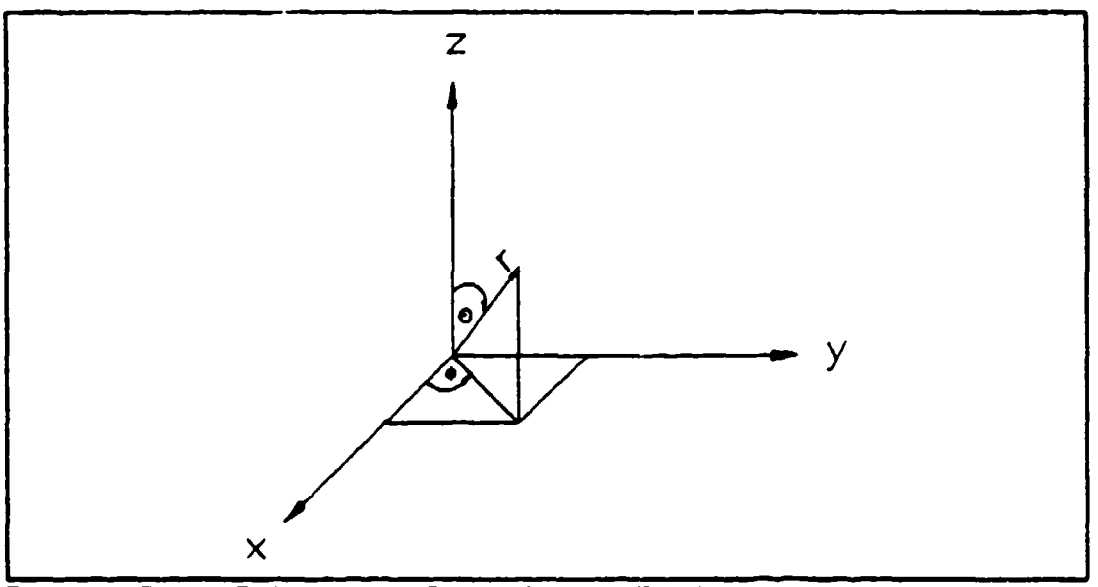

Figure 2-1 Spherical Coordinate System

This figure lends itself to the following set of basic equations.

$$x = r\sin\theta\cos\phi, \quad y = r\sin\theta\sin\phi, \quad z = r\cos\theta \qquad (2\text{-}1)$$

We now wish to impose that θ be restricted to small angles and we reduce this set of equations to,

$$x = r\theta\cos\phi, \quad y = r\theta\sin\phi, \quad z = r \qquad (2\text{-}2)$$

Next, we rotate the conventional spherical coordinate system and impose a cone symmetric about the z-axis with the vertex at the origin, and establish a free stream Mach number aligned with and pointing in the +z direction. This creates a shock cone that is also symmetric about the z-axis. Figure 2-2 below shows this.

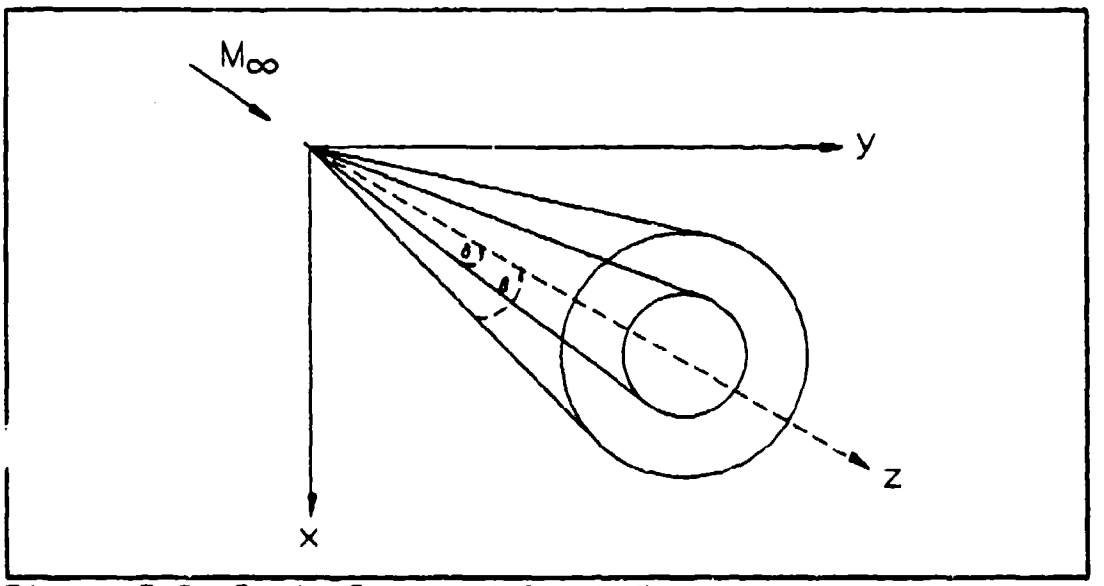

Figure 2-2 Basic Cone and Shock Cone

We now want to construct a non-conical body that will have a flow field that remains conical between the body compression surface and the shock surface. This is done using the procedure in reference 14.

To begin, we define the trailing edge of the free stream surface. In this thesis we will use a sixth-order polynomial to describe this line. Now, we trace undisturbed free streamlines (i.e., streamlines parallel to M_∞) upstream until we intersect the shock cone, thus describing the freestream surface. Next, we trace corresponding streamlines through the shock layer until we intersect the base plane of the cone, thus describing the compression surface of the waverider.

When we determine the streamlines in the compression surface that correspond to those in the freestream surface we require the aid of figure 2-3. Imagine that we pass a plane through the axis of the basic cone. This plane then identifies corresponding streamlines for the freestream and compression surfaces. For example, we may choose any point on the trailing edge of the freestream surface and pass a plane through the axis of the basic cone which also intersects this point. Now staying in the plane we trace upstream until we intersect the shock. Then we trace back a streamline that intersects the shock and stays in the plane until we get back to the base of the cone. Now if we sweep the plane from point

to point along the freestream surface we define the compression surface. Therefore, simply by describing the trailing edge of the freestream surface we have means to determine the entire shape of the waverider body.

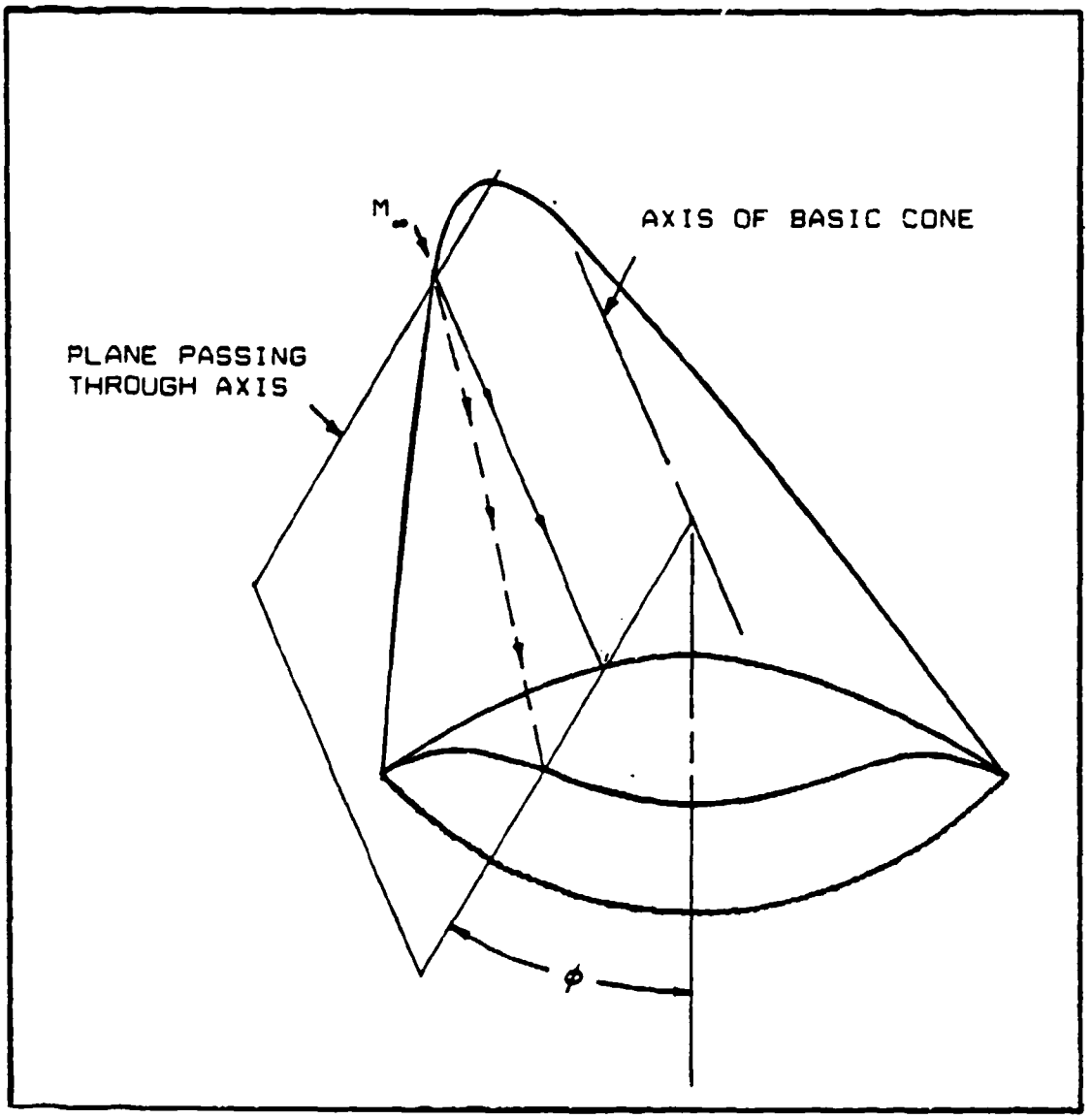

Figure 2-3

According to reference 14, the freestream and compression surfaces are described by

$$r\theta = r_s(\Phi)\beta \tag{2-3}$$

$$r(\theta_c^2 - \delta^2)^{1/2} = r_s(\Phi)(\beta^2 - \delta^2)^{1/2} \tag{2-4}$$

where r is a line from the origin of our coordinate system to any arbitrary point on the freestream or compression surface, θ is the angle between r and the axis of the cone (z-axis), and r_s is the line from the origin to the intersection of the compression and freestream surfaces. Also, β and δ are the half angles for the shock cone and the basic cone respectively. Figure 2-4 below shows a 2-D side view of these definitions.

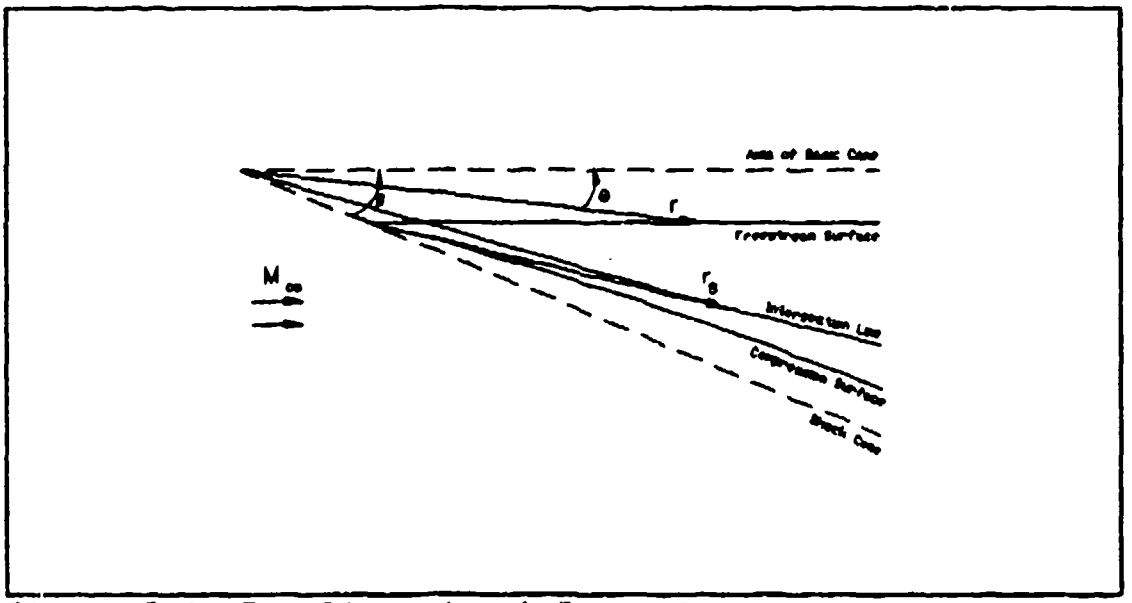

Figure 2-4 Two Dimensional Side View

2.3 The base plane view

We would like to represent the trailing edge of the free-stream surface by a 4-term, sixth-order polynomial like the following

$$x = A + By^2 + Cy^4 + Dy^6 \qquad (2\text{-}5)$$

A representation of this form will allow us to be symmetric about a plane passing through the z-axis in the x-direction. Consider a base plane representation as is shown below in figure 2-5 along with the above equation (2-5).

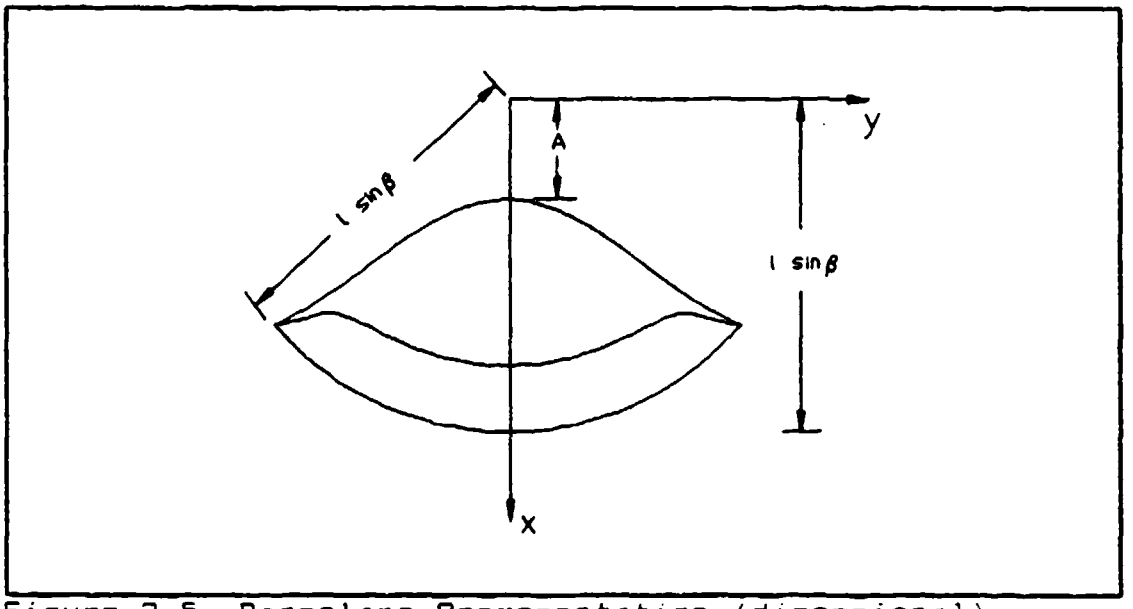

Figure 2-5 Baseplane Representation (dimensional)

We can see from equation (2-5) that,

$$x = A \text{ when } y = 0 \qquad (2\text{-}6)$$

Also, considering figure 2-4 we have the distance from the origin to the shock as $l\sin\beta$. Note that this is also the distance from the origin to the intersection of the two

surfaces since the shock remains conical. This perhaps suggest that we normalize with $l\sin\beta$. However, considering the relationship between β and δ given in reference 14 as,

$$\sigma \equiv \frac{\beta}{\delta} = \left[\frac{(\gamma+1)}{2} + \frac{1}{(M_\infty \delta)^2}\right]^{1/2} \qquad (2\text{-}7)$$

we choose to normalize with $l\sin\delta$ or $l\delta$ since we have restricted ourselves to small angles. Dividing equation (2-5) by $l\delta$ yields

$$x/(l\delta) = A/(l\delta) + 1/(l\delta)[By^2 + Cy^4 + Dy^6] \qquad (2\text{-}8)$$

Now as a matter of convenience since B, C, and D are as yet arbitrary we will define them in the following way

$$B = b_2/(l\delta), \quad C = b_4/(l\delta)^3, \quad D = b_6/(l\delta)^5 \qquad (2\text{-}9)$$

where b_2, b_4, and b_6 are yet to be described. Also, we will define $A/(l\delta)$ as a new parameter with the symbol R_0. Doing this we rewrite equation (2-8) as,

$$X = R_0 + b_2Y^2 + b_4Y^4 + b_6Y^6 \qquad (2\text{-}10)$$

where,

$$X = x/(l\delta), \quad Y = y/(l\delta) \qquad (2\text{-}11)$$

This normalized system renders the following new baseplane representation shown in figure 2-6. It is this new normalized system that we will use to develop a method of determining an infinite variety of waverider baseplane shapes.

This system allows the following conditions:

i) $X = R_0$ when $Y = 0$

ii) $X = \sigma\cos\Phi_1$ when $Y = \sigma\sin\Phi_1$

Additionally, we will require that the slope at the tip of the waverider be between zero and Φ_1. This helps to prevent double intersections with the compression surface. We will call this condition three.

iii) $0 \leq dX/dY \leq \Phi_1$

The four terms of equation (2-11) are determined using these conditions. Substitute condition ii) into (2-11) to yield,

$$\sigma\cos\Phi_1 = R_0+b_2\sigma^2\sin^2\Phi_1+b_4\sigma^4\sin^4\Phi_1+b_6\sigma^6\sin^6\Phi_1 \qquad (2\text{-}12)$$

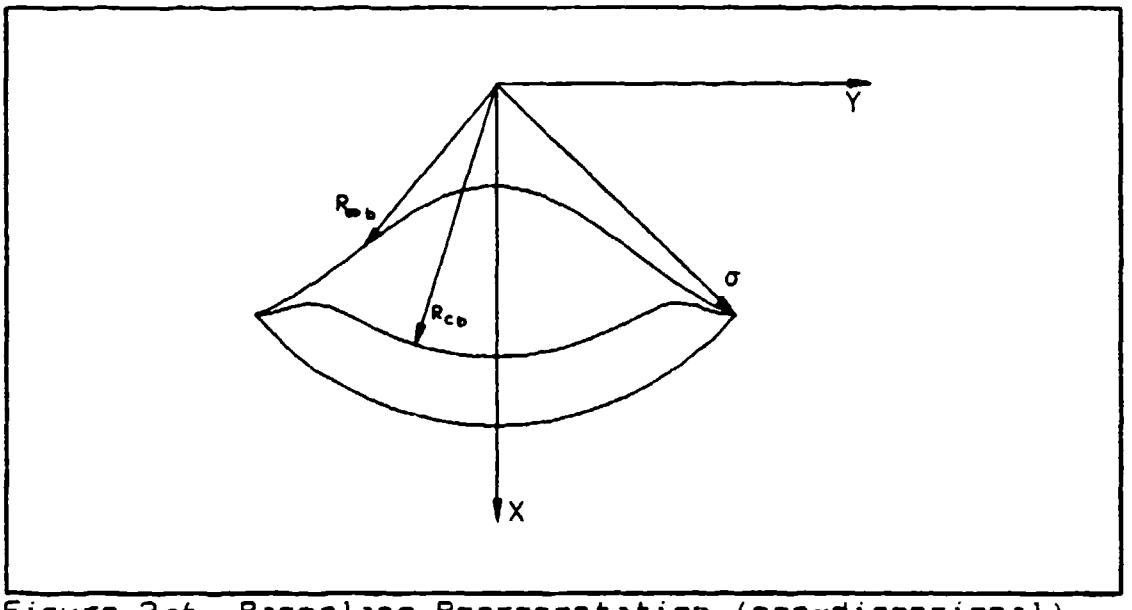

Figure 2-6 Baseplane Representation (non-dimensional)

We see that in order for (2-12) to hold we must choose R_0, Φ_1, b_2, b_4, and b_6 accordingly. To do this we may choose any one variable to be dependent and let the others remain independent.

For example, choose b_2 to be the dependent variable. Solving equation (2-12) for b_2 yields,

$$b_2 = \frac{\sigma\cos\Phi_1 - R_0 - b_4\sigma^4\sin^4\Phi_1 - b_6\sigma^6\sin^6\Phi_1}{\sigma^2\sin^2\Phi_1} \qquad (2\text{-}13)$$

We may therefore use (2-10) to describe a general waverider freestream edge providing we use (2-13) to determine b_2 once we have arbitrarily chosen R_0, Φ_1, b_4, and b_6.

Additionally, we will restrict attention to the cases when condition (iii) holds as well. To see if (iii) holds we merely calculate $dX/dY = 2b_2Y + 4b_4Y^3 + 6b_6Y^5$ and see if the criterion is met.

We now have a means to make various freestream trailing edge shapes. Referring to the above coordinate system we see that the negative most value of Y is,

$$Y_{neg} = -\sigma\sin\Phi_1 \qquad (2\text{-}14)$$

and clearly the positive most value of Y is,

$$Y_{pos} = +\sigma\sin\Phi_1 \qquad (2\text{-}15)$$

All other values of Y must lie in between (2-14) and (2-15).

We therefore start at $Y = -\sigma\sin\Phi_1$ and march away in

small increments until we reach $Y = +\sigma\sin\Phi_1$. At each step along the way we stop and use (2-10) to determine X. We now have many X, Y data points available to plot the freestream edge. If the increments are significantly small we may use a straight line approximation in between data points.

The above is a procedure to determine the freestream edge in the base plane. We now develop the procedure to determine the compression surface. Recall figure 2-6. At each set of points X, Y we may calculate R_{eb} by using the Pytnagorean theorem

$$R_{eb} = (X^2 + Y^2)^{1/2} \qquad (2\text{-}16)$$

where R_{eb} is the distance from the origin of the base plane coordinate system too a point on the surface of the freestream edge in the base plane.

Now we must determine the compression surface that goes with a chosen freestream surface. This is accomplished in reference 14 and is given as

$$R_{cb} = [1 + (\sigma^2 - 1)R^2_{eb}/\sigma^2]^{1/2} \qquad (2\text{-}17)$$

We will now define the X, Y data points for the compression surface as X_c and Y_c to prevent confusion. To determine the X_c, Y_c data points for the compression surface we use simple trigonometric relations,

$$X_c = R_{cb}\cos\Phi, \quad Y_c = R_{cb}\sin\Phi \qquad (2\text{-}18)$$

But, $\cos\Phi = X/R_{eb}$ and $\sin\Phi = Y/R_{eb}$ and we rewrite (2-18) as

$$X_c = X(R_{cb}/R_{eb}), \quad Y_c = Y(R_{cb}/R_{eb}) \qquad (2\text{-}19)$$

The above gives a systematic way to explore virtually an infinite number of waverider base plane shapes. All we need do is choose different variables subject to the given conditions and plot our picture.

We will now look at arbitrary crossections of the waverider viewed from a base plane perspective.

2.4 Arbitrary Crossectional Views

The freestream surface at any arbitrary cross section is still given by the general equation,

$$X = R_0 + b_2Y^2 + b_4Y^4 + b_6Y^6 \qquad (2\text{-}20)$$

however the range of Y is clearly not the same. Recall figure 2-3. From the figure we can see that Φ_z is dependent on location along the Z axis. Note Φ_z is the angle between the Z-axis and the outermost value of Y.

Now recall condition ii) given earlier. We can use the same condition at any arbitrary cross section simply by replacing Φ_1 with Φ_z and σ with σ_z. This gives,

$$X = \sigma_z\cos\Phi_z \text{ when } Y = \sigma_z\sin\Phi_z \qquad (2\text{-}21)$$

substituting (2-21) into (2-20) gives,

$$\sigma_z\cos\Phi_z = R_0+b_2\sigma_z^2\sin^2\Phi_z+b_4\sigma_z^4\sin^4\Phi_z+b_6\sigma_z^6\sin^6\Phi_z \qquad (2\text{-}22)$$

There are two unknowns in (2-22). They are σ_z and Φ_z. Considering figure (2-7) below we can produce a relationship that will give us σ_z.

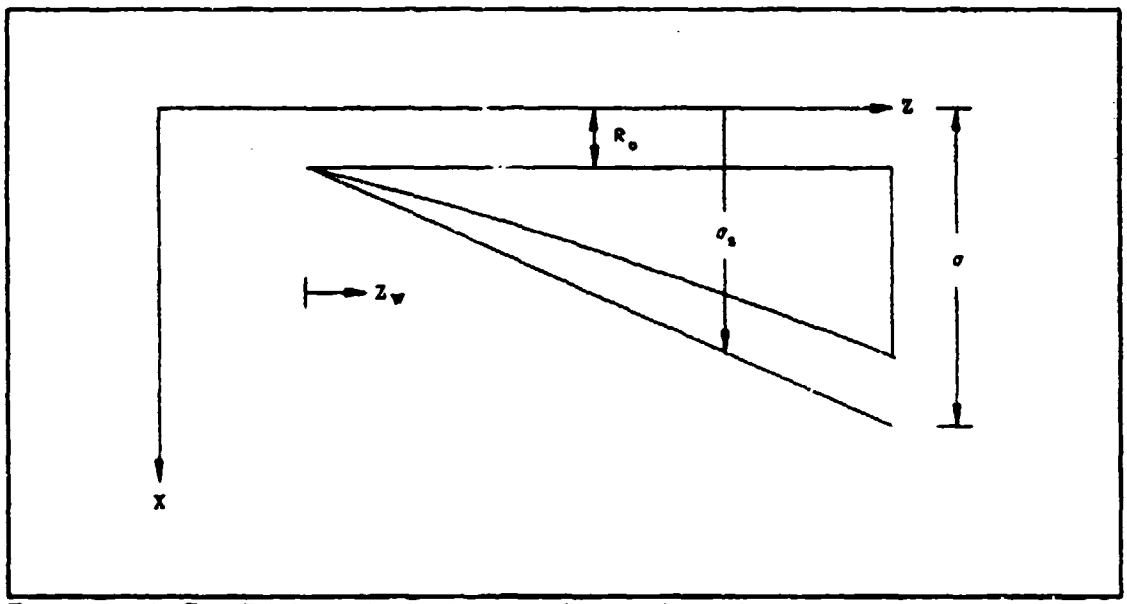

Figure 2-7 Side View (non-dimensional)

Recall that σ_z is the distance from the Z axis to the line of intersection of the shock and waverider body (in the non-dimensional system). But, this is also the distance from the Z axis to the shock in the X-direction. Therefore simple triangle relations give us,

$$\sigma_z = R_0 + Z_w/l_w(\sigma - R_0) \qquad (2\text{-}23)$$

where Z_w/l_w is the percentage back from the leading edge. i.e., 0.1, 0.35 etc...

Now equation (2-23) gives us σ_z, and then (2-22) will give us Φ_z. Due to the difficulty of solving (2-22) for Φ_z, we may use a numerical, instead of analytical approach to solving it. Once Φ_z and σ_z are known the free stream edge is simply plotted as before by replacing σ and Φ_1 by σ_z and Φ_z in

equations (2-14) and (2-15). We may call these equations (2-14) and (2-15) modified.

We now proceed to determine the compression surface at an arbitrary cross section. Recall equation (2-4) describing the compression surface,

$$r^2(\theta_c^2 - \delta^2) = r_s^2(\Phi)(\beta^2 - \delta^2) \qquad (2\text{-}24)$$

Dividing through by l^2 we obtain,

$$(r^2/l^2)(\theta_c^2 - \delta^2) = r_s^2(\Phi)/l^2(\beta^2 - \delta^2) \qquad (2\text{-}25)$$

Now we define θ_{eb} as the angle between r and the Z-axis where r is a line from the origin to any point on the free-stream trailing edge in the base plane. With this definition then we can say that,

$$l\theta_{eb} = r_s\beta \qquad (2\text{-}26)$$

where r_s is a line from the origin to the point of intersection of the two surfaces. Dividing through by δ we obtain,

$$l\theta_{eb}/\delta = r_s\beta/\delta = r_s\sigma \qquad (2\text{-}27)$$

and solving for θ_{eb}/δ yields,

$$\theta_{eb}/\delta = r_s\sigma/l \qquad (2\text{-}28)$$

Now θ_{eb}/δ is also equal to R_{eb} and we can write,

$$R_{eb} = r_s\sigma/l \qquad (2\text{-}29)$$

or

$$r_s^2/l^2 = R_{eb}^2/\sigma^2 \qquad (2\text{-}30)$$

Substituting (2-30) into (2-25) gives,

$$(r^2/l^2)(\theta_c^2 - \delta^2) = (R_{eb}^2/\sigma^2)(\beta^2 - \delta^2) \qquad (2\text{-}31)$$

and dividing through by δ^2 yields,

$$r^2/l^2(\theta_c^2/\delta^2 - 1) = R_{eb}^2/\sigma^2(\beta^2/\delta^2 - 1) \qquad (2\text{-}32)$$

Solving (2-32) for θ_c^2/δ^2 and replacing r with z yields,

$$\theta_c^2/\delta^2 = 1 + (l^2/z^2)[(\sigma^2 - 1)R_{eb}^2(\Phi)/\sigma^2] \qquad (2\text{-}33)$$

We note that $\theta_c^2/\delta^2 = R_{cb}^2$ and therefore (2-33) is remarkably close to equation (2-17) except for the factor l^2/z^2.

Since we want to view the arbitrary cross section from a base plane perspective we want to project θ_c onto the base plane. Figure 2-8 below represents this.

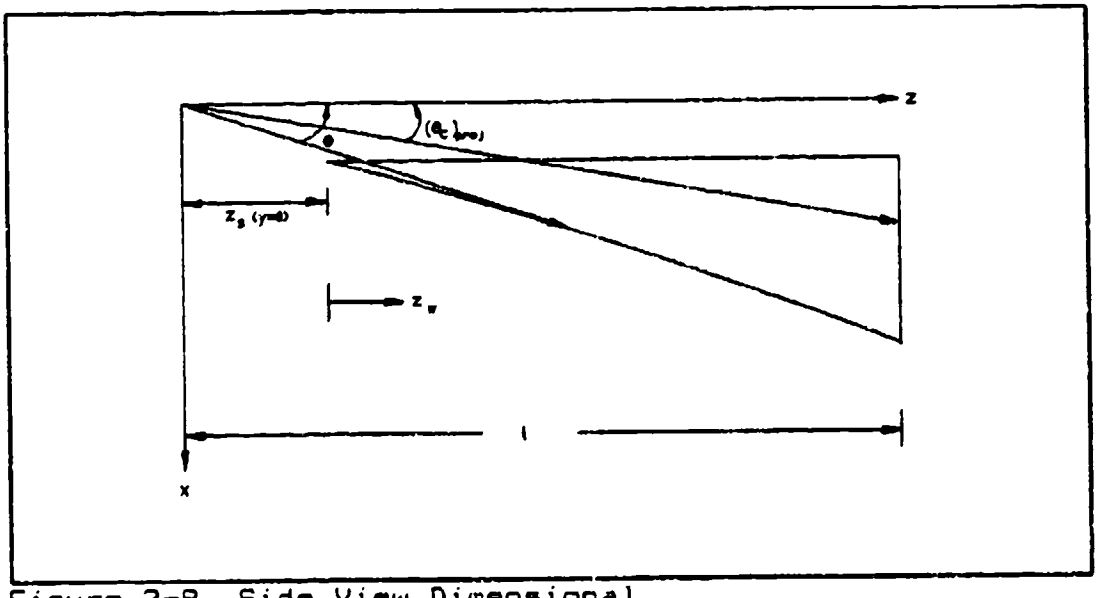

Figure 2-8 Side View Dimensional

We see that,

$$z\theta_c = l(\theta_c)_{proj} \qquad (2\text{-}34)$$

or

$$(\theta_c)_{proj} = z\theta_c/l \qquad (2\text{-}35)$$

Substituting (2-35) into (2-33) yields,

$$(R_{cb}^2)_{proj} = z^2/l^2 + (\sigma^2 - 1)R_{ob}^2(\Phi)/\sigma^2 \qquad (2\text{-}36)$$

From the above figure we see that,

$$z_w = z - R_0 l/\sigma \qquad (2\text{-}37)$$

and

$$l_w = l - R_0 l/\sigma = l(1 - R_0/\sigma) \qquad (2\text{-}38)$$

Equation (2-38) lets us normalize (2-36) with lw. Solving (2-38) for l and substituting into (2-37) we get after rearranging,

$$z_w/l_w = (z/l - R_0/\sigma)/(1 - R_0/\sigma) \qquad (2\text{-}39)$$

We now solve (2-39) for z/l to yield,

$$z/l = (z_w/l_w)(1 - R_0/\sigma) + R_0/\sigma \qquad (2\text{-}40)$$

Now substitute (2-40) into (2-36) to give the desired result,

$$(R_{cb}^2)_{proj} = (z_w/l_w(1-R_0/\sigma)+R_0/\sigma)^2+(\sigma^2-1)R_{ob}^2(\Phi)/\sigma^2 \qquad (2\text{-}41)$$

We now determine X_c, Y_c data points to plot the arbitrary cross section compression surface. We recall equations (2-14) and (2-15) modified.

$$Y_{neg} = -\sigma_z \sin\Phi_z, \quad Y_{pos} = +\sigma_z \sin\Phi_z \qquad (2\text{-}42)$$

Now start at Y_{neg} and march away in small increments until you reach Y_{pos}. At each step along the way stop and calculate X

according to equation (2-20) and R_{eb} according to equation (2-16). We can now determine $(R_{cb})_{proj}$ using (2-41). With $(R_{cb})_{proj}$ known we determine X_c, Y_c with the following simple trigonometric relations,

$$X_c = X(R_{cb})_{proj}/R_{eb} \qquad (2\text{-}43)$$

$$Y_c = Y(R_{cb})_{proj}/R_{eb} \qquad (2\text{-}44)$$

Note that equations (2-43) and (2-44) are similar to equations (2-19). Also in equation (2-41), z_w/l_w is an arbitrary input value depending on what cross section is being viewed. For example, if it is desired to view the cross-section at say 30% from the leading edge then $z_w/l_w = 0.30$.

We now have a systematic way to view the waverider shape at any arbitrary cross section from the leading edge to the base plane. Figure 2-9 below gives an example of the results using this procedure. The figure shows a base plane perspective of the waverider at 0.1 intervals from the leading edge.

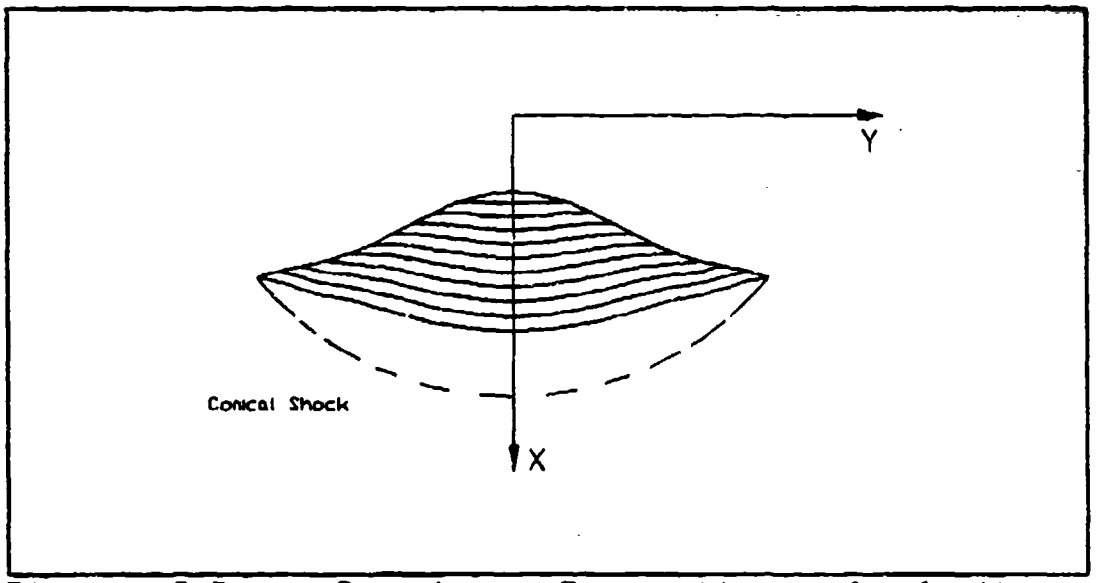

Figure 2-9 Baseplane Perspective of Arbitrary Crossections

2.5 The Top (planform) View

To determine the planform view of the waverider we consider the following coordinate system. We note that along the freestream surface $r\theta$ is a constant, and if we project to the base plane we see that $r\theta = r_s\beta$. Therefore we have

$$r\theta = r_s\beta = \text{constant} \tag{2-45}$$

We now establish a relationship between l and l_w . We can see that from figure 2-10a,

$$l - l_w = z_s(y=0) \tag{2-46}$$

and from figure 2-10b, $\theta = \beta$ when r is drawn to the leading edge of the waverider where the shock intersects the body. Redrawing figure 2-10b we have

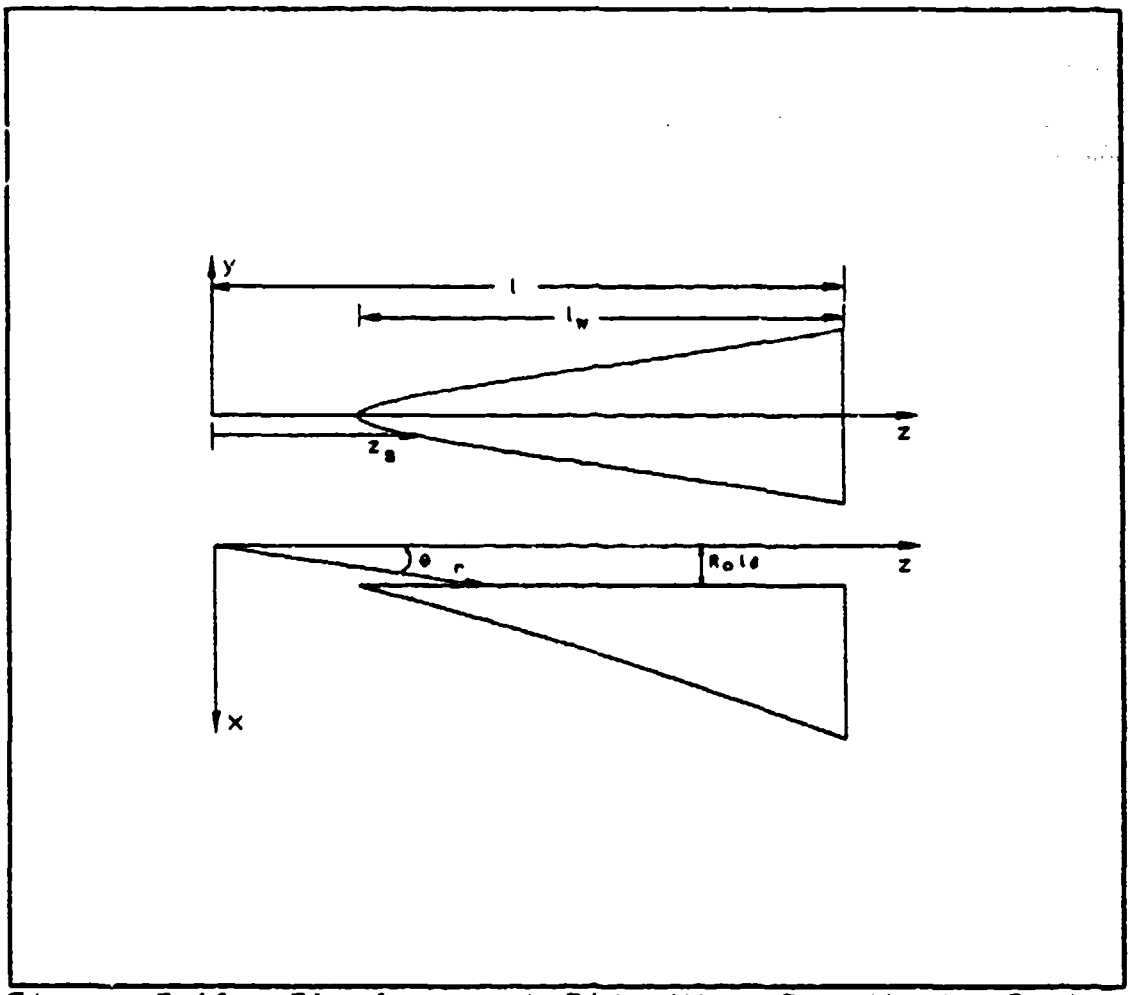

Figure 2-10 Planform and Side View Coordinate System (dimensional)

Now using basic trigonometry we see that,

$$z_s(y=0) = R_0 l\delta/\tan\beta \qquad (2\text{-}47)$$

but using small angle approximations $\tan\beta = \beta$, therefore

$$z_s(y=0) = R_0 l\delta/\beta = R_0 l/\sigma \qquad (2\text{-}48)$$

Substituting (2-48) into (2-46) we have

$$l - l_w = R_0 l/\sigma$$

or

$$l_w = l(1-R_0 l/\sigma) \qquad (2\text{-}49)$$

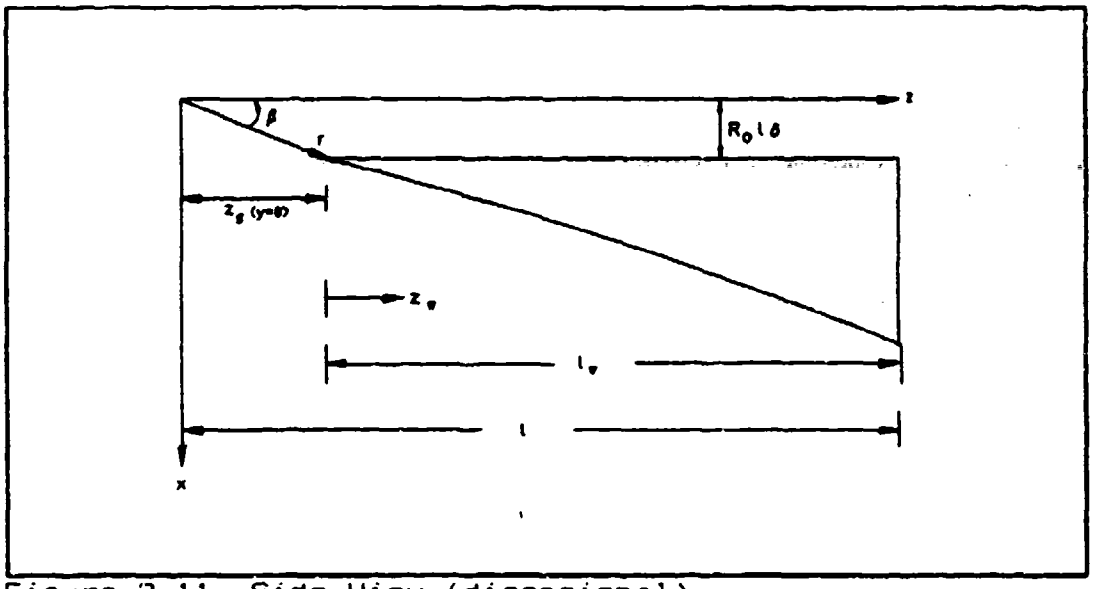

Figure 2-11 Side View (dimensional)

Equation (2-49) gives us a relationship between l and l_w .

Now at the base plane r = l, therefore

$$l\theta_{eb} = r_s\beta = \text{constant}$$

Dividing through by δ and rearranging we obtain

$$\theta_{eb}/\delta = r_s\beta/(l\delta) = r_s\sigma/l \qquad (2\text{-}50)$$

Recall that θ and r_s vary for a given shape and δ, β, and σ do not. Now $\theta_{eb}/\delta = R_{eb}(\phi)$ and this gives us

$$R_{eb}(\phi) = r_s\sigma/l \qquad (2\text{-}51)$$

For small angles $r_s = z_s$ and we rewrite (2-51) as,

$$z_s/l = R_{eb}(\phi)/\sigma \qquad (2\text{-}52)$$

Now recall from our spherical coordinate system that,

$$y = r\theta\sin\phi, \quad z = r \qquad (2\text{-}53)$$

or

$$y = z\theta\sin\phi \qquad (2\text{-}54)$$

Along the boundary (where the shock and body intersect) θ =

β. Replacing z with r_s and dividing through by l we have,

$$y/l = r_s\beta\sin\Phi/l \qquad (2\text{-}55)$$

but $r_s/l = R_{eb}(\Phi)/\sigma$ from (2-52). Therefore substituting yields,

$$y/l = R_{eb}(\Phi)\delta\sin\Phi \qquad (2\text{-}56)$$

Equations (2-52) and (2-56) give us a way of drawing the planform view normalized with l. However, it may be more convenient to normalize with l_w. Using (2-49) to accomplish this we have,

$$z_s/l_w = R_{eb}(\Phi)/(\sigma - R_0) \qquad (2\text{-}57)$$

$$y_s/l_w = R_{eb}(\Phi)\delta\sin\Phi/(1 - R_0/\sigma) \qquad (2\text{-}58)$$

Equations (2-57) and (2-58) give us a method of plotting our waverider as viewed from the top normalized with l_w. The appendix of this thesis devotes much of its bulk to showing various planform and baseplane views of different waveriders determined by a choice of different parameters in equation (2-10).

2.6 Three Dimensional Views

Development of a three-dimensional view of an arbitrary waverider shape can be an extension of the arbitrary cross section and planform views presented earlier. Adams[16] has developed a code using this analysis to present a 3-D view. Several views are presented in appendix H using this code.

CHAPTER 3

Surface Skin-Friction Coefficients

3.1 Introductory Remarks

In this chapter we wish to derive expressions for the average skin-friction coefficients for both the freestream and compression surfaces. Although these expressions will be approximate, they will reflect the proper trends for variations in Reynolds number, Mach number, and surface wall temperature. Since the pressure is constant on the freestream surface of the waverider and varies slowly along an inviscid streamline on the compression surface, we will assume that the friction coefficient can be modeled after a flat plate for the freestream surface and a wedge for the compression surface. In both cases, the pressure gradient along an inviscid surface streamline is zero. We shall use the momentum-integral formulation for compressible boundary layers.

3.2 Momentum-Integral Equation for Flat Plates and Wedges

The momentum-integral equation for zero pressure gradient is given by reference 18 as,

$$\frac{d\Theta}{dx} = \frac{\tau_w}{\rho_e U_e^2} \qquad (3\text{-}1)$$

Where Θ is the compressible momentum thickness given by,

$$\Theta = \int_0^{\delta} \frac{\rho U}{\rho_e U_e} \left(1 - \frac{U}{U_e}\right) dy \qquad (3\text{-}2)$$

and τ_w is the surface stress determined by,

$$\tau_w = \mu_w \left(\frac{\partial U}{\partial y}\right)_w \qquad (3\text{-}3)$$

Here x and y are measured along and normal to the surface in the usual way, as shown in figure 3-1. The thickness of the boundary layer is denoted by $\delta=\delta(x)$. The subscripts e and w denote conditions at the outer edge of the boundary layer and at the wall surface.

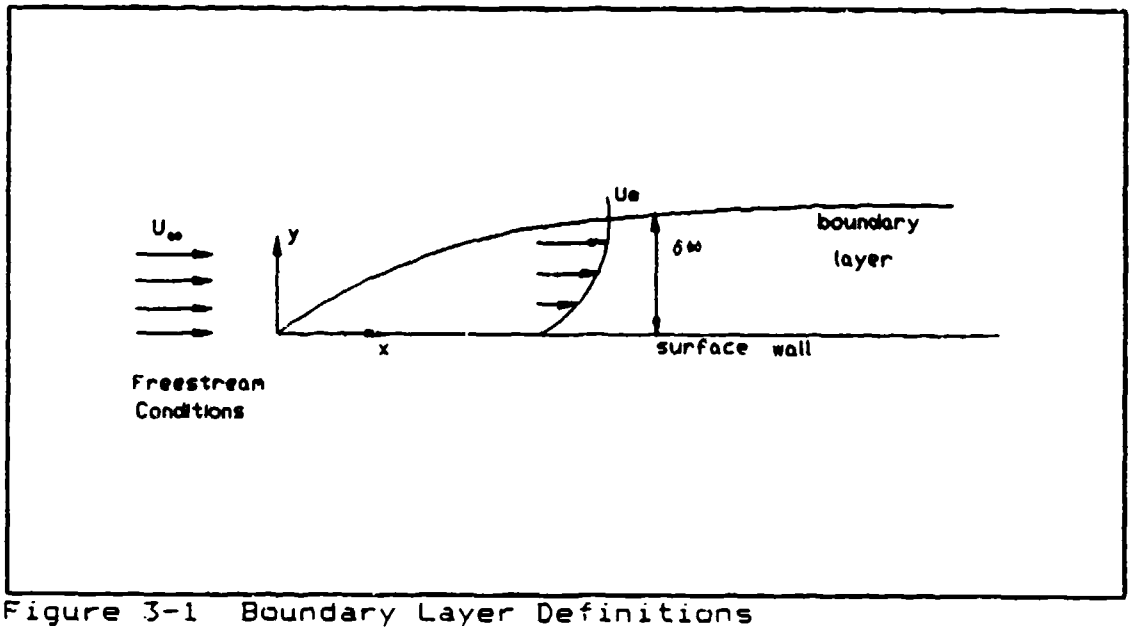

Figure 3-1 Boundary Layer Definitions

To account for compressibility effects, we introduce a transformed normal coordinate Y defined by,

$$dY = \frac{\rho}{\rho_e} dy \tag{3-4}$$

The momentum thickness can now be written as,

$$\theta = \int_0^{\Delta} \frac{U}{U_e}\left(1 - \frac{U}{U_e}\right) dY \tag{3-5}$$

where $Y = \Delta$ is the location of the outer edge of the boundary layer for the transformed coordinate. The wall friction is given by,

$$\tau_w = \frac{\rho_w \mu_w}{\rho_e}\left(\frac{\partial U}{\partial Y}\right)_w \tag{3-6}$$

3.3 Approximate Solution Based on Assumed Velocity Profile

An approximate solution for the momentum integral equation can be obtained by using an assumed velocity profile having the form,

$$\frac{U}{U_e} = f\left(\frac{Y}{\Delta}\right) \tag{3-7}$$

The momentum integral and wall friction can now be expressed as

$$\theta = \Delta \alpha_2 \tag{3-8a}$$

$$\tau_w = \frac{\rho_w \mu_w}{\rho_e} \frac{U_e}{\Delta} \alpha_1 \tag{3-8b}$$

where

$$\alpha_2 = \int_0^1 \frac{U}{U_e}\left(1 - \frac{U}{U_e}\right) d\left(\frac{Y}{\Delta}\right) \tag{3-9a}$$

$$\alpha_1 = \left[\frac{\partial(U/U_e)}{\partial(Y/\Delta)}\right]_w \tag{3-9b}$$

For this problem, we assume that the pressure gradient is zero and that the wall temperature is a constant, and thus that α_1 and α_2 are constants that depend only on the assumed velocity profile. The momentum-integral equation (3-1) can now be expressed as,

$$\frac{\Delta d\Delta}{dx} = C_w \frac{\mu_e}{\rho_e U_e} \frac{\alpha_1}{\alpha_2} \tag{3-10}$$

where

$$C_w = \frac{\rho_w \mu_w}{\rho_e \mu_e} \tag{3-11}$$

For this problem, the right side of equation (3-10) is a constant. Thus we can integrate it without difficulty, subject to the boundary condition $\Delta(0) = 0$, and obtain

$$\Delta = \sqrt{C_w \frac{2\alpha_1}{\alpha_2} \frac{\mu_e x}{\rho_e U_e}} \tag{3-12}$$

We thus obtain the well-known result for flat plates that the transformed boundary-layer thickness grows like the square root of x.

The local skin friction can now be obtained from equation (3-8b). The local skin-friction coefficient, based on the external-flow conditions is,

$$C_{f_e} \equiv \frac{\sqrt{2\,\alpha_1\,\alpha_2\,C_w}}{\sqrt{R_{ex_e}}} \tag{3-13}$$

where

$$R_{ex_e} \equiv \frac{\rho_e U_e x}{\mu_e} \tag{3-14}$$

is the Reynolds number based on the external flow conditions. Equation (3-13) has the same form as that obtained from the classical Blasius equation for constant-density flow past a flat plate. For compressible flow, the factor C_w depends on the assumed viscosity-temperature relation. The factor $\alpha_1\alpha_2$ depends on the assumed velocity profile.

3.4 Viscosity-Temperature Power-Law Relation

In this analysis, we shall assume the viscosity-temperature power-law relation

$$\frac{\mu}{\mu_e} = \left(\frac{T}{T_e}\right)^{\omega} \tag{3-15}$$

where ω is a constant usually taken to lie in the range $.5 \leq \omega \leq 1$, depending on the temperatures involved in the problem. Generally, ω is taken to be about 3/4.

For the special case $\omega = 1$, equation (3-15) takes the form

$$\frac{T_e}{T} \frac{\mu}{\mu_e} = 1 \tag{3-16}$$

Since the pressure is a constant across the boundary layer, we have for a thermally perfect gas ($P = \rho RT$) that $\frac{T_e}{T} = \frac{\rho}{\rho_e}$, and thus that

$$\frac{\rho \mu}{\rho_e \mu_e} = 1 \tag{3-17}$$

For this case, therefore, we have that $C_w = 1$. Thus for $\omega = 1$, C_{fe} from equation (3-13) has the same form as for incompressible flow, provided that ρ and μ are evaluated at the external flow conditions.

If $\omega \neq 1$, equation (3-15) can be written in the form

$$\frac{\mu}{\mu_e} = C \frac{T}{T_e} \tag{3-18}$$

where

$$C \equiv \frac{\rho \mu}{\rho_e \mu_e} = \left(\frac{T}{T_e}\right)^{\omega - 1} \tag{3-19}$$

Equation (3-18) is sometimes referred to as the Chapman-Rubesin form of the viscosity-temperature law, when C is taken as some constant or some function of x, but not as a function of y. For our purposes here, since T is a function of y, we will consider that C is also a function of y, given by equation (3-19). It correspondingly follows that,

$$C_w = \left(\frac{T_w}{T_e}\right)^{\omega - 1} \tag{3-20}$$

3.5 Assumed Velocity Profile

We shall assume that $U/U_e = f(Y/\Delta)$ has the specific form following the Karman-Pohlhausen technique. Namely, a fourth-order polynomial having the form,

$$\frac{U}{U_e} = A\left(\frac{Y}{\Delta}\right) + B\left(\frac{Y}{\Delta}\right)^2 + C\left(\frac{Y}{\Delta}\right)^3 + (1-A-B-C)\left(\frac{Y}{\Delta}\right)^4 \tag{3-21}$$

This expression satisfies the condition at the outer edge of the boundary layer that $U/U_e(1) = 1$. The constants A, B, and C are as follows to meet boundary conditions.

$$A = \left[\frac{\partial(U/U_e)}{\partial(Y/\Delta)}\right]_w = \alpha_1 \tag{3-22a}$$

$$B = \frac{1}{2}\left[\frac{\partial^2(U/U_e)}{\partial(Y/\Delta)^2}\right]_w \tag{3-22b}$$

$$C = (-2 - B) \tag{3-22c}$$

To specify A and B and thus C, we start by noting from the boundary-layer momentum differential equation that at the wall

$$\left[\frac{\partial}{\partial y}\left(\mu \frac{\partial U}{\partial y}\right)\right]_w = 0 \tag{3-23a}$$

provided the pressure gradient along the wall is zero. In terms of the transformed variable Y, this is

$$\left[\frac{\partial}{\partial Y}\left(C \mu_e \frac{\partial U}{\partial Y}\right)\right]_w = 0 \tag{3-23b}$$

Since μ_e does not depend on Y, we can expand equation (3-23b) and get

$$\begin{aligned}\left(\frac{\partial^2 U}{\partial Y^2}\right)_w &= -\left(\frac{\partial \ln C}{\partial Y}\right)_w \left(\frac{\partial U}{\partial Y}\right)_w \\ &= -\left(\frac{\partial \ln C}{\partial T}\right)_w \left(\frac{\partial T}{\partial Y}\right)_w \left(\frac{\partial U}{\partial Y}\right)_w \\ &= -\frac{(\omega - 1)}{T_w}\left(\frac{\partial T}{\partial Y}\right)_w \left(\frac{\partial U}{\partial Y}\right)_w\end{aligned} \tag{3-24}$$

Equation (3-22) provides a relation between the first and second derivative of the velocity at the wall, that is, between A and B. It is useful to place it in an alternative form. We note along with the expressions (3-3) and (3-6) at the wall that we have similar expressions for the heat flux

at the wall:

$$q_w = -k_w \left(\frac{\partial T}{\partial y}\right)_w = -\frac{\rho_w k_w}{\rho_e}\left(\frac{\partial T}{\partial Y}\right)_w \tag{3-25}$$

Consequently, equation (3-24) can be written alternatively as

$$\left(\frac{\partial^2 U}{\partial Y^2}\right)_w = \frac{(\omega - 1)}{T_w}\frac{P_r}{C_p}\frac{q_w}{\tau_w}\left(\frac{\partial U}{\partial Y}\right)_w^2 \tag{3-26}$$

where

$$P_r = C_p \mu_w / k_w \tag{3-27}$$

is the Prandtl number evaluated at the wall, and C_p is the specific heat at constant pressure. We assume that both P_r and C_p are constants.

It is further useful to introduce the Stanton number as the dimensionless heat-transfer coefficient:

$$S_T = \frac{q_w}{\rho_e U_e C_p (T_w - T_{aw})} \tag{3-28}$$

Here the Stanton number is based on the external flow conditions, and T_{aw} is the adiabatic wall temperature, to be specified later. Note that if heat is transferred from the fluid to the wall, then $T_w < T_{aw}$ and $q_w < 0$. In terms of S_T and C_f, defined by equation (3-13), we can rewrite equation (3-24) as

$$\left[\frac{\partial^2(U/U_e)}{\partial(Y/\Delta)^2}\right] = (\omega-1)\frac{(T_w - T_{aw})}{T_w}\frac{2P_r S_T}{C_f}\left[\frac{\partial(U/U_e)}{\partial(Y/\Delta)}\right]_w^2 \qquad (3\text{-}29a)$$

or

$$B = \frac{(\omega-1)}{2}\frac{(T_w - T_{aw})}{T_w}\frac{2P_r S_T}{C_f}A^2 \qquad (3\text{-}29b)$$

The factor $2S_T/C_f$ is known as the Reynolds-analogy factor. It will be specified later. Note when $\omega = 1$ that $B = 0$, and also when C is a constant or a function of x only that B again is zero.

Since B is a function of A, we need a condition on the assumed profile (3-19) to determine A. To do this, we assume the following condition at the outer edge of the boundary layer:

$$\left[\frac{\partial(U/U_e)}{\partial(Y/\Delta)}\right]_{Y=\Delta} = 0 \qquad (3\text{-}30)$$

This gives,

$$A + 2B + 3C + 4(1-A-B-C) = 0$$

substituting the relations for B and C yield,

$$DA^2 + 3A - 6 = 0 \qquad (3\text{-}31)$$

where

$$D = \frac{(\omega-1)}{2}\frac{(T_w - T_{aw})}{T_w}\frac{2P_r S_T}{C_f} \qquad (3\text{-}32)$$

Solving the quadratic equation for A gives

$$A = 12/(3 + \sqrt{(9+24D)}) \qquad (3\text{-}33)$$

When D = 0, then A = 2, and the velocity profile reduces to

$$\frac{U}{U_e} = 2\left(\frac{Y}{\Delta}\right) - 2\left(\frac{Y}{\Delta}\right)^3 + \left(\frac{Y}{\Delta}\right)^4 \qquad (3\text{-}34)$$

3.6 Effects of Mach Number and Heat Transfer on the Friction Coefficient

The momentum-thickness parameter α_2 can now be evaluated from the basic definition equation (3-9a):

$$\alpha_2 = 1/35 + 4A/15 - A^2/9 + DA^2(1/14 - 9A/140 - DA^2/105) \qquad (3\text{-}35a)$$

Since A depends on the factor D from equation (3-33), then α_2 depends on D only. Using the relationships from reference 17,

$$A = 2 + \frac{\Lambda}{6}, \qquad \Lambda = -2B \qquad (3\text{-}35b)$$

and that $D = BA^2$ allows us to write (3-35a) in the same manner as is done in the same reference namely,

$$\alpha_2 = \frac{1}{63}\left(\frac{37}{5} - \frac{\Lambda}{15} - \frac{\Lambda^2}{144}\right) \qquad (3\text{-}35c)$$

When D = 0, that is, when $\omega = 1$ or when $T_w = T_{aw}$ (no heat transfer), then A = 2. We then have $a_2 \approx 0.1175$. Likewise for this case we have $C_w = 1$, and the factor $\sqrt{(2a_1a_2)}$ appearing in the friction coefficient C_{fe}, equation (3-13), takes the value,

$$\sqrt{(2a_1a_2)} \approx 0.685.$$

The correct value for this factor evaluated by the Blasius profile form laminar boundary-layer theory is 0.664. Thus, for this case, the profile from equation (3-34) leads to an error of 3 percent.

Although this error is quite acceptable for our present purposes, the important utility of the present analysis lies in the result for a_2, equation (3-35), that produces combined results for $\omega \neq 1$ and for wall heat transfer, and for which there are no corresponding analytical results from the differential-equation analysis of compressible laminar boundary-layer theory. To proceed further, we need to evaluate the factor D, and to do this we need expressions for the adiabatic wall temperature and the Reynolds analogy factor. We shall thus assume the relations

$$T_{aw} = T_e \left(1 + \sqrt{P_r}\, \frac{\gamma - 1}{2}\, M_e^2\right) \tag{3-36}$$

$$2S_T/C_f = P_r^{-2/3} \tag{3-37}$$

which are well known approximations for flat plates and wedges. The factor D thus becomes

$$D = \frac{\omega - 1}{2} P_r^{1/3} \left[1 - \frac{T_e}{T_w} \left(1 + \sqrt{P_r} \, \frac{\gamma - 1}{2} \, M_e^2 \right) \right] \tag{3-38}$$

With these results, we now have the general functional dependence

$$C_{fe} = f \left(R_{exe}, M_e, \frac{T_e}{T_w}, P_r, \omega, \gamma \right) \tag{3-39}$$

By means of equation (3-20) we can write equation (3-13) as

$$C_{fe} = \frac{\sqrt{2 \alpha_1 \alpha_2}}{\sqrt{R_{exe}}} \left(\frac{T_e}{T_w} \right)^{\frac{1-\omega}{2}} \tag{3-40}$$

with the factor $f(2\alpha_1\alpha_2)$ being a function of D as given by equation (3-38). For adiabatic walls, the results simplify since D = 0, and we have

$$C_{fe} = \frac{0.685}{\sqrt{R_{exe}}} \, \frac{1}{\left(1 + \sqrt{P_r} \, \frac{\gamma - 1}{2} \, M_e^2 \right)^{\frac{1-\omega}{2}}}$$

The factor $C_{fe} f(R_{exe})$ is plotted versus M_e in figure 3-2 for $\gamma = 1.4$, $\omega = 0.7$, $P_r = 0.72$. It can be seen that increasing the external-flow Mach number can reduce the local

skin-friction coefficient considerably.

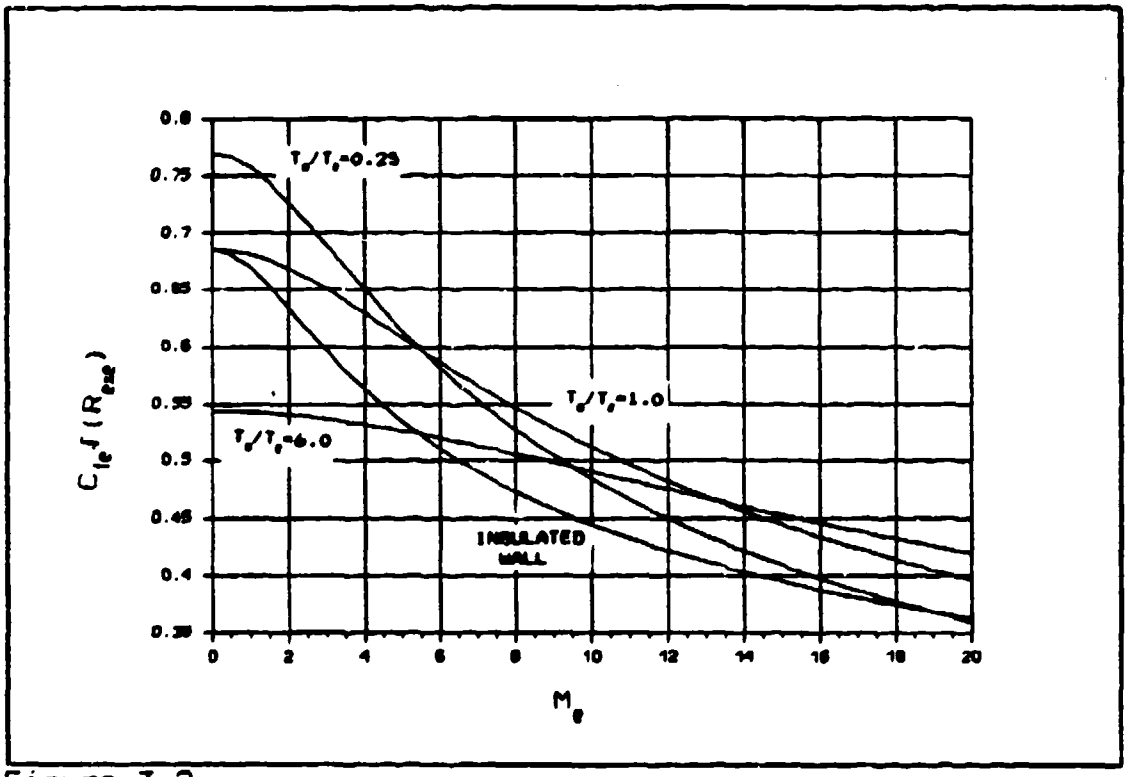

Figure 3-2

Figure 3-2 also shows two curves for when the wall temperature is held fixed, that is, for T_w/T_e = 1 and 6. Again these curves are calculated by means of equations (3-39), (3-36), (3-33) and (3-31). Again, the local skin friction coefficient decreases as M_e increases. These curves are in agreement with corresponding results obtained by numerical integration of the similarity boundary-layer equations of reference 19 and 20.

3.7 Application to Waverider Freestream Surface

For flat plates the external conditions are the same as the freestream conditions. Since the inviscid surface streamlines are straight lines with zero pressure gradient on the upper freestream surface of the waverider, we can apply the previous formulas for C_{fe} by replacing the subscript e with the subscript ∞. In doing this we ignore the fact that there is actually a cross flow in the boundary layer. This occurs because the boundary layer originates at different locations along the leading edge. In a subsequent section, we will obtain an average skin friction coefficient for the freestream wetted surface by integrating the local skin-friction coefficient along each straight streamline on the freestream surface and then integrating again across the span of the surface. This approximate result can be obtained straight forwardly and provides a simple means for making parametric studies of friction drag.

3.8 Compression Surface of the Waverider

For the compression surface of the waverider, the external conditions for the boundary layer are not the same as the freestream conditions because the inviscid surface streamlines pass through the conical bow shock. To express the local skin-friction coefficient and the local Reynolds number in terms of the freestream conditions, we therefore rewrite equation (3-13) as follows:

$$C_{f_\infty} \equiv \frac{2\tau_w}{\rho_\infty U_\infty^2} = \frac{\rho_e U_e^2}{\rho_\infty U_\infty^2} C_{fe}$$

$$= \frac{\rho_e U_e^2}{\rho_\infty U_\infty^2} \left(\frac{T_e}{T_w}\right)^{\frac{1-\omega}{2}} \frac{\sqrt{2\,\alpha_1\alpha_2}}{\sqrt{\frac{\rho_e U_e \mu_\infty}{\rho_\infty U_\infty \mu_e} Re_{x\infty}}}$$

$$= \sqrt{\frac{\rho_e}{\rho_\infty}} \left(\frac{U_e}{U_\infty}\right)^{3/2} \left(\frac{T_e}{T_\infty}\right)^{\omega/2} \left(\frac{T_e}{T_w}\right)^{\frac{1-\omega}{2}} \frac{\sqrt{2\,\alpha_1\alpha_2}}{\sqrt{Re_{x\infty}}} \qquad (3\text{-}42)$$

where

$$Re_{x\infty} = \frac{\rho_\infty U_\infty x}{\mu_\infty} \qquad (3\text{-}43)$$

For a thermally perfect gas we have

$$\frac{\rho_e}{\rho_\infty} = \frac{P_e}{P_\infty} \frac{T_\infty}{T_e} \qquad (3\text{-}44)$$

Thus, when the density is eliminated in favor of the pressure, equation (3-42) becomes

$$C_{f_\infty} = \sqrt{\frac{P_e}{P_\infty}} \left(\frac{U_e}{U_\infty}\right)^{3/2} \left(\frac{T_\infty}{T_w}\right)^{\frac{1-\omega}{2}} \frac{\sqrt{2\,\alpha_1\alpha_2}}{\sqrt{Re_{x\infty}}} \qquad (3\text{-}45)$$

The inviscid surface streamlines on the compression side of the waverider lie in a plane, and the pressure increases slowly along the streamline. Although the boundary layer has

a cross flow and is thus actually three dimensional, we assume these effects are small enough to ignore, and thus the boundary layer along an inviscid surface streamline behaves nearly as that of a flat plate. Further, we assume that the external flow conditions are given by the conditions immediately behind the conical bow shock. If we evaluate these conditions by hypersonic small-disturbance theory then we have

$$\frac{U_e}{U_\infty} \approx 1 \tag{3-46a}$$

$$\frac{P_e}{P_\infty} \approx 1 + \gamma K_\delta^2 \tag{3-46b}$$

$$\frac{(\gamma-1)M_\infty^2 + 2}{(\gamma-1)M_e^2 + 2} = \frac{T_e}{T_\infty} = 1 + \frac{(\gamma-1)}{2} K_\delta^2 \left(2 - \frac{1}{\sigma^2}\right) \tag{3-46c}$$

where

$$\sigma^2 = \frac{(\gamma+1)}{2} + \frac{1}{K_\delta^2} \tag{3-46d}$$

and $K_\delta \equiv M_\infty \delta$. Equation (3-45) now takes the form

$$C_{f\infty} = \sqrt{\frac{P_e}{P_\infty}} \left(\frac{T_\infty}{T_w}\right)^{\frac{1-\omega}{2}} \frac{\sqrt{2\,\alpha_1\alpha_2}}{\sqrt{R_{e_{x\infty}}}} \tag{3-47}$$

The factor $(\alpha_1\alpha_2)_e$ must be evaluated such that T_e and M_e in the factor D are calculated in terms of the infinity conditions

by means of equation (3-46c).

We may simplify equation (3-47) by writing it in terms of the freestream skin friction coefficient given by equation (3-40). Doing so gives,

$$C_{f_\infty} = K(C_{f_\infty})_{fs} \tag{3-48}$$

where

$$K = \sqrt{\frac{P_e}{P_\infty}} \sqrt{\frac{(\alpha_1\alpha_2)_e}{\alpha_1\alpha_2}} \tag{3-49}$$

In the factor K the dominant term is $\sqrt{(P_e/P_\infty)}$ since $\sqrt{((\alpha_1\alpha_2)_e/(\alpha_1\alpha_2))}$ is close to unity. In fact it is unity when Pr = 1.

3.9 Average Skin Friction Coefficients

The average skin friction coefficient is determined by summing up all of the local coefficients along each streamline and then dividing through by the wetted area of the surface.

Considering figure 3-3 below, we have for the average skin friction coefficient for the freestream surface

$$\overline{C_{ff}} = \frac{2\int_s \int_{z_s}^{\ell} C_{f_\infty} dz\, ds}{2\int_s \int_{z_0}^{\ell} dz\, ds} \tag{3-50}$$

In this section we will skip the details of the analysis of the above equation and save it for appendix A. However, after this analysis we have,

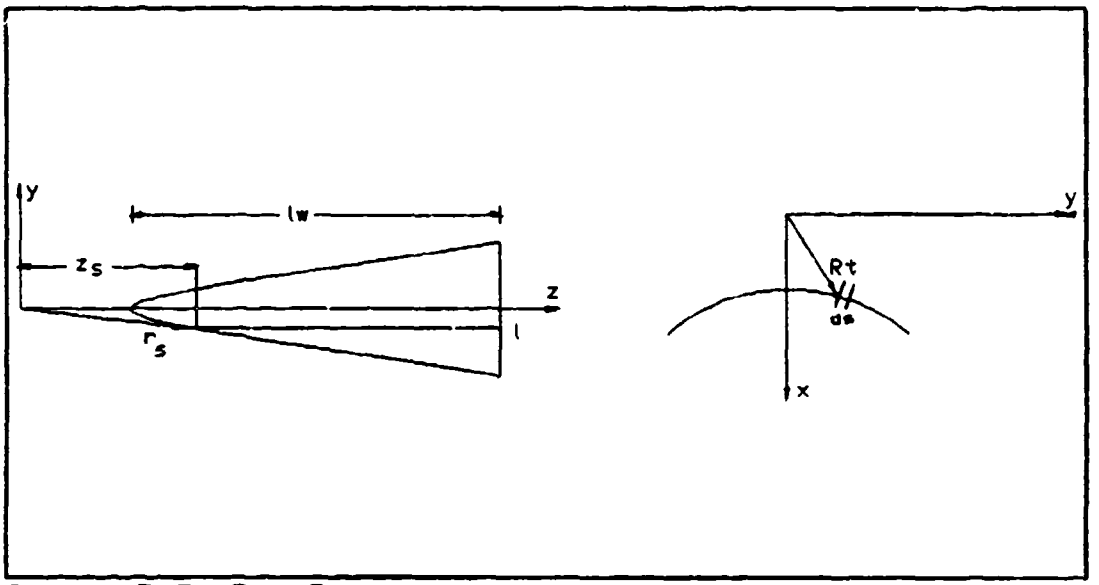

Figure 3-3 The Freestream Surface

$$\overline{C_{ff}} = \frac{\sqrt{1-R_0/\sigma}\; C_{ff}\; 2\int_0^{Y_s}\sqrt{1-R_t/\sigma}\,\sqrt{1+(dX/dY)^2}\,dY}{\int_0^{Y_s}(1-R_t/\sigma)\,\sqrt{1+(dX/dY)^2}\,dY} \qquad (3\text{-}51)$$

The reader may choose any numerical integration scheme desired to evaluate the integrals.

Now, to determine the average skin friction coefficient for the compression surface we will make the assumption that the wetted area for the compression surface is approximately

the same as that of the freestream surface. Using this approximation gives for the compression surface,

$$\overline{C_{fc}} = \sqrt{1-R_0/\sigma}\; C_{fc}\; \frac{2\int_0^{Y_t}\sqrt{1-R_t/\sigma}\,\sqrt{1+(dX/dY)^2}\,dY}{\int_0^{Y_t}(1-R_t/\sigma)\,\sqrt{1+(dX/dY)^2}\,dY} \qquad (3\text{-}52)$$

In equations (3-51) and (3-52) above C_{ff} and C_{fc} are the local skin friction coefficients determined using the analysis of the previous sections.

3.10 Estimation of Total Drag

A good discussion on various types of Drag is presented in reference 21. Here, we will begin with the following definition

$$D = D_w + D_f + D_b \qquad (3\text{-}53)$$

where D_w is the wave drag, D_f is the skin friction drag and D_b is the base drag.

The wave drag exists at supersonic/hypersonic speeds and is caused by static pressure gradients across the shock wave. We will define the wave drag as

$$D_w = qA_bC_w \qquad (3\text{-}54)$$

where $q = 1/2\ \rho_\infty U_\infty^2$, A_b is the base area of the waverider and C_w is the wave drag coefficient.

The skin friction drag is caused by shearing stresses over the wetted surface of the body. We will define the friction drag as

$$D_f = q\overline{C_{ft}}(S_{wf} + S_{wc}) \tag{3-55}$$

where S_{wf} and S_{wc} represent the wetted surface area of the freestream and compression surfaces respectively. Also, $\overline{C_{ft}}$ is the average total skin friction coefficient. However, using the analysis of the previous sections we can rewrite (3-55) as

$$D_f = q(S_{wf}\overline{C_{ff}} + S_{wc}C_{fc}) \tag{3-56}$$

or using the results of equation (3-48) we have,

$$D_f = q\overline{C_{ff}}(S_{wf} + KS_{wc}) \tag{3-57}$$

The base drag is caused by the blunt end of a body. This is because the pressure at the base is usually not the same as the surrounding infinity conditions. We will ignore this effect however, as is usually done when comparing different configurations[14]. Thereby setting $P_b = P_\infty$.

Ignoring the base drag and combining equations (3-51) and (3-50) into (3-49) gives

$$D = q(C_wA_b + \overline{C_{ff}}S_{wf} + C_{fc}S_{wc}) \tag{3-58}$$

or using the results of (3-57) we have

$$D = q[C_wA_b + \overline{C_{ff}}(S_{wf} + KS_{wc})] \tag{3-59}$$

It may be more convenient to have the total drag in terms of the average total skin friction coefficient. Equating (3-

55) and (3-57) and solving for $\overline{C_{ff}}$ yields,

$$\overline{C_{ff}} = \overline{C_{ft}}[(S_{wf} + S_{wc})/(S_{wf} + KS_{wc})] \qquad (3\text{-}60)$$

Substituting (3-60) into (3-59) gives,

$$D = q[C_{w}A_{b} + \overline{C_{ft}}(S_{wf} + S_{wc})] \qquad (3\text{-}61)$$

where

$$\overline{C_{ft}} = \overline{C_{ff}}[(S_{wf} + KS_{wc})/(S_{wf} + S_{wc})] \qquad (3\text{-}62)$$

In the appendix to this thesis we present the lift-to-drag ratio as well as the average total skin friction coefficient for each particular configuration shown.

CHAPTER 4

Comparing Configurations

4.1 Introductory Remarks

Here we will describe what happens as we change different parameters of the waverider configuration. In order to do this we must establish a basic shape from which we will base our comparisons. Once the basic configuration is chosen then we will discuss what happens when we change the coefficients of Y of equation (2-10) namely, b_2, b_4, and b_6. After this we will compare shapes with different values for R_0, Φ_1, and δ and include a discussion on the Mach number and Reynolds number.

4.2 The Basic Waverider Configuration

The basic shape is chosen to have the parameters shown below in table 4.1

Table 4-1
Basic Configuration Parameters

Φ	δ	Mach Number	Reynolds Number	γ
50°	8	10	$1X10^6$	1.4
R_0	b_2	b_4	b_6	slope
0.5	0.903	-1.0	0.437	25°

The basic parameters were chosen arbitrarily except for b_2 and b_6. The value of b_6 was chosen such that the slope at the edge of the waverider freestream surface was 25°. This value is in between the limits imposed by condition iii) of chapter 2. The value of b_2 was fixed according to equation (2-13). These basic configuration parameters resulted in the waverider configuration shown below in figure 4-1.

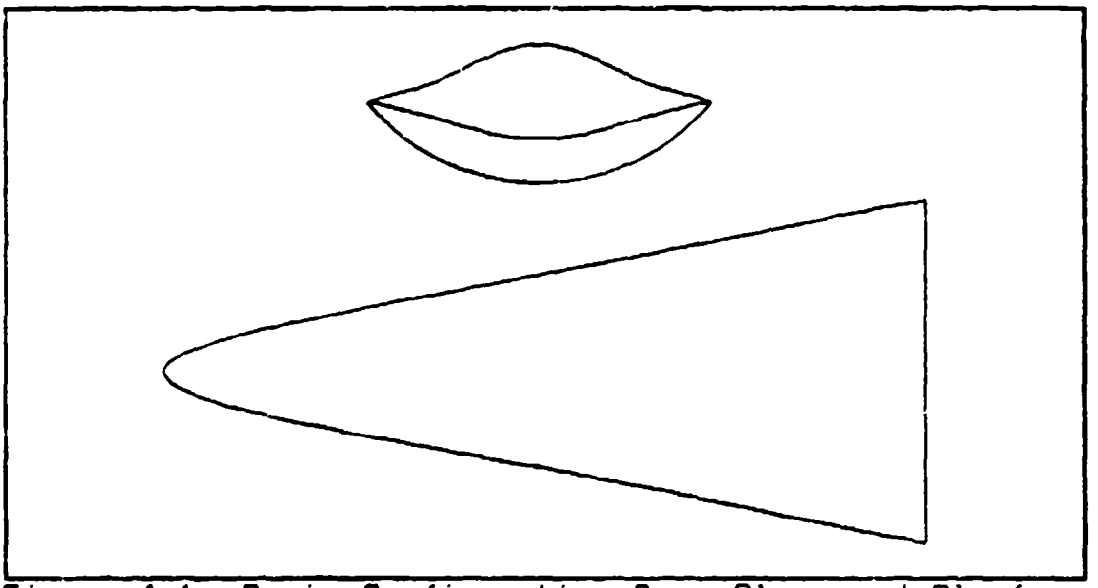

Figure 4-1 Basic Configuration Base Plane and Planform Views

We will now vary these parameters and see how the basic configuration changes.

2.3 Changing the Coefficients of Y of the Equation Describing the Freestream Edge in the Base Plane With Consideration of the Edge Slope

Here, we will hold the parameters, Φ_1, δ, M, Rey, and constant and vary in a systematic way the coefficients of Y equation (2-10).

Suppose we want to change b_4 from a -1.0 as shown in table 4.1, to a -2.0. This is easily done. However, due to equation (2-13) changing b4 will result in a different value of b_2 as well. We must also keep in mind the imposed condition of the slope at the edge of the waverider. Changing b_4 will also change the slope at the edge of the waverider. We can however, keep the slope at a constant value by letting b_6 change by a suitable amount. Table 4-2 below shows what happens when we change b_4 from -1.0 to -2.0, holding R_0 and the edge slope constant. Also, figure 4-2 shows the corresponding waverider configuration.

Table 4-2

Φ	δ	Mach Number	Reynolds Number	γ
50°	8	10	$1X10^6$	1.4
R_0	b_2	b_4	b_6	slope
0.5	1.405	-2.0	0.935	25°

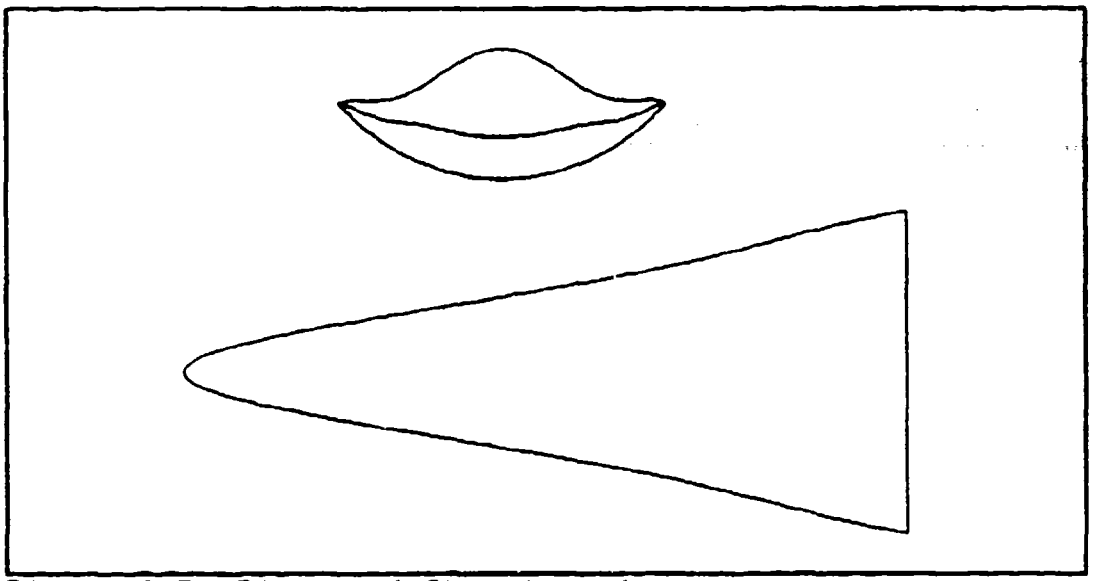

Figure 4-2 Effect of Changing b4

This discussion shows the inherent complexities of changing what may seem to be a rather simple variable. By changing b_4 we discovered that b_2 and b_6 must also change.

Suppose now instead of changing b_4 we want to change the freestream edge slope from 25° to its maximum limit of 50°. This is accomplished by changing the value of b_6 or b_4. However, for the sake of simplicity we will hold b_4 at its previous value of -1.0. Setting dX/dY = 50 and solving gives a new value of b_6 and b_2. Table 4-3 below shows this, and figure 4-3 shows the corresponding waverider configuration.

A similar approach to the above analysis can be done if we want the slope of the freestream edge at its minimum value.

We must also ask ourselves what are the aerodynamic and geometric consequences of changing the values of b_4. Analysis

Table 4-3

Φ	δ	Mach Number	Reynolds Number	γ
50°	8	10	$1X10^6$	1.4
R_0	b_2	b_4	b_6	slope
0.5	0.795	1.9	0.544	50°

has shown that the viscous lift to drag ratio may increase or decrease with a change in b_4. The deciding factor is the initial value of b_4. However, the change in magnitude of the viscous L/D appears to change only rather slightly.

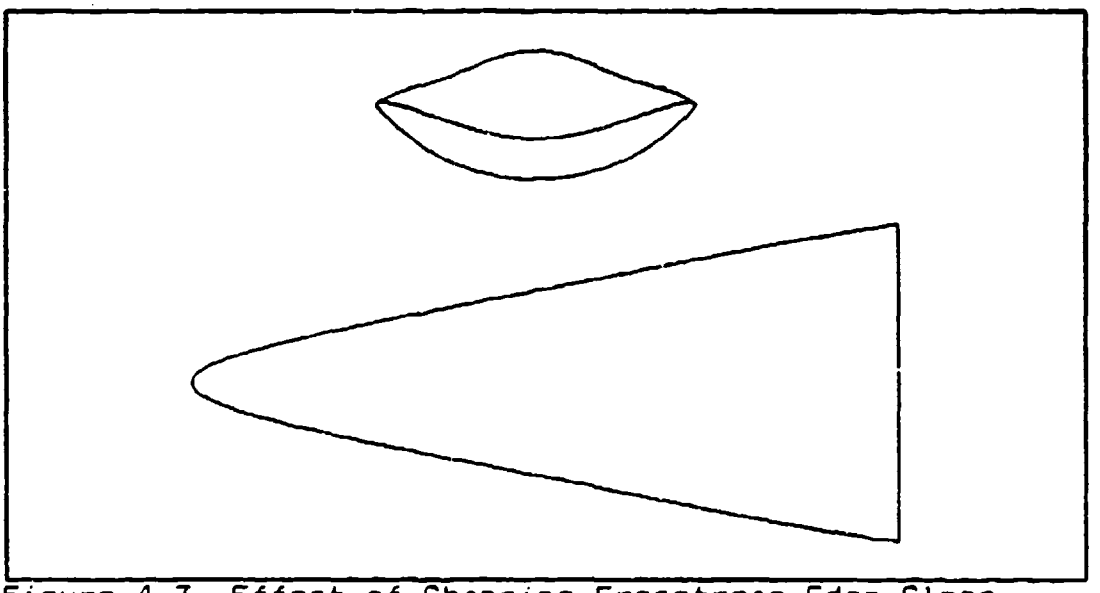

Figure 4-3 Effect of Changing Freestream Edge Slope

Similarly, the effects of changing the edge slope in general has a minor effect on the aerodynamic values. However, a slope of 50° usually gave higher L/D ratios; although in some cases this was not true.

4.4 Changing R_0 in the Equation Describing the Freestream Edge

When changing R_0, we might say that there is no effect on the edge slope. However, a further investigation tells us that, even though dX/dY has no R_0 terms in it, the value of b_2 does depend on R_0. Since the slope is dependent on b2 we see that changing R_0 will result in a changing tip slope. We can however keep the tip slope constant by changing b_6 as done before.

A more dramatic affect caused by changing R_0 is the non-dimensional length of the waverider. This is easily seen by equation (2-38). Also, figure (4-4) below shows this result. We can see that small values of R_0 will result in more slender configurations. We define the aspect ratio for these configurations as b/l_w. Where b is the maximum distance across the base of the waverider. Therefore the smaller the aspect ratio the more slender the waverider. Aspect ratios are given for each configuration shown in the Appendix.

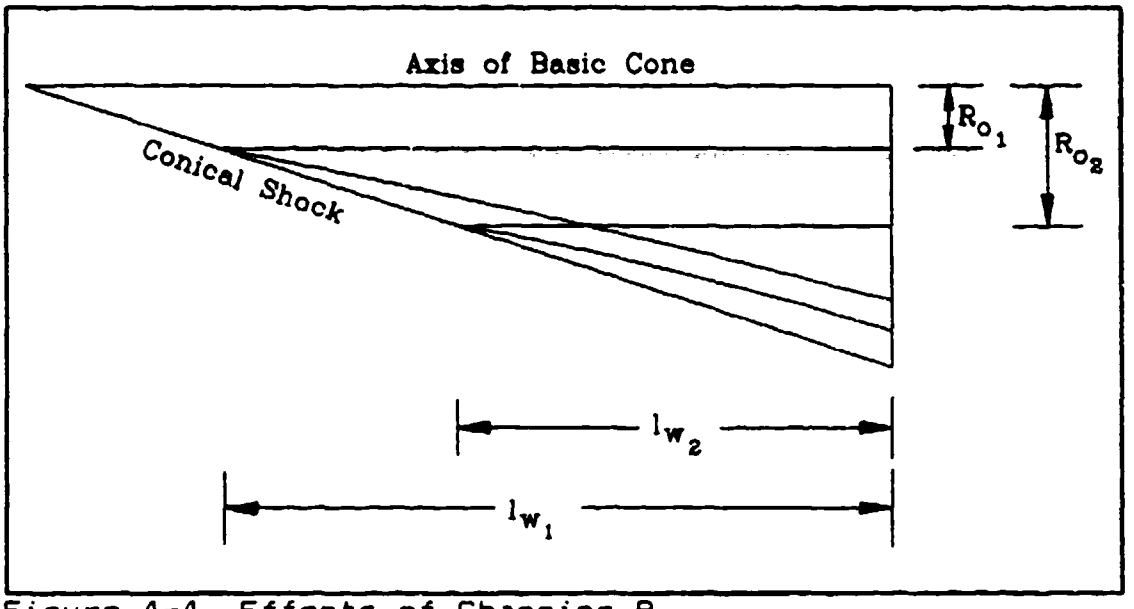

Figure 4-4 Effects of Changing R_0

Analysis shows in general that small values of R_0 usually result in better viscous lift to drag ratios.

Another effect on the waverider that occurs with a change in R_0 is the shock stand off distance. Smaller values of R_0 result in the shock being a greater distance away from the compression surface. This can be seen in the above figure. There are other factors that determine the shock stand off distance and these will be discussed as they occur.
Changing R_0 also significantly changes the shape of the base plane configuration as is shown below in figures 4-5a,b.

In figures 4-5a,b the value of the edge slope and the value of b_4 is kept constant. In general, larger values of R_0 cause the freestream surface to be flatter.

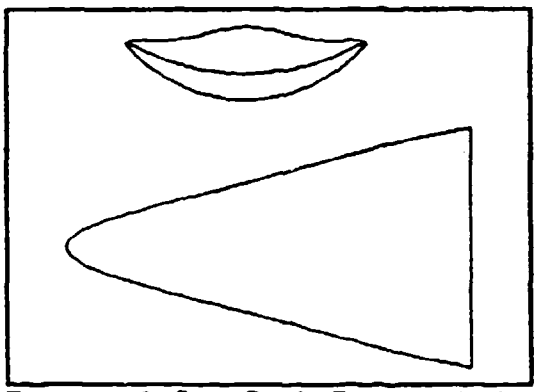

Figure 4-5a R_0=0.7, b_4=-1.0, slope=25°

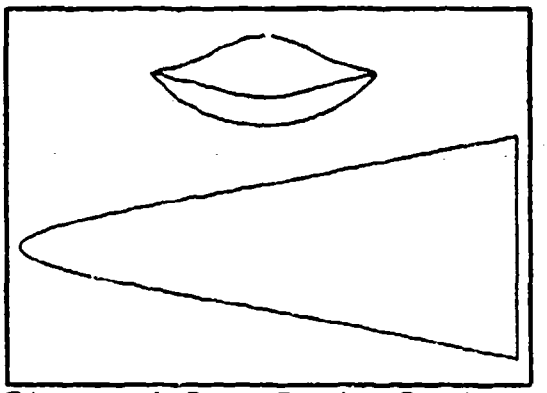

Figure 4-5b Basic Config. R_0=0.5, b_4=-1.0, slope=25°

4.5 Changing the Parameter Φ_1

When we change Φ_1 the most significant change in the waverider shape that is first noticed is the change in maximum span or width; all other parameters remaining the same. Equations (2-14) and (2-15) give us the positive and negative most values of Y, which allow us to determine the span of the waverider. Clearly a decrease in Φ_1 decreases the span. A decrease in the span decreases the aspect ratio and increases the slenderness of the waverider.

If we change Φ_1 holding R_0 and b_4 constant, we get a new value for b_2 according to equation (2-13). Also, b_6 will have to change to keep the slope at the edge constant or within limits according to condition iii). Figures 4-6a,b show two configurations with identical δ, b_4, and tip slope but with different Φ_1's

We see from this that a change in Φ_1 causes a significant change in the waverider shape; not only in span but also in the curvature of the freestream and compression surface. However, there is no change in the length of the waverider.

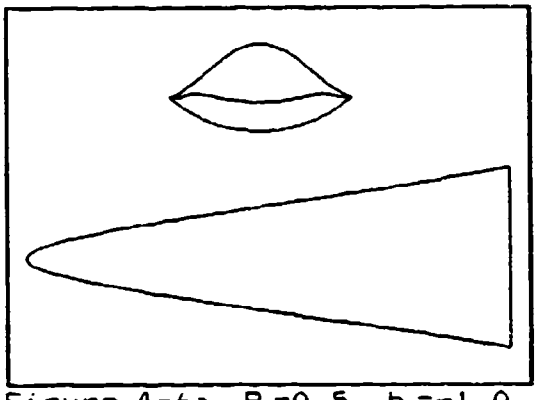

Figure 4-6a R_0=0.5, b_4=-1.0, slope=25°, Φ_1=40°

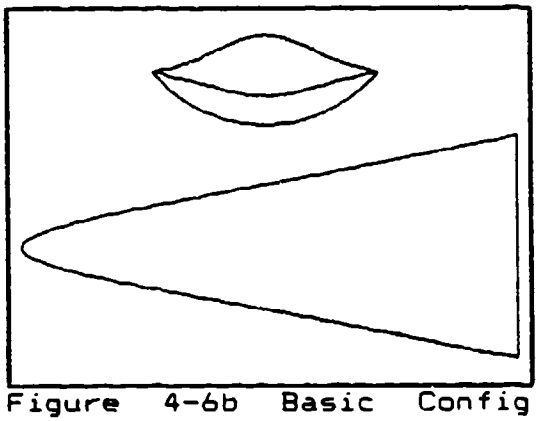

Figure 4-6b Basic Config R_0=0.5, b_4=-1.0, slope=25°, Φ_1=50°

4.6 Changing the Parameter δ

When we change δ the value of σ changes. This has an effect on the standoff distance between the shock and the compression surface of the waverider body. To see this we look at the definition of σ from chapter 3.

$$\sigma^2 = \frac{(\gamma+1)}{2} + \frac{1}{K_\delta^2} \qquad (4-1)$$

where $K_\delta = M_\infty \delta$.

We can see from equation (4-1) that a decrease in δ will result in an increase in σ. This causes the separation

between β and δ to increase; which affects the shock standoff distance. The standoff distance becomes important when considering design of engine and engine inlet conditions. Below in figures 4-7a,b we show different waveriders with the same R_0, Φ_1, b4, and tip slope but with different δ's.

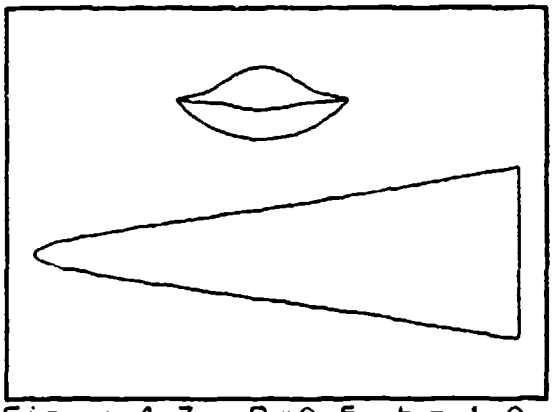

Figure 4-7a R_0=0.5, b_4=-1.0, δ=6, Φ_1=50, slope=25°

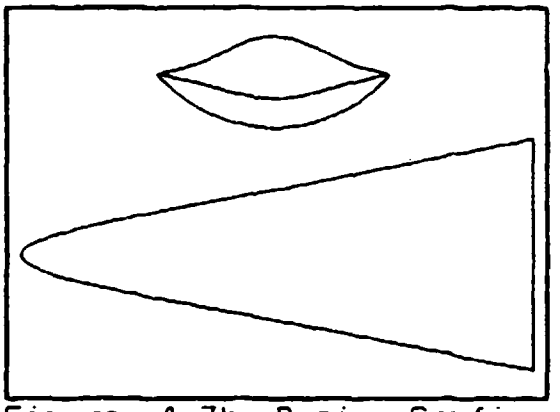

Figure 4-7b Basic Config. R_0=0.5, b_4=-1.0, δ=8, Φ_1=50, slope=25°

Again, changing δ and therefore σ, results in a change of b_2 according to equation (2-13) and a change in b_4 or b_6 to meet the slope condition on the edge of the waverider freestream surface. These changes cause the curvature of the freestream and compression surfaces to vary.

4.7 Changing the Mach Number

Varying the mach number has a similar effect as changing δ as we see from equation (4-1). An increase in M will cause

the standoff distance to be smaller just as an increase in δ will do. The only difference will be the magnitude of the change. Again we must take into account how changes affect σ and therefore b_2, b_4, and b_6.

4.8 Changing the Reynolds Number

We realize that M has a role in the determination of the Reynolds number. However, lets assume the Mach number will remain constant. This leaves altitude and the length of the waverider as the deciding factors of the value of the Reynolds number.

Figure 4-8 below shows L/D vs. Reynolds number for the basic configuration shown in figure 4-1.

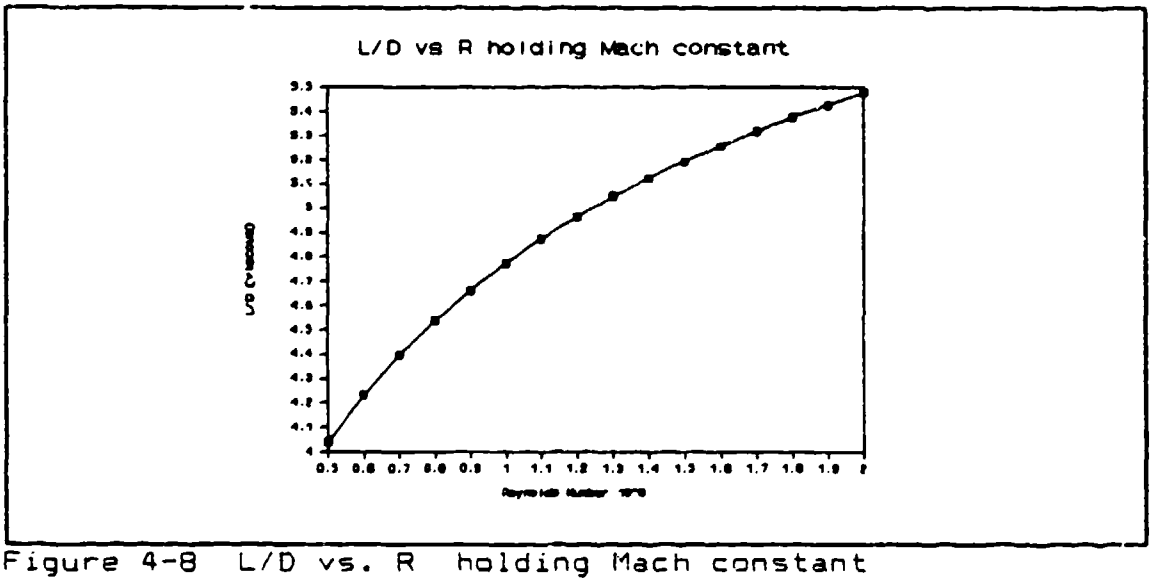

Figure 4-8 L/D vs. R holding Mach constant

CHAPTER 5

Conclusion

5.1 Summary

The two primary goa' established in chapter 1 have been accomplished. In the appendices, a catalogue of over 100 shapes is presented. This catalogue shows variations of waveriders that can be generated by axisymmetric flow past a cone and is the result of the first goal.

As discussed earlier there can be an infinite number of waverider shapes so as yet the catalogue is incomplete. However, one may get an idea and a feel for waverider shapes by studying the appendices.

Chapter 3 is the result of the second primary goal. Here we developed an analytical method of estimating the skin friction coefficient -- where as before only numerical methods existed. An average total skin friction coefficient is presented in the appendices for each arbitrary waverider shape.

5.2 Results and Discussions

The best waverider shape depends on the designers main goals. As in all design processes one is usually faced with compromise. For example the waverider with the best lift-to-

drag ratio will probably not have the best volume-to-area ratio.

The following table is a tool to help in the design process. In the table we can see the effects of certain geometric and aerodynamic values when we vary parameters that affect the shape of the waverider. When using the table the results are given such that all other parameters are held constant. For example, lc ing Φ_1 will in general result in a lower value of L/D the other parameters are held constant; namely, R_0 and b_4. The table doesn't give magnitudes of change only direction of change. In some cases the effect of a change cannot be determined ahead of time. An example would be the effect in the volume-to-area ratio with a change in b_4. Lowering b_4 may result in either an increase or decrease in the volume-to-area ratio depending on the original value of b_4.

TABLE 5-1
EFFECT OF LOWERING (Φ_1, R_0, and b_4)

	Φ_1	R_0	b_4
L/D	↓	↓	↓
V/V_L	↓↑	↑	↓
$V^{2/3}/S_p$	↑	↑	↓↑
SSD	—	↑	—
b/l_w	↓	↓	—

Following this chapter in appendices B through H a catalogue of over 100 shapes is presented. All of the configurations presented are based on Mach number of 10 and Reynolds number of 10^6. The lift-to-drag ratios were calculated and found to lie in a range from 4.32 to 5.06 while the average skin friction coefficient ranged from 0.00176 to 0.00205. The volume to area ratio $V^{2/3}/S_p$ ranged from 0.224 to 0.153. In the table under each view are various geometric and aerodynamic values. Some of them are compared with what we call the idealized waverider. Reference 14 describes this ideal waverider. The freestream surface of the ideal waverider is given by,

$$X = |Y\cot\Phi_1| \qquad (5\text{-}1)$$

where the lines about the term on the right represent the absolute value. Note than in the above equation there is no term representing the value of R_0. This is because R_0 is zero in this case.

REFERENCES

[1]Townend, L.H., "Research and Design for Lifting Reentry," Progress in Aerospace and Science, Vol. 19, No. 1, 1979, pp 1-80.

[2]Stollery, J.L., "What has Aerospace Research Led to?", Aerospace, Sept. 1982, p. 14.

[3]Kuchemann, D., The Aerodynamic Design of Aircraft, Pergamon Press, New York, 1978, Chap. 8.

[4]Hemsch, M.J. and Nielsen, J.N., Tactical Missile Aerodynamics, AIAA Progress in Aeronautics and Astronautics Series, edited by M. Summerfield, New York, 1986.

[5]Rasmussen, M.L., "Waverider Configurations Derived from Inclined Circular and Elliptic Cones," Journal of Spacecraft and Rockets, Vol. 17, No. 6, Nov.-Dec. 1980, pp. 537-545.

[6]Rasmussen, M.L., Daniel, D.C., and Jischke, M.L., "Supersonic Aerodynamics of a Class of Cone-Derived Waveriders," 12th Navy Symposium on Aero-ballistics, David W. Taylkor Naval Ship research and development Center, Bethesda, MD, May 1981.

[7]Rasmussen, M.L., Jischke, M.C., and Daniel, D.C., "Experimental Forces and Moments on Cone-Derived Waveriders for M_∞ = 1 to 5," Journal of Spacecraft and Rockets, vol. 19, No. 6, Nov.-Dec. 1982, pp. 592-598.

[8]Rasmussen, M.L. and Broadaway, R.T., "Viscous Effects on the Performance of Cone-Derived Waveriders," AIAA Paper No. 83-2084, AIAA Flight Conference, Gatlinburg, TN, August 1983.

[9]Kim, B.S., Rasmussen, M.L., and Jischke, M.C., "Optimization of Waverider Configurations Generated from Axisymmetric conical flows," Journal of Spacecraft and Rockets, Vol. 20, No. 5, Sept.-Oct. 1983, pp. 461-469.

[10]Rasmussen, M.L., "Aerodynamics of Cone-Derived Waveriders and Related Lifting Bodies," Air Force Armament Laboratory Report AFATL-TR-84-70, Eglin AFB, Florida, March 1985.

[11]Rasmussen, M.L., "Experiments on a Slender Waverider Configuration with and without an Inlet," Air Force Armament Laboratory Report AFATL-TR-86-07, Eglin AFB, Florida, March 1985.

[12]Rasmussen, M.L. and Clement, L., "Cone-Derived Waveriders with Longitudinal Curvature," Journal of Spacecraft and Rockets, Vol. 23, No. 5, Sept.-Oct. 1986, pp. 461-469.

[13]Bowcutt, K.G., Anderson, J.D., and Capriotte, D., "Viscous Optimized Hypersonic Waveriders," AIAA Paper No. 87-0272, AIAA 25th Aerospace Sciences Meeting, Reno, NV, Jan. 1987.

[14]Rasmussen, M.L. and Stevens, D.R., "On Waverider Shapes Applied to Aero-Space Plane Forebody Configurations," AIAA Paper No. 87-2550, AIAA 5th Applied Aerodynamics Conference, Monterey, CA, August 1987.

[15]Lin, S-C. and Rasmussen, M.L., "Cone-Derived Waveriders with Combined Transverse and Longitudinal Curvature," AIAA Paper No. 88-0371, AIAA 26th Aerospace Sciences Meeting, Reno, NV, Jan. 1988.

[16]Adams, C.F., "3-Dimensional Waverider Program," Special Report, University of Oklahoma 1988

[17]Schlicting, H., Boundary Layer Theory, McGraw Hill, 7th Edition, 1979, Chap. 10.

[18]White, F.M., Viscous Fluid Flow, McGraw Hill, 1974, Chapter 7.

[19]Kuethe, A.M. and Chow, C-Y., Foundations of Aerodynamics: Bases of Aerodynamic Design, John Wiley & Sons, 3rd Edition, 1976, Chap. 16

[20]Van Driest, E. R., Investigation of Laminar Boundary Layer in Compressible Fluids Using the Crocco Method, NACA TN 2597, 1952

[21]McCormick, B.W., Aerodynamics, Aeronautics, and Flight Mechanics, John Wiley & Sons, 1979, Chap. 4.

Appendix A

Development of Equation 3-51

We begin by establishing a few definitions that will be used later in this analysis. Consider the second part of figure 3-3 and we may say without much effort,

$$ds = \sqrt{(dx)^2+(dy)^2}$$

$$= \sqrt{1+(dx/dy)^2}\,dy \qquad A.1$$

Next, consider equations (2-5) and (2-20). From these we can show that,

$$dx/dy = dX/dY \qquad A.2$$

and also that,

$$dx = l\delta dX, \quad dy = l\delta dY \qquad A.3$$

Now considering the first part of figure 3-3 we may write that the wetted surface area of the freestream surface is,

$$S_{W_\infty} = 2\int_s\int_{z_s}^{l} dz\,ds$$

$$= 2\int_s (l - z_s)\,ds \qquad A.4$$

Now since we are using small angles we have,

$$z_s \approx r_s \qquad A.5$$

Therefore,

$$S_{W_\infty} = 2\int_s (l - r_s)\,ds \qquad A.6$$

$$= 2l\int_s \left(1 - \frac{r_s}{l}\right) ds$$

Now use equation (2-29) and that $R_t = R_{eb}$ to give,

$$S_{W\infty} = 2\ell \int_s (1 - R_t/\sigma)\, ds \qquad A.7$$

and substituting A.1 yields,

$$S_{W\infty} = 2\ell \int_0^{Y_\ell} (1 - R_t/\sigma) \sqrt{1 + (dx/dy)^2}\, dy \qquad A.8$$

Now if we substitue relationships A.2 and A.3 we have,

$$S_{W\infty} = 2\ell^2\delta \int_0^{Y_\ell} (1 - R_t/\sigma) \sqrt{1 + (dX/dY)^2}\, dY \qquad A.9$$

Recall equation (3-50)

$$\overline{C_{ff}} = \frac{2\int_s \int_{zs}^{\ell} C_{f_\infty} dz\, ds}{2\int_s \int_{zs}^{\ell} dz\, ds} \qquad A.10$$

where C_{f_∞} is the local skin friction coefficient for the fresstream surface. Substituting A.4 into A.10 yields,

$$\overline{C_{ff}} = \frac{2}{S_{W\infty}} \int_s \int_{zs}^{\ell} C_{f\infty} dz\, ds \qquad A.11$$

Using equation (3-40) and replacing the subscript e with ∞ according to section 3.7 yields,

$$\overline{C_{ff}} = \frac{2}{S_{w\infty}} \int_s \int_{zs}^{\ell} \frac{\sqrt{2\,\alpha_1 \alpha_2}}{\sqrt{R_{ex_\ell}}} \left(\frac{T_\infty}{T_w}\right)^{\frac{1-\omega}{2}} dz\, ds$$

$$= \frac{2}{S_{w\infty}} \frac{\sqrt{2\,\alpha_1 \alpha_2}}{\sqrt{\rho_\infty U_\infty / \mu_\infty}} \left(\frac{T_\infty}{T_w}\right)^{\frac{1-\omega}{2}} \int_s \int_{zs}^{\ell} \frac{dz\, ds}{\sqrt{z - z_s}}$$

$$= \frac{4}{S_{w\infty}} \frac{\sqrt{2\,\alpha_1 \alpha_2}}{\sqrt{\rho_\infty U_\infty / \mu_\infty}} \left(\frac{T_\infty}{T_w}\right)^{\frac{1-\omega}{2}} \int_s \sqrt{\ell - z_s}\, ds$$

$$= \frac{4}{S_{w\infty}} \frac{\sqrt{2\,\alpha_1 \alpha_2}}{\sqrt{\rho_\infty U_\infty / \mu_\infty}} \left(\frac{T_\infty}{T_w}\right)^{\frac{1-\omega}{2}} \ell^{1/2} \int_s \sqrt{1 - z_s/\ell}\, ds$$

$$= \frac{4}{S_{w\infty}} \frac{\sqrt{2\,\alpha_1 \alpha_2}}{\sqrt{\rho_\infty U_\infty \ell_w / \mu_\infty}} \left(\frac{T_\infty}{T_w}\right)^{\frac{1-\omega}{2}} \ell \sqrt{\ell_w/\ell} \int_s \sqrt{1 - z_s/\ell}\, ds \qquad \text{A.12}$$

Now recall from equation (3-28) that,

$$\ell_w = \ell(1 - R_0/\sigma) \qquad \text{A.13}$$

substituting yields,

$$\overline{C_{ff}} = \frac{4}{S_{w\infty}} \sqrt{2\,\alpha_1 \alpha_2} \left(\frac{T_\infty}{T_w}\right)^{\frac{1-\omega}{2}} \frac{\ell\sqrt{1 - R_0/\sigma}}{\sqrt{R_{ex_\infty}}} \int_s \sqrt{1 - z_s/\ell}\, ds \qquad \text{A.14}$$

We may now make the substitutions of equation (3-40) and equations A.1, A.2, and A.3 to yield

$$\overline{C_{ff}} = \frac{C_{f\infty}}{S_{w\infty}} 4 \sqrt{1 - R_0/\sigma}\, \ell^2 \delta \int_0^{Y_\ell} \sqrt{1 - R_\ell/\sigma}\, \sqrt{1 + (dX/dY)^2}\, dY \qquad \text{A.15}$$

Now substitue equation A.9 to give us the desired result equation (3-51)

$$\overline{C_{ff}} = \frac{C_{f_\infty}\, 2\sqrt{1-R_0/\sigma}\int_0^{Y_t}\sqrt{1-R_t/\sigma}\,\sqrt{1+(dX/dY)^2}\,dY}{\int_0^{Y_t}(1-R_t/\sigma)\sqrt{1+(dX/dY)^2}\,dY} \qquad A.16$$

APPENDIX B

Presented here are configurations that have the following parameters held fixed:

$$\Phi_1 = 60, \quad \delta = 8, \quad M = 10, \quad Rey = 1X10^6$$

The following parameters are varied:

R_0 from 0.2 to 0.4

b_4 from 0.0 to -3.0

The values of b_2 and b_6 are such that equation 2-13 and condition (iii) holds.

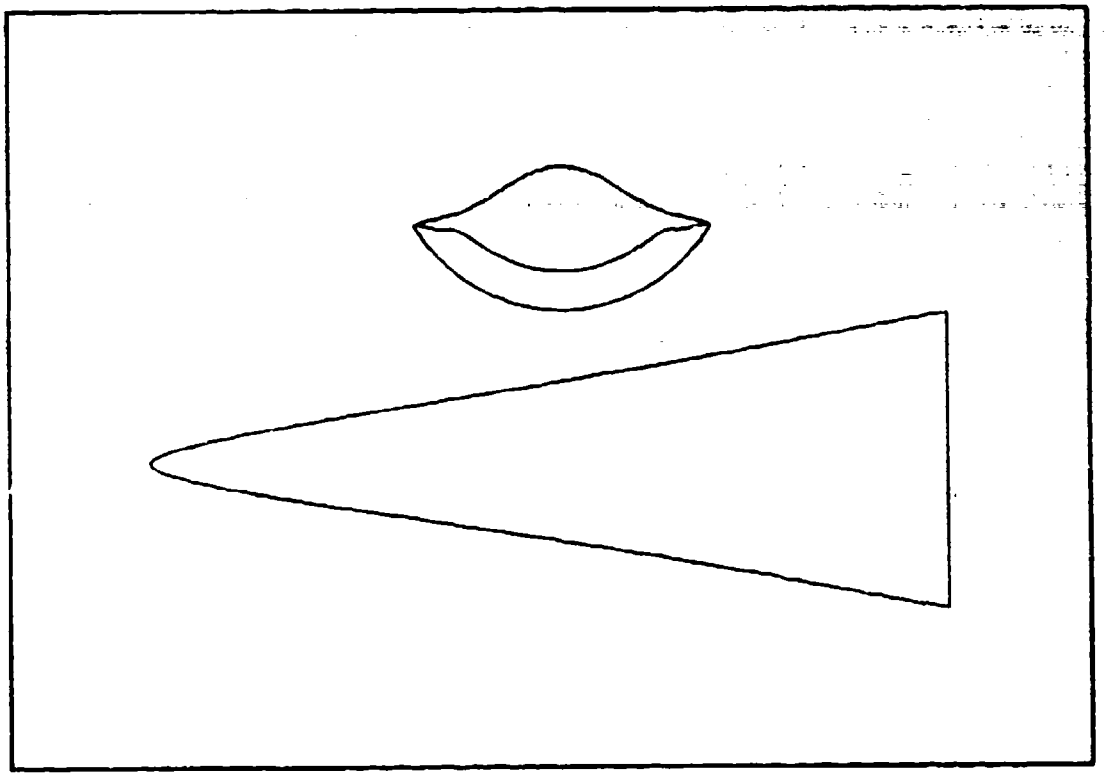

Figure B.1

Table B.1

Phi :60.0	Delta = 8.0	Mach :10.0	Rey = 0.10E+07	Gamma = 1.40
Y = 0.200 + 1.057 Y^2 + -1.000 Y^4 + 0.352 Y^6				
Cftav = 0.001947	CL = 0.043795		CD = 0.009691	
Sw/Sp = 2.152777	V^(2/3)/Sp = 0.212266		(L/D)vis = 4.519036	
Ab/Abi = 0.870890	V/Vi = 0.774453		Sp/Spi = 0.901519	
b/lw = 0.372398	SSD = 0.300503			

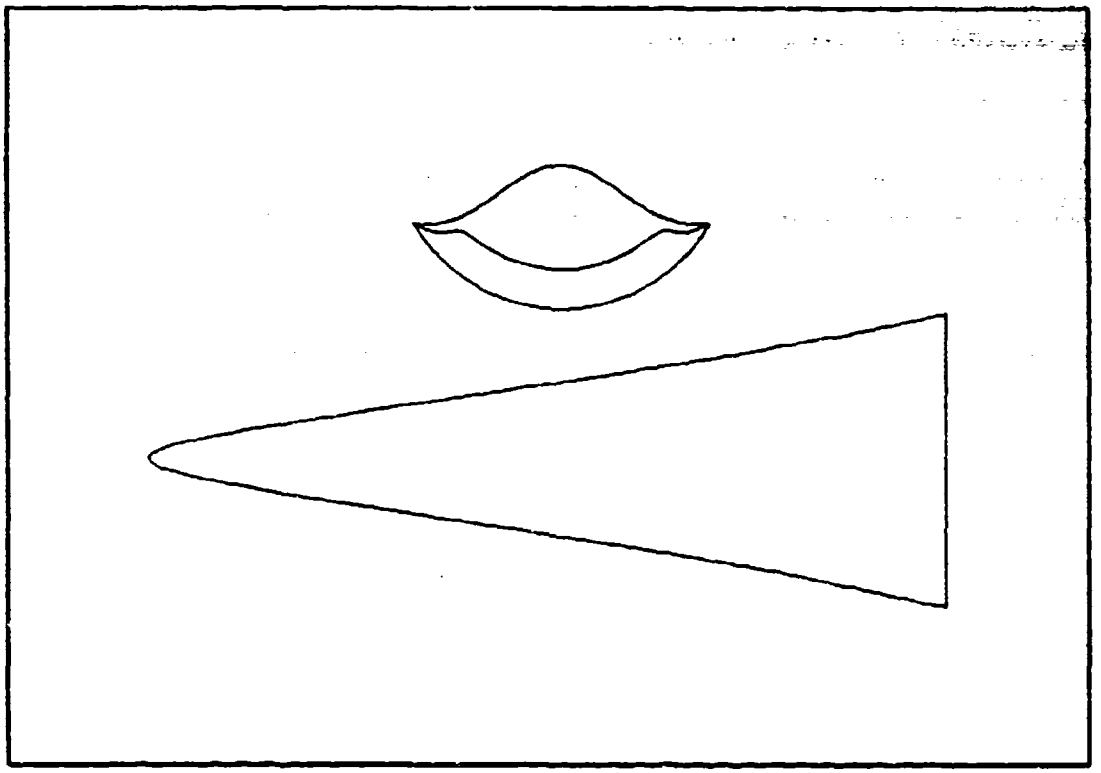

Figure B.2

Table B.2

Phi =60.0	Delta = 8.0	Mach =10.0	Rey = 0.10E+07	Gamma = 1.40
X = 0.200 + 1.171 Y^2 + -1.000 Y^4 + 0.283 Y^6				
Cftav = 0.001951	CL = 0.043789		CD = 0.009684	
Sw/Sp = 2.180042	V^(2/3)/Sp = 0.212500		(L/D)vis = 4.521998	
Ab/Abi = 0.835673	V/Vi = 0.743075		Sp/Spi = 0.876035	
b/lw = 0.372398	SSD = 0.300503			

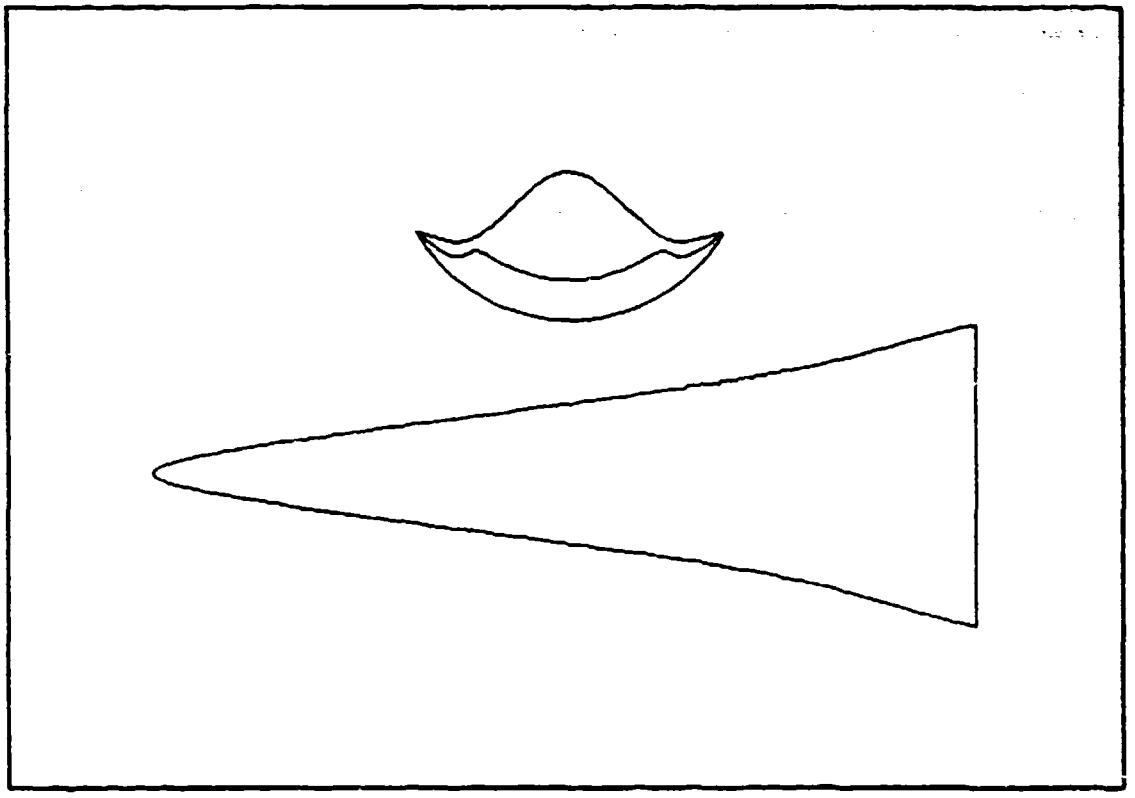

Figure B.3

Table B.3

Phi =60.0	Delta = 8.0	Mach =10.0	Rey = 0.10E+07	Gamma = 1.40
Y = 0.200 + 1.812 Y^2 + -2.000 Y^4 + 0.673 Y^6				
Cftav = 0.001973	CL = 0.043690	CD = 0.009756		
Sw/Sp = 2.263438	V^(2/3)/Sp = 0.211051	(L/D)vis = 4.478099		
Ab/Abi = 0.756626	V/Vi = 0.655907	Sp/Spi = 0.811647		
b/lw = 0.372398	SSD = 0.300503			

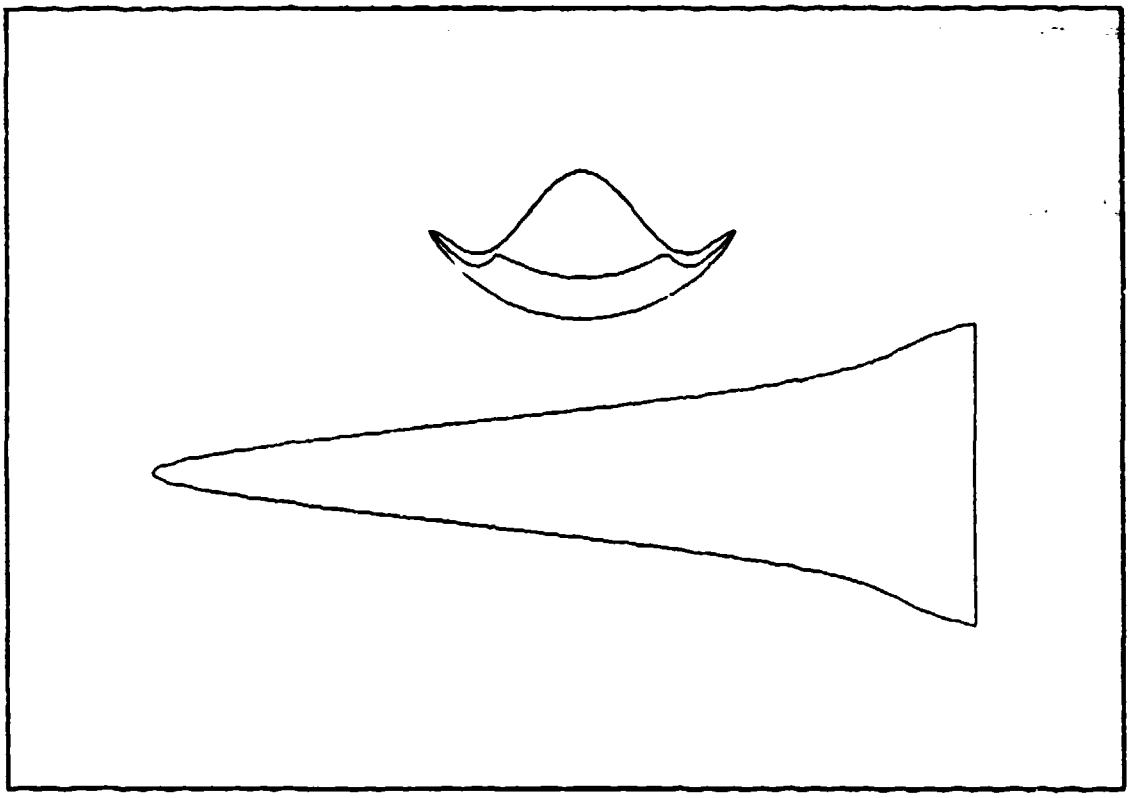

Figure B.4

Table B.4

Phi =60.0	Delta = 8.0	Mach =10.0	Rey = 0.10E+07	Gamma = 1.40
Y = 0.200 + 2.457 Y^2 + -3.000 Y^4 + 1.061 Y^6				
Cftav = 0.002009		CL = 0.043637		CD = 0.009994
Sw/Sp = 2.399271		V^(2/3)/S· = 0.212883		(L/D)vis = 4.366130
Ab/Abi = 0.676559		V/Vi = 0.579832		Sp/Spi = 0.741174
b/lw = 0.372398		SSD = 0.300503		

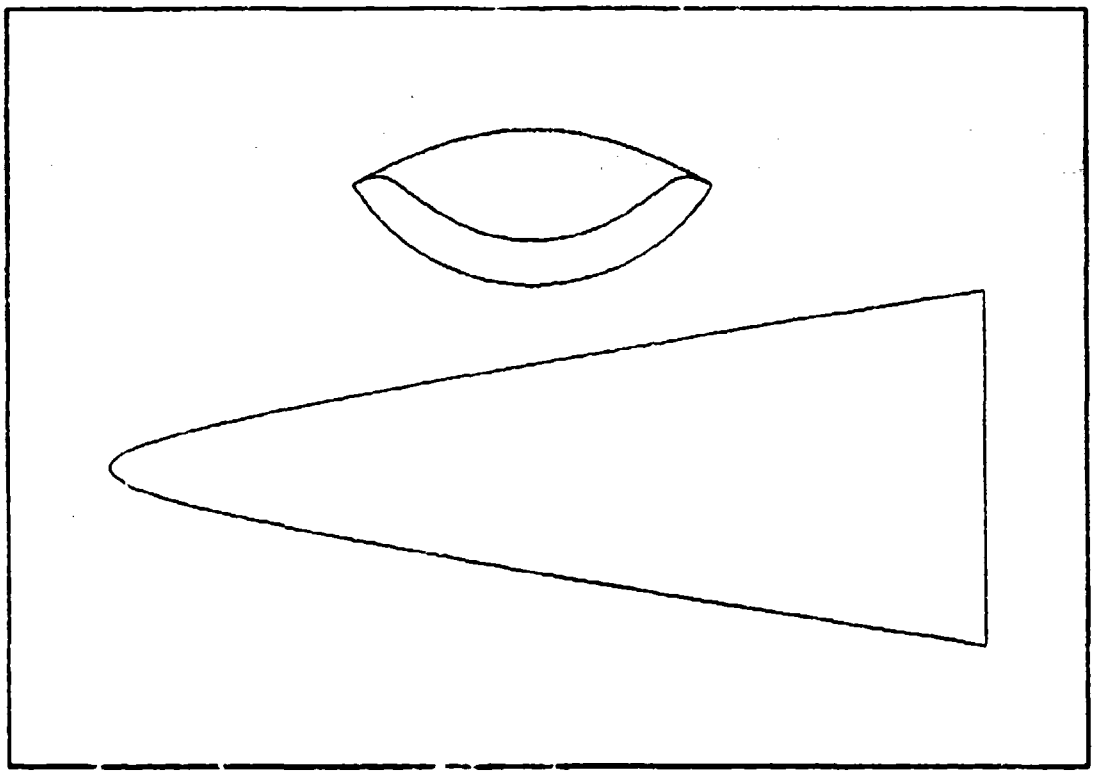

Figure B.5

Table B.5

Phi =60.0	Delta = 8.0	Mach =10.0	Rey = 0.10E+07	Gamma = 1.40
X = 0.300 + 0.297 Y^2 + 0.000 Y^4 + -0.013 Y^6				
Cftav = 0.001918	CL = 0.043599		CD = 0.008593	
Sw/Sp = 2.107515	V^(2/3)/Sp = 0.207946		(L/D)vis = 4.545040	
Ab/Abi = 0.878447	V/Vi = 0.743837		Sf = 0.895832	
b/lw = 0.409313	SSD = 0.290236			

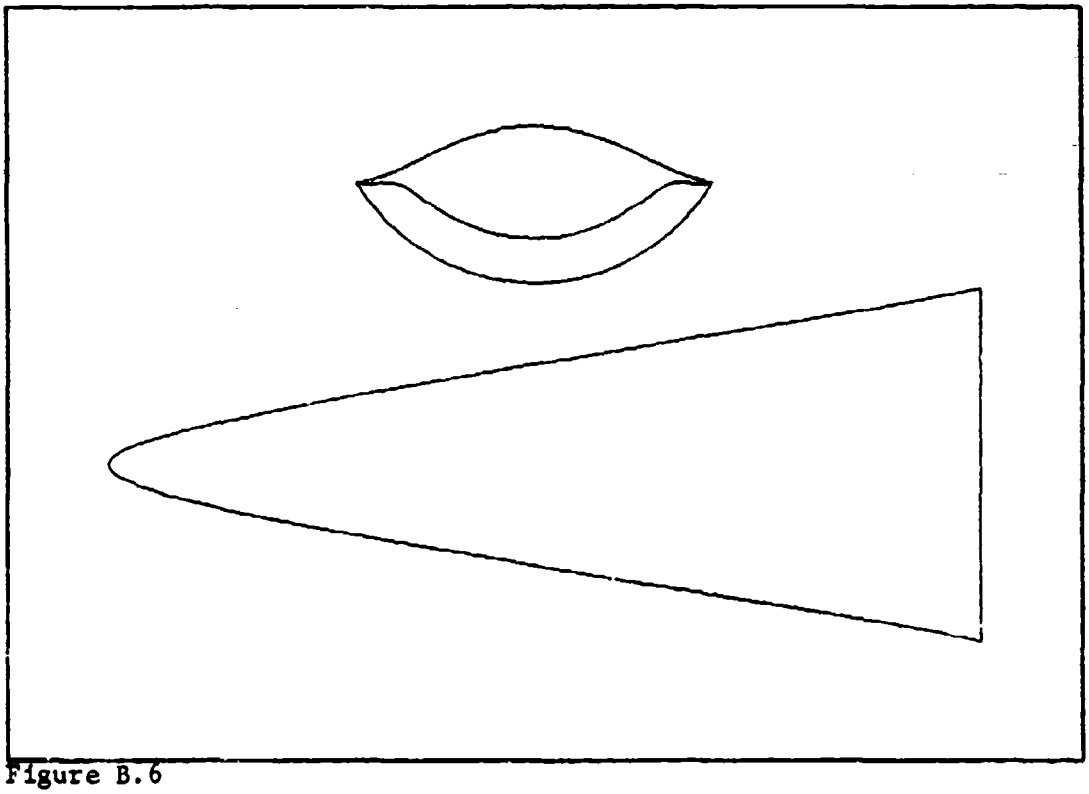

Figure B.6

Table B.6

Phi =60.0	Delta = 8.0	Mach =10.0	Rey = 0.10E+07	Gamma = 1.40
Y = 0.300 + 0.411 Y^2 + 0.000 Y^4 + -0.082 Y^6				
Cftav = 0.001918	CL = 0.043578		CD = 0.009516	
Sw/Sp = 2.106905	V^(2/3)/Sp = 0.207258		(L/D)vis = 4.579339	
Ab/Abi = 0.843229	V/Vi = 0.710444		Sp/Spi = 0.871710	
b/lw = 0.409313	SSD = 0.290236			

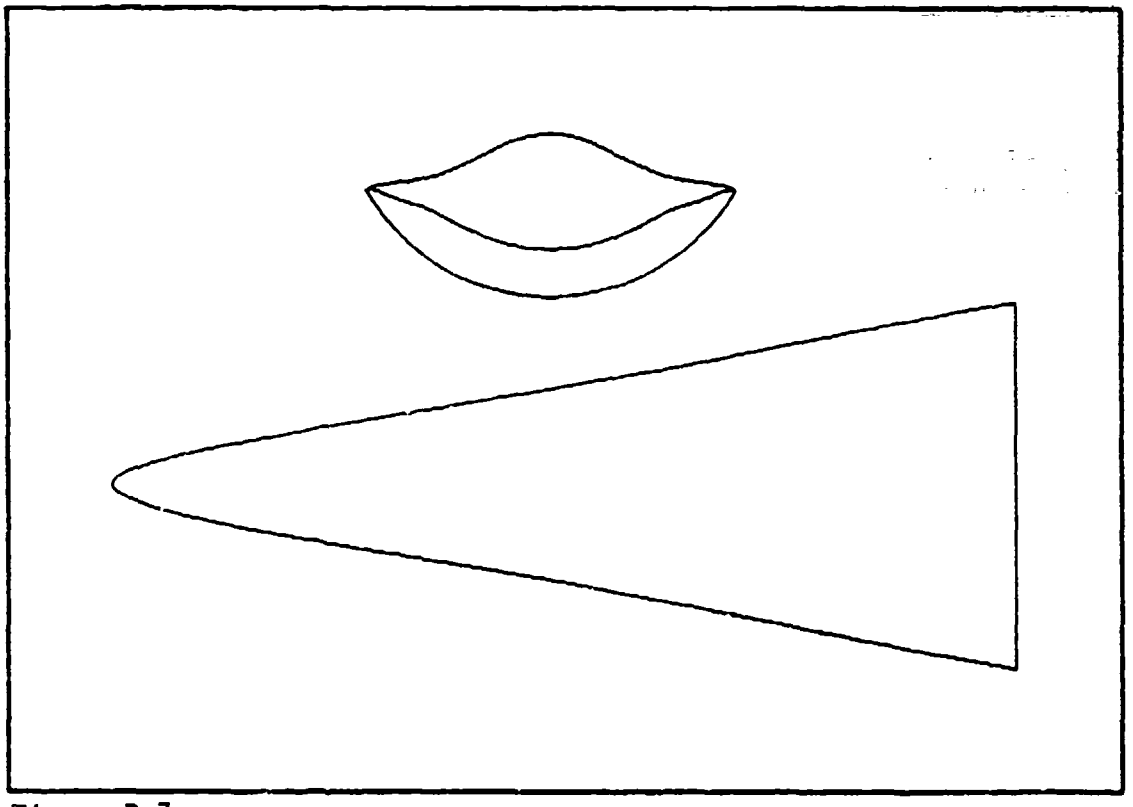

Figure B.7

Table B.7

Phi :60.0	Delta : 8.0	Mach :10.0	Rey : 0.10E+07	Gamma : 1.40
Y : 0.300 + 0.940 Y^2 + -1.000 Y^4 + 0.376 Y^6				
Cftav : 0.001932		CL : 0.043448	CD : 0.009450	
Sw/Sp : 2.102324		V^(2/3)/Sp : 0.203256	(L/D)vis : 4.597868	
Ab/Abi : 0.798890		V/Vi : 0.647930	Sp/Spi : 0.835926	
b/lw : 0.409313		SSD : 0.256236		

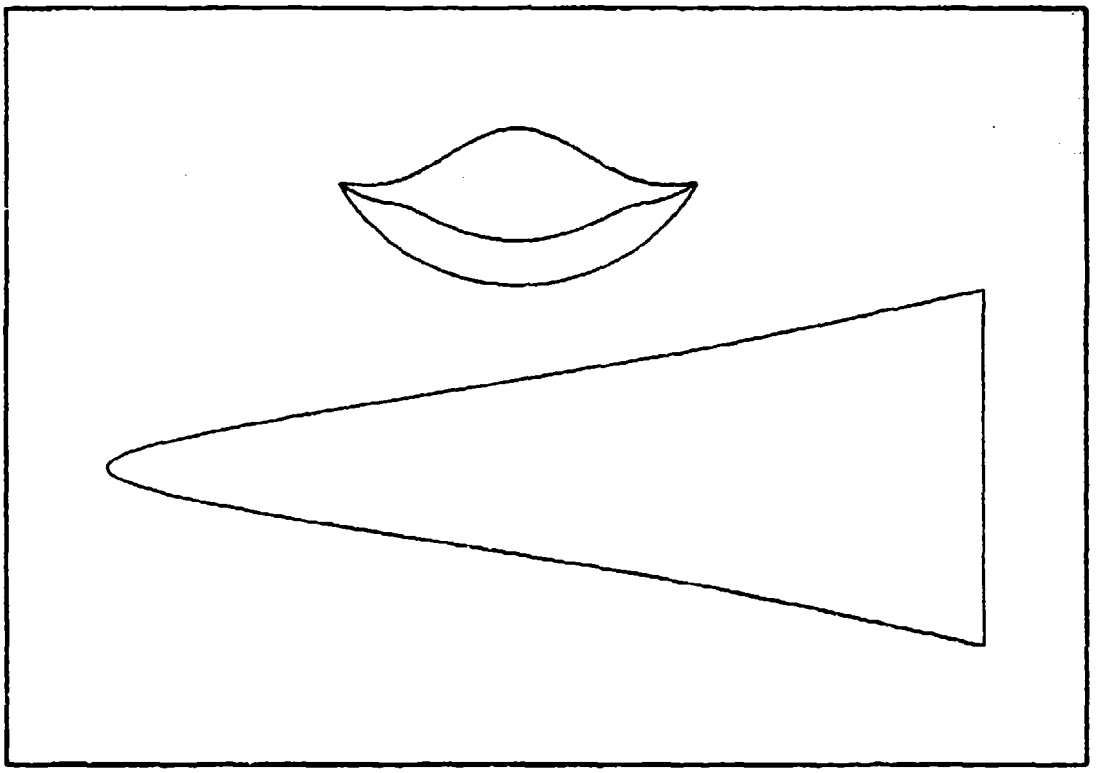

Figure B.8

Table B.8

Phi =60.0	Delta = 8.0	Mach =10.0	Rey = 0.10E+07	Gamma = 1.40
Y = 0.300 + 1.056 Y^2 + -1.000 Y^4 + 0.306 Y^6				
Cftav = 0.001939	CL = 0.043437		CD = 0.009431	
Sw/Sp = 2.121517	V^(2/3)/Sp = 0.203593		(L/D)vis = 4.605786	
Ab/Abi = 0.763162	V/Vi = 0.818193		Sp/Spi = 0.808807	
b/lw = 0.409313	SSD = 0.290236			

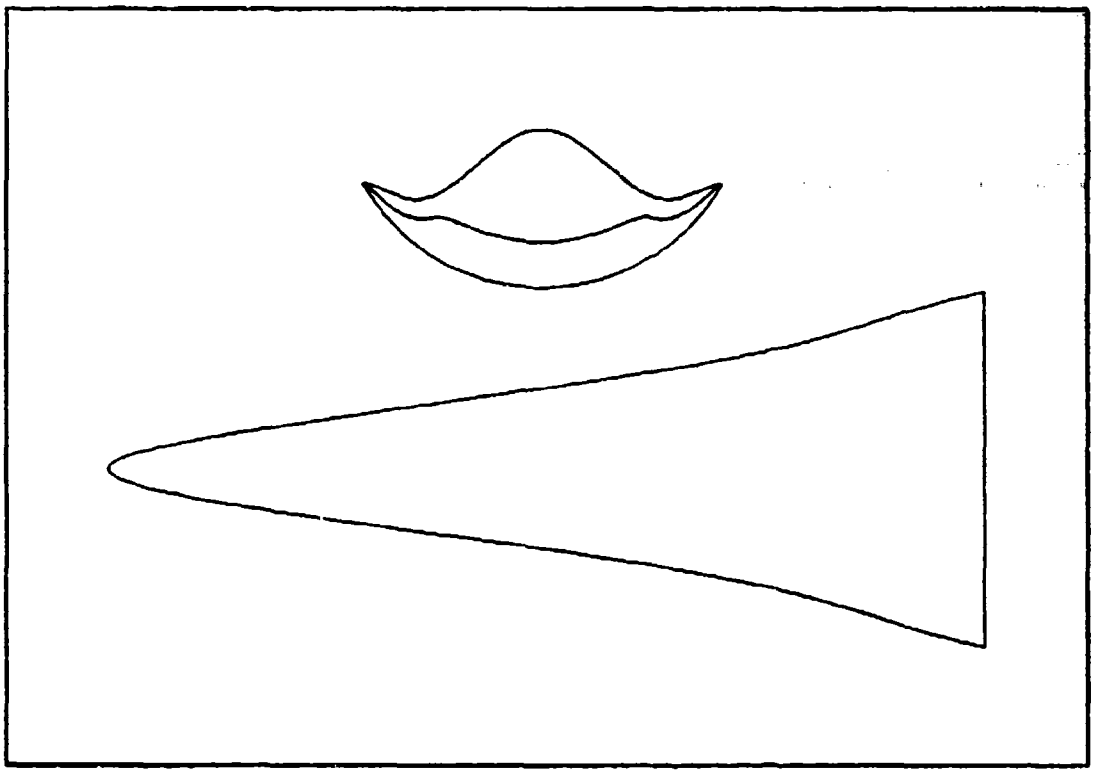

Figure B.9

Table B.9

Phi =60.0	Delta = 8.0	Mach =10.0	Rey = 0.10E+07	Gamma = 1.40
Y = 0.300 + 1.697 Y^2 + -2.000 Y^4 + 0.696 Y^6				
Cftav = 0.001874	CL = 0.043324		CD = 0.009531	
Sw/Sp = 2.200773	V^(2/3)/Sp = 0.202616		(L/D)vis = 4.545457	
Ab/Abi = 0.684115	V/Vi = 0.538133		Sp/Spi = 0.740933	
b/lw = 0.409313	SBD = 0.290236			

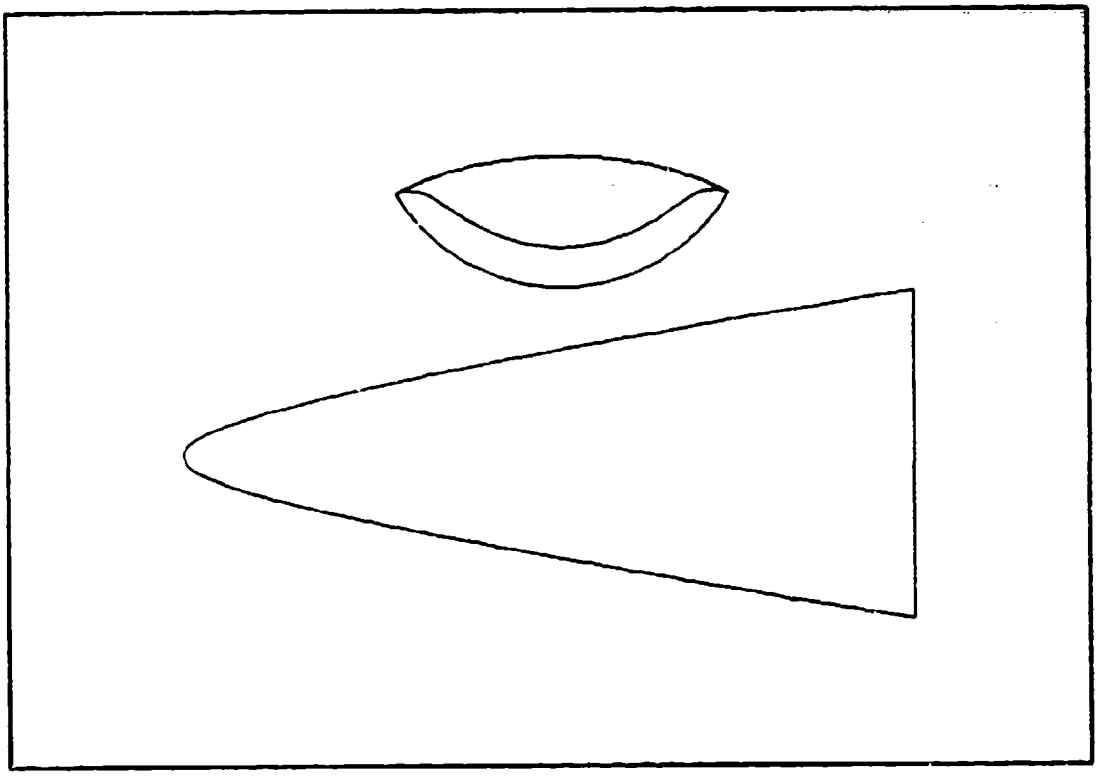

Figure B.10

Table B.10

Phi =60.0	Delta = 8.0	Mach =10.0	Rey = 0.10E+07	Gamma = 1.40
I = 0.400 + 0.180 Y^2 + 0.000 Y^4 + 0.011 Y^6				
Cftav = 0.001891		CL = 0.043239	CD = 0.009377	
Sw/Sp = 2.077541		V^(2/3)/Sp = 0.198999	(L/D)vis = 4.611255	
Ab/Abi = 0.806447		V/Vi = 0.821062	Sp/Spi = 0.830038	
b/lw = 0.454352		SSD = 0.276033		

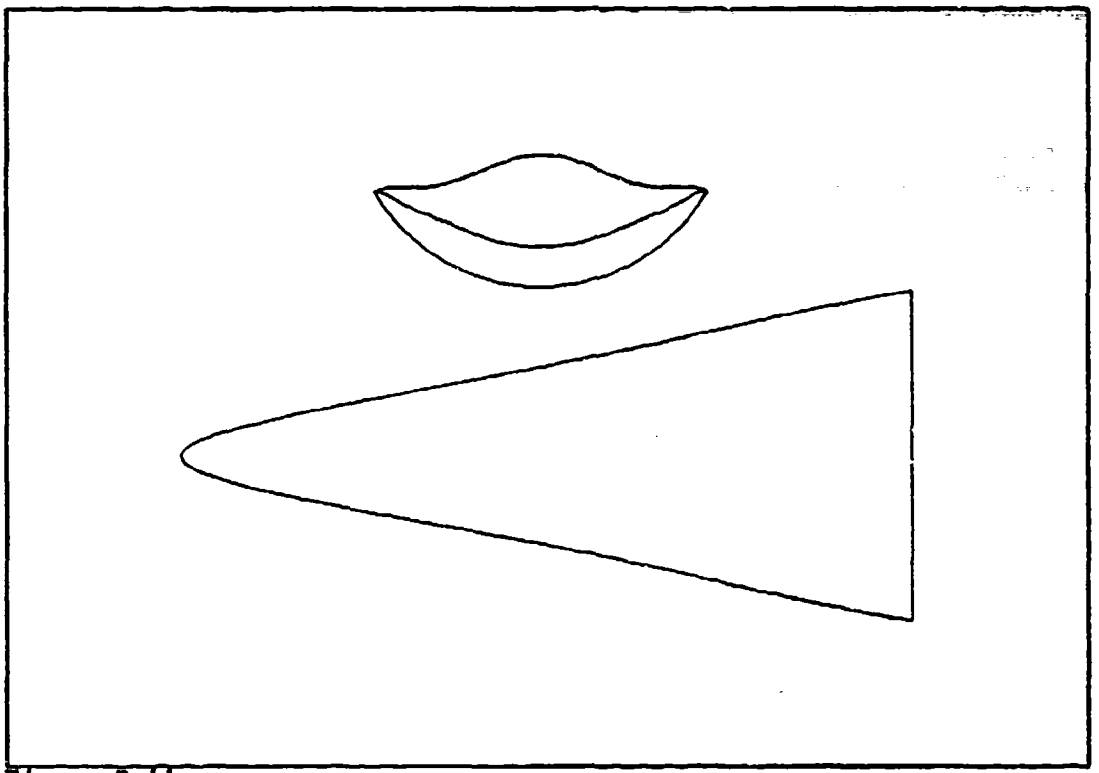

Figure B.11

Table B.11

Phi =60.0	Delta = 8.0	Mach =10.0	Rey = 0.10E+07	Gamma = 1.40
I = 0.400 + 0.829 Y^2 + -1.000 Y^4 + 0.396 Y^6				
Cftav = 0.001927	CL = 0.043063		CD = 0.009289	
Sw/Sp = 2.077201	V^(2/3)/Sp = 0.194364		(L/D)vis = 4.635796	
Ab/Abi = 0.724848	V/Vi = 0.530231		Sp/Spi = 0.764733	
b/lw = 0.454352	SSD = 0.276033			

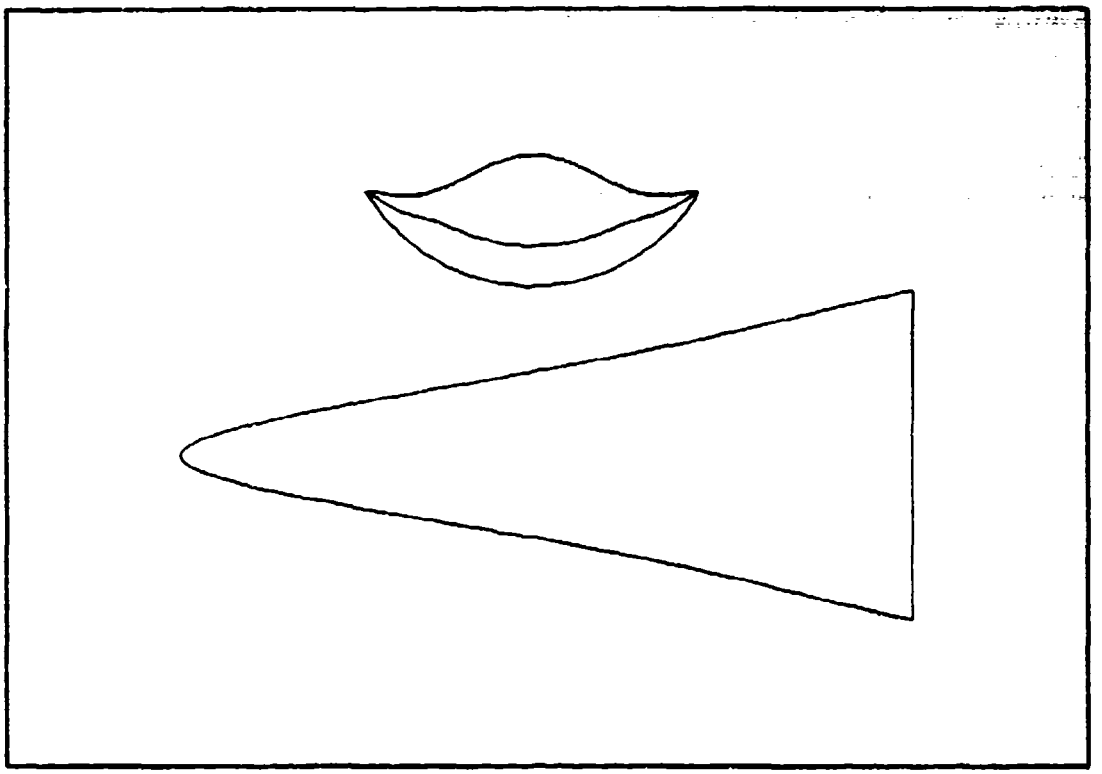

Figure B.12

Table B.12

Phi =60.0	Delta = 8.0	Mach =10.0	Rey = 0.10E+07	Gamma = 1.40
Y = 0.400 + 0.938 Y^2 + -1.000 Y^4 + 0.330 Y^6				
Cftav = 0.001937	CL = 0.043048		CD = 0.009268	
Sw/Sp = 2.089441	V^(2/3)/Sp = 0.194770		(L/D)vis = 4.644742	
Ab/Abi = 0.691162	V/Vi = 0.504332		Sp/Spi = 0.736157	
b/lw = 0.454352	SSD = 0.276033			

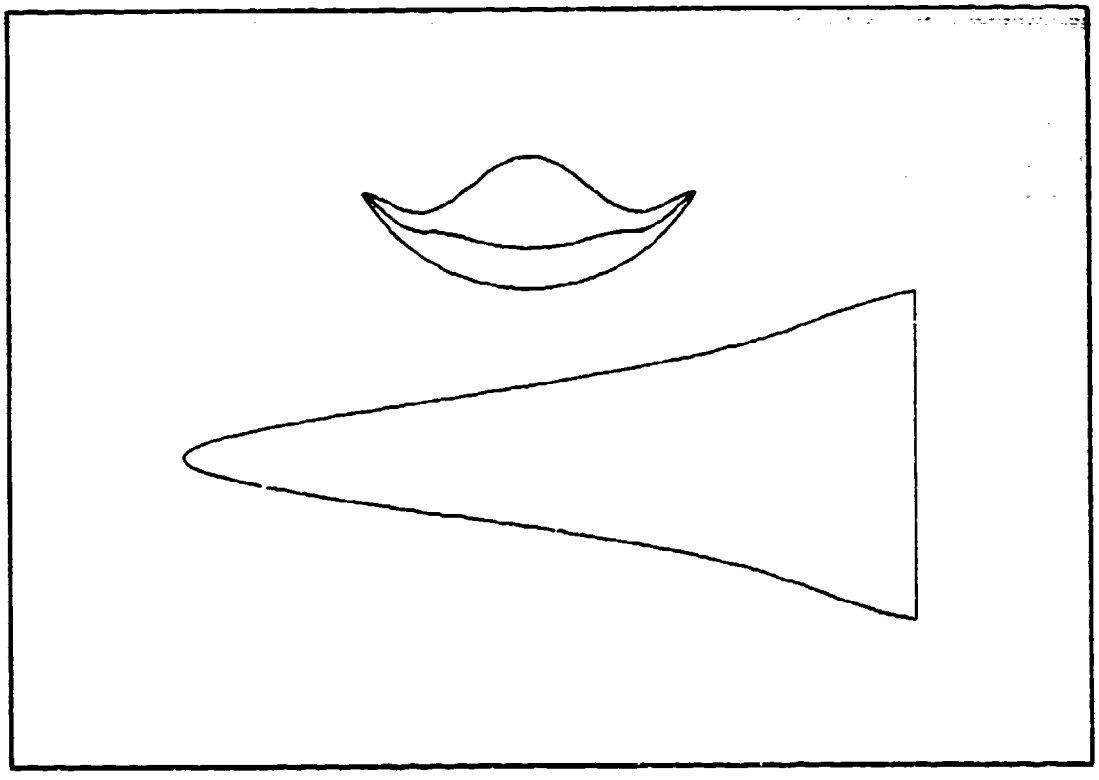

Figure B.13

Table B.13

Phi =60.0	Delta = 8.0	Mach =10.0	Rey = 0.10E+07	Gamma = 1.40
Y = 0.400 + 1.577 Y^2 + -2.000 Y^4 + 0.721 Y^6				
Cftav = 0.001987	CL = 0.042925		CD = 0.009398	
Sw/Sp = 2.164243	V^(2/3)/Sp = 0.194121		(L/D)vis = 4.567488	
Ab/Abi = 0.612625	V/Vi = 0.432013		Sp/Spi = 0.668012	
b/lw = 0.454852	SSD = 0.276033			

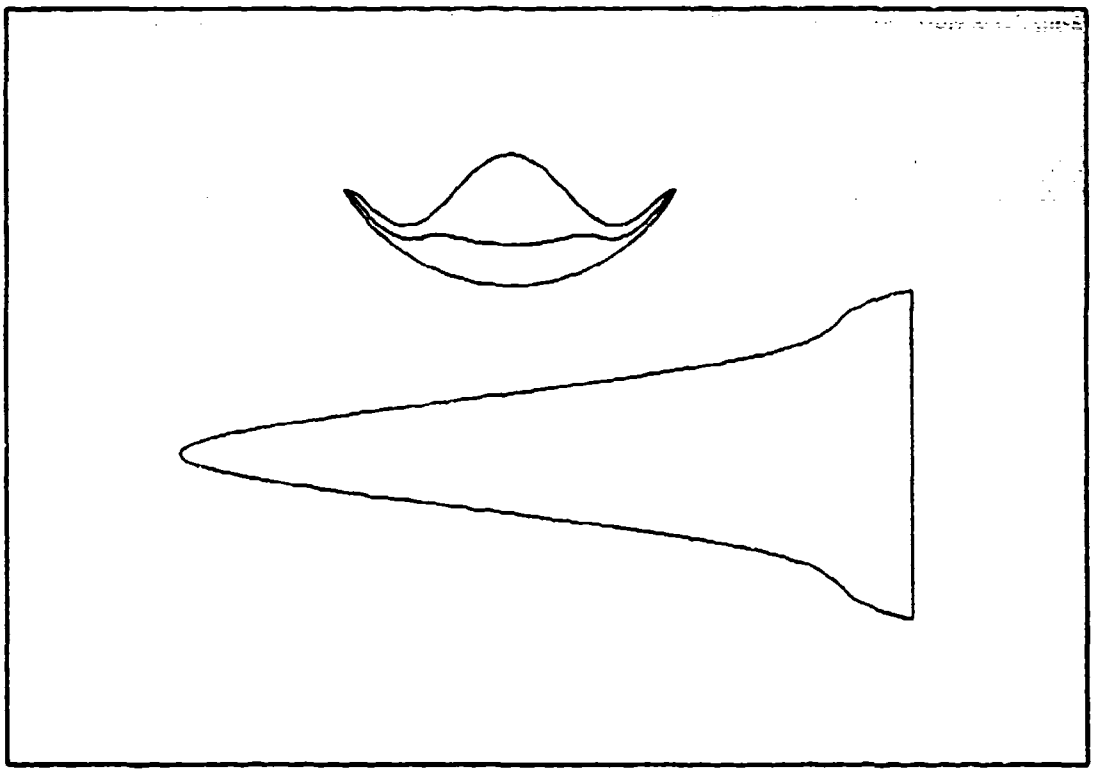

Figure B.14

Table B.14

Phi =60.0	Delta = 8.0	Mach =10.0	Rey = 0.10E+07	Gamma = 1.40
Y = 0.400 + 2.220 Y^2 + -3.000 Y^4 + 1.110 Y^6				
Cftav = 0.002045	CL = 0.042875		CD = 0.009654	
Sw/Sp = 2.281403	V^(2/3)/Sp = 0.197759		(L/D)vis = 4.441051	
Ab/Abi = 0.533069	V/Vi = 0.371700		Sp/Spi = 0.593176	
b/lw = 0.454352	SSD = 0.276033			

APPENDIX C

Presented here are configurations that have the following parameters held fixed:

$$\Phi_1 = 50, \quad \delta = 8, \quad M = 10, \quad Rey = 1X10^6$$

The following parameters are varied:

R_0 from 0.3 to 0.7

b_4 from 0.0 to -3.0

The values of b_2 and b_6 are such that equation 2-13 and condition (iii) holds.

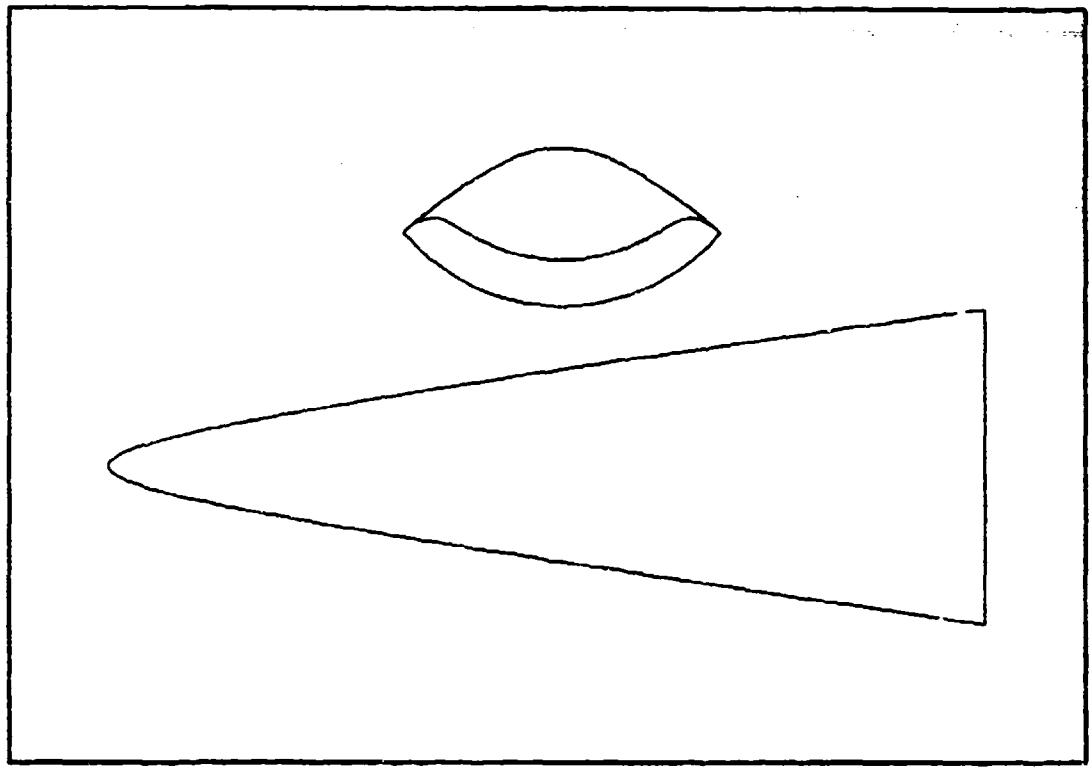

Figure C.1

Table C.1

Phi =50.0	Delta = 8.0	Mach =10.0	Rey = 0.10E+07	Gamma = 1.40
Y = 0.300 + 0.792 Y^2 + -0.400 Y^4 + 0.147 Y^6				
Cftav = 0.001905	CL = 0.043800		CD = 0.009381	
Sw/Sp = 2.154487	V^(2/3)/Sp = 0.210144		(L/D)vis = 4.647765	
Ab/Abi = 0.885660	V/Vi = 0.754987		Sp/Spi = 0.896308	
b/lw = 0.362059	SSD = 0.290236			

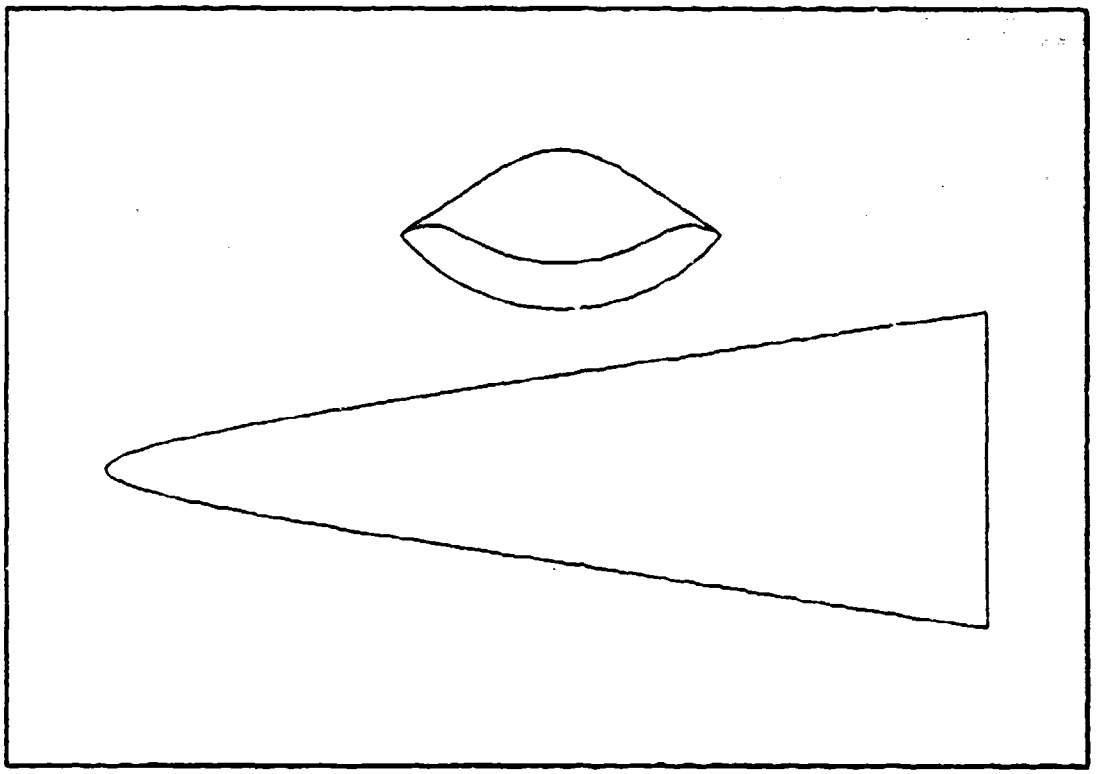

Figure C.2

Table C.2

Phi =50.0	Delta = 8.0	Mach =10.0	Rey = 0.10E+07	Gamma = 1.40
Y = 0.300 + 0.993 T^2 + -0.800 T^4 + 0.346 T^6				
Cftav = 0.001906	CL = 0.043558		CD = 0.009344	
Sw/Sp = 2.151257	V^(2/3)/Sp = 0.209198		(L/D)vis = 4.661775	
Ab/Abi = 0.865016	V/Vi = 0.729159		Sp/Spi = 0.879708	
b/lw = 0.362059	SSD = 0.290236			

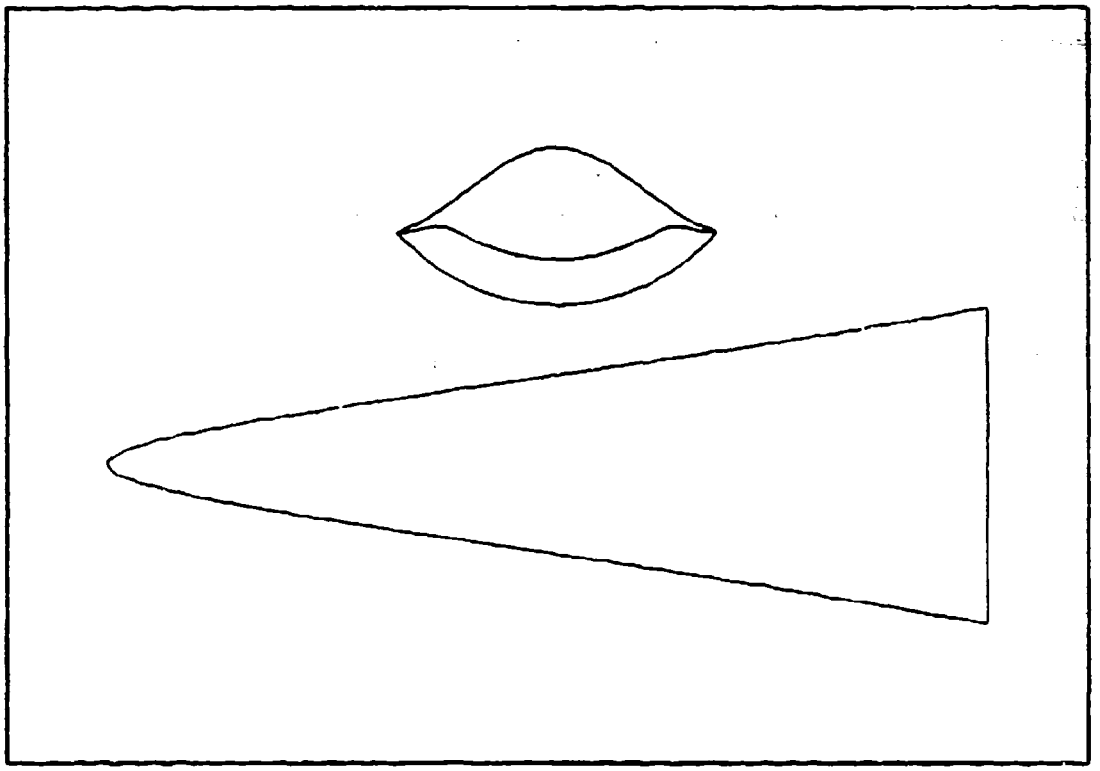

Figure C.3

Table C.3

Phi =50.0	Delta = 8.0	Mach =10.0	Rey = 0.10E+07	Gamma = 1.40
Y = 0.300 + 1.100 Y^2 + -0.800 Y^4 + 0.240 Y^6				
Cftav = 0.001906	CL = 0.043545		CD = 0.009335	
Sw/Sp = 2.167182	V^(2/3)/Sp = 0.209543		(L/D)vis = 4.664793	
Ab/Abi = 0.837507	V/Vi = 0.703896		Sp/Spi = 0.857857	
b/lw = 0.362059	SSD = 0.290236			

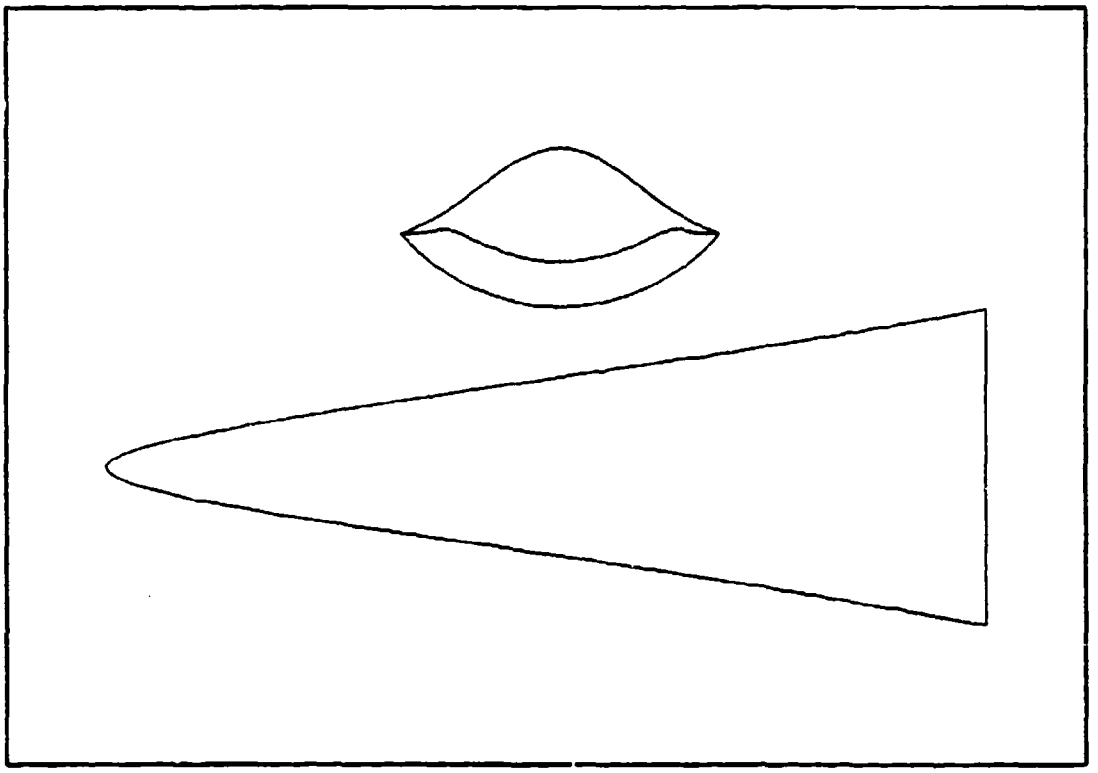

Figure C.4

Table C.4

Phi =50.0	Delta = 8.0	Mach =10.0	Rey = 0.10E+07	Gamma = 1.40
Y = 0.300 + 1.201 Y^2 + -1.000 Y^4 + 0.339 Y^6				
Cftav = 0.001907		CL = 0.043525	CD = 0.009328	
Sw/Sp = 2.170346		V^(2/3)/Sp = 0.209224	(L/D)vis = 4.666131	
Ab/Abi = 0.827055		V/Vi = 0.691601	Sp/Spi = 0.849130	
b/lw = 0.362059		SSD = 0.290236		

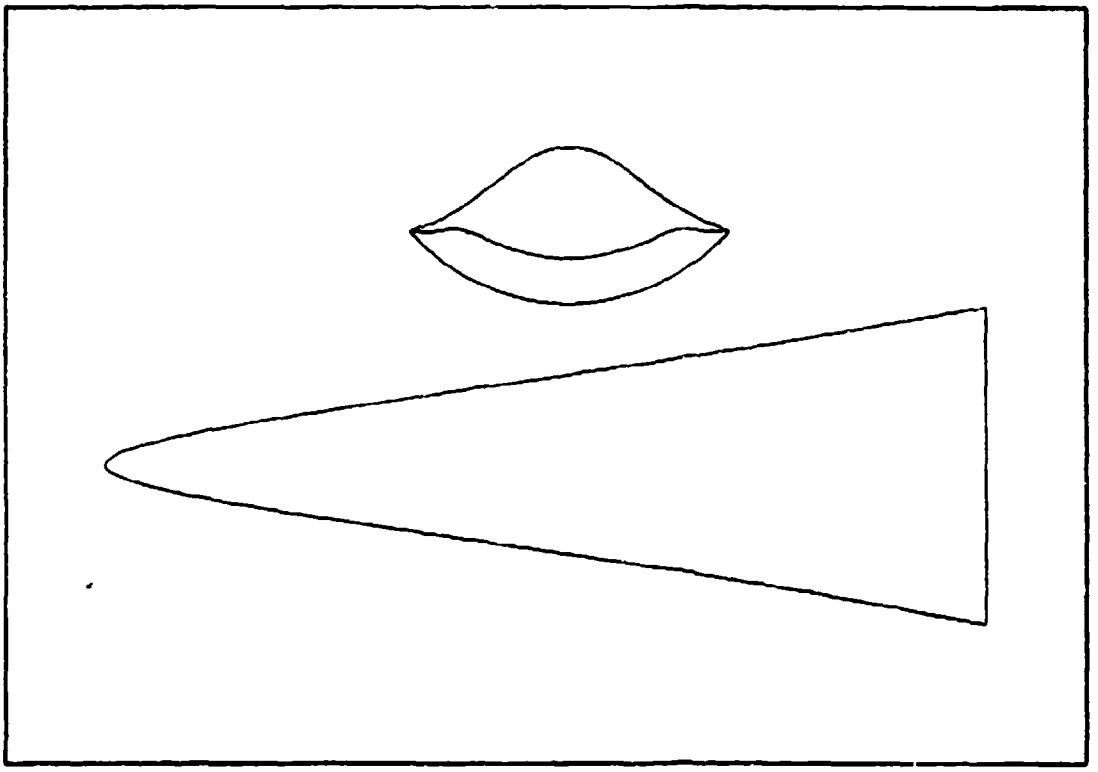

Figure C.5

Table C.5

Phi =50.0	Delta = 8.0	Mach =10.0	Rey = 0.10E+07	Gamma = 1.40
X = 0.300 + 1.302 Y^2 + -1.200 Y^4 + 0.438 Y^6				
Cftav = 0.001908	CL = 0.043507		CD = 0.009325	
Sw/Sp = 2.174980	V^(2/3)/Sp = 0.208944		(L/D)vis = 4.665699	
Ab/Abi = 0.816603	V/Vi = 0.879505		Sp/Spi = 0.840323	
b/lw = 0.362059	SSD = 0.290236			

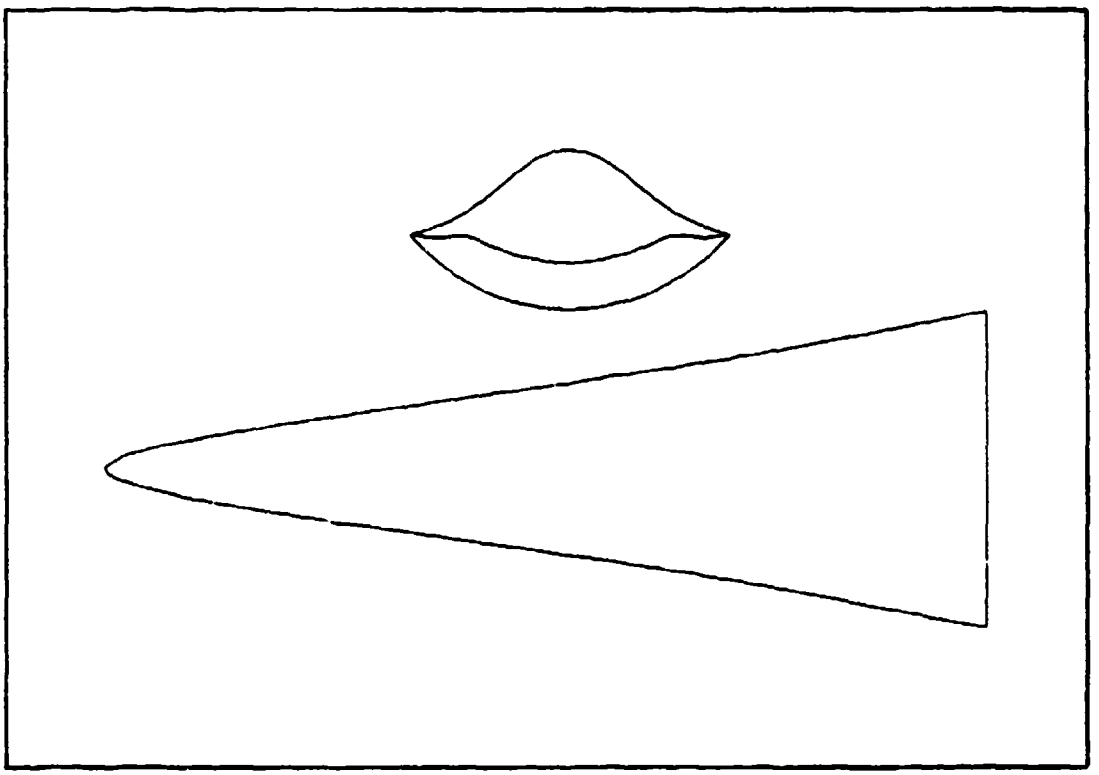

Figure C.6

Table C.6

Phi =50.0	Delta = 8.0	Mach =10.0	Rey = 0.10E+07	Gamma = 1.40
Y = 0.300 + 1.503 Y^2 + -1.600 Y^4 + 0.637 Y^6				
Cftav = 0.001911	CL = 0.043470	CD = 0.009329		
Sw/Sp = 2.187994	V^(2/3)/Sp = 0.208499	(L/D)vis = 4.659933		
Ab/Abi = 0.795958	V/Vi = 0.656134	Sp/Spi = 0.822696		
b/lw = 0.362059	SSD = 0.290236			

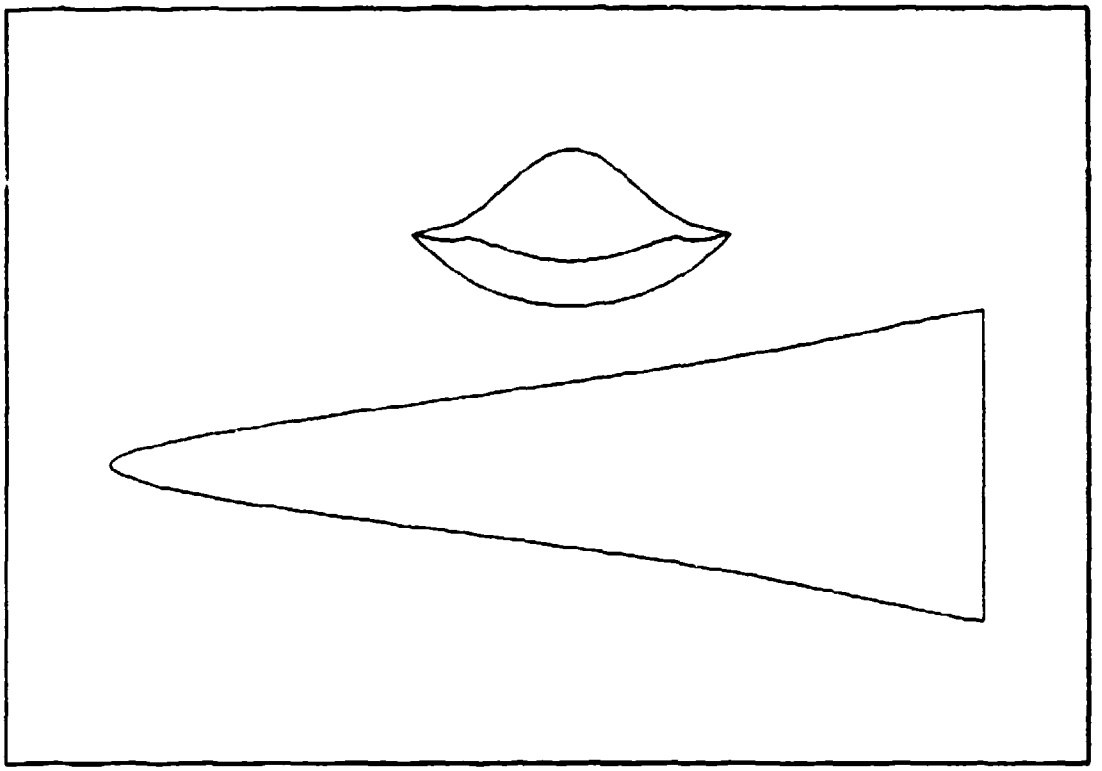

Figure C.7

Table C.7

Phi =50.0	Delta = 8.0	Mach =10.0	Rey = 0.10E+07	Gamma = 1.40
Y = 0.300 + 1.704 Y^2 + -2.000 Y^4 + 0.836 Y^6				
Cftav = 0.001915	CL = 0.043437	CD = 0.009345		
Sw/Sp = 2.205945	V^(2/3)/Sp = 0.208223	(L/D)vis = 4.648007		
Ab/Abi = 0.775313	V/Vi = 0.633565	Sp/Spi = 0.804787		
b/lw = 0.362059	SSD = 0.290236			

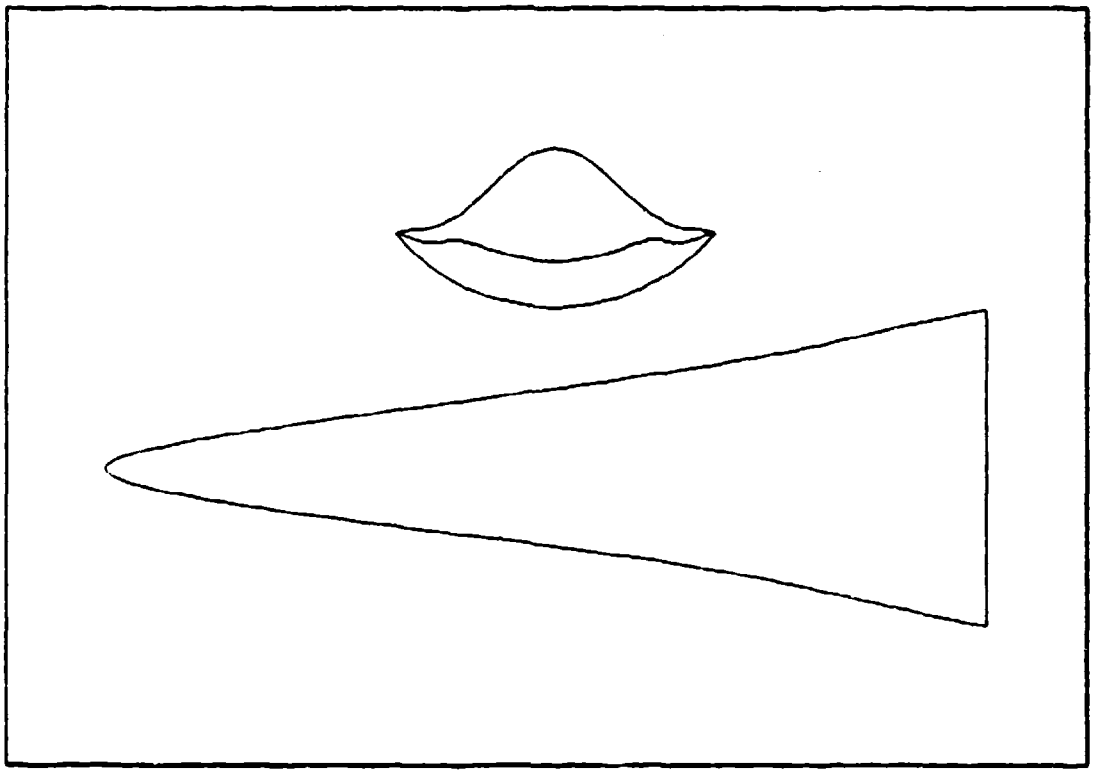

Figure C.8

Table C.8

Phi =50.0	Delta = 8.0	Mach =10.0	Rey = 0.10E+07	Gamma = 1.40
X = 0.300 + 1.905 Y^2 + -2.400 Y^4 + 1.035 Y^6				
Cftav = 0.001921	CL = 0.043405		CD = 0.009374	
Sw/Sp = 2.228375	V^(2/3)/Sp = 0.208129		(L/D)vis = 4.630399	
Ab/Abi = 0.754669	V/V1 = 0.611813		Sp/Spi = 0.786616	
b/lw = 0.362059	SSD = 0.290236			

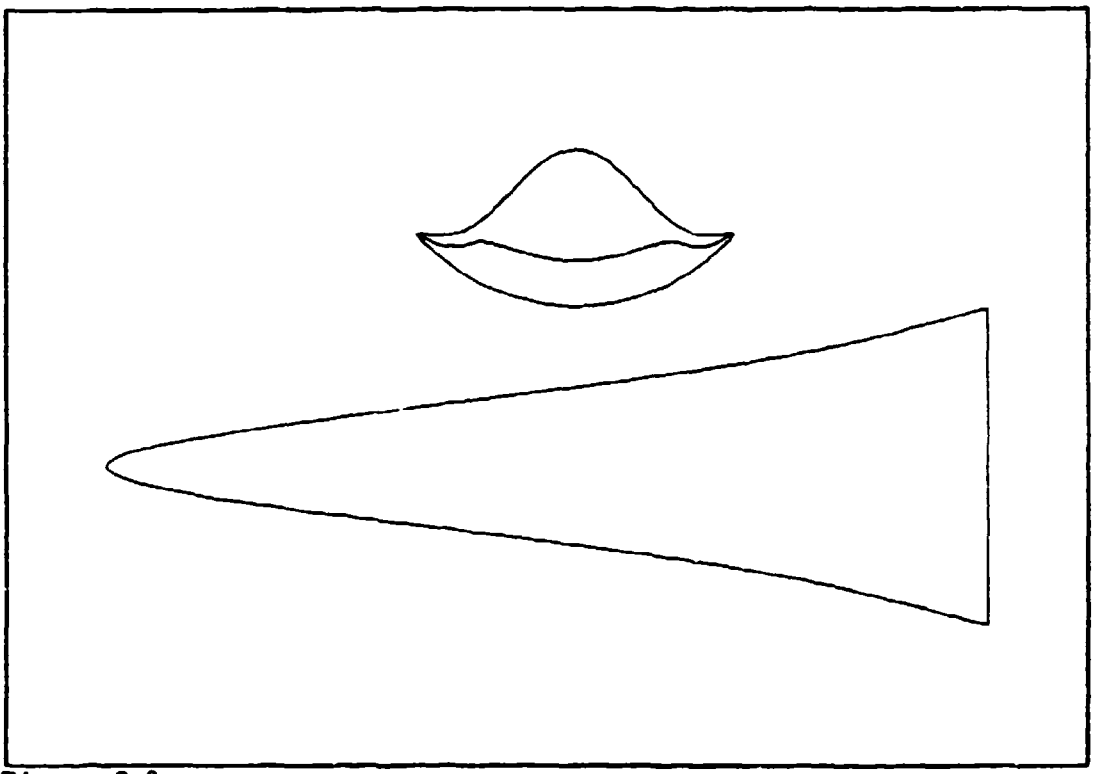

Figure C.9

Table C.9

Phi =50.0	Delta = 8.0	Mach =10.0	Rey = 0.10E+07	Gamma = 1.40
Y = 0.300 + 2.013 Y^2 + -2.400 Y^4 + 0.928 Y^6				
Cftav = 0.001926		CL = 0.043415		CD = 0.009424
Sw/Sp = 2.264482		V^(2/3)/Sp = 0.209875		(L/D)vis = 4.606875
Ab/Abi = 0.726901		V/Vi = 0.591549		Sp/Spi = 0.762748
b/lw = 0.362059		SSD = 0.290238		

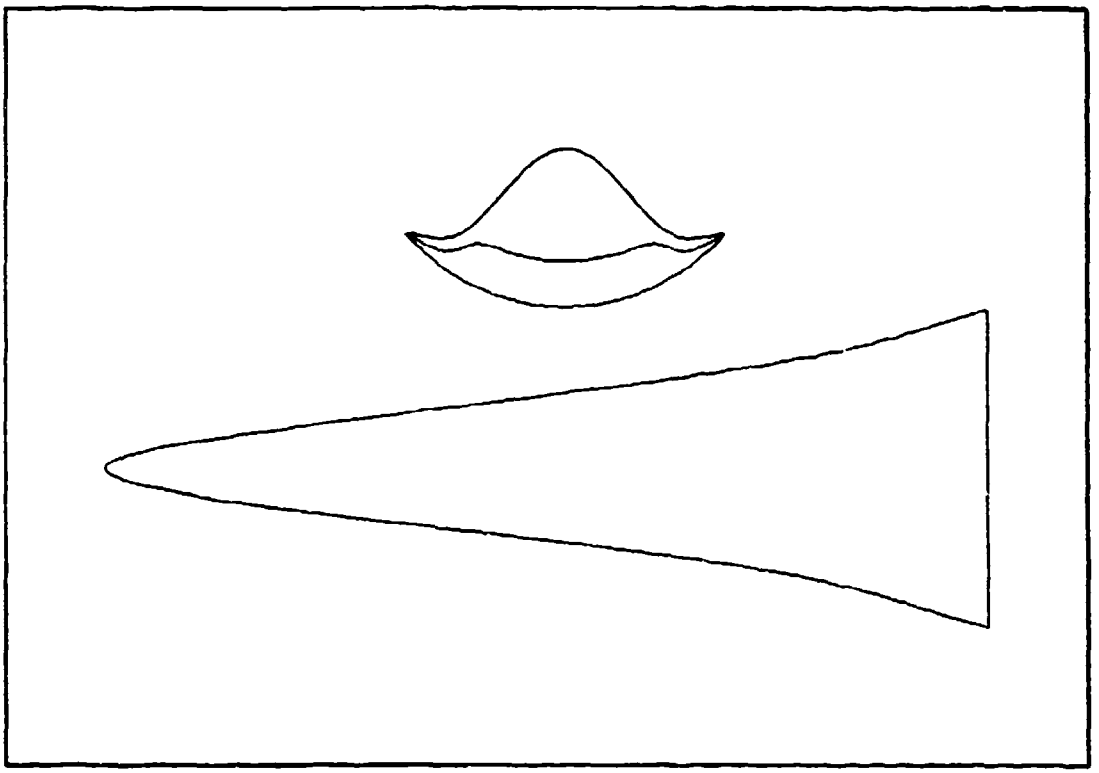

Figure C.10

Table C.10

Phi :50.0	Delta = 8.0	Mach :10.0	Rey = 0.10E+07	Gamma = 1.40
Y = 0.300 + 2.312 Y^2 + -3.000 Y^4 + 1.229 Y^6				
Cftav = 0.001936	CL = 0.043382	CD = 0.009498		
Sw/Sp = 2.308484	V^(2/3)/Sp = 0.210525	(L/D)vis = 4.567349		
Ab/Abi = 0.696582	V/Vi = 0.562402	Sp/Spi = 0.735208		
b/lw = 0.362059	SSD = 0.290238			

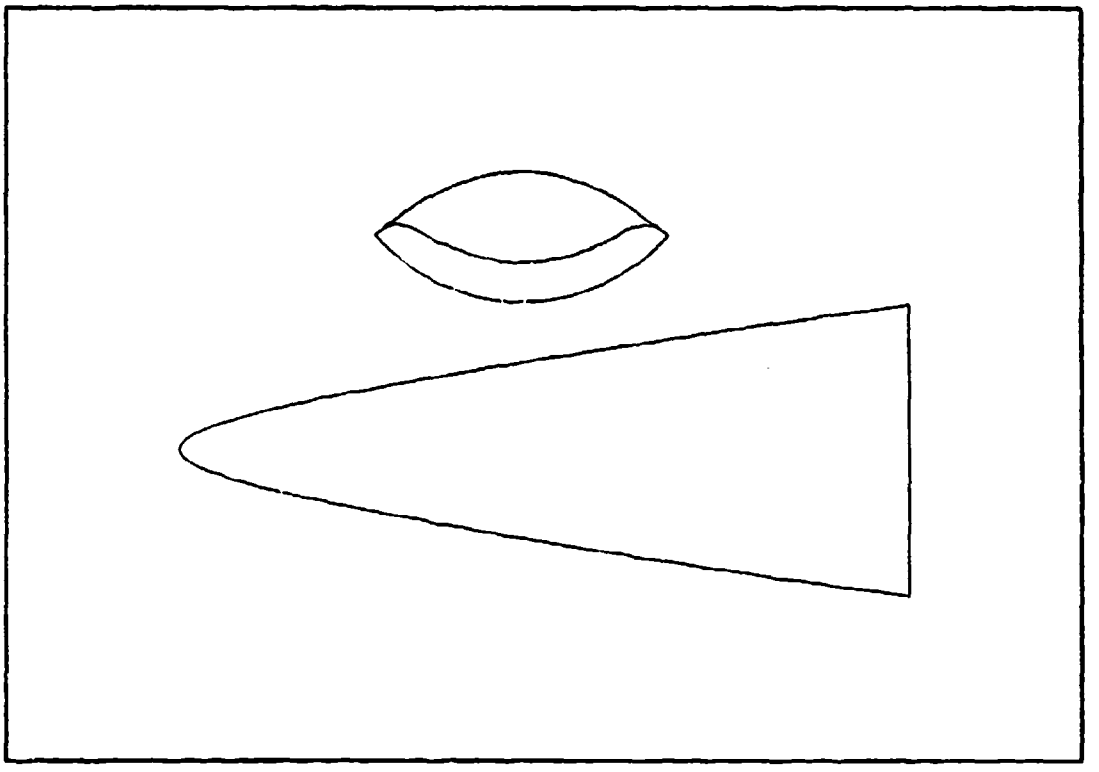

Figure C.11

Table C.11

Phi :50.0	Delta = 8.0	Mach :10.0	Rey = 0.10E+07	Gamma = 1.40
Y = 0.400 + 0.441 Y^2 + 0.000 Y^4 + -0.002 Y^6				
Cftav = 0.001882	CL = 0.043288	CD = 0.009180		
Sw/Sp = 2.106585	V^(2/3)/Sp = 0.202395	(L/D)vis = 4.713079		
Ab/Abi = 0.829852	V/Vi = 0.649641	Sp/Spi = 0.841907		
b/lw = 0.401898	SSD = 0.276033			

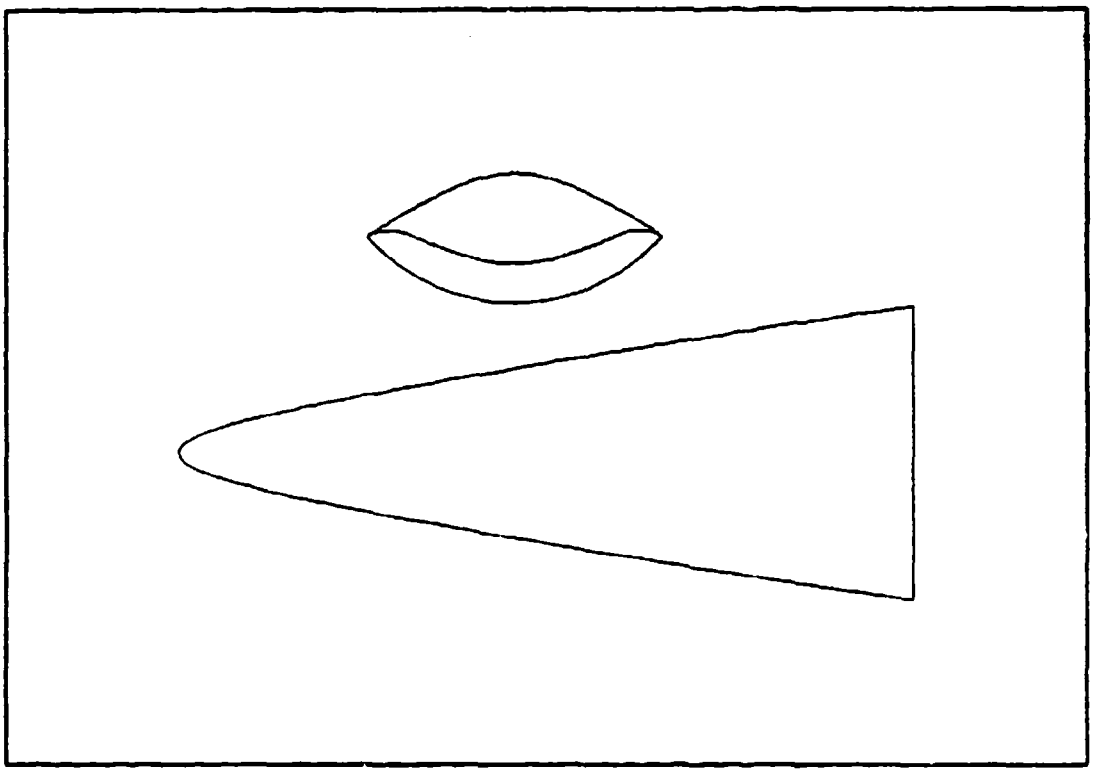

Figure C.12

Table C.12

Phi =50.0	Delta = 8.0	Mach =10.0	Rey = 0.10E+07	Gamma = 1.40
I = 0.400 + 0.642 Y^2 + -0.400 Y^4 + 0.197 Y^6				
Cftav = 0.001887	CL = 0.043220		CD = 0.009145	
Sw/Sp = 2.093222	V^(2/3)/Sp = 0.201318		(L/D)vis = 4.726161	
Ab/Abi = 0.809208	V/Vi = 0.624954		Sp/Spi = 0.824831	
b/lw = 0.401898	SSD = 0.276033			

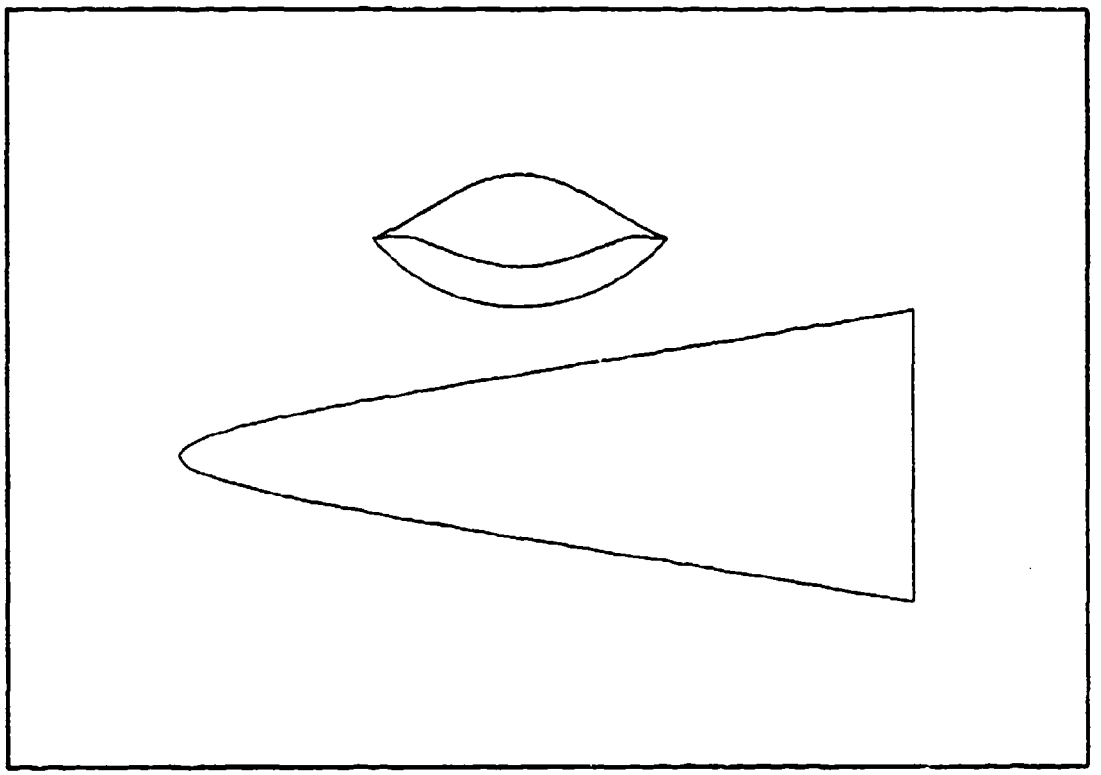

Figure C.13

Table C.13

Phi =50.0	Delta = 8.0	Mach =10.0	Rey = 0.10E+07	Gamma = 1.40
I = 0.400 + 0.750 Y^2 + -0.400 Y^4 + 0.090 Y^6				
Cftav = 0.001889	CL = 0.043199	CD = 0.009122		
Sw/Sp = 2.106453	V^(2/3)/Sp = 0.201476	(L/D)vis = 4.735799		
Ab/Abi = 0.781440	V/Vi = 0.600359	Sp/Spi = 0.802415		
b/lw = 0.401898	SSD = 0.276033			

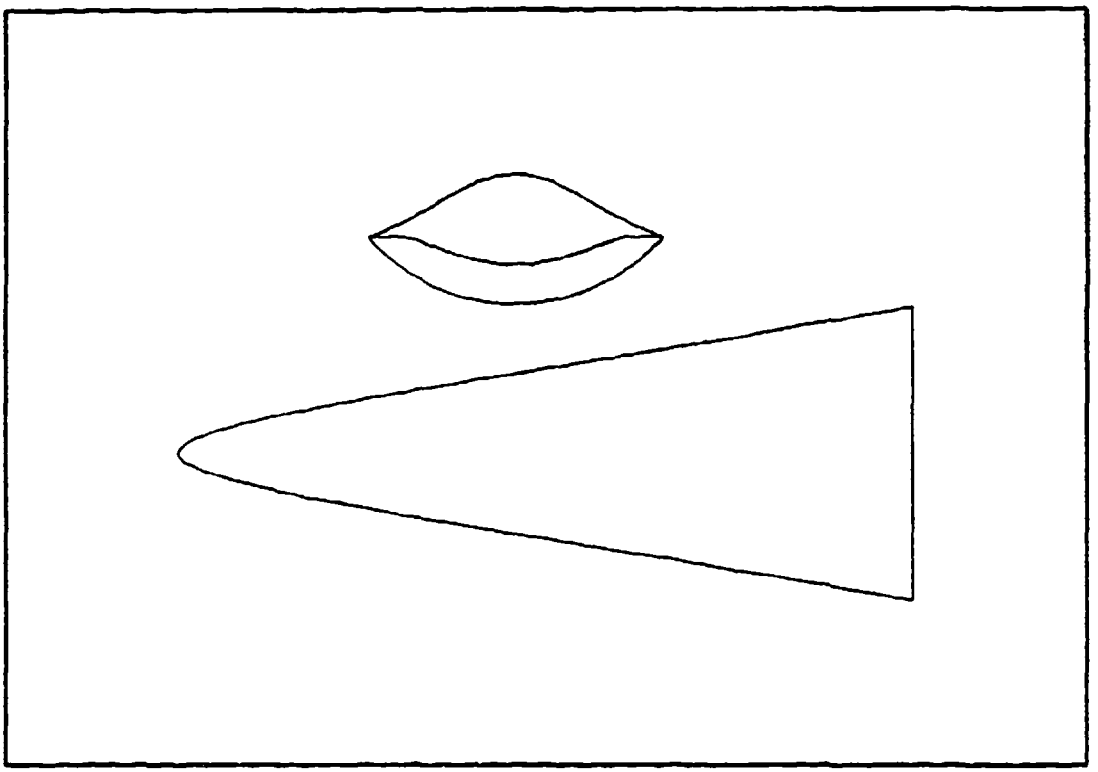

Figure C.14

Table C.14

Phi =50.0	Delta = 8.0	Mach =10.0	Rey = 0.10E+07	Gamma = 1.40
I = 0.400 + 0.851 Y^2 + -0.600 Y^4 + 0.189 Y^6				
Cftav = 0.001892	CL = 0.043177		CD = 0.009115	
Sw/Sp = 2.107503	V^(2/3)/Sp = 0.201090		(L/D)vis = 4.736885	
Ab/Abi = 0.770988	V/Vi = 0.588658		Sp/Spi = 0.793473	
b/lw = 0.401898	SSD = 0.276033			

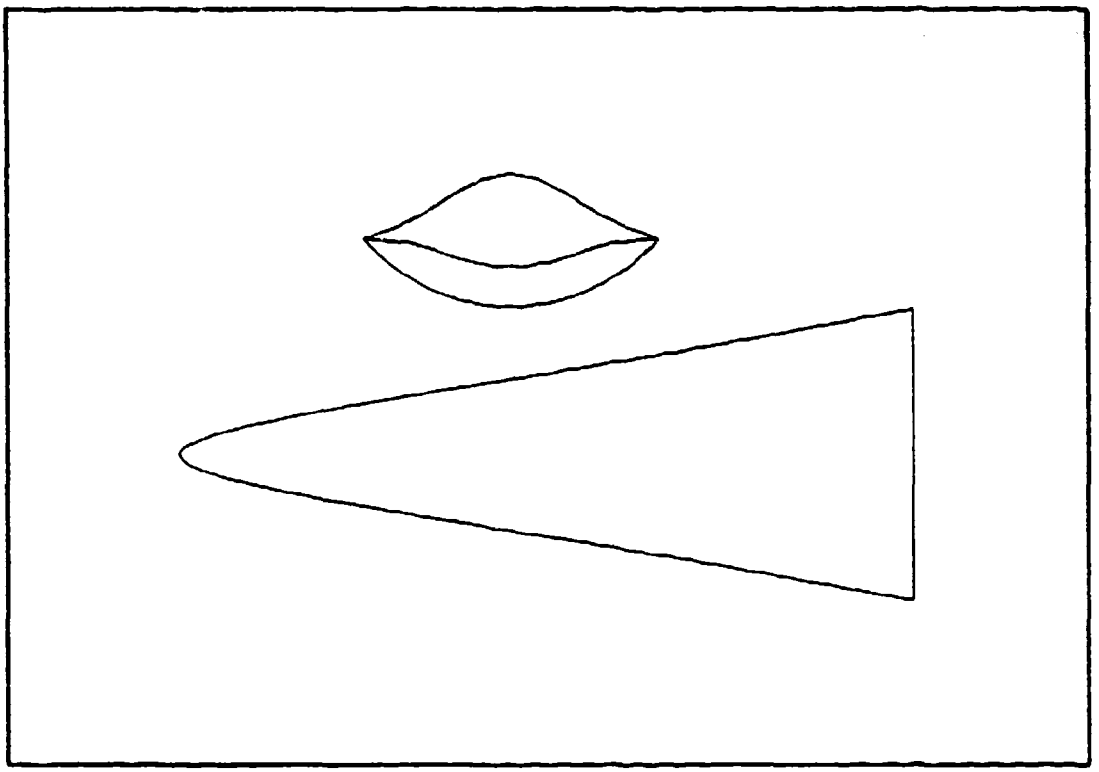

Figure C.15

Table C.15

Phi =50.0	Delta = 8.0	Mach =10.0	Rey = 0.10E+07	Gamma = 1.40
Y = 0.400 + 1.052 Y^2 + -1.000 Y^4 + 0.388 Y^6				
Cftav = 0.001898	CL = 0.043133	CD = 0.009111		
Sw/Sp = 2.113615	V^(2/3)/Sp = 0.200432	(L/D)vis = 4.734126		
Ab/Abi = 0.750343	V/Vi = 0.566081	Sp/Spi = 0.775592		
b/lw = 0.401898	SSD = 0.276033			

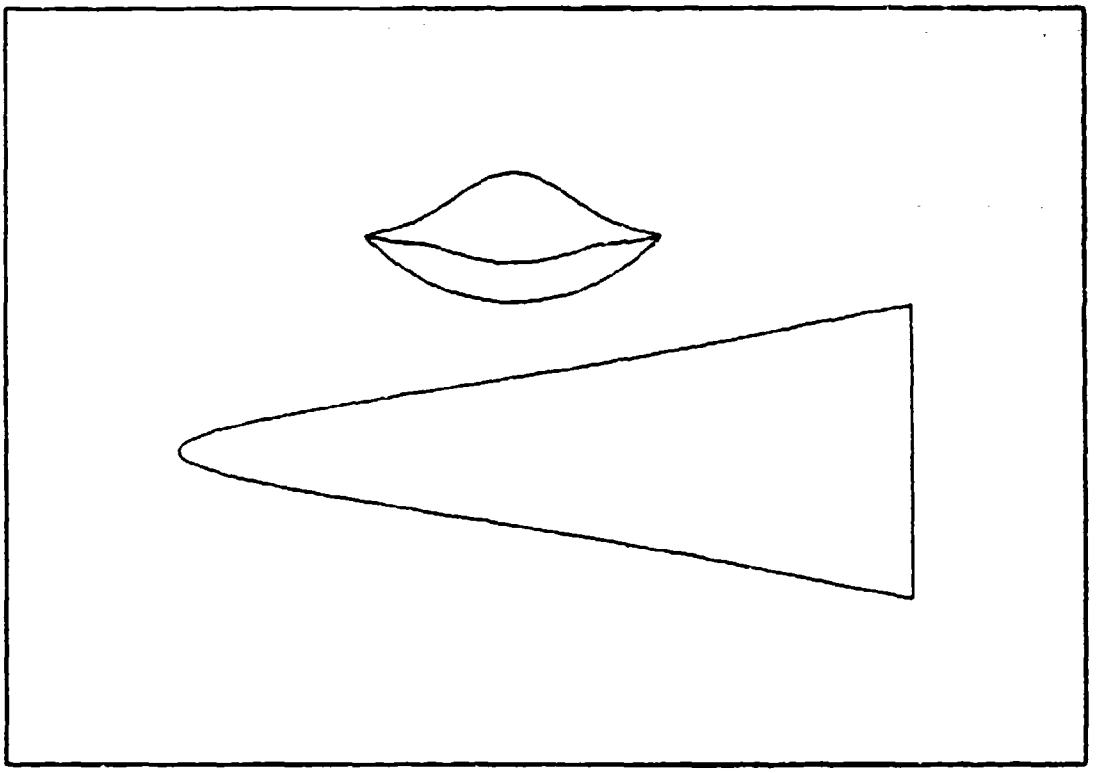

Figure C.16

Table C.16

Phi =50.0	Delta = 8.0	Mach =10.0	Rey = 0.10E+07	Gamma = 1.40
X = 0.400 + 1.253 Y^2 + -1.400 Y^4 + 0.587 Y^6				
Cftav = 0.001905	CL = 0.043082		CD = 0.009120	
Sw/Sp = 2.124808	V^(2/3)/Sp = 0.199939		(L/D)vis = 4.725195	
Ab/Abi = 0.729698	V/Vi = 0.544315		Sp/Spi = 0.757447	
b/lw = 0.401898	SSD = 0.276033			

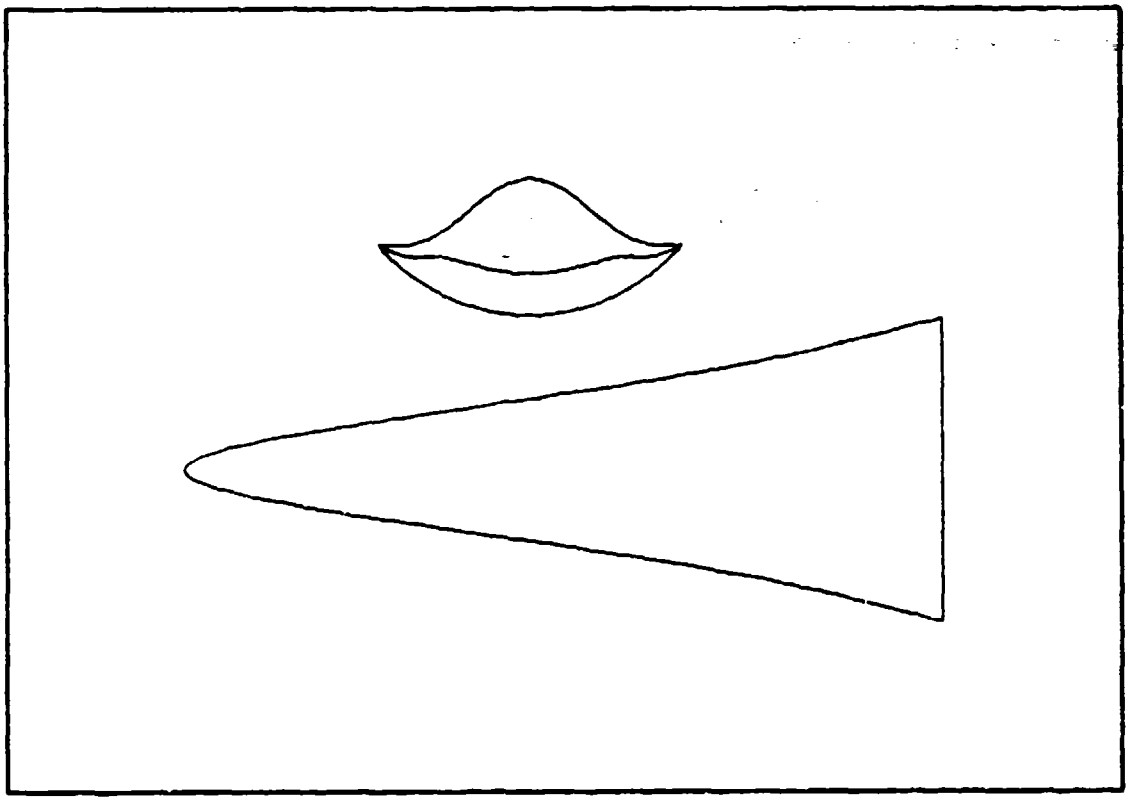

Figure C.17

Table C.17

Phi :50.0	Delta : 8.0	Mach :10.0	Rey : 0.10E+07	Ganma : 1.40
Y = 0.400 + 1.562 Y^2 + -1.800 Y^4 + 0.879 Y^6				
Cftav : 0.001919	CL : 0.043054		CD : 0.009171	
Sw/Sp : 2.167452	V^(2/3)/Sp : 0.201086		(L/D)vis : 4.694574	
Ab/Abi : 0.681286	V/Vi : 0.503584		Sp/Spi : 0.715070	
b/lw : 0.401898	SSD : 0.276033			

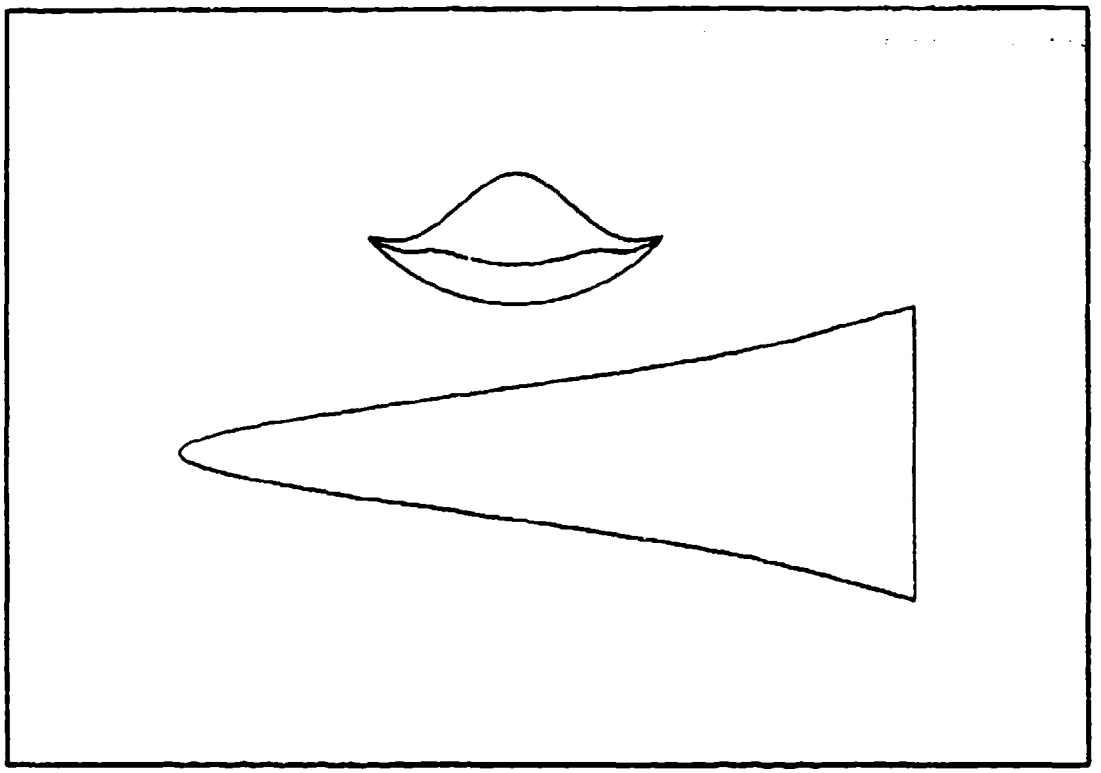

Figure C.18

Table C.18

Phi :50.0	Delta = 8.0	Mach =10.0	Rey = 0.10E+07	Gamma = 1.40
X = 0.400 + 1.763 Y^2 + -2.200 Y^4 + 0.878 Y^6				
Cftav = 0.001928	CL = 0.043024		CD = 0.009211	
Sw/Sp = 2.190453	V^(2/3)/Sp = 0.201283		(L/D)vis = 4.671057	
Ab/Abi = 0.660641	V/Vi = 0.484482		Sp/Spi = 0.696187	
b/lw = 0.401898	SSD = 0.276033			

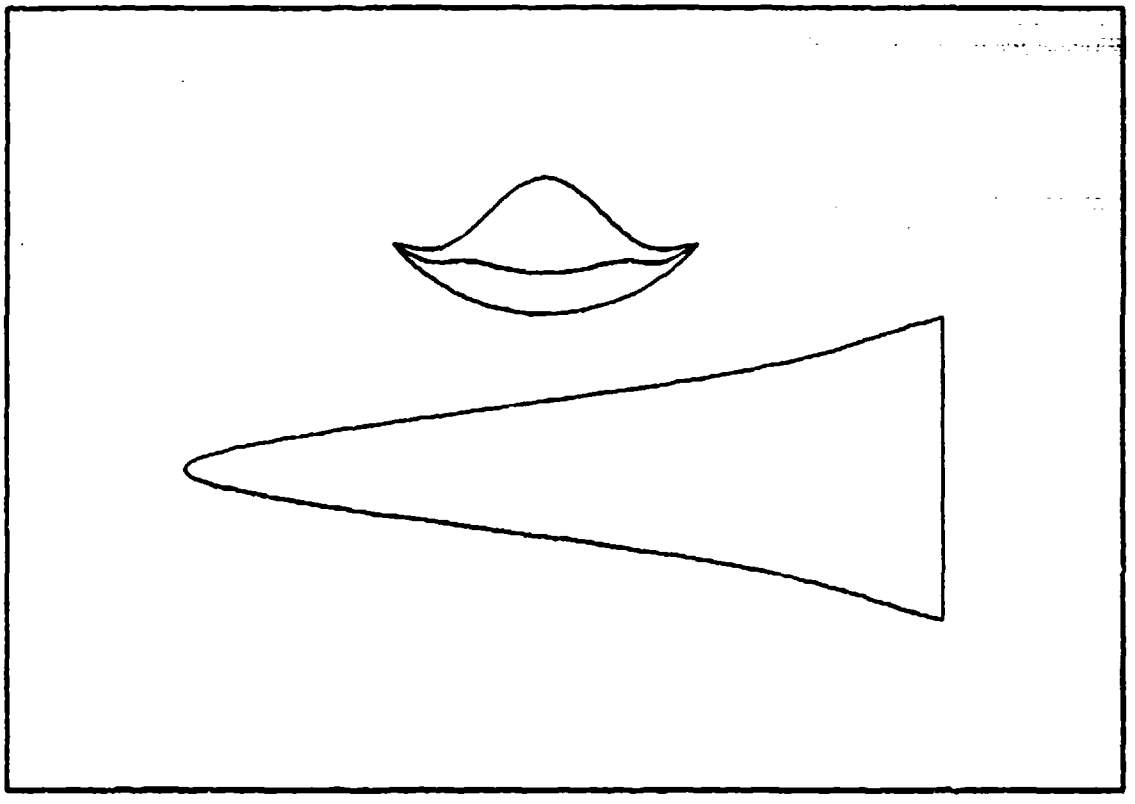

Figure C.19

Table C.19

Phi =50.0	Delta = 8.0	Mach =10.0	Rey = 0.10E+07	Gamma = 1.40
Y = 0.400 + 1.964 Y^2 + -2.800 Y^4 + 1.077 Y^6				
Cftav = 0.001938	CL = 0.042999		CD = 0.009261	
Sw/Sp = 2.217187	V^(2/3)/Sp = 0.201728		(L/D)vis = 4.643071	
Ab/Abi = 0.639996	V/Vi = 0.466241		Sp/Spi = 0.677104	
b/lw = 0.401898	SSD = 0.276033			

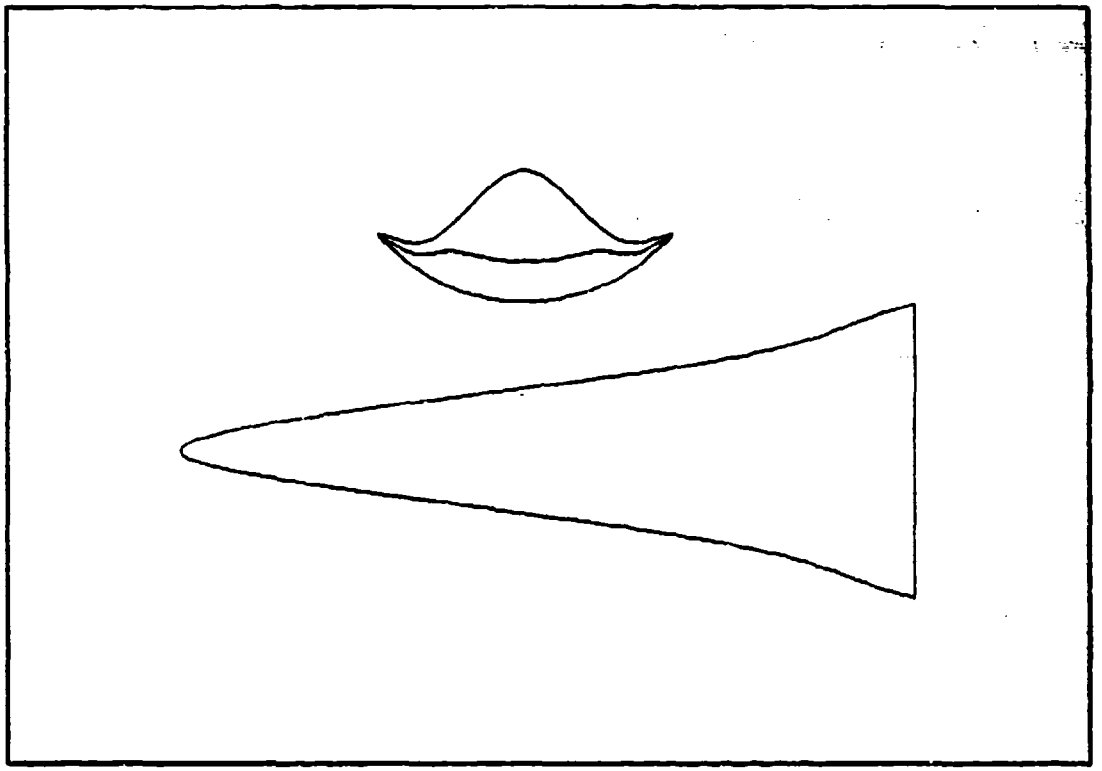

Figure C.20

Table C.20

Phi =50.0	Delta = 8.0	Mach =10.0	Rey = 0.10E+07	Gamma = 1.40
Y = 0.400 + 2.165 Y^2 + -3.000 Y^4 + 1.276 Y^6				
Cftav = 0.001948	CL = 0.042978		CD = 0.009321	
Sw/Sp = 2.247369	V^(2/3)/Sp = 0.202447		(L/D)vis = 4.611121	
Ab/Abi = 0.619351	V/Vi = 0.448869		Sp/Spi = 0.657835	
b/lw = 0.401898	SBD = 0.276033			

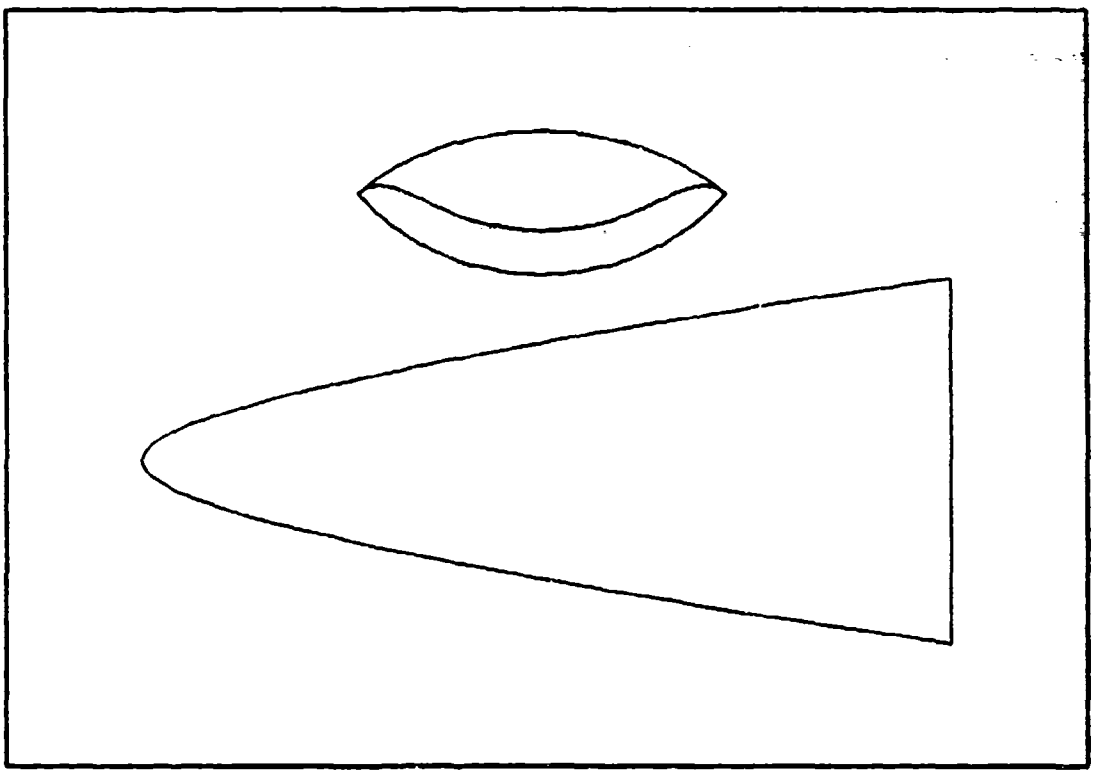

Figure C.21

Table C.21

Phi =50.0	Delta = 0.0	Mach =10.0	Rey = 0.10E+07	Gamma = 1.40
Y = 0.500 + 0.292 Y^2 + 0.000 Y^4 + 0.047 Y^6				
Citav = 0.001862	CL = 0.042867		CD = 0.008987	
Sw/Sp = 2.070644	V^(2/3)/Sp = 0.193480		(L/D)vis = 4.769799	
Ab/Abi = 0.753140	V/Vi = 0.529250		Sp/Spi = 0.768223	
b/lw = 0.451589	SSD = 0.258054			

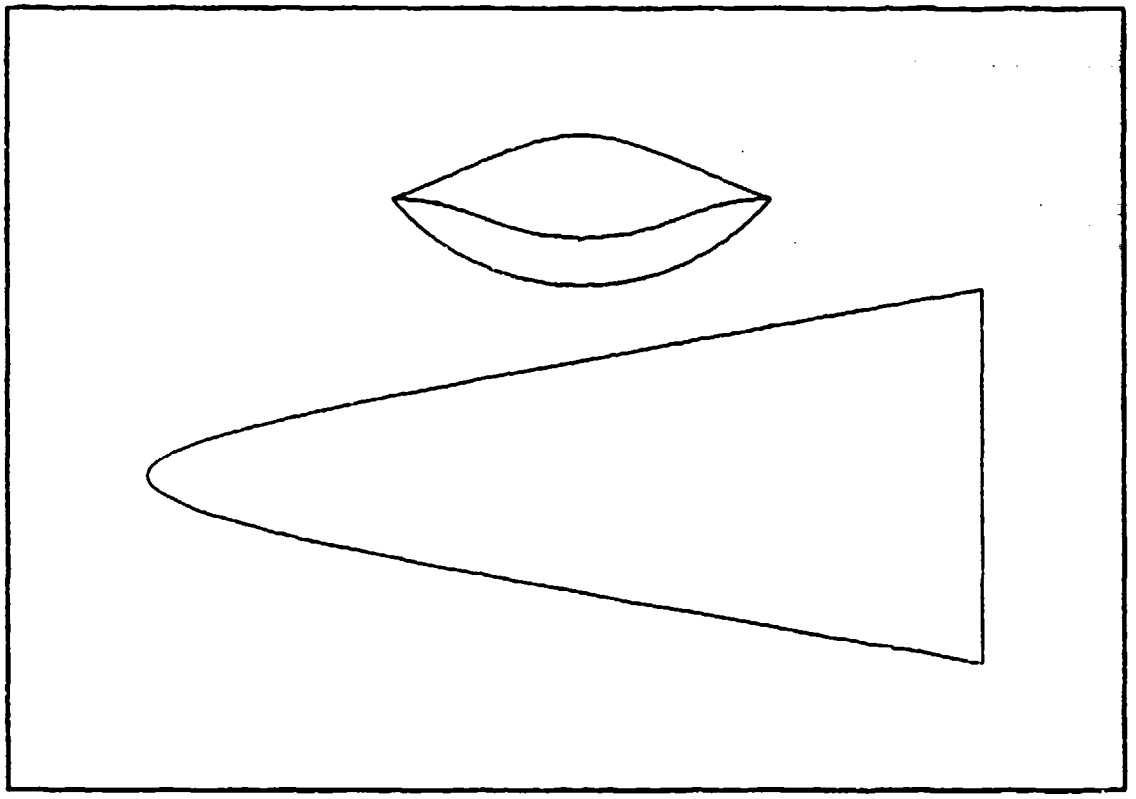

Figure C.22

Table C.22

Phi =50.0	Delta = 8.0	Mach =10.0	Rey = 0.10E+07	Gamma = 1.40
X = 0.500 + 0.601 Y^2 + -0.400 Y^4 + 0.139 Y^6				
Cftav = 0.001877	CL = 0.042788		CD = 0.008942	
Sw/Sp = 2.067719	V^(2/3)/Sp = 0.192469		(L/D)vis = 4.784766	
Ab/Abi = 0.704728	V/Vi = 0.483839		Sp/Spi = 0.727426	
b/lw = 0.451589	SSD = 0.258054			

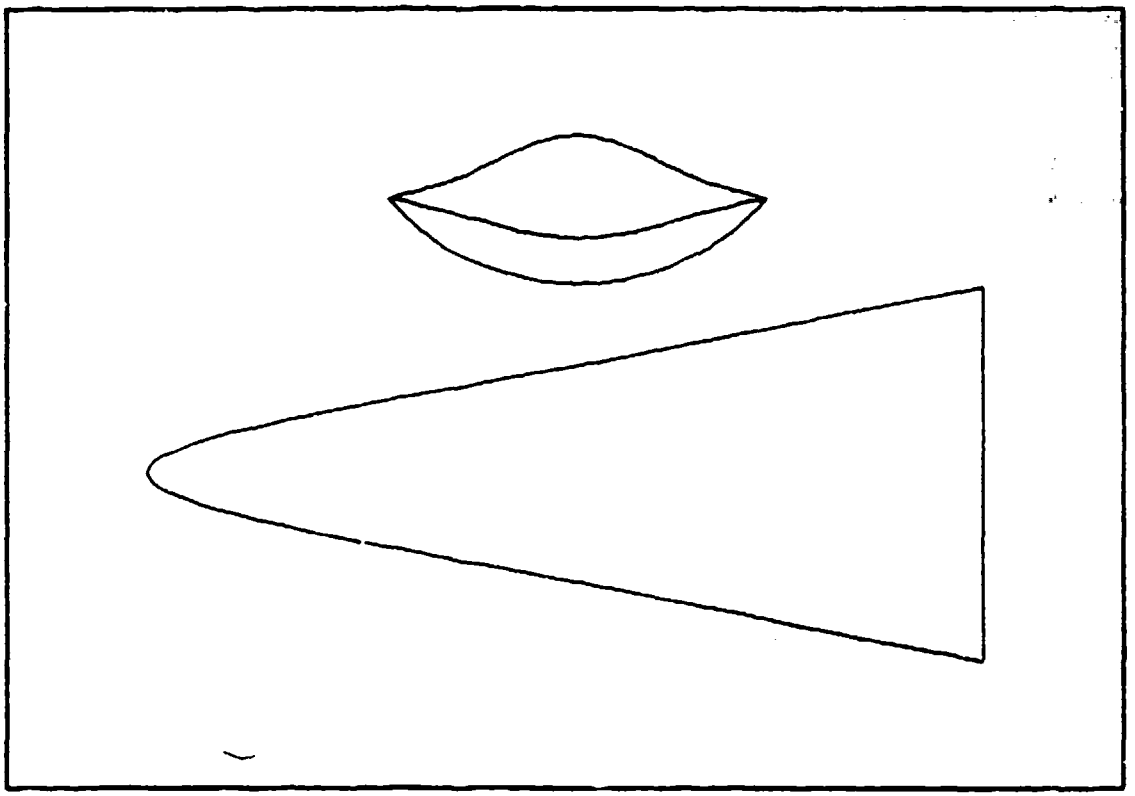

Figure C.23

Table C.23

Phi =50.0	Delta = 8.0	Mach =10.0	Rey = 0.10E+07	Gamma = 1.40
Y = 0.500 + 0.903 Y^2 + -1.000 Y^4 + 0.437 Y^6				
Cftav = 0.001894	CL = 0.042716	CD = 0.008949		
Sw/Sp = 2.075381	V^(2/3)/Sp = 0.191391	(L/D)vis = 4.773218		
Ab/Abi = 0.673631	V/Vi = 0.452648	Sp/Spi = 0.899733		
b/lw = 0.451589	SSD = 0.258054			

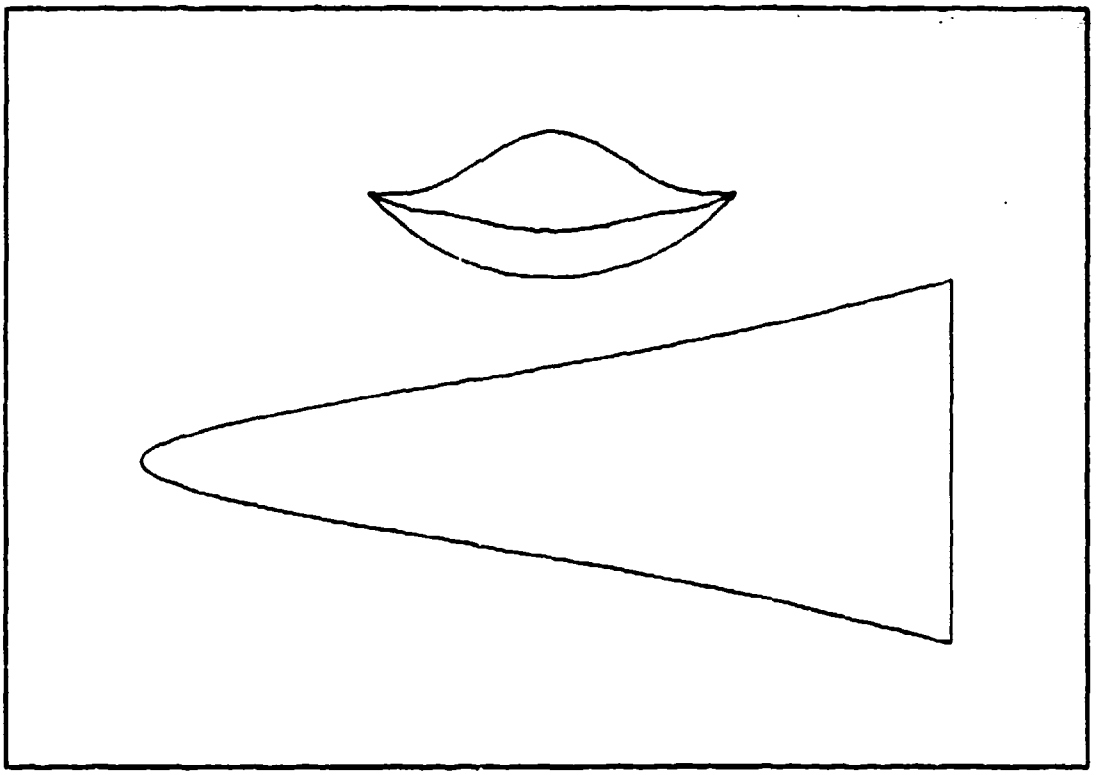

Figure C.24

Table C.24

Phi =50.0	Delta = 8.0	Mach =10.0	Rey = 0.10E+07	Gamma = 1.40
Y = 0.500 + 1.212 Y^2 + -1.400 Y^4 + 0.529 Y^6				
Cftav = 0.001915	CL = 0.042664		CD = 0.008987	
Sw/Sp = 2.105614	V^(2/3)/Sp = 0.192161		(L/D)vis = 4.747234	
Ab/Abi = 0.825218	V/Vi = 0.414169		Sp/Spi = 0.656853	
b/lw = 0.451589	SSD = 0.258054			

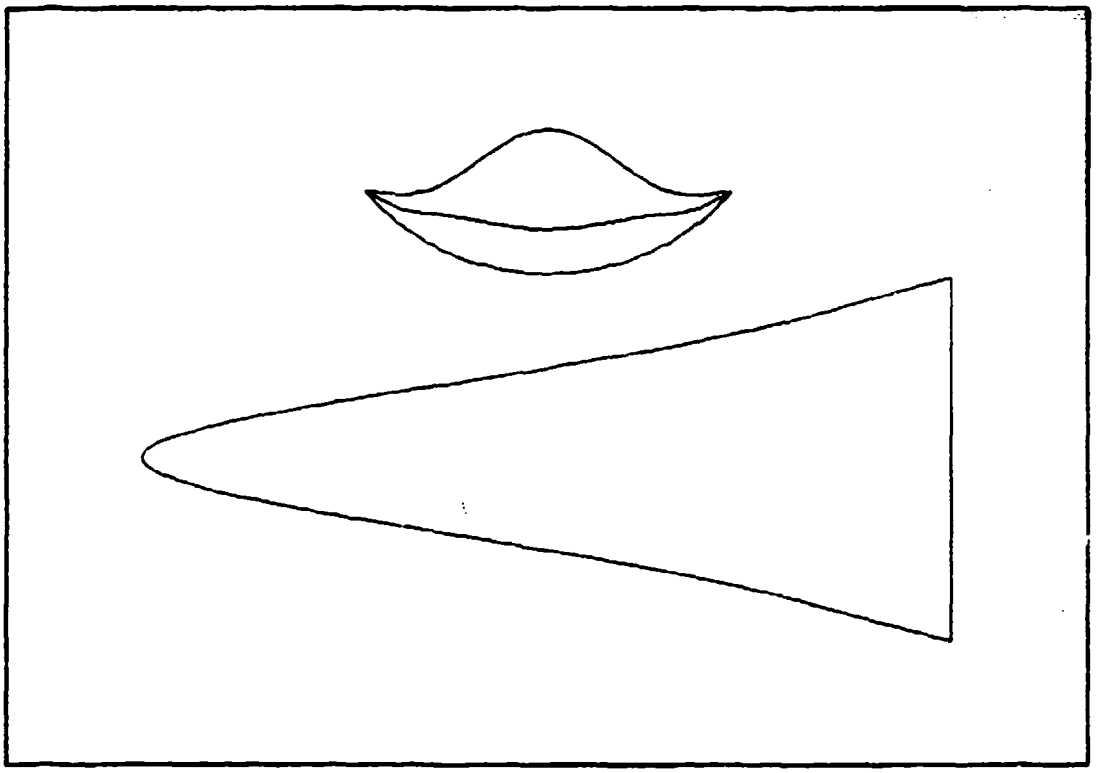

Figure C.25

Table C.25

Phi =50.0	Delta = 8.0	Mach =10.0	Rey = 0.10E+07	Gamma = 1.40
I = 0.500 + 1.413 Y^2 + -1.800 Y^4 + 0.728 Y^6				
Cftav = 0.001927	CL = 0.042628	CD = 0.009025		
Sw/Sp = 2.124140	V^(2/3)/Sp = 0.192207	(L/D)vis = 4.723290		
Ab/Abi = 0.604573	V/Vi = 0.396348	Sp/Spi = 0.637721		
b/lw = 0.451589	SSD = 0.258054			

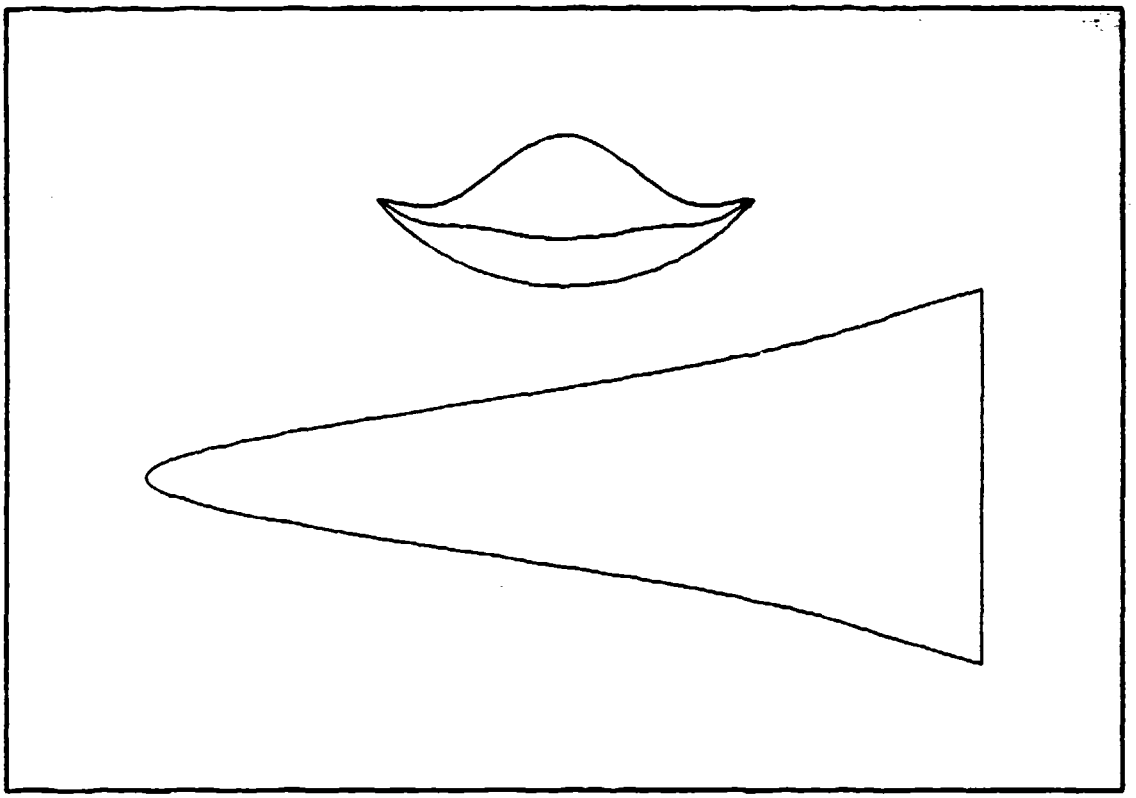

Figure C.26

Table C.26

Phi =50.0	Delta = 8.0	Mach =10.0	Rey = 0.10E+07	Gamma = 1.40
I = 0.500 + 1.614 Y^2 + -2.200 Y^4 + 0.927 Y^6				
Cftav = 0.001941	CL = 0.042597	CD = 0.009073		
Sw/Sp = 2.146518	V^(2/3)/Sp = 0.192518	(L/D)vis = 4.694764		
Ab/Abi = 0.583929	V/Vi = 0.379397	Sp/Spi = 0.618405		
b/lw = 0.451589	SSD = 0.258054			

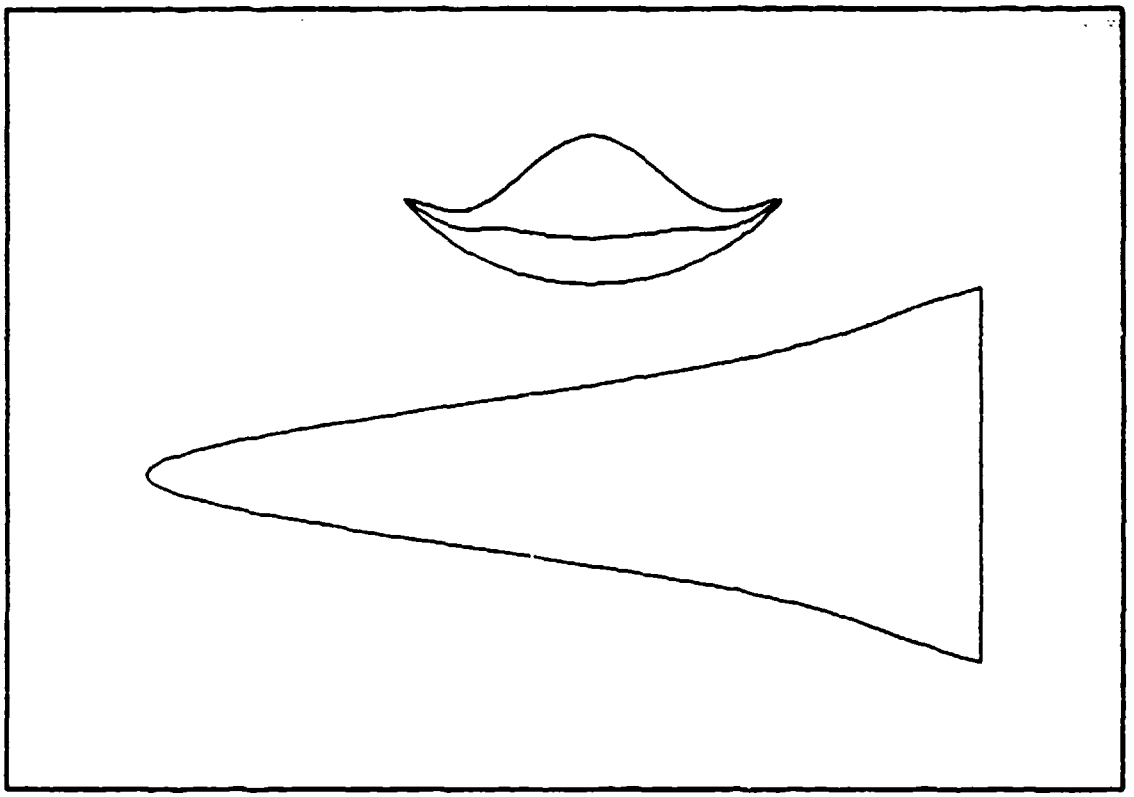

Figure C.27

Table C.27

Phi =50.0	Delta = 8.0	Mach =10.0	Rey = 0.10E+07	Gamma = 1.40
Y = 0.500 + 1.815 Y^2 + -2.600 Y^4 + 1.126 Y^6				
Cftav = 0.001955		CL = 0.042571		CD = 0.009131
Sw/Sp = 2.172462		V^(2/3)/Sp = 0.193128		(L/D)vis = 4.662208
Ab/Abi = 0.563284		V/Vi = 0.363326		Sp/Spi = 0.598916
b/lw = 0.451589		SSD = 0.258054		

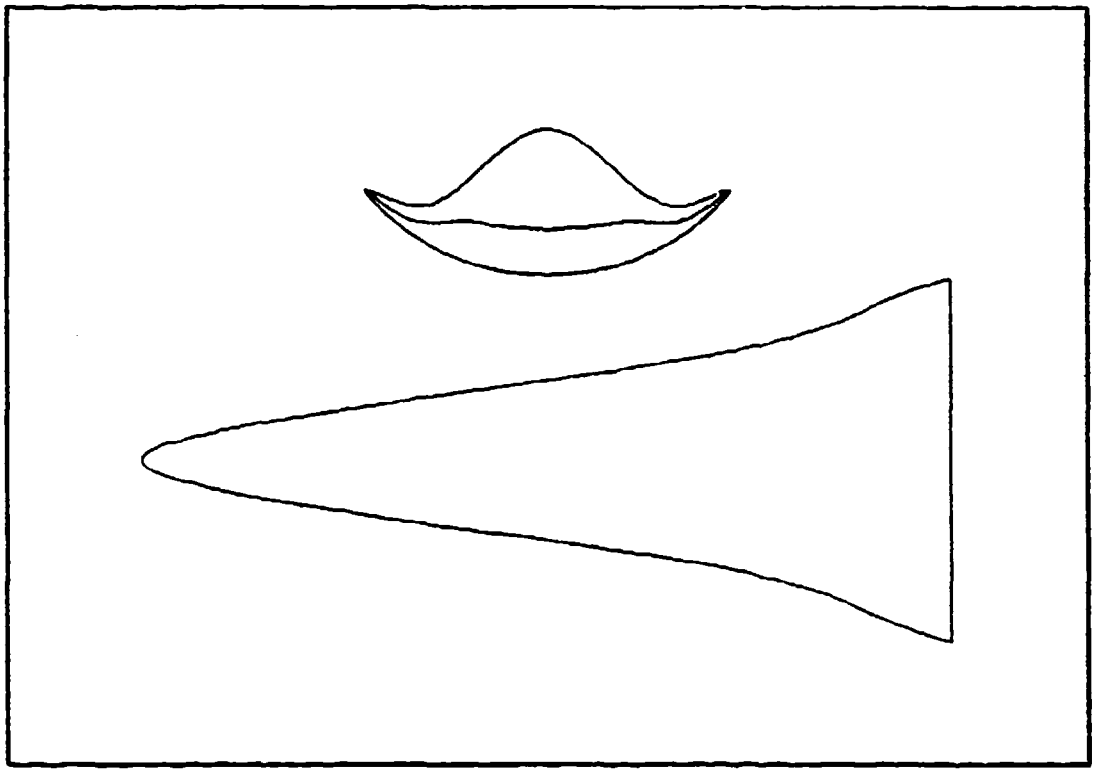

Figure C.28

Table C.28

Phi :50.0	Delta = 8.0	Mach :10.0	Rey = 0.10E+07	Gamma = 1.40
Y = 0.500 + 2.016 Y^2 + -3.000 Y^4 + 1.325 Y^6				
Cftav = 0.001969	CL = 0.042552	CD = 0.009198		
Sw/Sp = 2.201684	V^(2/3)/Sp = 0.194077	(L/D)vis = 4.626232		
Ab/Abi = 0.542639	V/Vi = 0.348142	Sp/Spi = 0.579266		
b/lw = 0.451589	SSD = 0.258054			

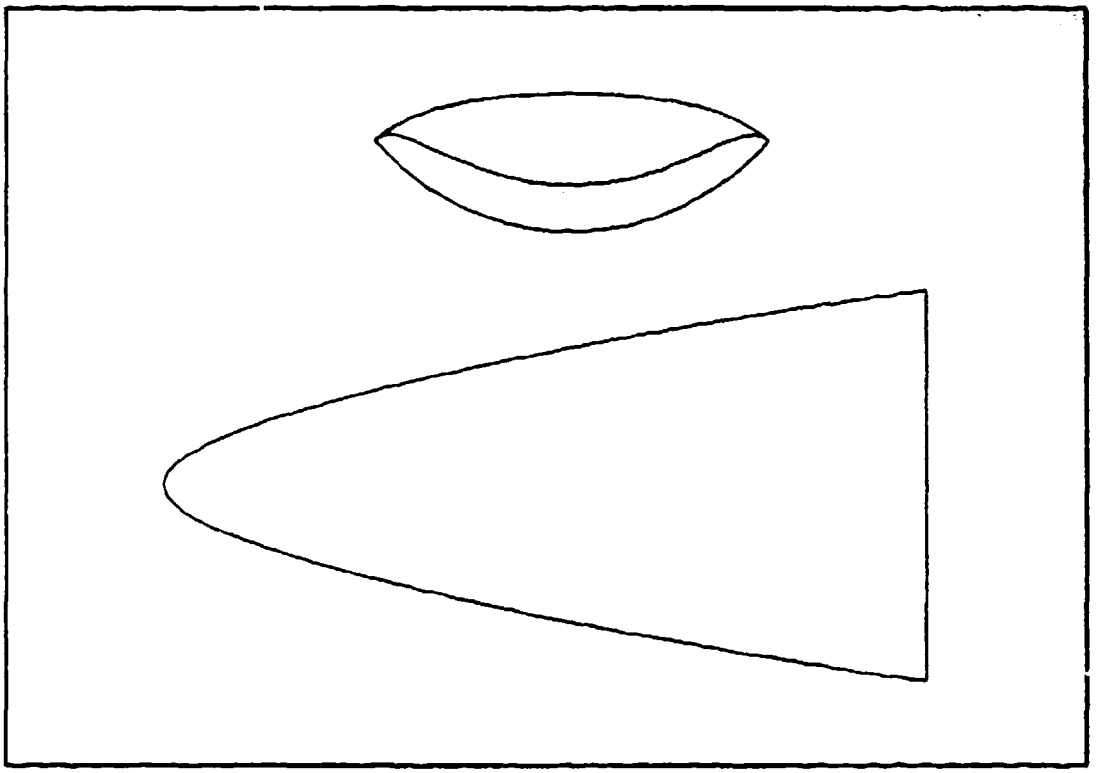

Figure C.29

Table C.29

Phi =50.0	Delta = 8.0	Mach =10.0	Rey = 0.10E+07	Gamma = 1.40
X = 0.600 + 0.143 Y^2 + 0.000 Y^4 + 0.096 Y^6				
Cftav = 0.001841	CL = 0.042447		CD = 0.008833	
Sw/Sp = 2.051067	V^(2/3)/Sp = 0.184276		(L/D)vis = 4.805467	
Ab/Abi = 0.676428	V/Vi = 0.421012		Sp/Spi = 0.692483	
b/lw = 0.515302	SSD = 0.236489			

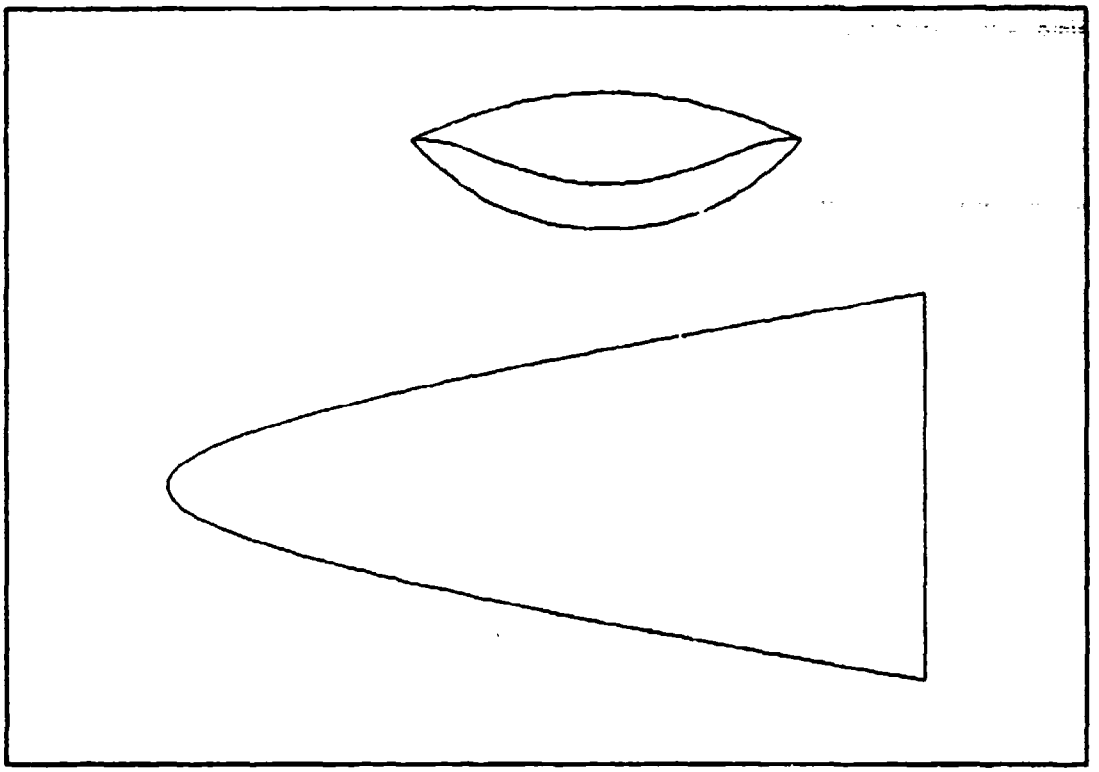

Figure C.30

Table C.30

Phi =50.0	Delta = 8.0	Mach =10.0	Rey = 0.10E+07	Gamma = 1.40
I = 0.600 + 0.251 Y^2 + 0.000 Y^4 + -0.011 Y^6				
Cftav = 0.001851	CL = 0.042412	CD = 0.008800		
Sw/Sp = 2.045426	V^(2/3)/Sp = 0.184069	(L/D)vis = 4.819488		
Ab/Abi = 0.648661	V/Vi = 0.399285	Sp/Spi = 0.669200		
b/lw = 0.515302	SSD = 0.236489			

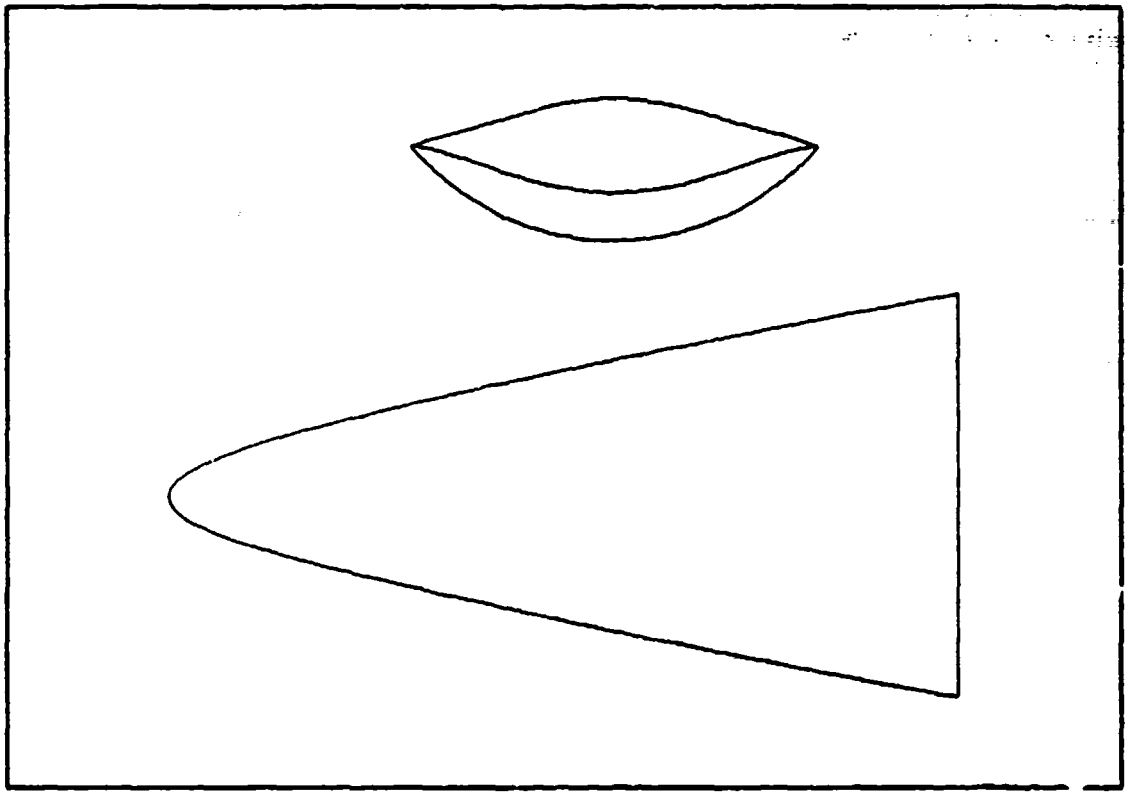

Figure C.31

Table C.31

Phi =50.0	Delta = 8.0	Mach =10.0	Rey = 0.10E+07	Gamma = 1.40
I = 0.600 + 0.452 Y^2 + -0.400 Y^4 + 0.188 Y^6				
Cftav = 0.001867	CL = 0.042357	CD = 0.008801		
Sw/Sp = 2.043804	V^(2/3)/Sp = 0.183058	(L/D)vis = 4.812601		
Ab/Abi = 0.628016	V/Vi = 0.379612	Sp/Spi = 0.650607		
b/lw = 0.515302	SSD = 0.236489			

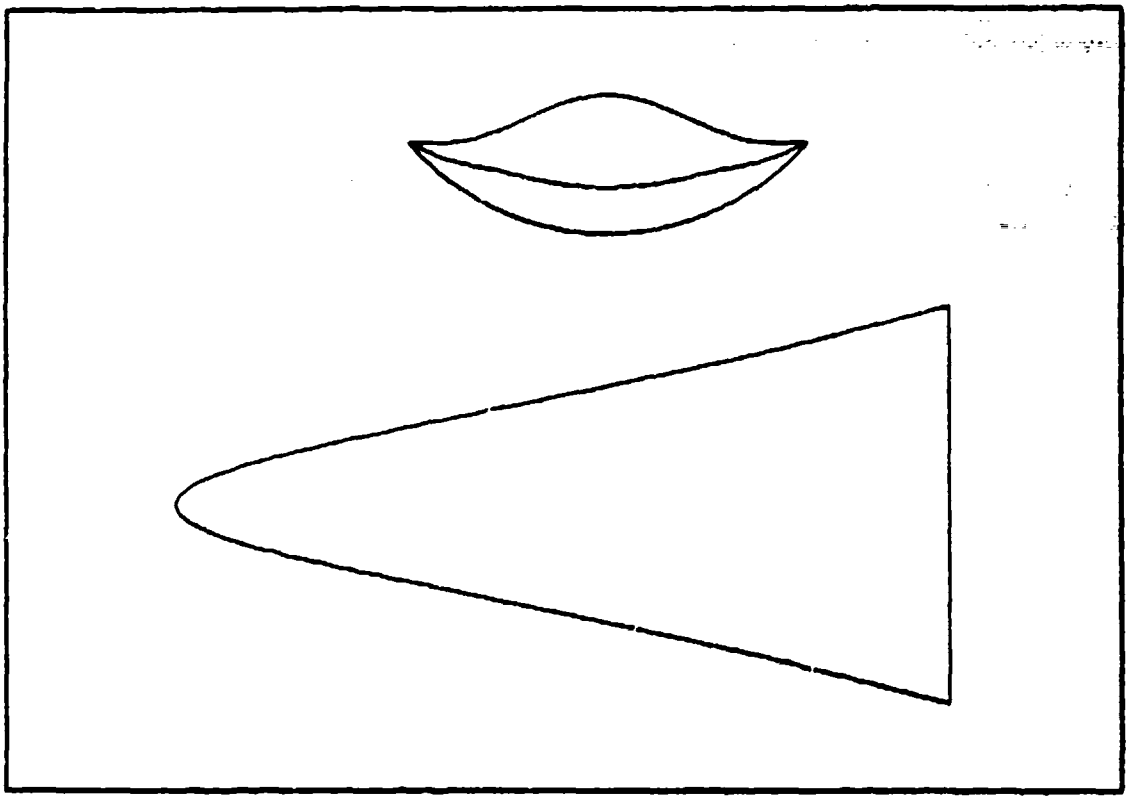

Figure C.32

Table C.32

Phi =50.0	Delta = 8.0	Mach =10.0	Rey = 0.10E+07	Gamma = 1.40
I = 0.600 + 0.862 Y^2 + -1.000 Y^4 + 0.379 Y^6				
Cftav = 0.001906	CL = 0.042262		CD = 0.008834	
Sw/Sp = 2.061863	V^(2/3)/Sp = 0.182863		(L/D)vis = 4.784272	
Ab/Abi = 0.569151	V/Vi = 0.333822		Sp/Spi = 0.597814	
b/lw = 0.515302	SBD = 0.236489			

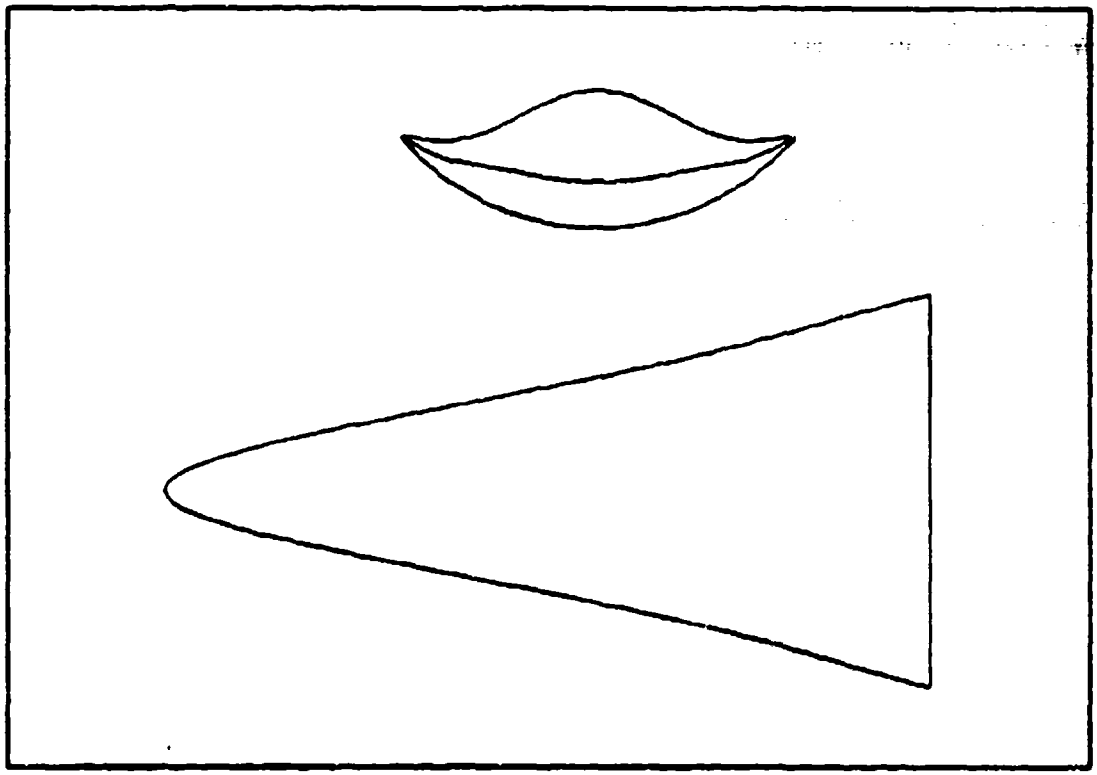

Figure C.33

Table C.33

Phi =50.0	Delta = 8.0	Mach =10.0	Rey = 0.10E+07	Gamma = 1.40
I = 0.600 + 1.068 Y^2 + -1.400 Y^4 + 0.578 Y^6				
Cftav = 0.001928	CL = 0.042220		CD = 0.008871	
Sw/Sp = 2.075419	Y^(2/3)/Sp = 0.182690		(L/D)vis = 4.759373	
Ab/Abi = 0.548506	V/Vi = 0.317303		Sp/Spi = 0.578473	
b/lw = 0.515302	SSD = 0.236469			

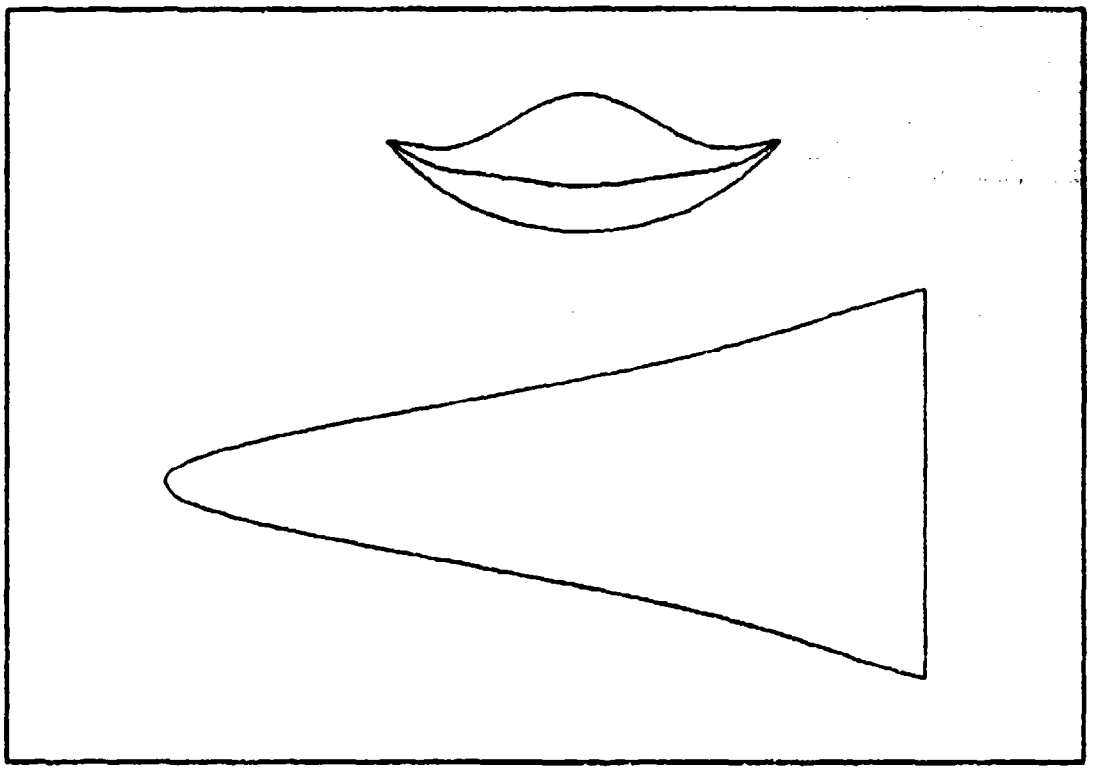

Figure C.34

Table C.34

Phi =50.0	Delta = 8.0	Mach =10.0	Rey = 0.10E+07	Gamma = 1.40
Y = 0.600 + 1.264 Y^2 + -1.800 Y^4 + 0.777 Y^6				
Cftav = 0.001942	CL = 0.042183		CD = 0.008919	
Sw/Sp = 2.092990	V^(2/3)/Sp = 0.182802		(L/D)vis = 4.729744	
Ab/Abi = 0.527861	V/Vi = 0.301664		Sp/Spi = 0.558962	
b/lw = 0.515302	SSD = 0.238489			

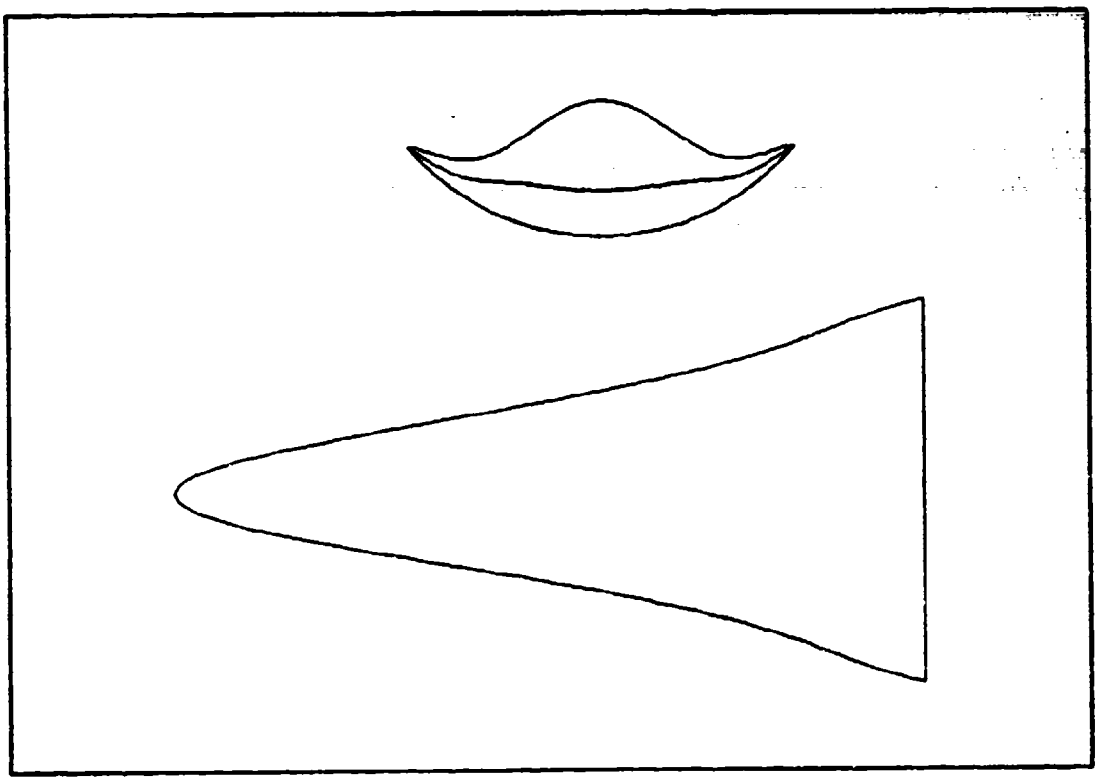

Figure C.35

Table C.35

Phi =50.0	Delta = 8.0	Mach =10.0	Rey = 0.10E+07	Gamma = 1.40
Y = 0.600 + 1.465 Y^2 + -2.200 Y^4 + 0.976 Y^6				
Cftav = 0.001961	CL = 0.042152		CD = 0.008976	
Sw/Sp = 2.114278	V^(2/3)/Sp = 0.183242		(L/D)vis = 4.695912	
Ab/Abi = 0.507217	V/Vi = 0.286913		Sp/Spi = 0.539290	
b/lw = 0.515302	SSD = 0.236489			

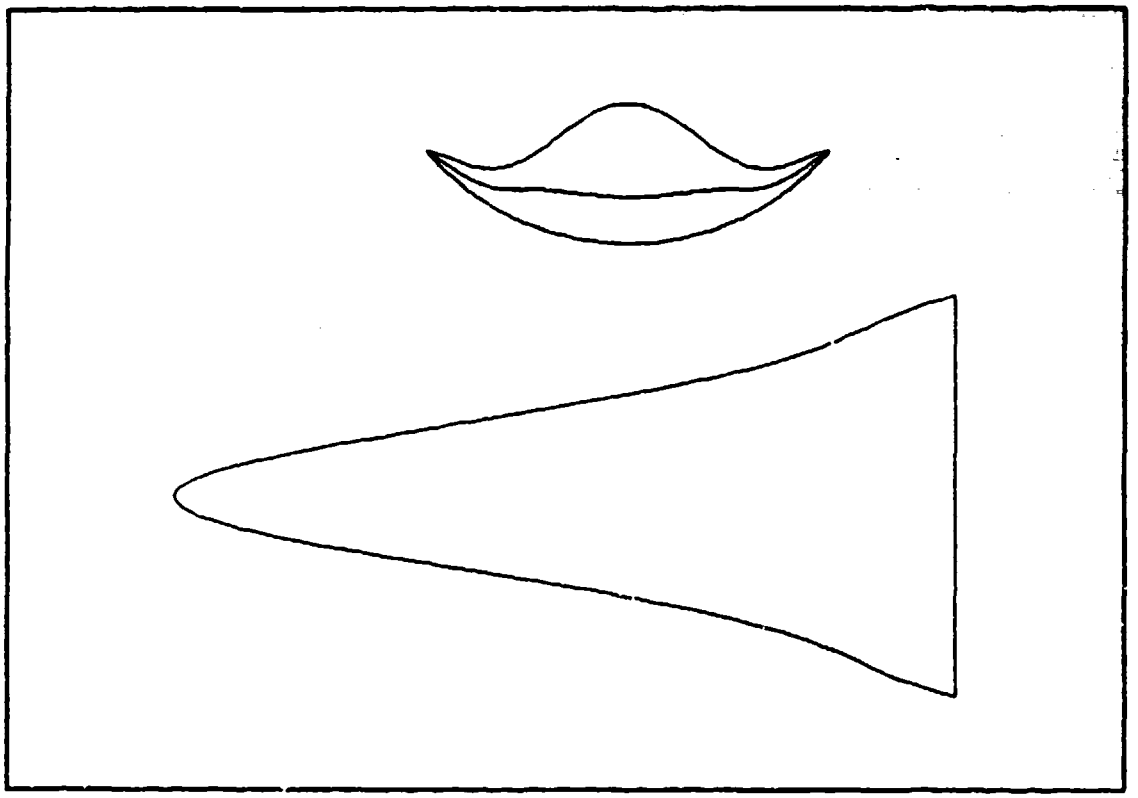

Figure C.36

Table C.36

Phi =50.0	Delta = 8.0	Mach =10.0	Rey = 0.10E+07	Gamma = 1.40
I = 0.600 + 1.666 Y^2 + -2.600 Y^4 + 1.175 Y^6				
Cftav = 0.001980	CL = 0.042127	CD = 0.009043		
Sw/Sp = 2.138979	V^(2/3)/Sp = 0.184060	(L/D)vis = 4.658574		
Ab/Abi = 0.486572	V/Vi = 0.273058	Sp/Spi = 0.519468		
b/lw = 0.515302	SSD = 0.236469			

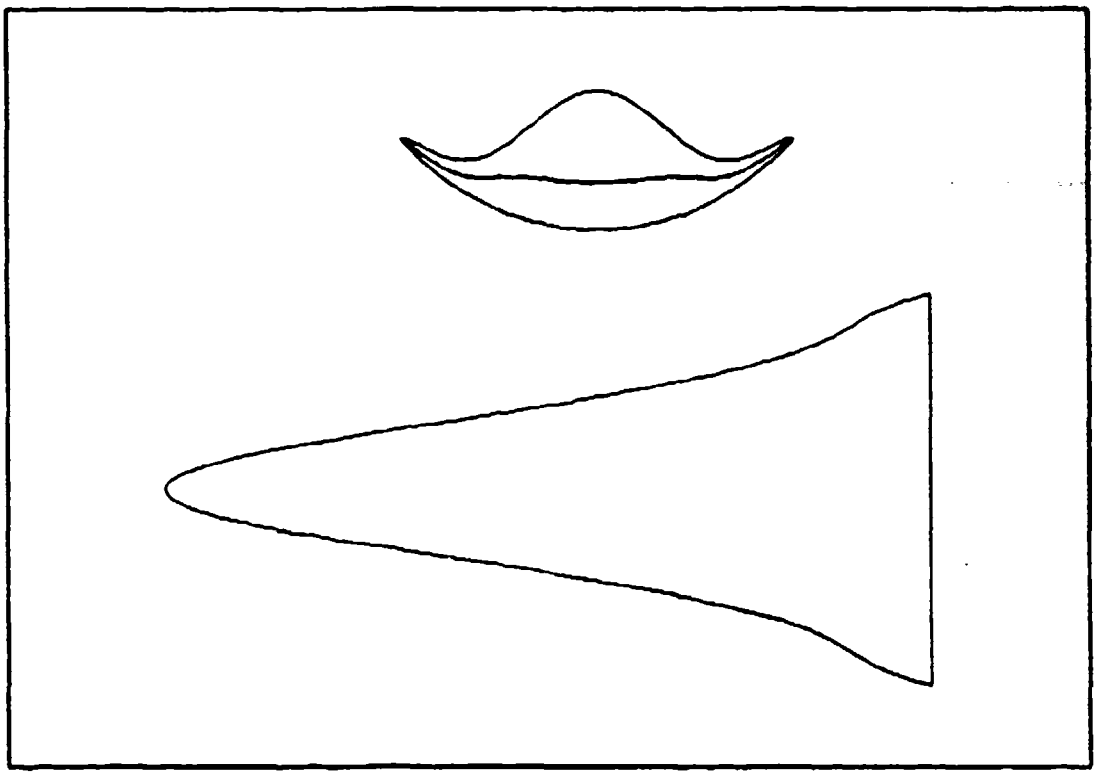

Figure C.37

Table C.37

Phi :50.0	Delta = 8.0	Mach :10.0	Rey = 0.10E+07	Gamma = 1.40
I = 0.600 + 1.867 Y^2 + -3.000 Y^4 + 1.374 Y^6				
Cftav = 0.001999	CL = 0.042110	CD = 0.009118		
Sw/Sp = 2.166782	V^(2/3)/Sp = 0.185314	(L/D)vis = 4.618535		
Ab/Abi = 0.465927	V/Vi = 0.260106	Sp/Spi = 0.499505		
b/lw = 0.515302	SSD = 0.236489			

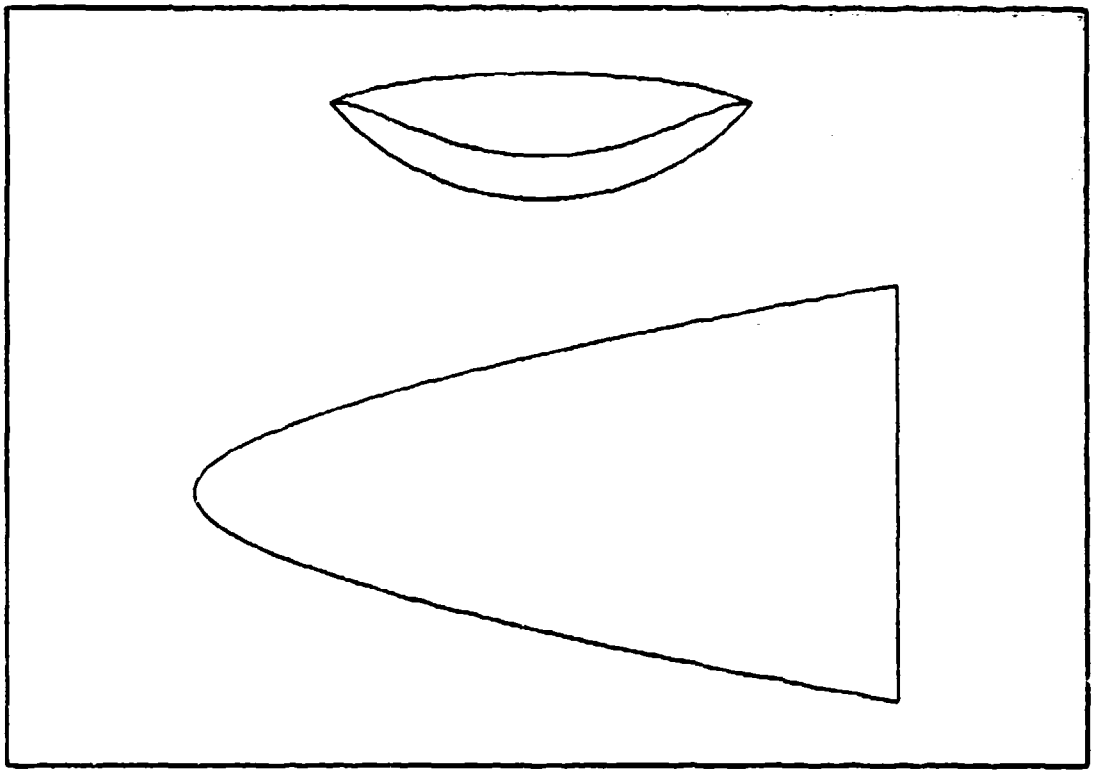

Figure C.38

Table C.38

Phi =50.0	Delta = 8.0	Mach =16.0	Rey = 0.10E+07	Gamma = 1.40
I = 0.700 + 0.102 Y^2 + 0.000 Y^4 + 0.038 Y^6				
Cftav = 0.001833	CL = 0.041972		CD = 0.008676	
Sw/Sp = 2.035391	V^(2/3)/Sp = 0.174208		(L/D)vis = 4.837829	
Ab/Abi = 0.571949	V/Vi = 0.305445		Sp/Spi = 0.591427	
b/lw = 0.599945	SSD = 0.211550			

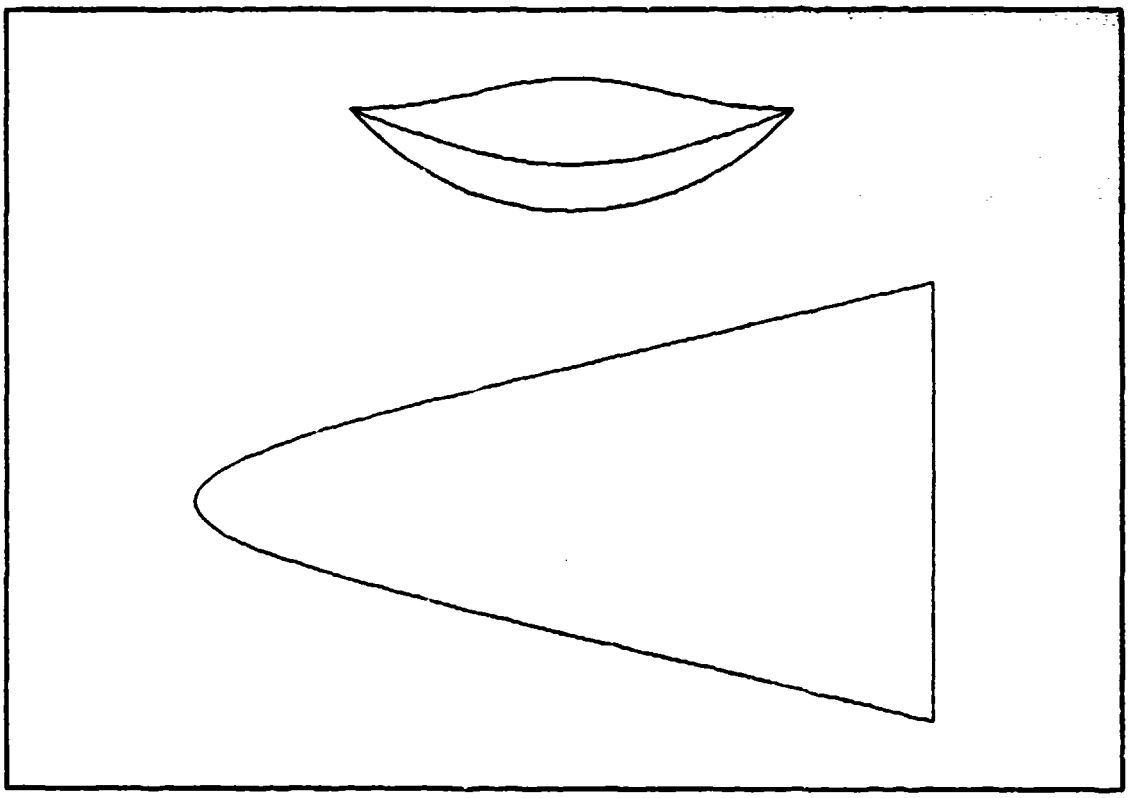

Figure C.39

Table C.39

Phi :50.0	Delta = 8.0	Mach :10.0	Rey = 0.10E+07	Gamma = 1.40
Y = 0.700 + 0.411 Y^2 + -0.400 Y^4 + 0.130 Y^6				
Cftav = 0.001875	CL = 0.041883	CD = 0.008686		
Sw/Sp = 2.033808	V^(2/3)/Sp = 0.173457	(L/D)vis = 4.821683		
Ab/Abi = 0.523536	V/Vi = 0.270647	Sp/Spi = 0.547973		
b/lw = 0.599945	SSD = 0.211550			

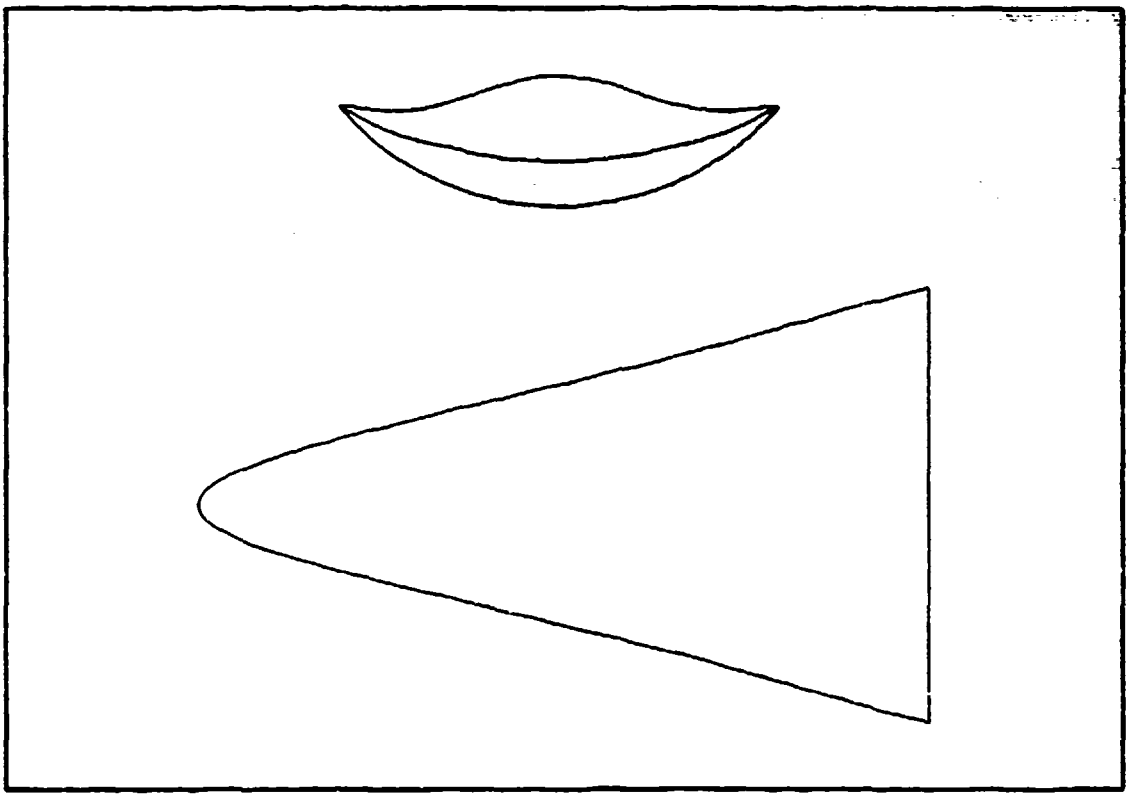

Figure C.40

Table C.40

Phi =50.0	Delta = 8.0	Mach =10.0	Rey = 0.10E+07	Gamma = 1.40
I = 0.700 + 0.712 Y^2 + -1.000 Y^4 + 0.429 Y^6				
Cftav = 0.001911	CL = 0.041807		CD = 0.008740	
Sw/Sp = 2.044167	V^(2/3)/Sp = 0.172623		(L/D)vis = 4.783686	
Ab/Abi = 0.492698	V/Vi = 0.247583		Sp/Spi = 0.518875	
b/lw = 0.599945	SSD = 0.211550			

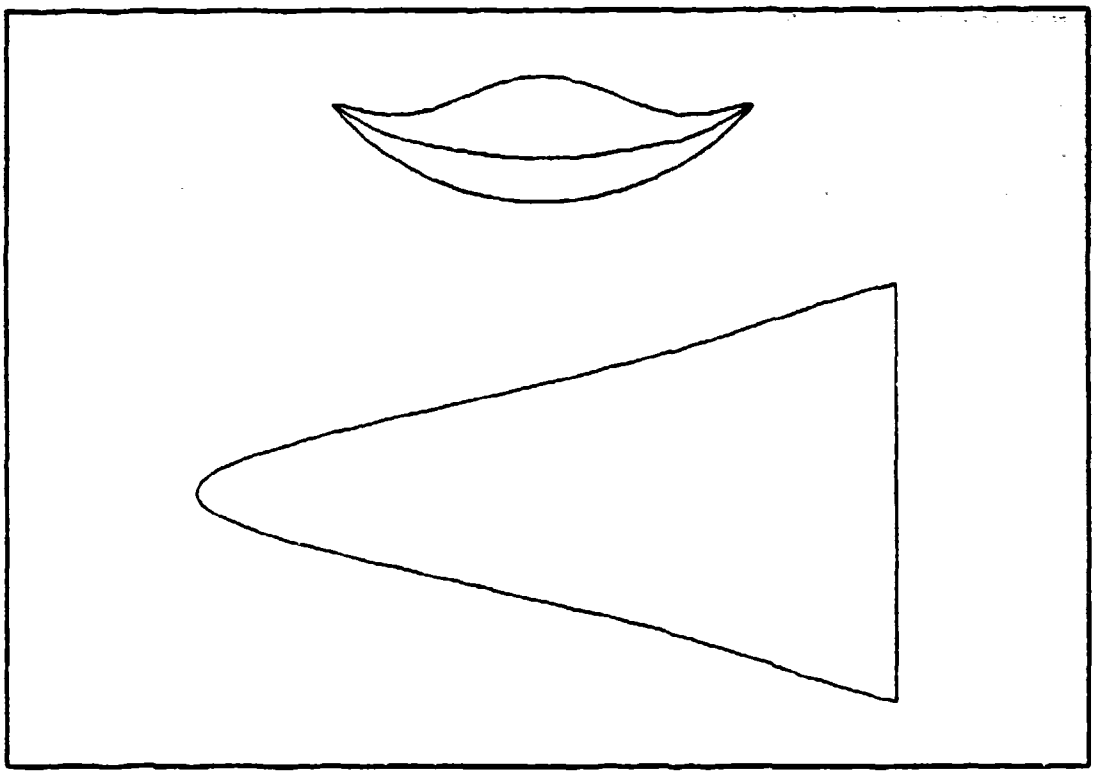

Figure C.41

Table C.41

Phi =50.0	Delta = 8.0	Mach =10.0	Rey = 0.10E+07	Gamma = 1.40
Y = 0.700 + 0.913 Y^2 + -1.400 Y^4 + 0.628 Y^6				
Cftav = 0.001936	CL = 0.041763	CD = 0.008788		
Sw/Sp = 2.056345	V^(2/3)/Sp = 0.172440	(L/D)vis = 4.752065		
Ab/Abi = 0.472053	V/Vi = 0.233263	Sp/Spi = 0.499199		
b/lw = 0.599945	SSD = 0.211550			

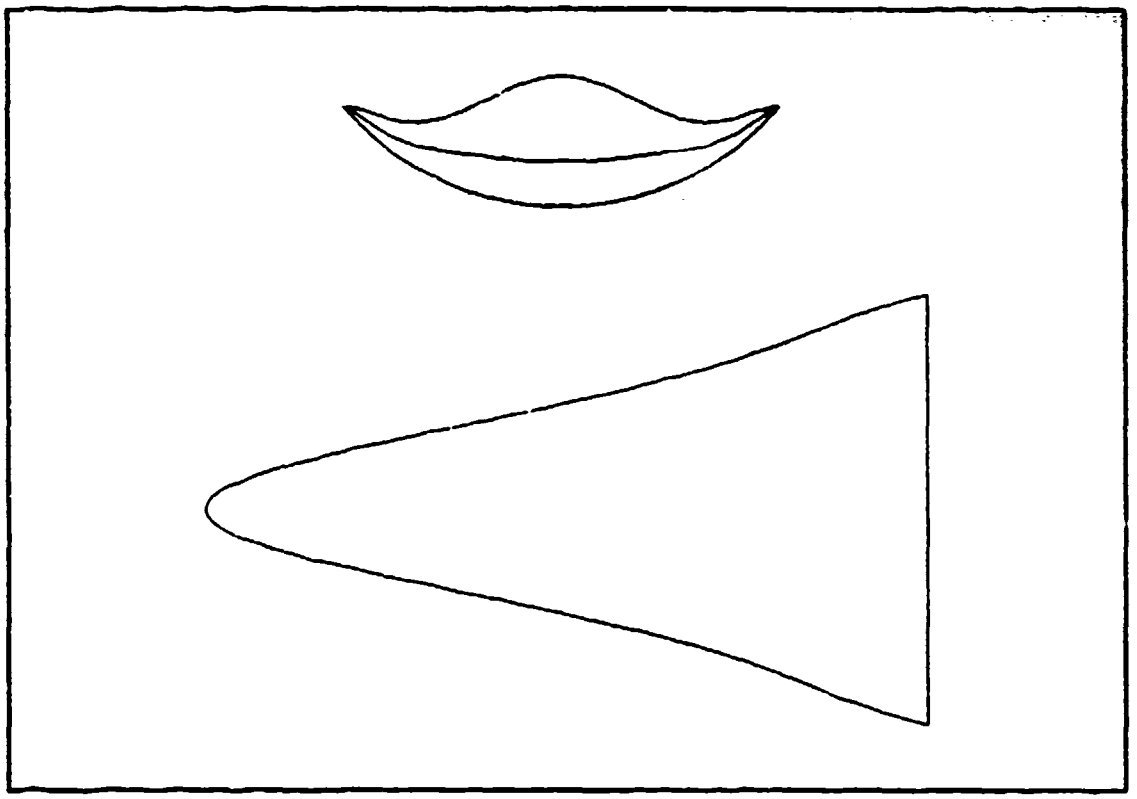

Figure C.42

Table C.42

Phi =50.0	Delta = 8.0	Mach =10.0	Rey = 0.10E+07	Gamma = 1.40
Y = 0.700 + 1.114 Y^2 + -1.800 Y^4 + 0.827 Y^6				
Cftav = 0.001961		CL = 0.041724		CD = 0.008847
Sw/Sp = 2.072390		V^(2/3)/Sp = 0.172614		(L/D)vis = 4.716013
Ab/Abi = 0.451409		V/Vi = 0.219838		Sp/Spi = 0.479373
b/lw = 0.599945		SSD = 0.211550		

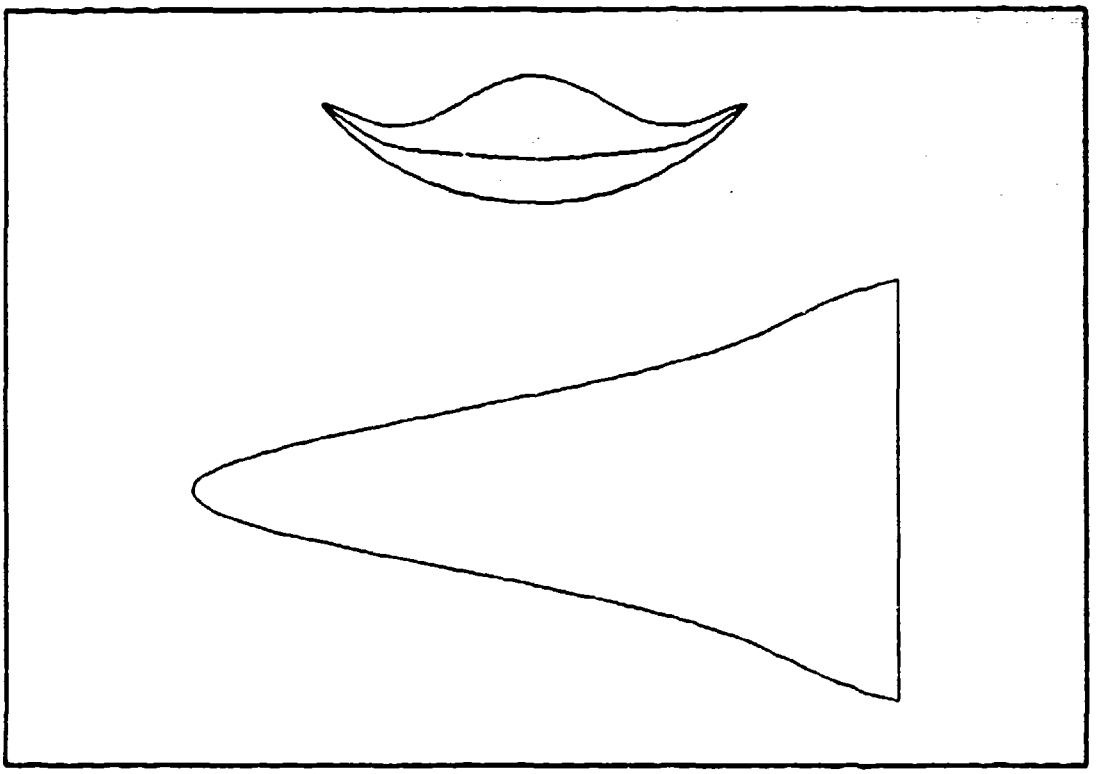

Figure C.43

Table C.43

Phi =50.0	Delta = 8.0	Mach =10.0	Rey = 0.10E+07	Gamma = 1.40
Y = 0.700 + 1.315 Y^2 + -2.200 Y^4 + 1.026 Y^6				
Cftav = 0.001987	CL = 0.041693		CD = 0.008916	
Sw/Sp = 2.091982	V^(2/3)/Sp = 0.173211		(L/D)vis = 4.676222	
Ab/Abi = 0.430764	V/Vi = 0.207317		Sp/Spi = 0.459405	
b/lw = 0.599945	SSD = 0.211550			

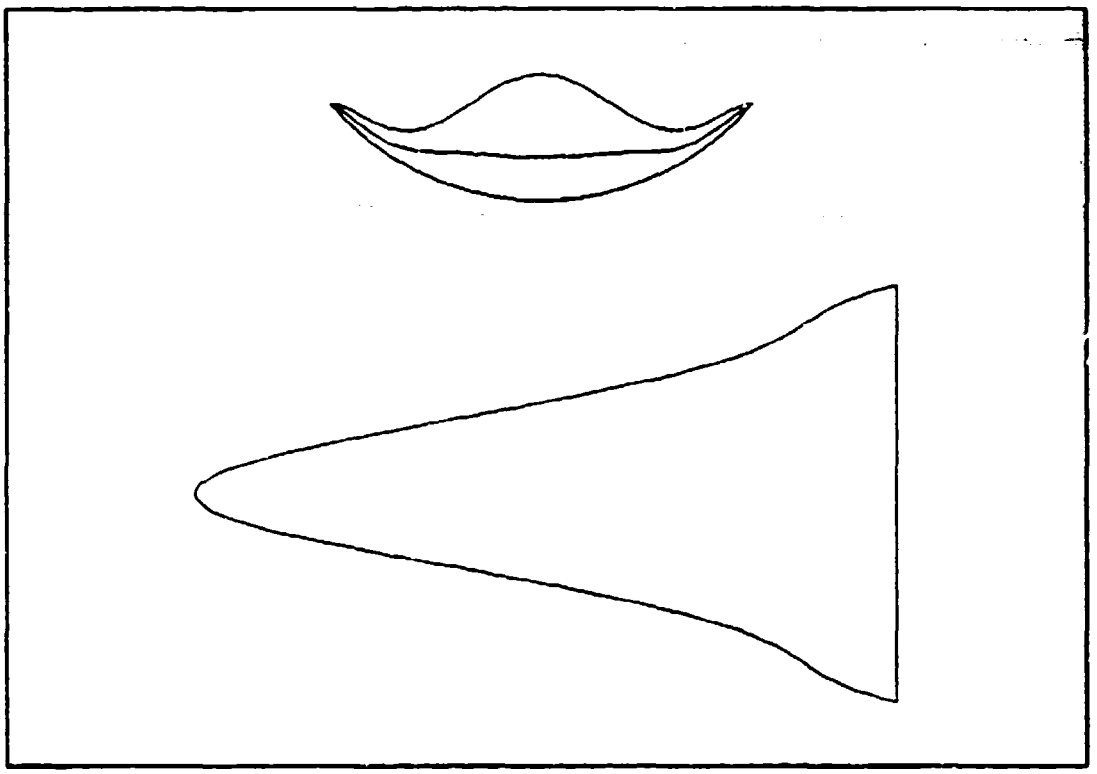

Figure C.44

Table C.44

Phi =50.0	Delta = 8.0	Mach =10.0	Rey = 0.10E+07	Gamma = 1.40
Y = 0.700 + 1.516 Y^2 + -2.600 Y^4 + 1.225 Y^6				
Cftav = 0.002013	CL = 0.041670		CD = 0.008993	
Sw/Sp = 2.114785	V^(2/3)/Sp = 0.174308		(L/D)vis = 4.633659	
Ab/Abi = 0.410119	V/Vi = 0.195705		Sp/Spi = 0.439305	
b/lw = 0.599945	SSD = 0.211550			

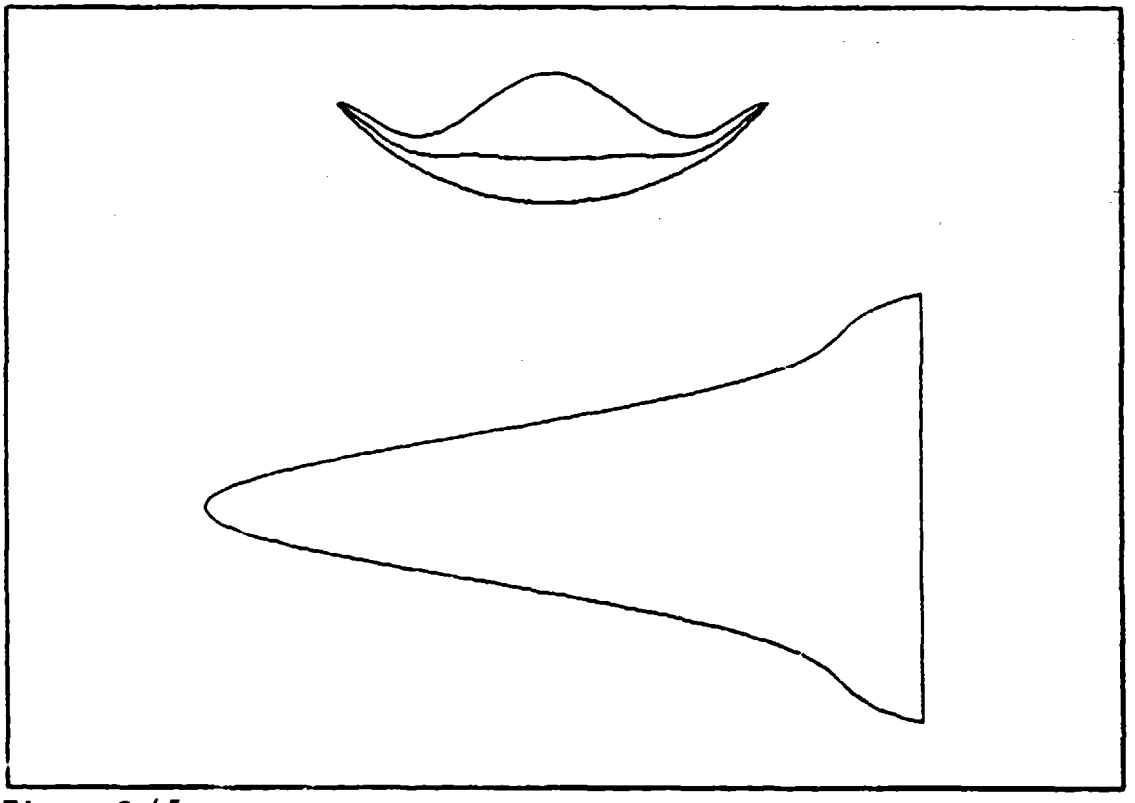

Figure C.45

Table C.45

Phi =50.0	Delta = 8.0	Mach =10.0	Rey = 0.10E+07	Gamma = 1.40
Y = 0.700 + 1.717 Y^2 + -3.000 Y^4 + 1.424 Y^6				
Cftav = 0.002039	CL = 0.041657	CD = 0.009076		
Sw/Sp = 2.140448	V^(2/3)/Sp = 0.176001	(L/D)vis = 4.589540		
Ab/Abi = 0.389474	V/Vi = 0.185009	Sp/Spi = 0.419079		
b/lw = 0.599945	SSD = 0.211550			

APPENDIX D

Presented here are configurations that have the following parameters held fixed:

$$\Phi_1 = 40, \quad \delta = 8, \quad M = 10, \quad Rey = 1X10^6$$

The following parameters are varied:

R_0 from 0.4 to 0.8

b_4 from 0.0 to -2.0

The values of b_2 and b_6 are such that equation 2-13 and condition (iii) holds.

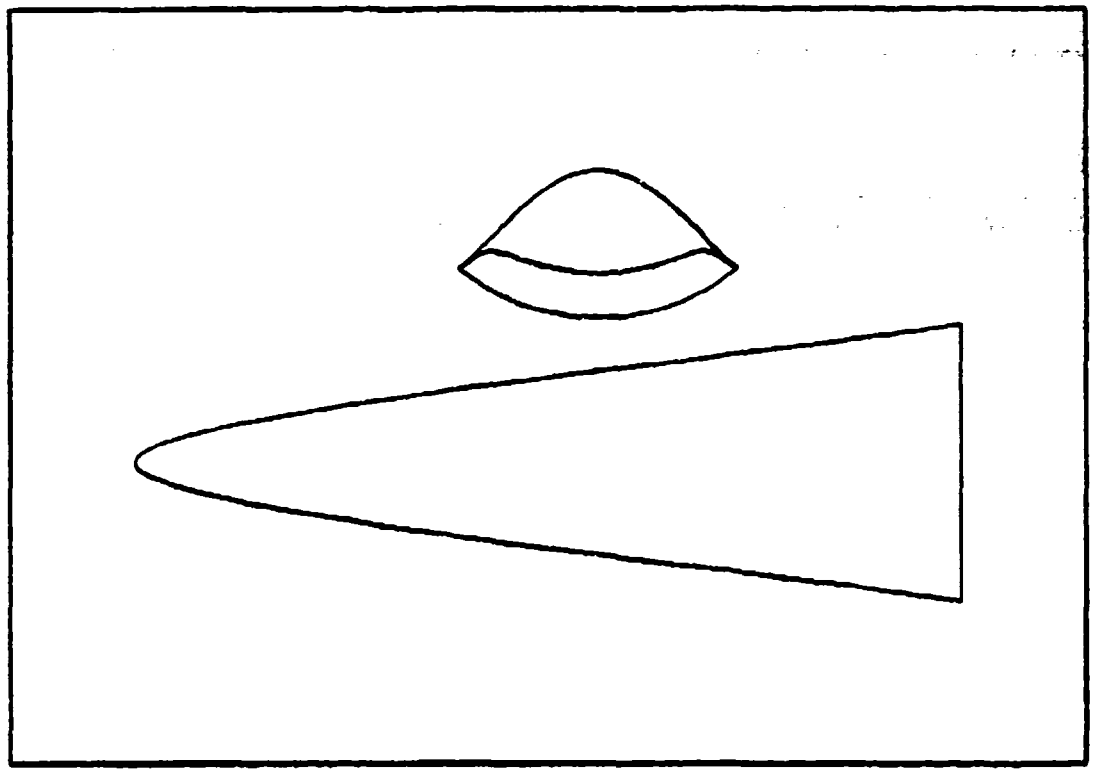

Figure D.1

Table D.1

Phi =40.0	Delta = 8.0	Mach =10.0	Rey = 0.10E+07	Gamma = 1.40
I = 0.400 + 1.070 Y^2 + 0.000 Y^4 + -0.436 Y^6				
Cftav = 0.001872	CL = 0.043280		CD = 0.000168	
Sw/Sp = 2.226448	Y^(2/3)/Sp = 0.210626		(L/D)vis = 4.725829	
Ab/Abi = 0.818486	Y/Yi = 0.646468		Sp/Spi = 0.826151	
b/lw = 0.337233	SSD = 0.270033			

D1

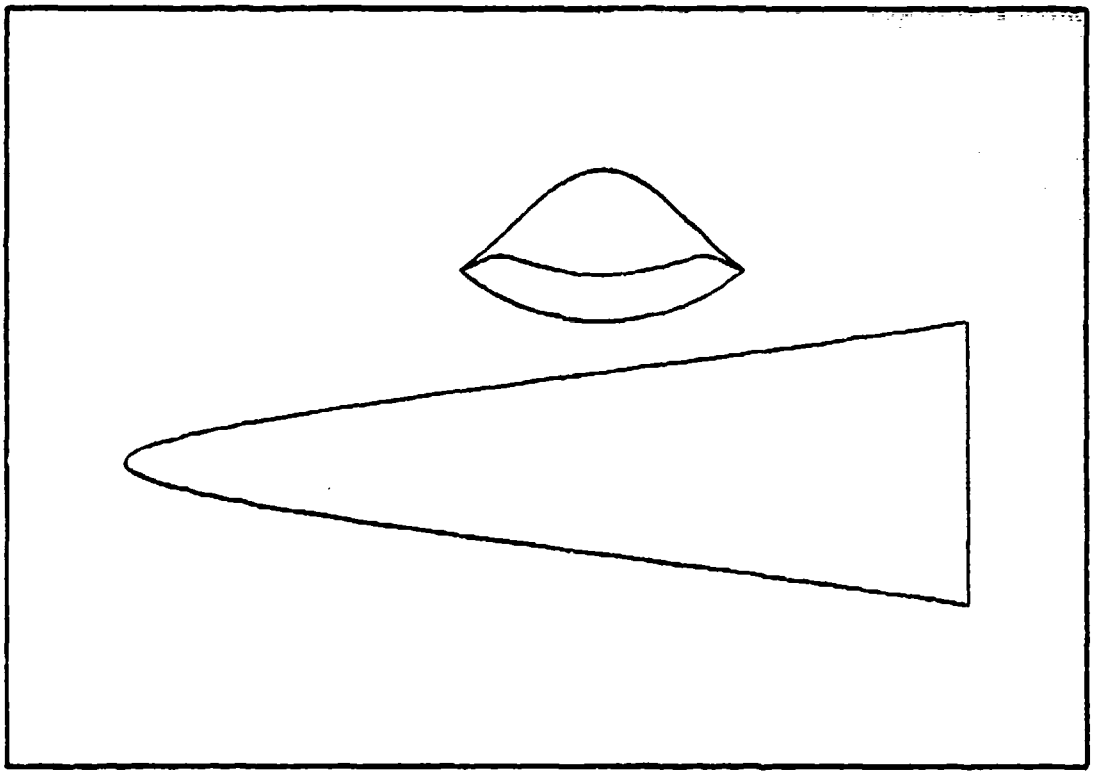

Figure D.2

Table D.2

Phi :40.0	Delta : 8.0	Mach :10.0	Rey : 0.10E+07	Gamma : 1.40
Y : 0.400 + 1.424 Y^2 + -1.600 Y^4 + 0.270 Y^6				
Cftav : 0.001875	CL : 0.043219		CD : 0.009140	
Sw/Sp : 2.227960	V^(2/3)/Sp : 0.209891		(L/D)vis : 4.728425	
Ab/Abi : 0.791594	V/Vi : 0.615215		Sp/Spi : 0.804055	
b/lw : 0.387233	SSD : 0.276033			

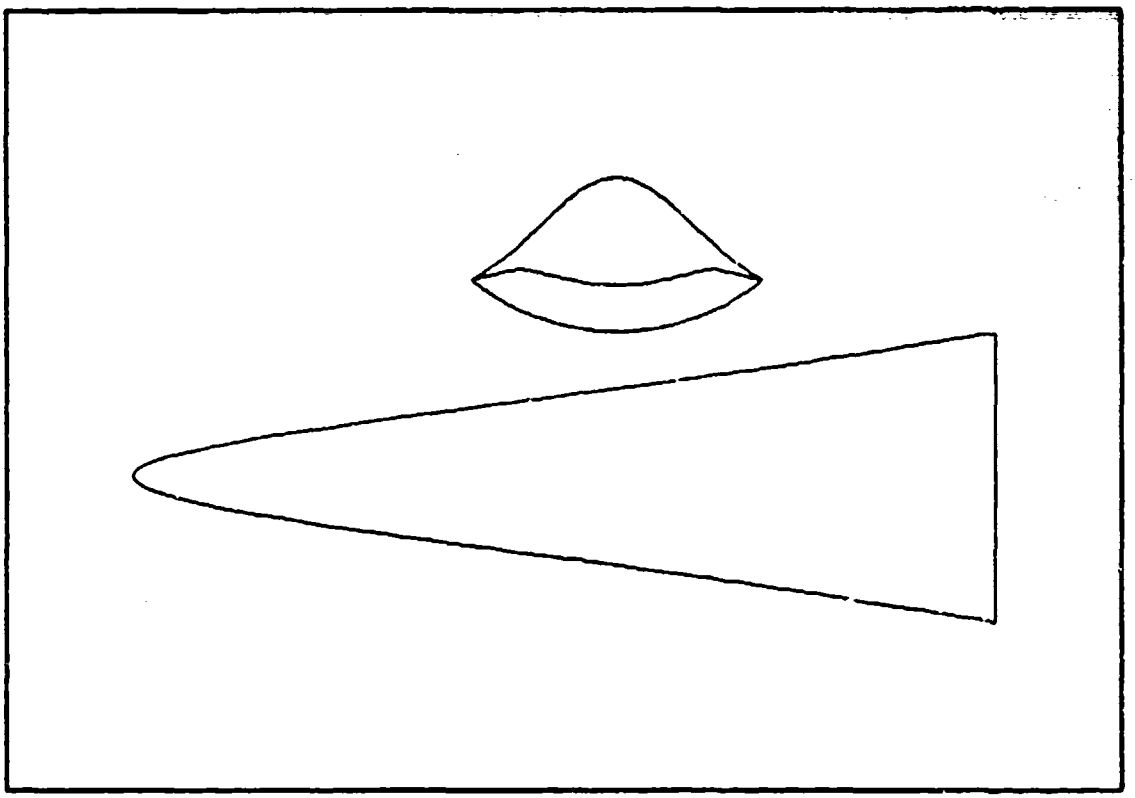

Figure D.3

Table D.3

Phi =40.0	Delta = 8.0	Mach =10.0	Rey = 0.10E+07	Gamma = 1.40
Y = 0.400 + 1.778 Y^2 + -2.000 Y^4 + 0.977 Y^6				
Cftav = 0.001879	CL = 0.043162	CD = 0.009145		
Sw/Sp = 2.240033	V^(2/3)/Sp = 0.209406	(L/D)vis = 4.719671		
Ab/Abi = 0.764796	V/Vi = 0.585466	Sp/Spi = 0.779723		
b/lw = 0.337233	SSD = 0.276033			

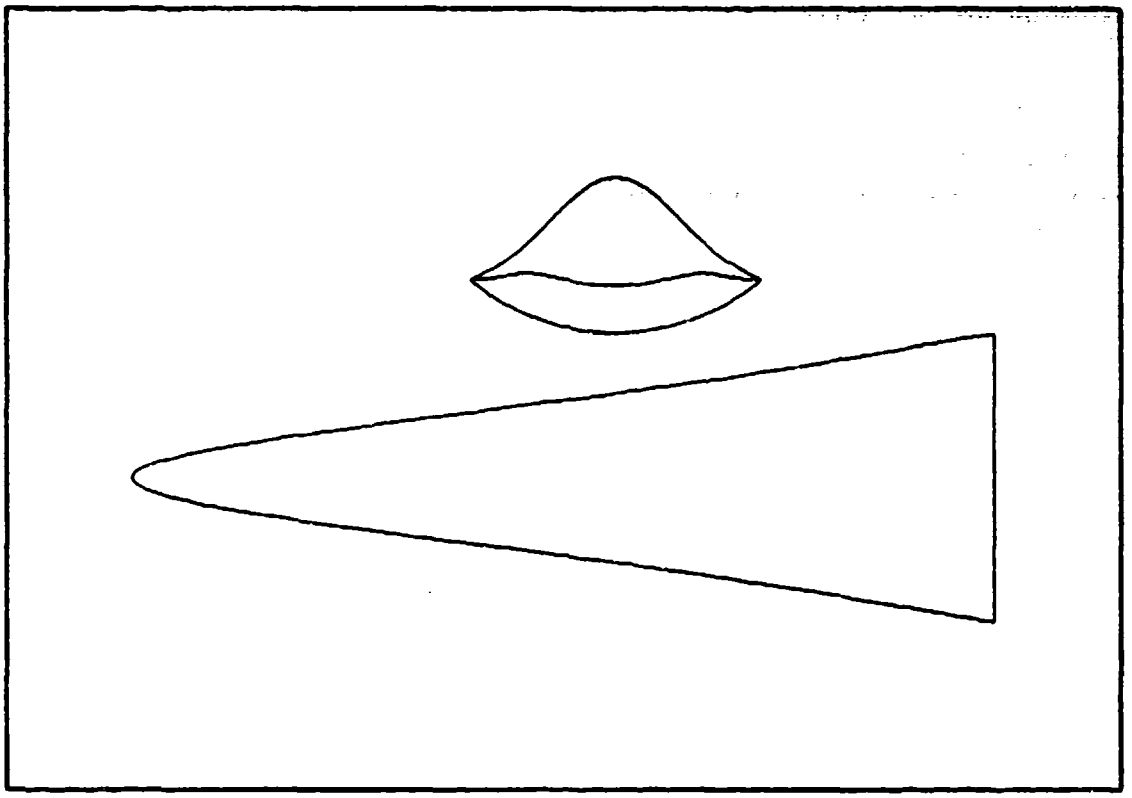

Figure D.4

Table D.4

Phi =40.0	Delta = 8.0	Mach =10.0	Rey = 0.10E+07	Gamma = 1.40
Y = 0.400 + 2.132 Y^2 + -3.000 Y^4 + 1.682 Y^6				
Cftav = 0.001883	CL = 0.043109	CD = 0.009172		
Sw/Sp = 2.262038	V^(2/3)/Sp = 0.209216	(L/D)vis = 4.700094		
Ab/Abi = 0.737809	V/Vi = 0.557007	Sp/Spi = 0.754930		
b/lw = 0.337233	SSD = 0.276033			

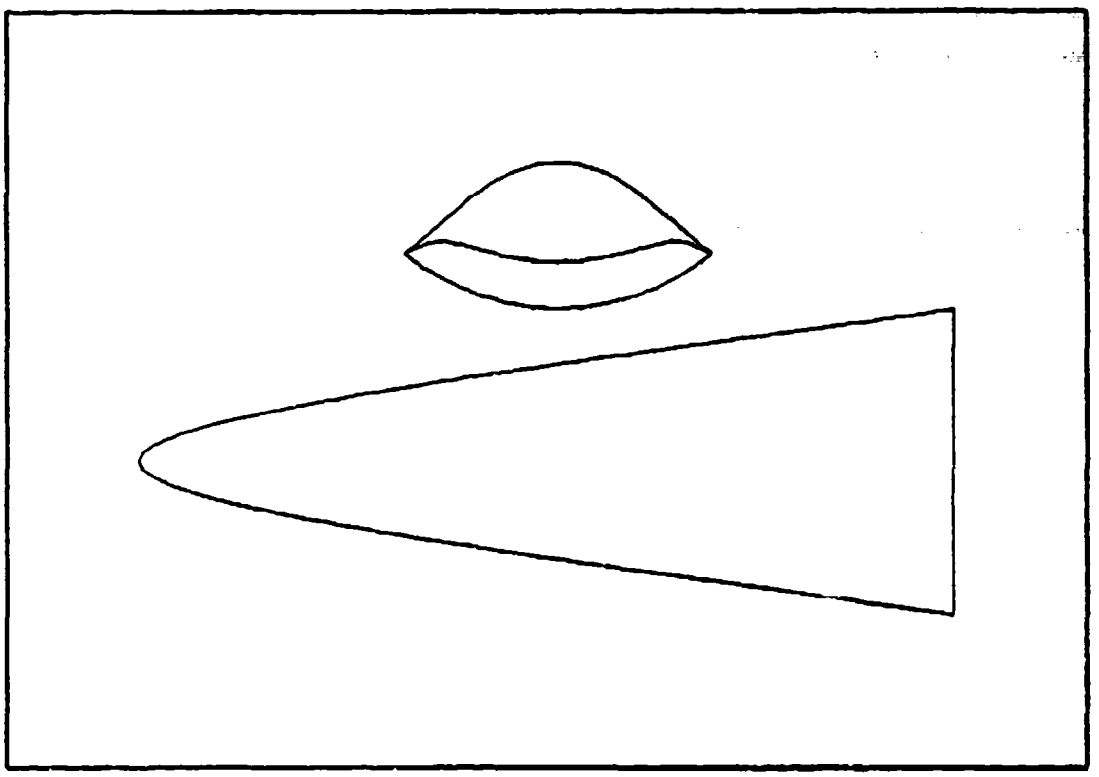

Figure D.5

Table D.5

Phi :40.0	Delta = 8.0	Mach :10.0	Rey = 0.10E+07	Gamma = 1.40
Y = 0.500 + 0.858 Y^2 + 0.000 Y^4 + -0.295 Y^6				
Cftav = 0.001859	CL = 0.042861		CD = 0.008915	
Sw/Sp = 2.151700	V^(2/3)/Sp = 0.201529		(L/D)vis = 4.807703	
Ab/Ab1 = 0.738083	V/V1 = 0.521240		Sp/Sp1 = 0.749808	
b/lw = 0.378929	SSD = 0.258054			

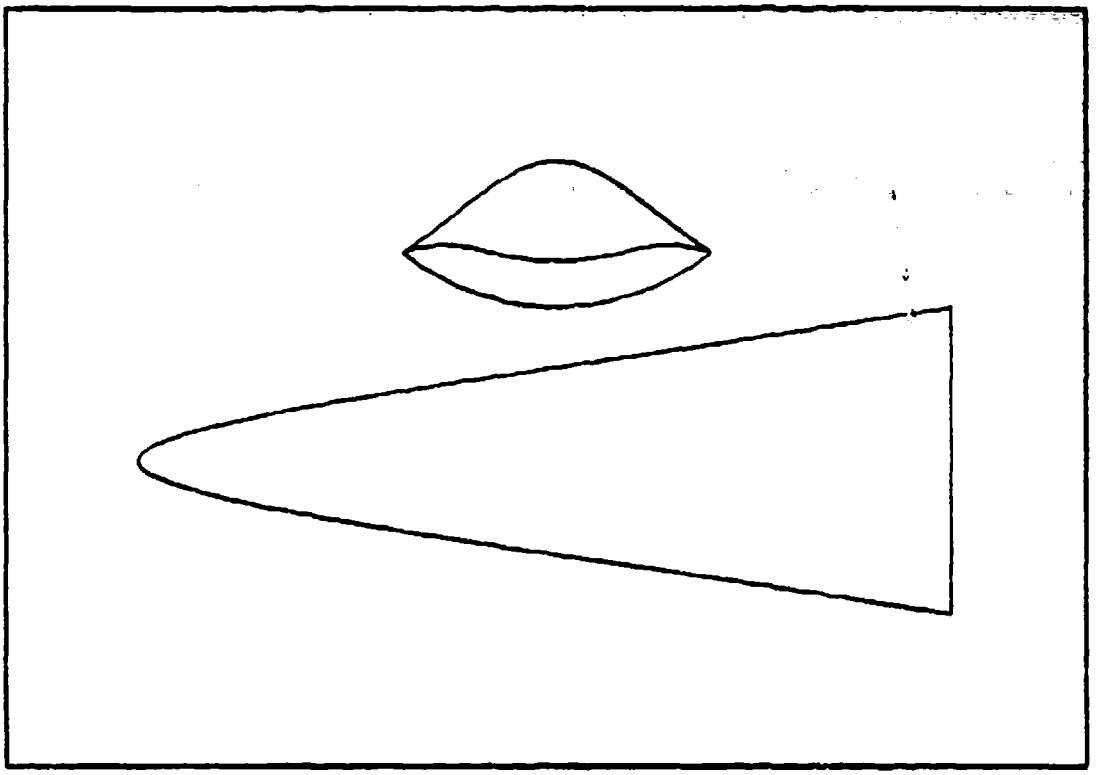

Figure D.6

Table D.6

Phi :40.0	Delta : 8.0	Mach :10.0	Rey : 0.10E+07	Gamma : 1.40
Y = 0.500 + 1.212 Y^2 + -1.000 Y^4 + 0.411 Y^6				
Cftav : 0.001868	CL : 0.042795		CD : 0.008912	
Sw/Sp : 2.154438	V^(2/3)/Sp : 0.200740		(L/D)vis : 4.801750	
Ab/Abi : 0.711191	V/Vi : 0.492838		Sp/Spi : 0.725149	
b/lw : 0.378929	SSD : 0.258054			

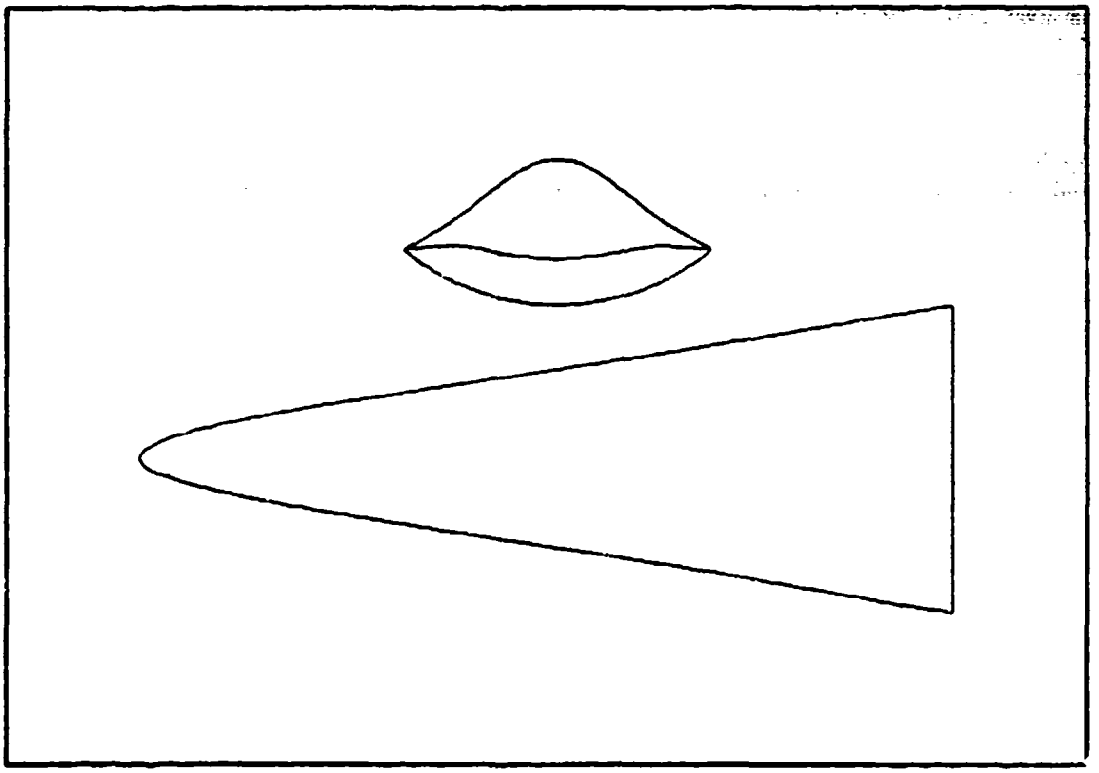

Figure D.7

Table D.7

Phi =40.0	Delta = 8.0	Mach =10.0	Rey = 0.10E+07	Gamma = 1.40
I = 0.500 + 1.566 Y^2 + -2.000 Y^4 + 1.118 Y^6				
Cftav = 0.001877	CL = 0.042733		CD = 0.008931	
Sw/Sp = 2.167306	V^(2/3)/Sp = 0.200233		(L/D)vis = 4.785007	
Ab/Abi = 0.684393	V/Vi = 0.465955		Sp/Spi = 0.700308	
b/lw = 0.378929	SSD = 0.258054			

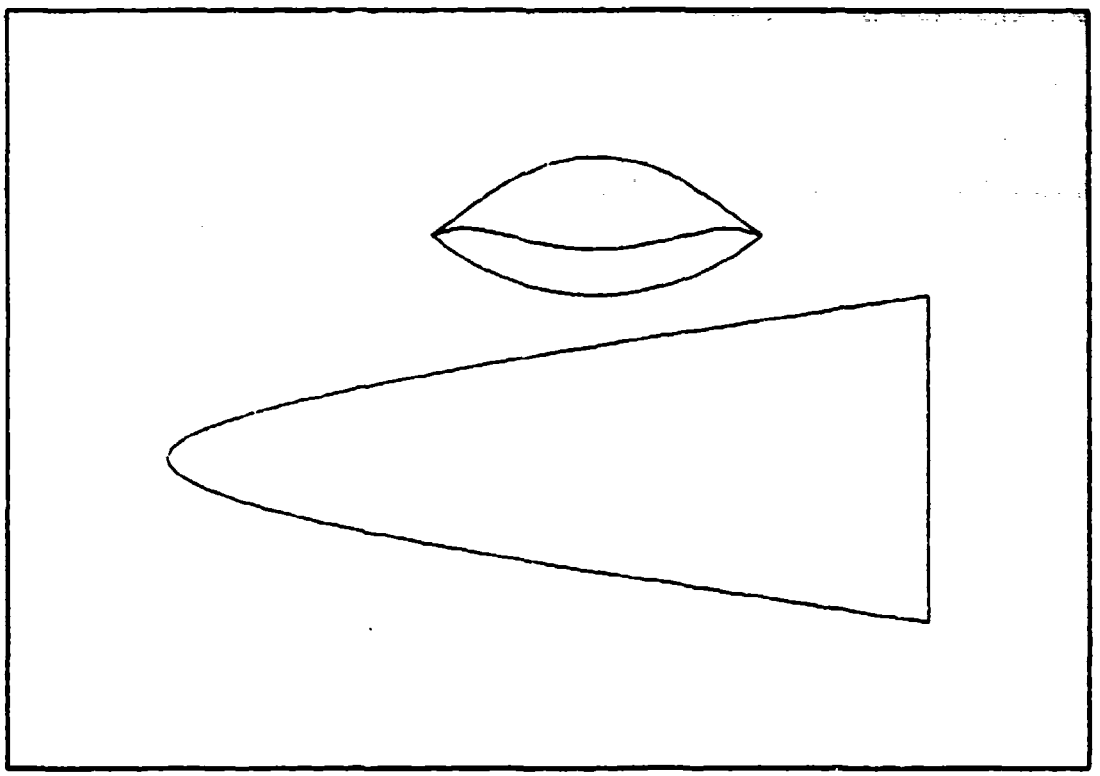

Figure D.8

Table D.8

Phi =40.0	Delta = 8.0	Mach =10.0	Rey = 0.10E+07	Gamma = 1.40
Y = 0.600 + 0.646 Y^2 + 0.000 Y^4 + -0.154 Y^6				
Cftav = 0.001847	CL = 0.042424		CD = 0.008715	
Sw/Sp = 2.095432	V^(2/3)/Sp = 0.191944		(L/D)vis = 4.868124	
Ab/Abi = 0.657681	V/Vi = 0.409299		Sp/Spi = 0.870060	
b/lw = 0.432390	SSD = 0.236489			

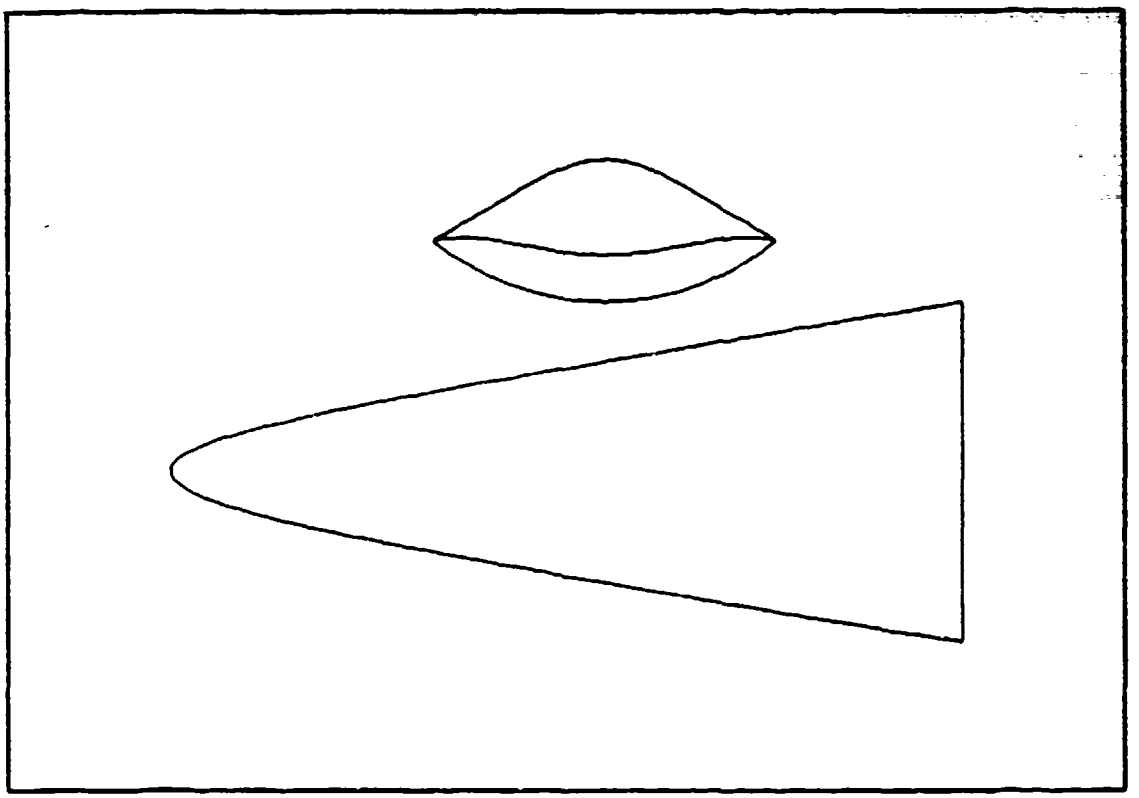

Figure D.9

Table D.9

Phi =40.0	Delta = 8.0	Mach =10.0	Rey = 0.10E+07	Gamma = 1.40
Y = 0.600 + 1.000 Y^2 + -1.000 Y^4 + 0.552 Y^6				
Cftav = 0.001862	CL = 0.042353	CD = 0.008725		
Sw/Sp = 2.097926	V^(2/3)/Sp = 0.191047	(L/D)vis = 4.853993		
Ab/Abi = 0.630788	V/Vi = 0.383805	Sp/Spi = 0.644953		
b/lw = 0.432390	SSD = 0.236489			

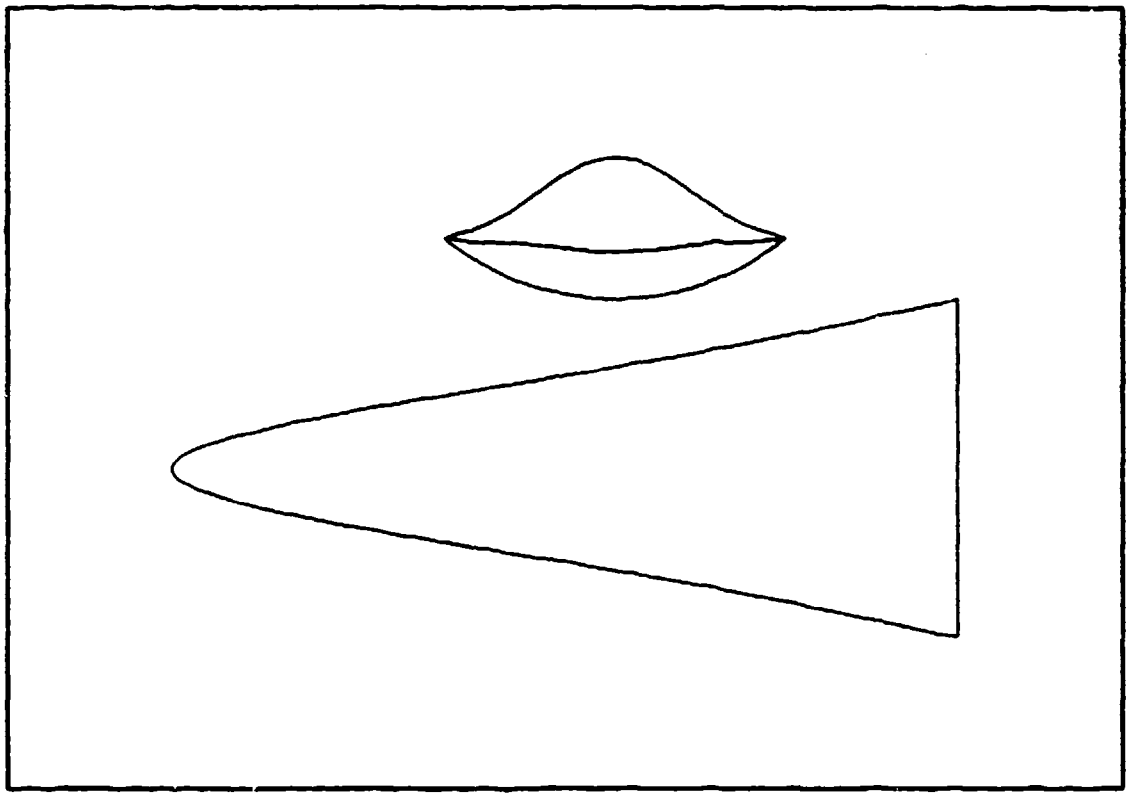

Figure D.10

Table D.10

Phi =40.0	Delta = 8.0	Mach =10.0	Rey = 0.10E+07	Gamma = 1.40
X = 0.600 + 1.457 Y^2 + -2.000 Y^4 + 1.053 Y^6				
Cftav = 0.001884	CL = 0.042278	CD = 0.008783		
Sw/Sp = 2.127193	V^(2/3)/Sp = 0.191596	(L/D)vis = 4.813523		
Ab/Abi = 0.584419	V/Vi = 0.347349	Sp/Spi = 0.801709		
b/lw = 0.432390	SSD = 0.236489			

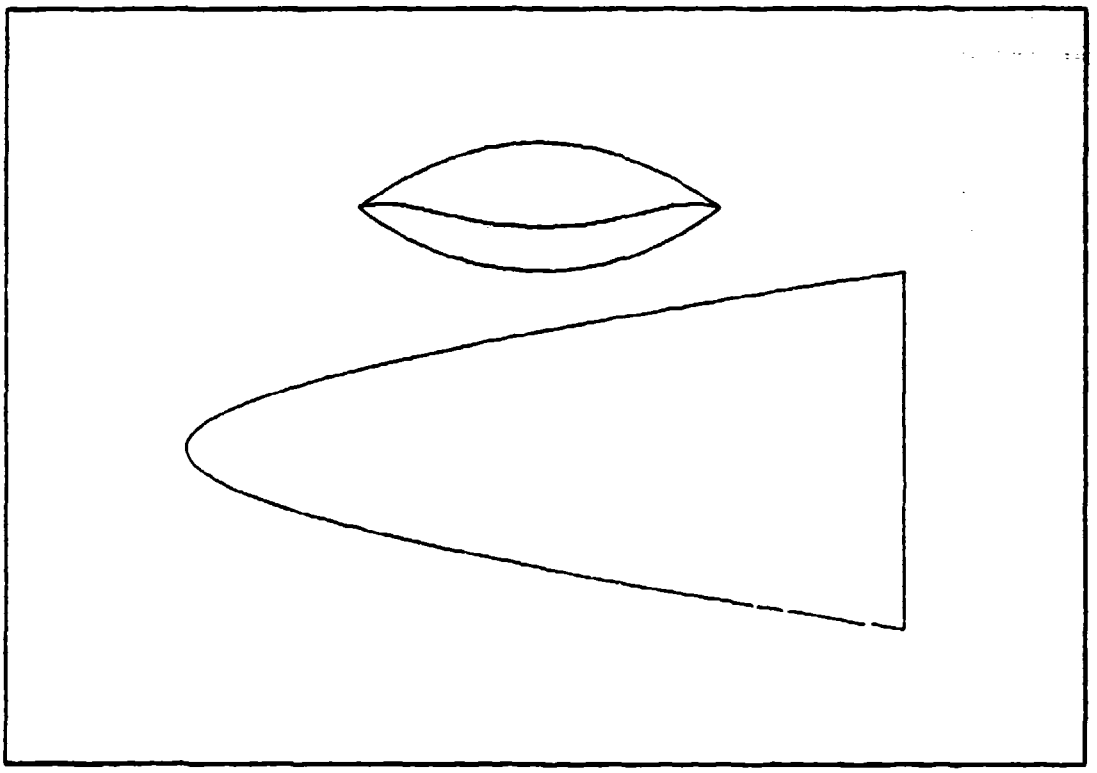

Figure D.11

Table D.11

Phi =40.0	Delta = 8.0	Mach =10.0	Rey = 0.10E+07	Gamma = 1.40
Y = 0.700 + 0.434 Y^2 + 0.000 Y^4 + -0.013 Y^6				
Cftav = 0.001833		CL = 0.041974		CD = 0.008546
Sw/Sp = 2.055271		V^(2/3)/Sp = 0.181677		(L/D)vis = 4.911695
Ab/Abi = 0.577278		V/Vi = 0.310836		Sp/Spi = 0.589272
b/lw = 0.503414		SSD = 0.211550		

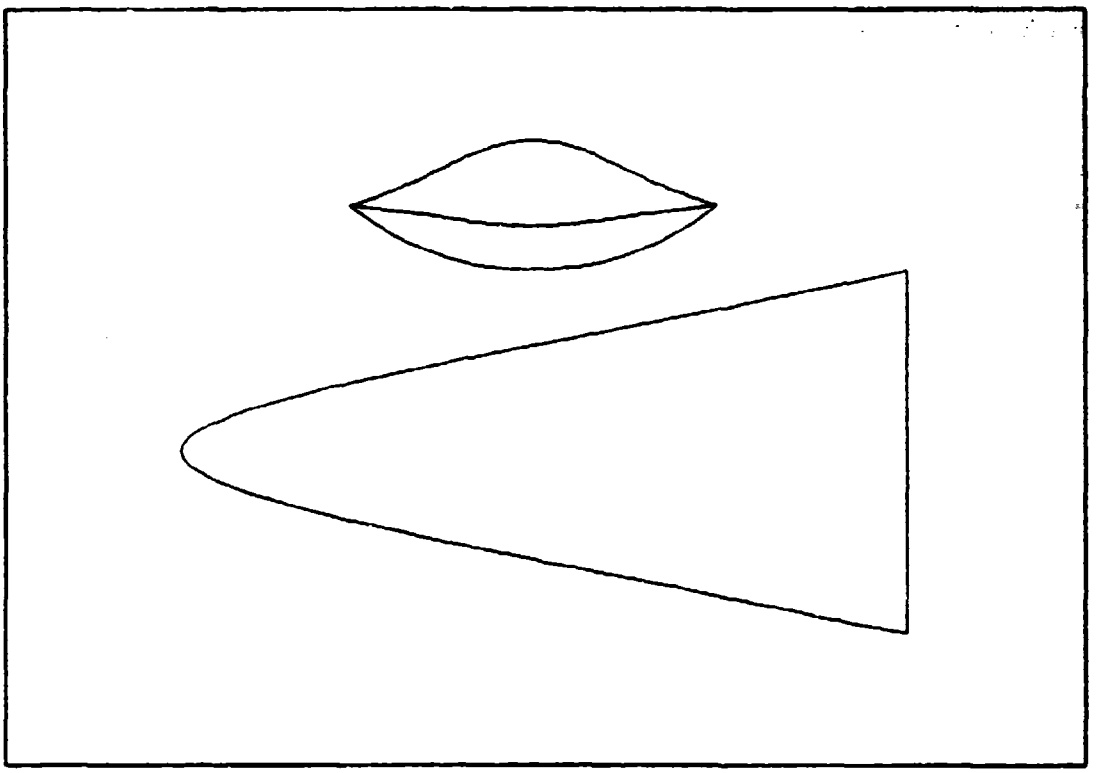

Figure D.12

Table D.12

Phi =40.0	Delta = 8.0	Mach =10.0	Rey = 0.10E+07	Gamma = 1.40
X = 0.700 + 0.891 Y^2 + -1.000 Y^4 + 0.487 Y^6				
Cftav = 0.001866	CL = 0.041880		CD = 0.008588	
Sw/Sp = 2.065478	V^(2/3)/Sp = 0.181381		(L/D)vis = 4.876789	
Ab/Ab1 = 0.530814	V/V1 = 0.276368		Sp/Sp1 = 0.545752	
b/lw = 0.503414	SSD = 0.211550			

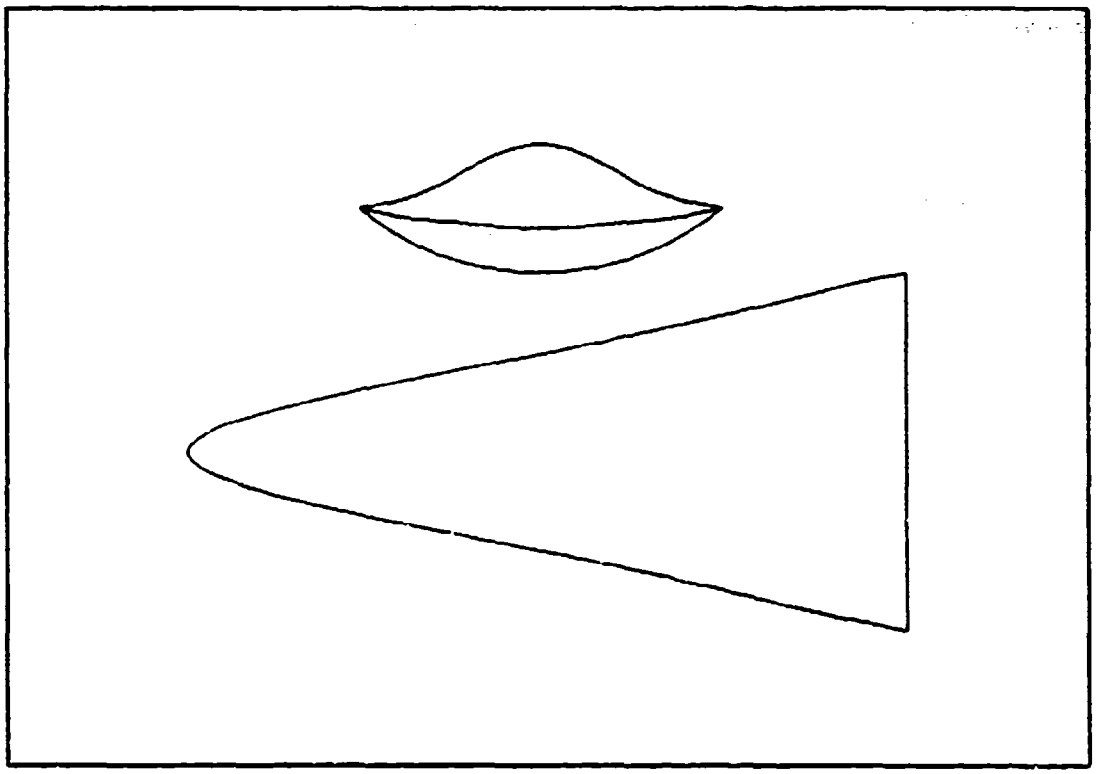

Figure D.13

Table D.13

Phi =40.0	Delta = 8.0	Mach =10.0	Rey = 0.10E+07	Gamma = 1.40
Y = 0.700 + 1.245 Y^2 + -2.000 Y^4 + 1.194 Y^6				
Cftav = 0.001891		CL = 0.041816		CD = 0.008642
Sw/Sp = 2.080921		V^(2/3)/Sp = 0.181055		(L/D)vis = 4.838609
Ab/Abi = 0.504016		V/Vi = 0.256373		Sp/Spi = 0.520036
b/lw = 0.503414		SSD = 0.211550		

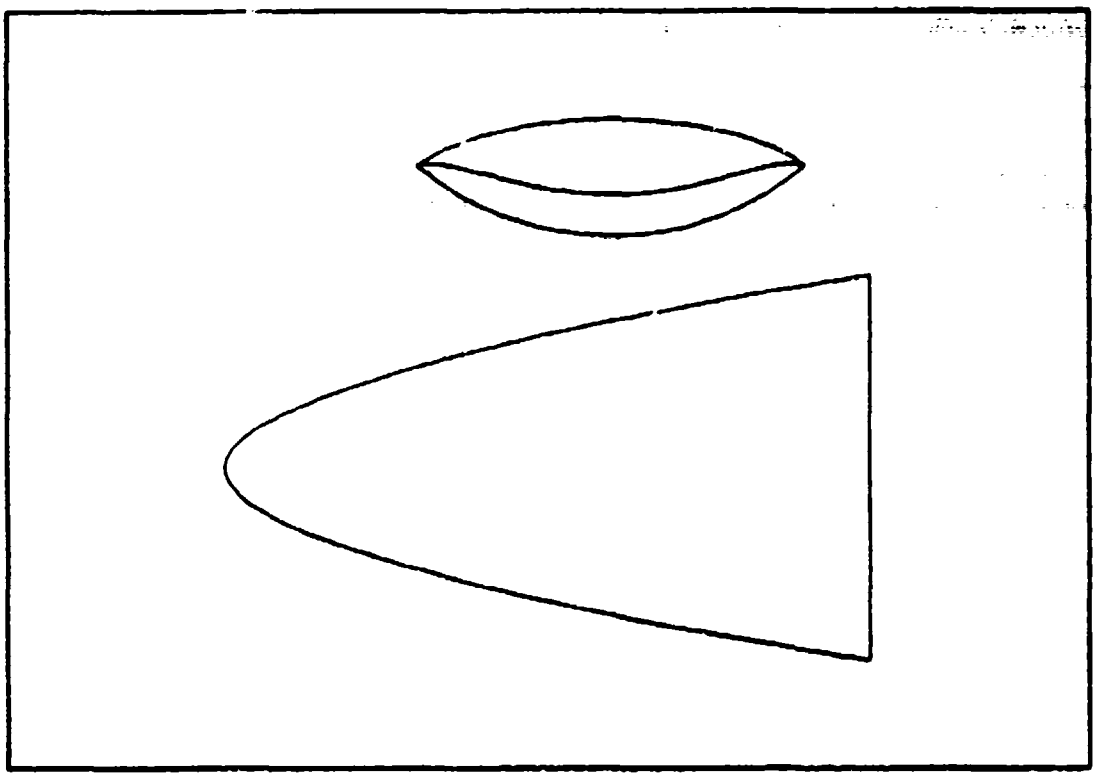

Figure D.14

Table D.14

Phi :40.0	Delta = 8.0	Mach =10.0	Rey = 0.10E+07	Gamma = 1.40
Y = 0.000 + 0.222 Y^2 + 0.000 Y^4 + 0.126 Y^6				
Cftav = 0.001814	CL = 0.041516		CD = 0.008402	
Sw/Sp = 2.031092	V^(2/3)/Sp = 0.170501		(L/D)vis = 4.941123	
Ab/Abi = 0.496875	V/Vi = 0.225988		Sp/Spi = 0.507682	
b/lw = 0.602357	SSD = 0.183460			

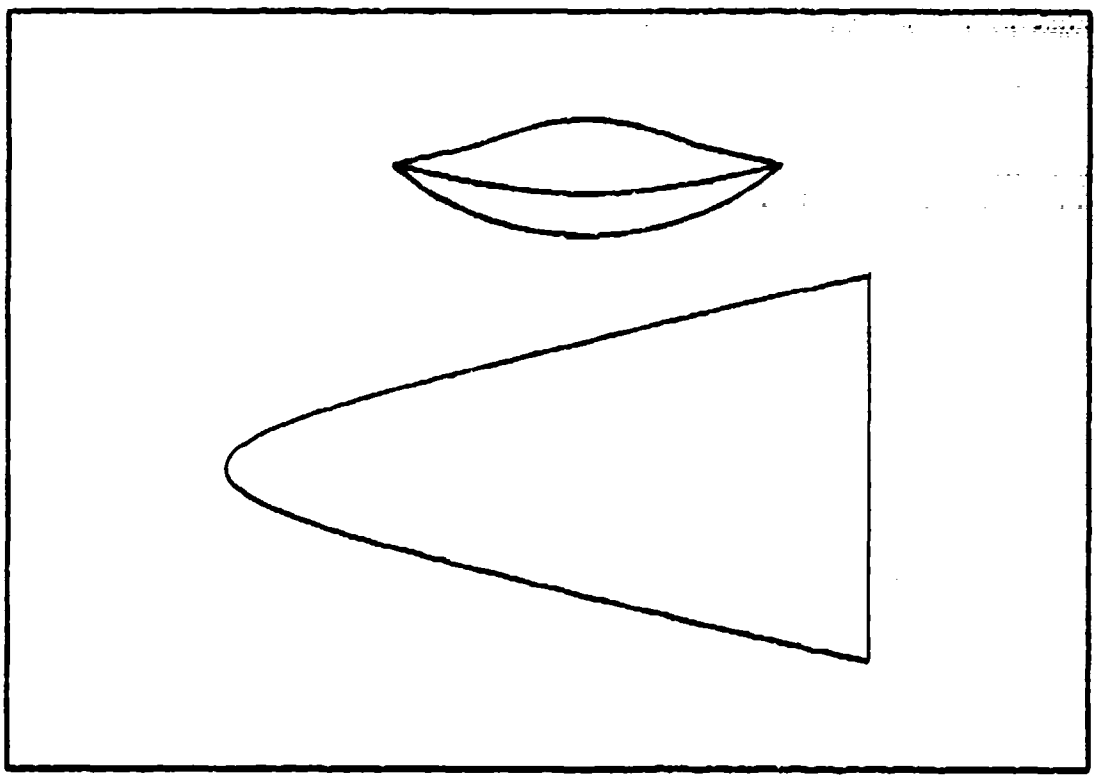

Figure D.15

Table D.15

Phi =40.0	Delta = 8.0	Mach =10.0	Rey = 0.10E+07	Gamma = 1.40
Y = 0.000 + 0.079 Y^2 + -1.000 Y^4 + 0.020 Y^6				
Cftav = 0.001864	CL = 0.041412		CD = 0.006462	
Sw/Sp = 2.035067	Y^(2/3)/Sp = 0.169021		(L/D)vis = 4.893869	
Ab/Abl = 0.450411	Y/Yl = 0.196078		Sp/Spl = 0.462694	
b/lw = 0.802357	SSD = 0.183460			

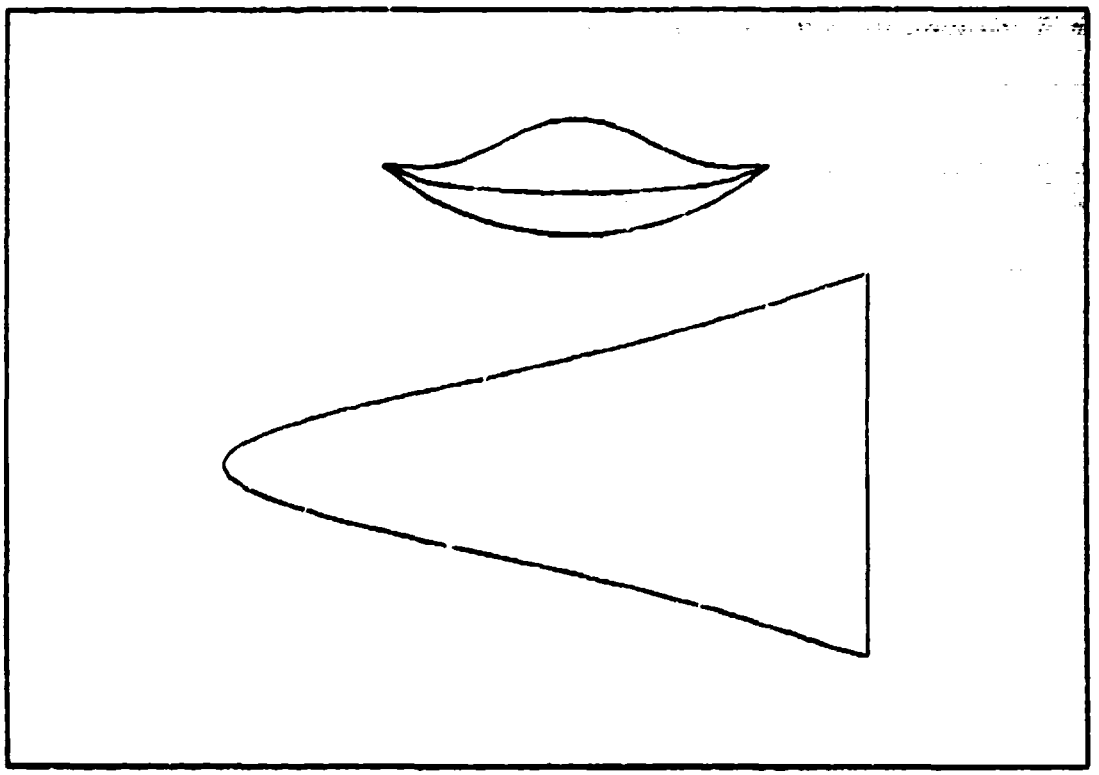

Figure D.16

Table D.16

Phi =40.0	Delta = 8.0	Mach =10.0	Rey = 0.10E+07	Gamma = 1.40
Y = 0.800 + 1.137 Y^2 + -2.000 Y^4 + 1.128 Y^6				
Cftav = 0.001915	CL = 0.041839		CD = 0.008571	
Sw/Sp = 2.061023	V^(2/3)/Sp = 0.171124		(L/D)vis = 4.823078	
Ab/Abi = 0.403946	V/Vi = 0.170474		Sp/Spi = 0.419171	
b/lw = 0.602357	SSD = 0.183460			

APPENDIX E

Presented here are configurations that have the following parameters held fixed:

$$\Phi_1 = 30, \quad \delta = 8, \quad M = 10, \quad Rey = 1X10^6$$

The following parameters are varied:

R_0 from 0.5 to 0.9

b_4 from 0.0 to -15.0

The values of b_2 and b_6 are such that equation 2-13 and condition (iii) holds.

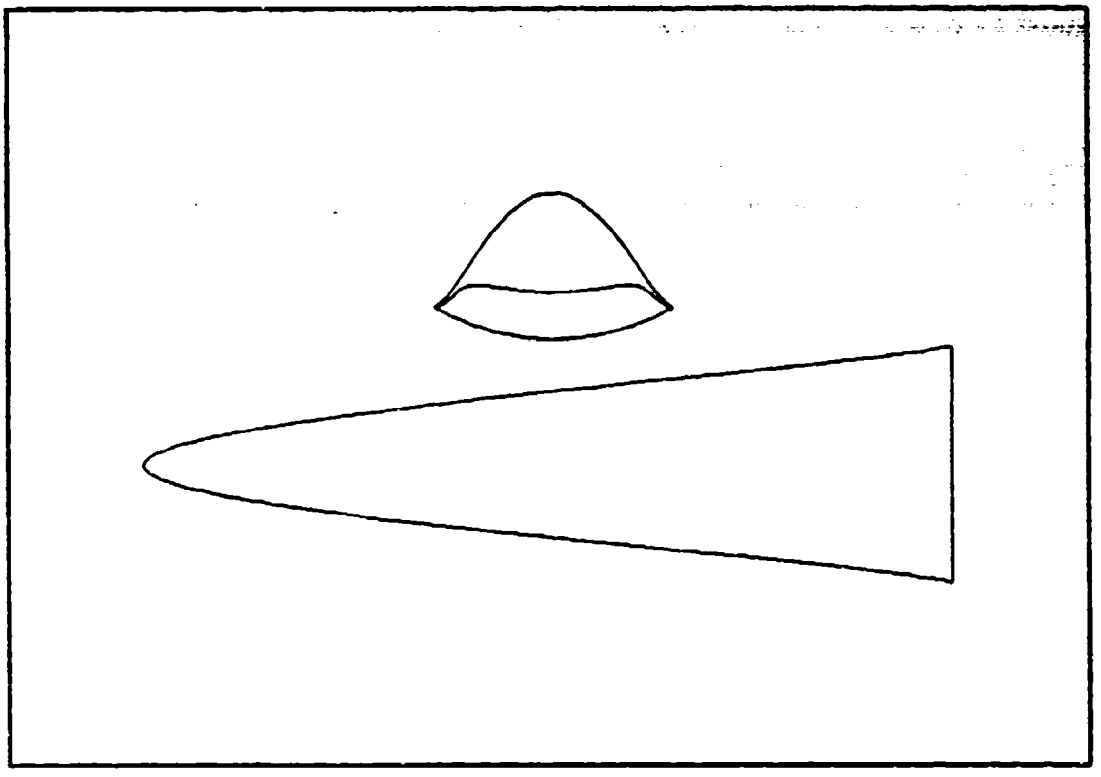

Figure E.1

Table E.1

Phi =30.0	Delta = 8.0	Mach =10.0	Rey = 0.10E+07	Gamma = 1.40
I = 0.500 + 2.019 Y^2 + 0.000 Y^4 + -2.943 Y^6				
Cftav = 0.001849	CL = 0.042870	CD = 0.009184		
Sw/Sp = 2.387981	V^(2/3)/Sp = 0.217357	(L/D)vis = 4.667721		
Ab/Abi = 0.725007	V/Vi = 0.515734	Sp/Spi = 0.732560		
b/lw = 0.294754	SSD = 0.258054			

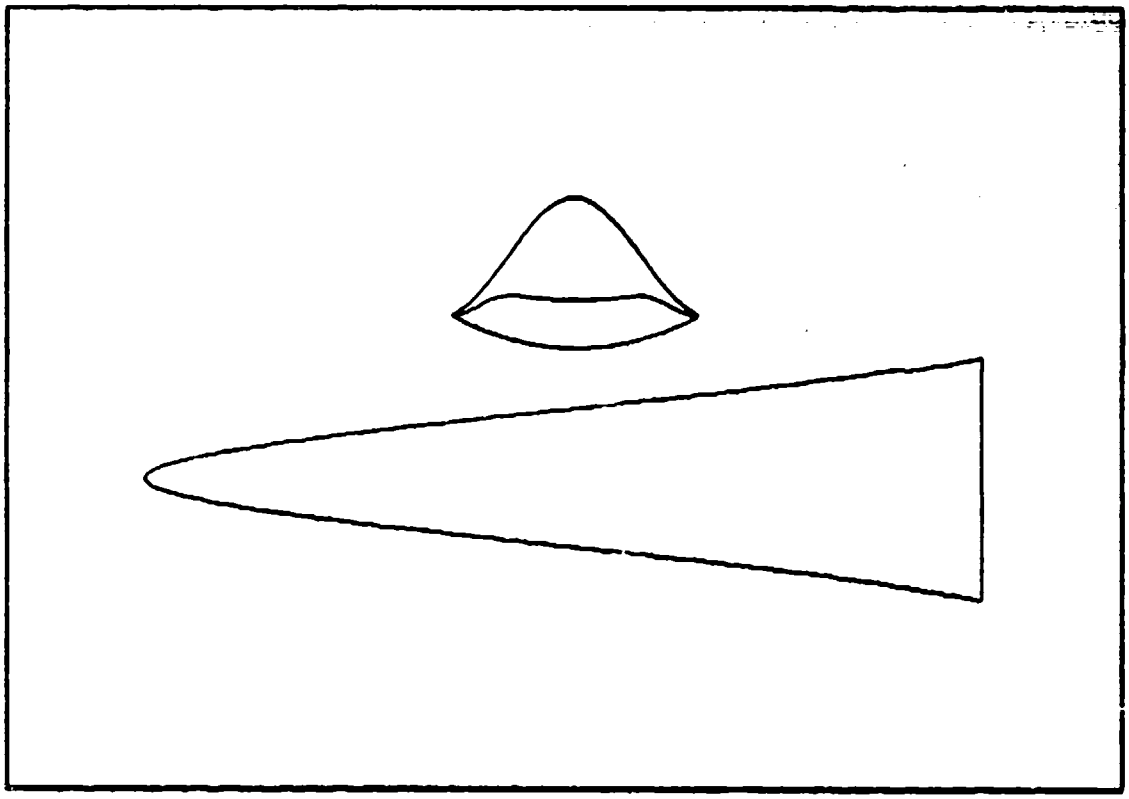

Figure E.2

Table E.2

Phi =30.0	Delta = 8.0	Mach =10.0	Rey = 0.10E+07	Gamma = 1.40
X = 0.500 + 3.089 Y^2 + -5.000 Y^4 + 2.895 Y^6				
Cftav = 0.001857	CL = 0.042758		CD = 0.009247	
Sw/Sp = 2.429212	V^(2/3)/Sp = 0.217310		(L/D)vis = 4.623816	
Ab/Abi = 0.674038	V/Vi = 0.464878		Sp/Spi = 0.683721	
b/lw = 0.294754	SSD = 0.258054			

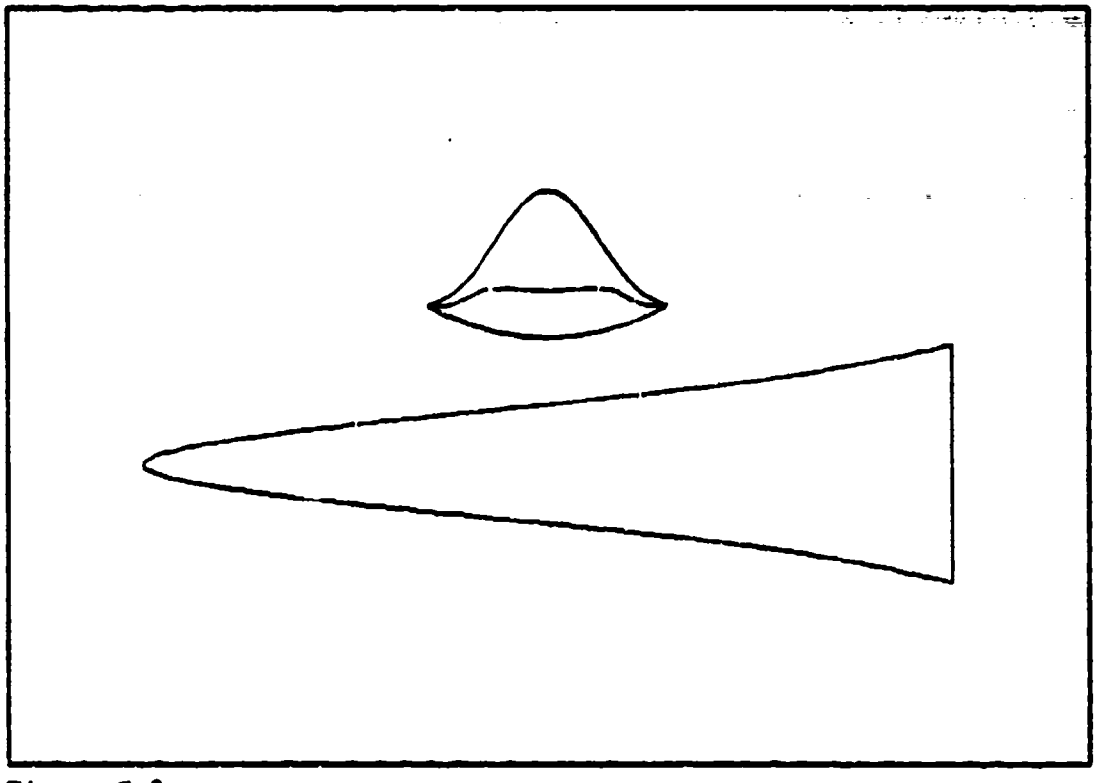

Figure E.3

Table E.3

Phi :30.0	Delta : 8.0	Mach :10.0	Rey : 0.10E+07	Gamma : 1.40
X : 0.500 + 4.160 Y^2 + -10.000 Y^4 + 8.733 Y^6				
Cftav : 0.001866	CL : 0.042671		CD : 0.009392	
Sw/Sp : 2.509903	Y^(2/3)/Sp : 0.218706		(L/D)vis : 4.543412	
Ab/Abi : 0.623966	V/Vi : 0.419516		Sp/Spi : 0.634407	
b/lw : 0.294754	SSD : 0.258054			

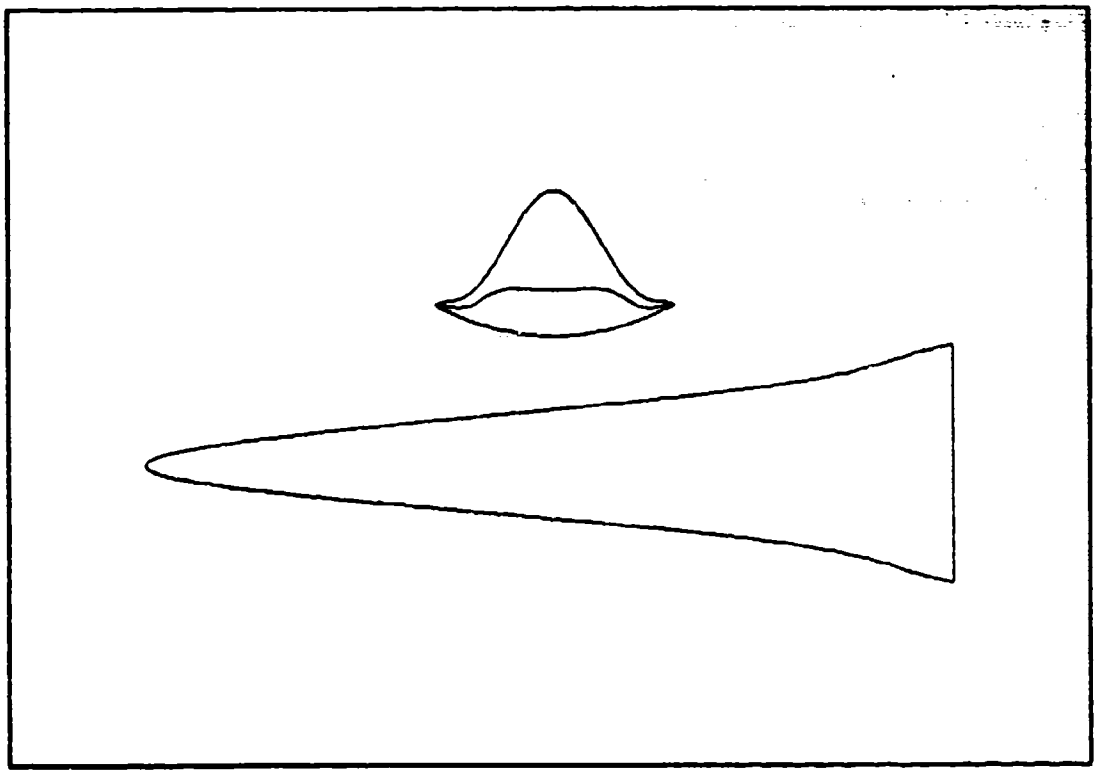

Figure E.4

Table E.4

Phi =30.0	Delta = 8.0	Mach =10.0	Rey = 0.10E+07	Gamma = 1.40
I = 0.500 + 5.212 Y^2 + -15.000 Y^4 + 14.670 Y^6				
Cftav = 0.001879	CL = 0.042616	CD = 0.009808		
Sw/Sp = 2.620803	V^(2/3)/Sp = 0.221677	(L/D)vis = 4.435354		
Ab/Abi = 0.574256	V/Vi = 0.380793	Sp/Spi = 0.586776		
b/lw = 0.294754	SSD = 0.258054			

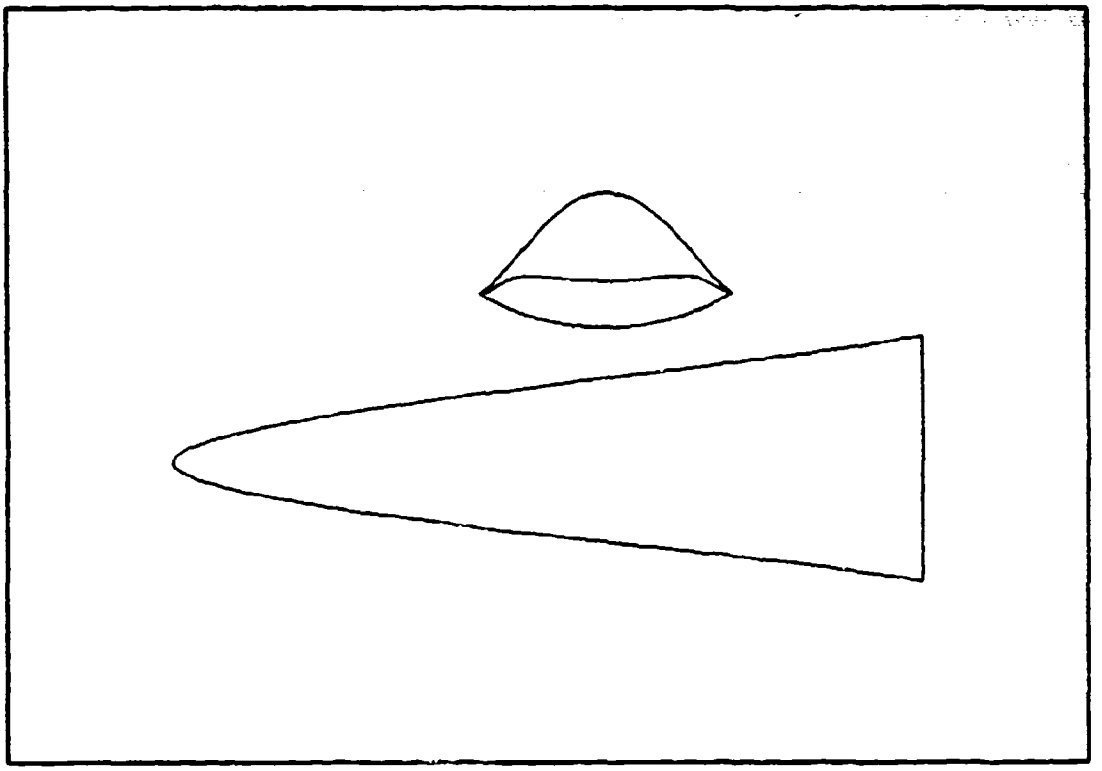

Figure E.5

Table E.5

Phi =30.0	Delta = 8.0	Mach =10.0	Rey = 0.10E+07	Gamma = 1.40
X = 0.600 + 1.669 Y^2 + 0.000 Y^4 + -2.306 Y^6				
Cftav = 0.001845	CL = 0.042420	CD = 0.008904		
Sw/Sp = 2.277009	V^(2/3)/Sp = 0.207252	(L/D)vis = 4.764273		
Ab/Abi = 0.641628	V/Vi = 0.400941	Sp/Spi = 0.649562		
b/lw = 0.336339	SSD = 0.236489			

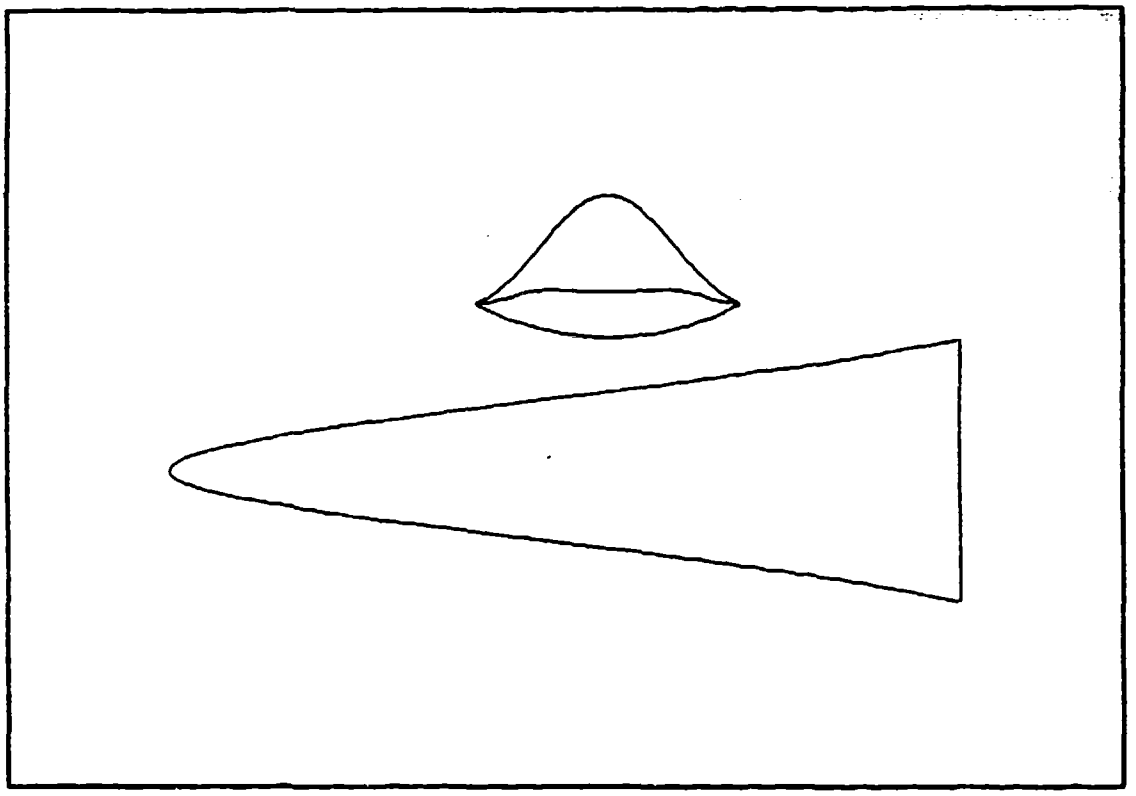

Figure E.6

Table E.6

Phi =30.0	Delta = 8.0	Mach =10.0	Rey = 0.10E+07	Gamma = 1.40
Y = 0.600 + 2.739 Y^2 + -5.000 Y^4 + 3.531 Y^6				
Cftav = 0.001863	CL = 0.042302	CD = 0.008987		
Sw/Sp = 2.317458	V^(2/3)/Sp = 0.207171	(L/D)vis = 4.707104		
Ab/Abi = 0.590635	V/Vi = 0.355951	Sp/Spi = 0.600247		
b/lw = 0.336339	SSD = 0.236489			

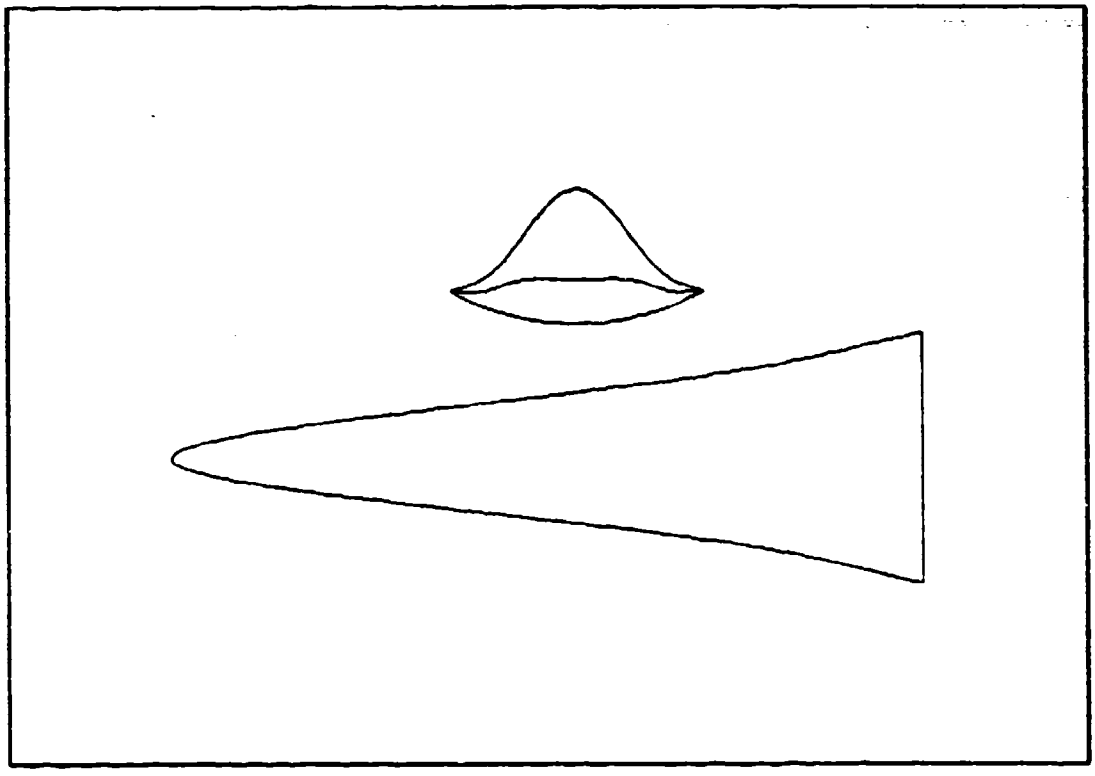

Figure E.7

Table E.7

Phi =30.0	Delta = 8.0	Mach =10.0	Rey = 0.10E+07	Gamma = 1.40
Y = 0.600 + 3.810 Y^2 + -10.000 Y^4 + 9.369 Y^6				
Cftav = 0.001881	CL = 0.042215	CD = 0.009155		
Sw/Sp = 2.399240	V^(2/3)/Sp = 0.208868	(L/D)vis = 4.611248		
Ab/Abi = 0.539665	V/Vi = 0.316522	Sp/Spi = 0.550550		
b/lw = 0.336339	SSD = 0.236489			

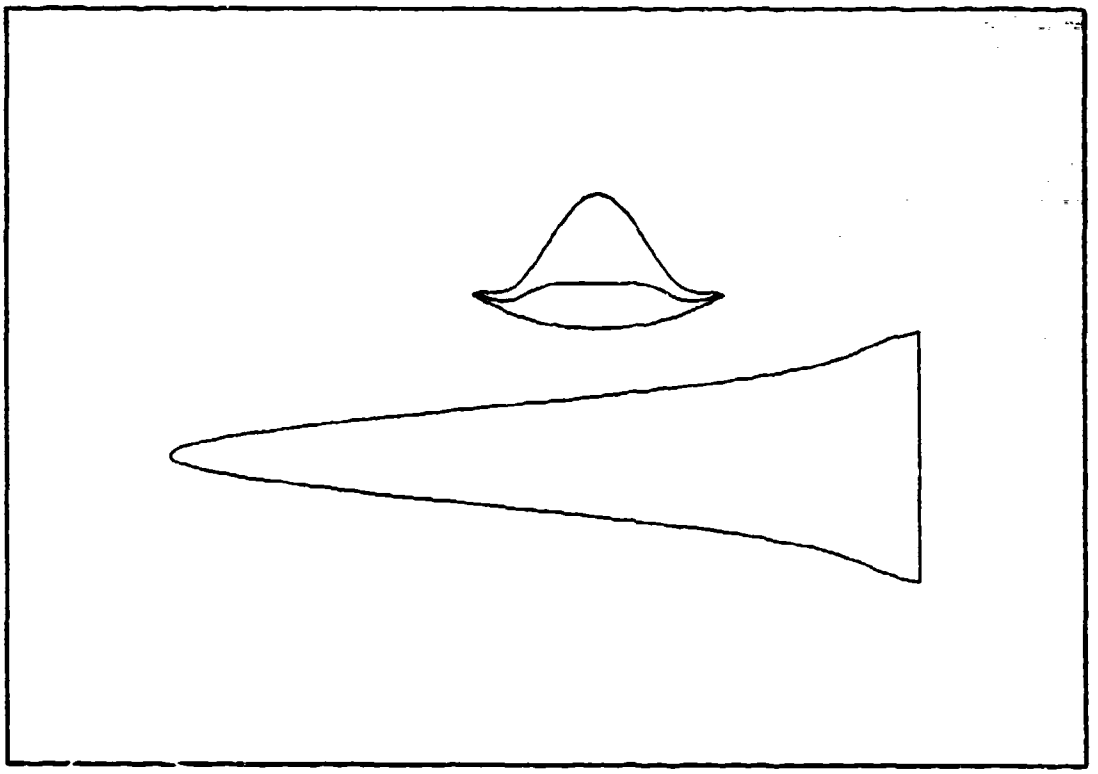

Figure E.8

Table E.8

Phi =30.0	Delta = 8.0	Mach =10.0	Rey = 0.10E+07	Gamma = 1.40
Y = 0.600 + 4.981 Y^2 + -15.000 Y^4 + 15.205 Y^6				
Cftav = 0.001902	CL = 0.042170	CD = 0.009410		
Sw/Sp = 2.518831	V^(2/3)/Sp = 0.213079	(L/D)vis = 4.481304		
Ab/Abi = 0.488651	V/Vi = 0.282666	Sp/Spi = 0.500467		
b/lw = 0.536339	SSD = 0.236489			

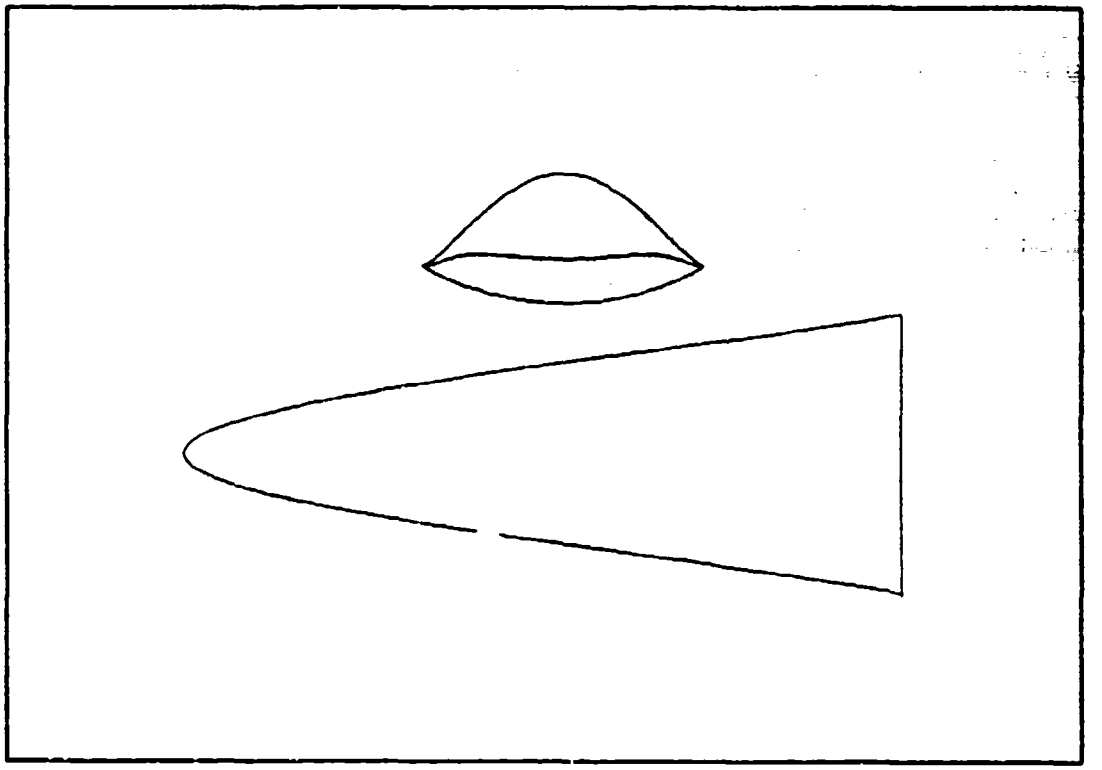

Figure E.9

Table E.9

Phi :30.0	Delta : 8.0	Mach :10.0	Rey : 0.10E+07	Gamma : 1.40
I : 0.700 + 1.318 Y^2 + 0.000 Y^4 + -1.867 Y^6				
Cftav : 0.001840	CL : 0.041957		CD : 0.008657	
Sw/Sp : 2.183216	V^(2/3)/Sp : 0.196271		(L/D)vis : 4.846644	
Ab/Abi : 0.558292	V/Vi : 0.300542		Sp/Spi : 0.565997	
b/lw : 0.391586	SSD : 0.211550			

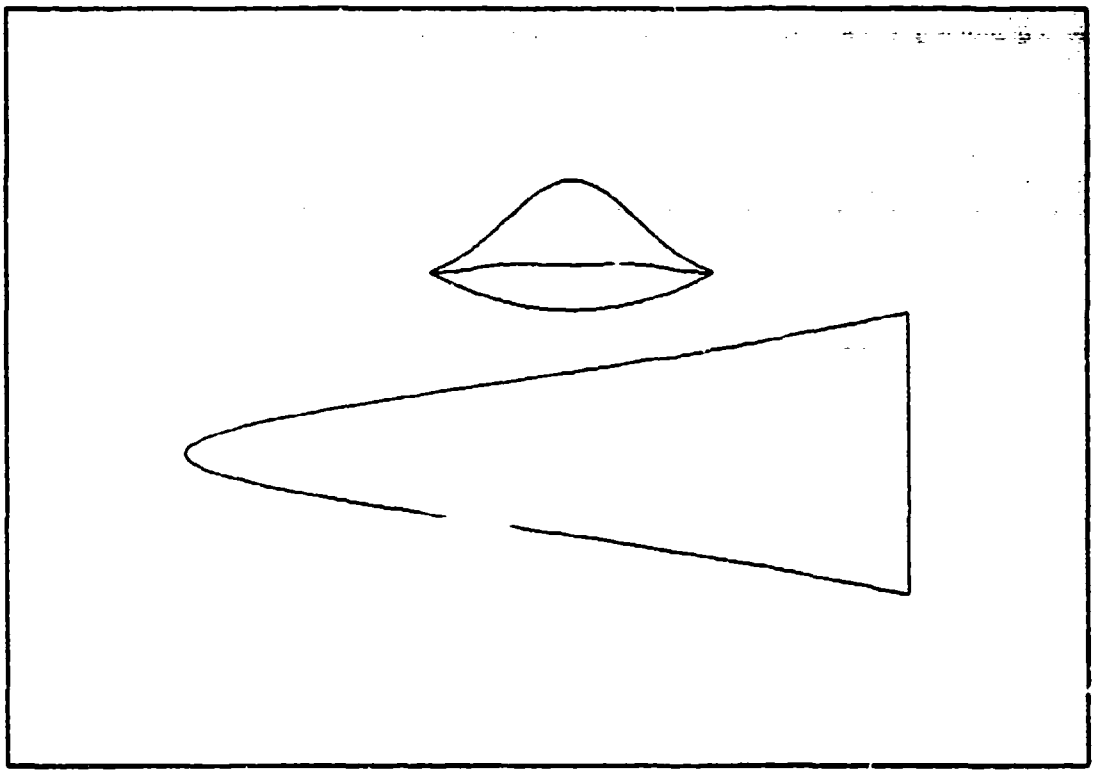

Figure E.10

Table E.10

Phi =30.0	Delta = 8.0	Mach =10.0	Rey = 0.19E+07	Gamma = 1.40
Y = 0.700 + 2.389 Y^2 + -5.000 Y^4 + 4.167 Y^6				
Cftav = 0.001871	CL = 0.041834		CD = 0.008763	
Sw/Sp = 2.221092	V^(2/3)/Sp = 0.196094		(L/D)vis = 4.774157	
Ab/Abi = 0.507235	V/Vi = 0.261449		Sp/Spi = 0.516250	
b/lw = 0.391586	SSD = 0.211550			

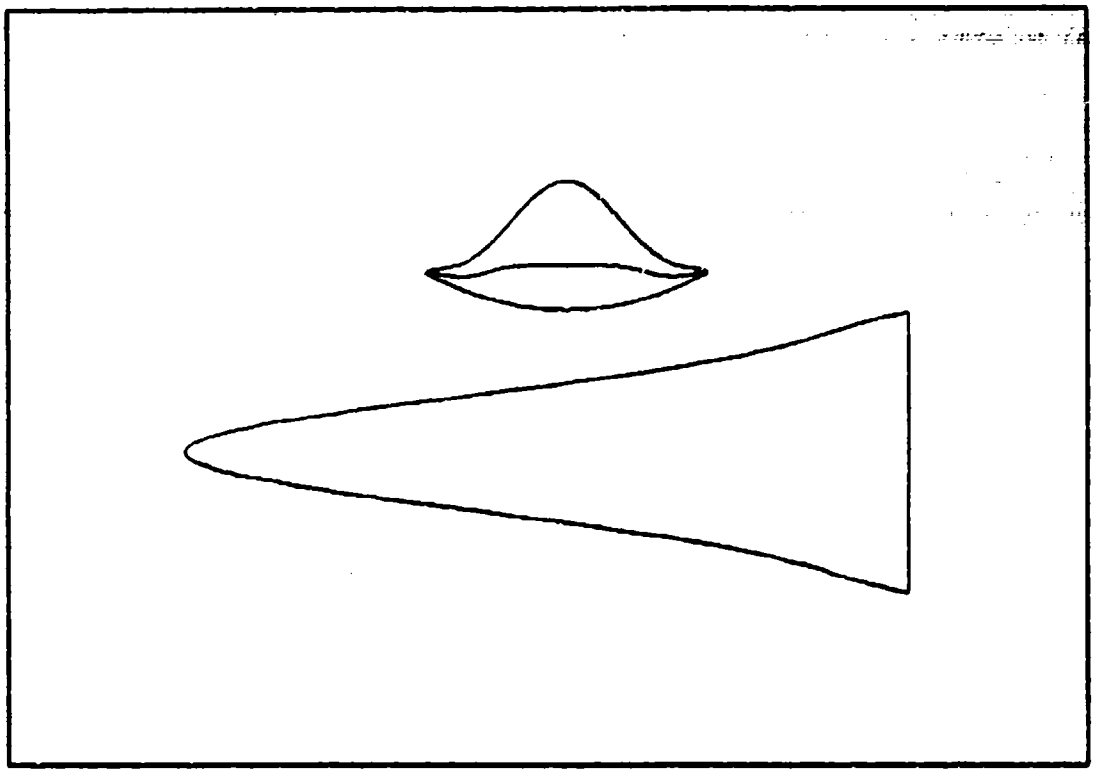

Figure E.11

Table E.11

Phi :30.0	Delta : 8.0	Mach :10.0	Rey : 0.10E+07	Gamma : 1.40
Y : 0.700 + 3.460 Y^2 + -10.000 Y^4 + 10.006 Y^6				
Cftav : 0.001903	CL : 0.041748		CD : 0.008959	
Sw/Sp : 2.302922	V^(2/3)/Sp : 0.198184		(L/D)vis : 4.658729	
Ab/Abi : 0.456286	V/Vi : 0.228006		Sp/Spi : 0.466260	
b/lw : 0.391586	SSD : 0.211550			

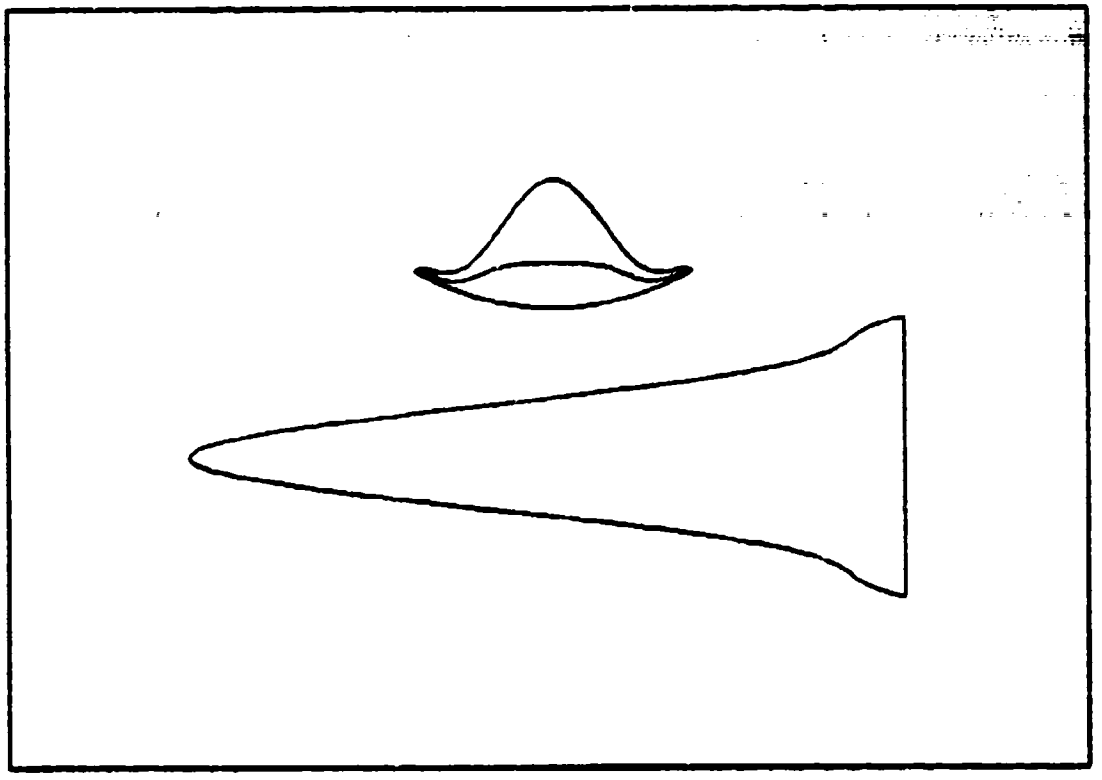

Figure E.12

Table E.12

Phi :30.0	Delta : 8.0	Mach :10.0	Rey : 0.10E+07	Gamma : 1.40
Y : 0.700 + 4.532 Y^2 + -15.000 Y^4 + 15.835 Y^6				
Cftav : 0.001936	CL : 0.041715		CD : 0.009249	
Sw/Sp : 2.424993	V^(2/3)/Sp : 0.203740		(L/D)vis : 4.510335	
Ab/Abi : 0.405119	V/Vi : 0.200114		Sp/Spi : 0.415759	
b/lw : 0.391586	SSD : 0.211550			

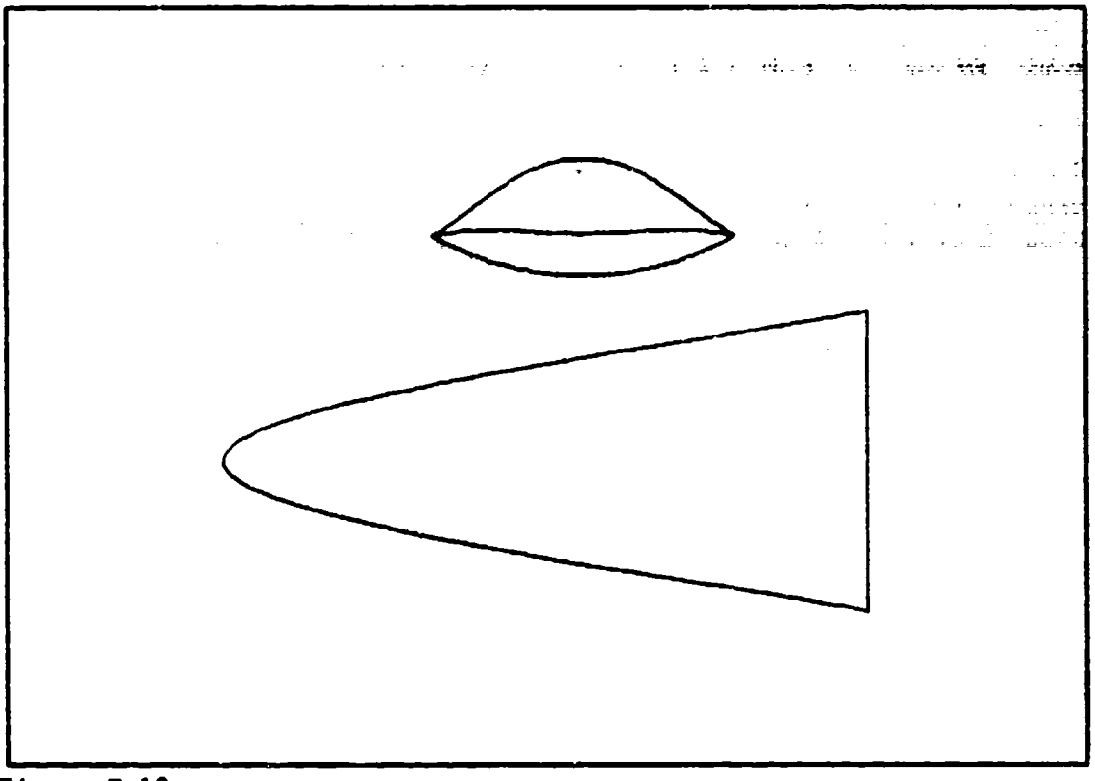

Figure E.13

Table E.13

Phi :30.0	Delta : 8.0	Mach :10.0	Rey : 0.10E+07	Gamma : 1.40
X : 0.800 + 0.968 Y^2 + 0.000 Y^4 + -1.033 Y^6				
Cftav : 0.001833	CL : 0.041485		CD : 0.008441	
Sw/Sp : 2.107252	V^(2/3)/Sp : 0.184133		(L/D)vis : 4.914905	
Ab/Abi : 0.474848	V/Vi : 0.214528		Sp/Spi : 0.481883	
b/lw : 0.468550	SSD : 0.183460			

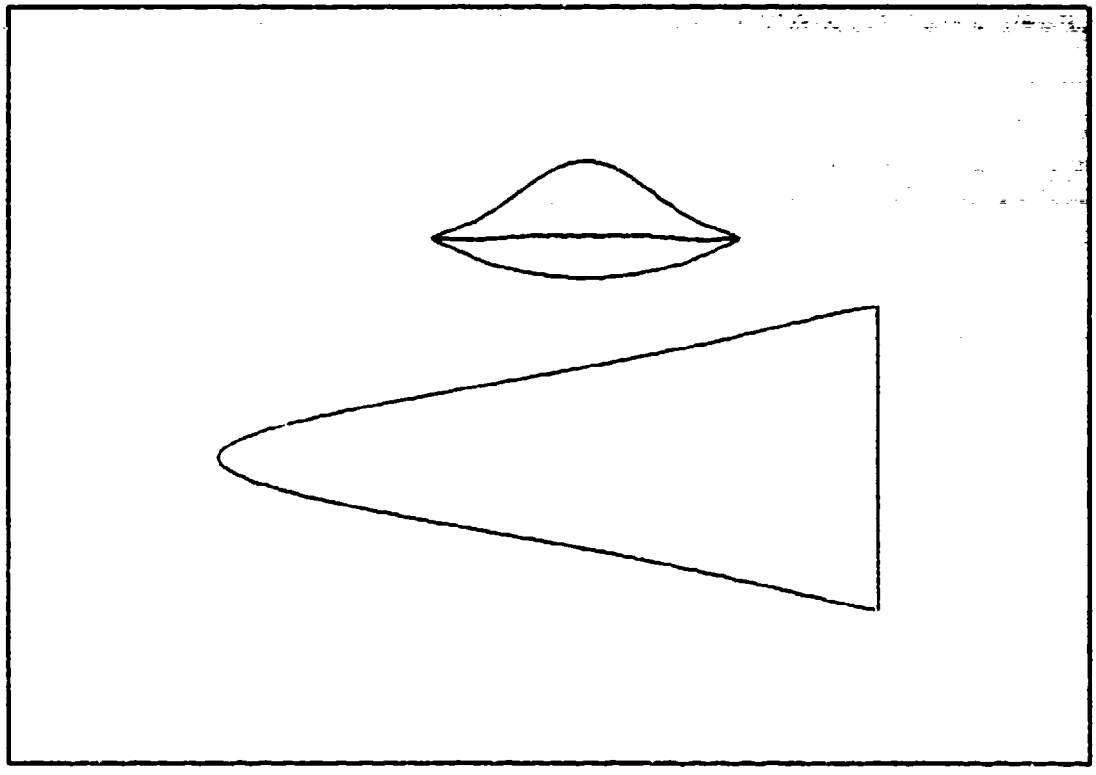

Figure E.14

Table E.14

Phi =30.0	Delta = 8.0	Mach =10.0	Rey = 0.10E+07	Gamma = 1.40
Y = 0.800 + 2.039 Y^2 + -5.000 Y^4 + 4.804 Y^6				
Cftav = 0.001883	CL = 0.041357		CD = 0.008576	
Sw/Sp = 2.140818	V^(2/3)/Sp = 0.183749		(L/D)vis = 4.822628	
Ab/Abi = 0.423856	V/Vi = 0.181456		Sp/Spi = 0.431872	
b/lw = 0.468550	SSD = 0.183460			

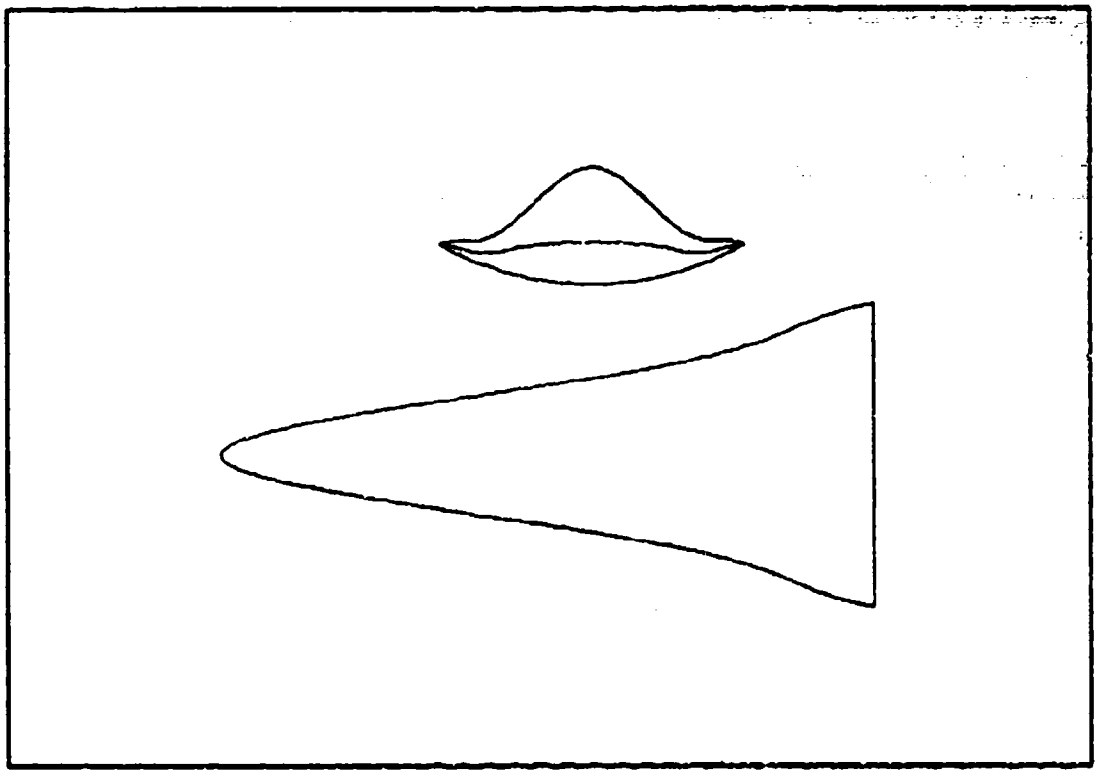

Figure E.15

Table E.15

Phi :30.0	Delta : 8.(	Mach :10.0	Rey : 0.10E+07	Gamma : 1.40
Y = 0.800 + 3.109 T^2 + -10.000 T^4 + 10.842 T^6				
Cftav : 0.001934	CL : 0.041275		CD : 0.008812	
Sw/Sp : 2.221630	V^(2/3)/Sp : 0.186425		(L/D)vis : 4.684116	
Ab/Abi : 0.372885	V/Vi : 0.154016		Sp/Spi : 0.381598	
b/lw : 0.466550	SSD : 0.183460			

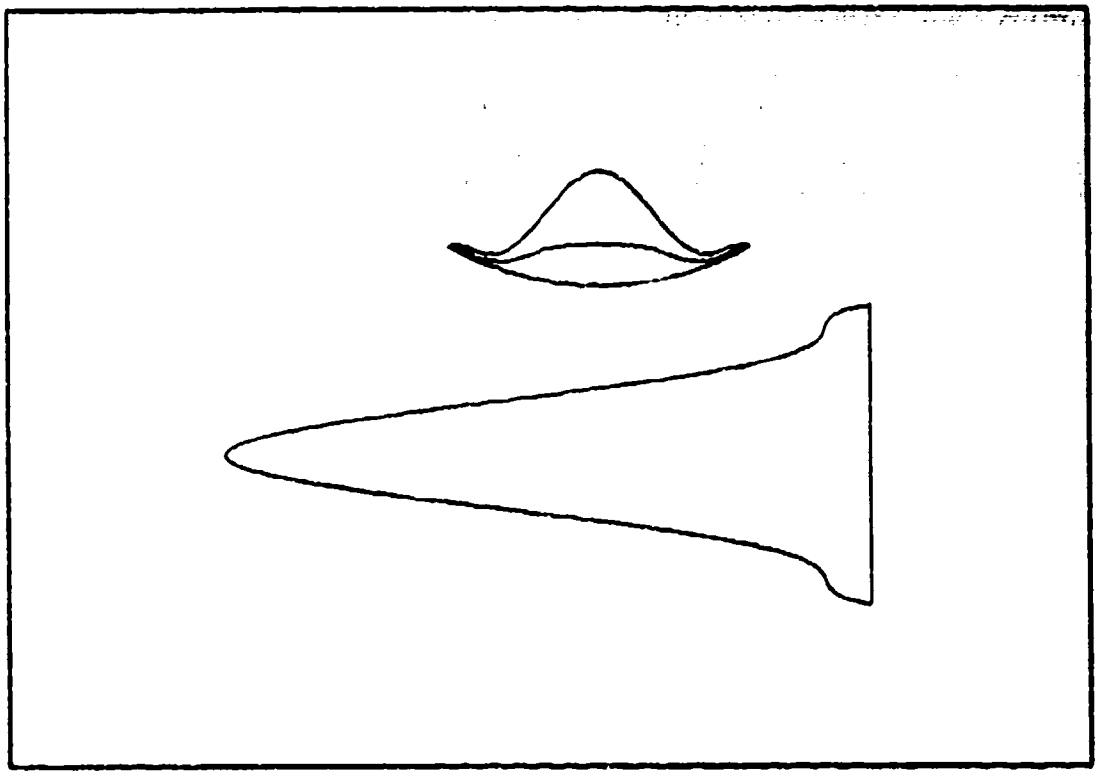

Figure E.16

Table E.16

Phi :36.0	Delta = 8.0	Mach =10.0	Rey = 0.10E+07	Gamma = 1.40
X = 0.800 + 4.100 Y^2 + -15.000 Y^4 + 16.481 Y^6				
Cftav = 0.001982		CL = 0.041260	CD = 0.009137	
Sw/Sp = 2.343656		V^(2/3)/Sp = 0.194103	(L/D)vis = 4.515485	
Ab/Abi = 0.321937		V/Vi = 0.132237	Sp/Spi = 0.331083	
b/lw = 0.466550		SSD = 0.163460		

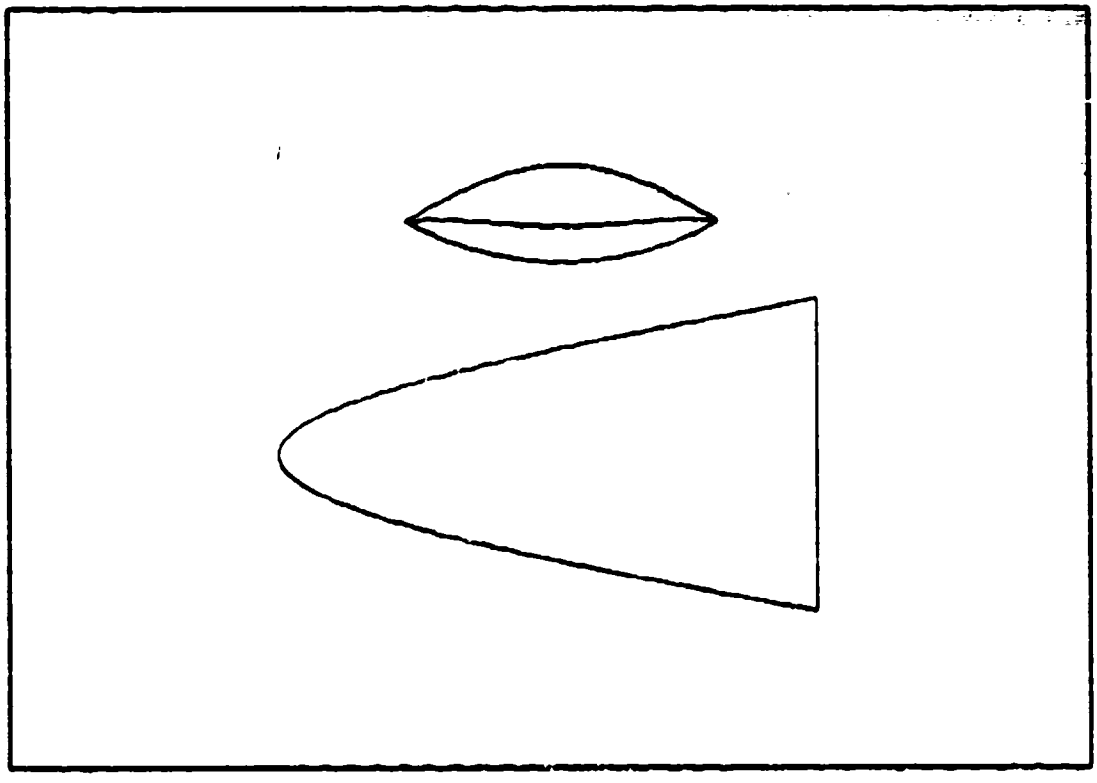

Figure E.17

Table E.17

Phi =30.0	Delta = 8.0	Mach =10.0	Rey = 0.10E+07	Gamma = 1.40
		Y = 0.900 + 0.618 Y^2 + 0.000 Y^4 + -0.397 Y^6		
Cftav = 0.001821		CL = 0.041009	CD = 0.008254	
Sw/Sp = 2.051210		V^(2/3)/Sp = 0.170417	(L/D)vis = 4.968442	
Ab/Abi = 0.391447		V/Vi = 0.143061	Sp/Spi = 0.397405	
b/lw = 0.583188		SSD = 0.152450		

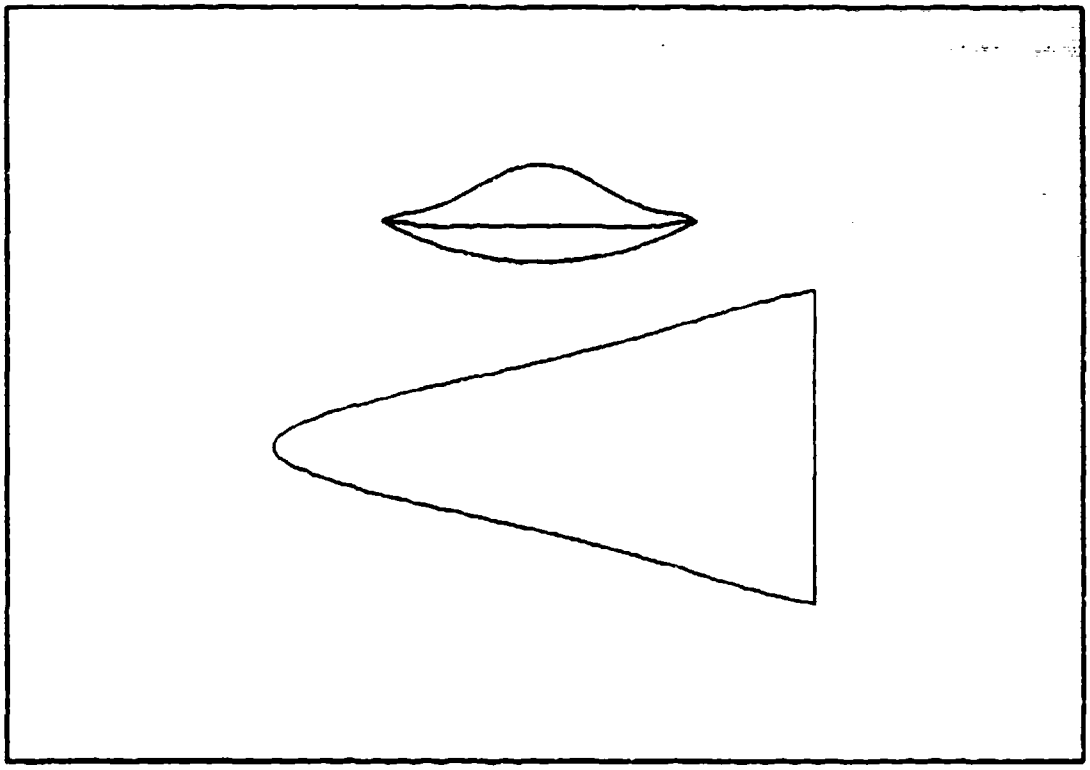

Figure E.18

Table E.18

Phi =30.0	Delta = 8.0	Mach =10.0	Rey = 0.10E+07	Gamma = 1.40
X = 0.900 + 1.688 Y^2 + -5.000 Y^4 + 5.442 Y^6				
Cftav = 0.001899	CL = 0.040875		CD = 0.008433	
Sw/Sp = 2.079087	V^(2/3)/Sp = 0.169635		(L/D)vis = 4.847222	
Ab/Abi = 0.340499	V/Vi = 0.116021		Sp/Spi = 0.347197	
b/lw = 0.583168	SSD = 0.152450			

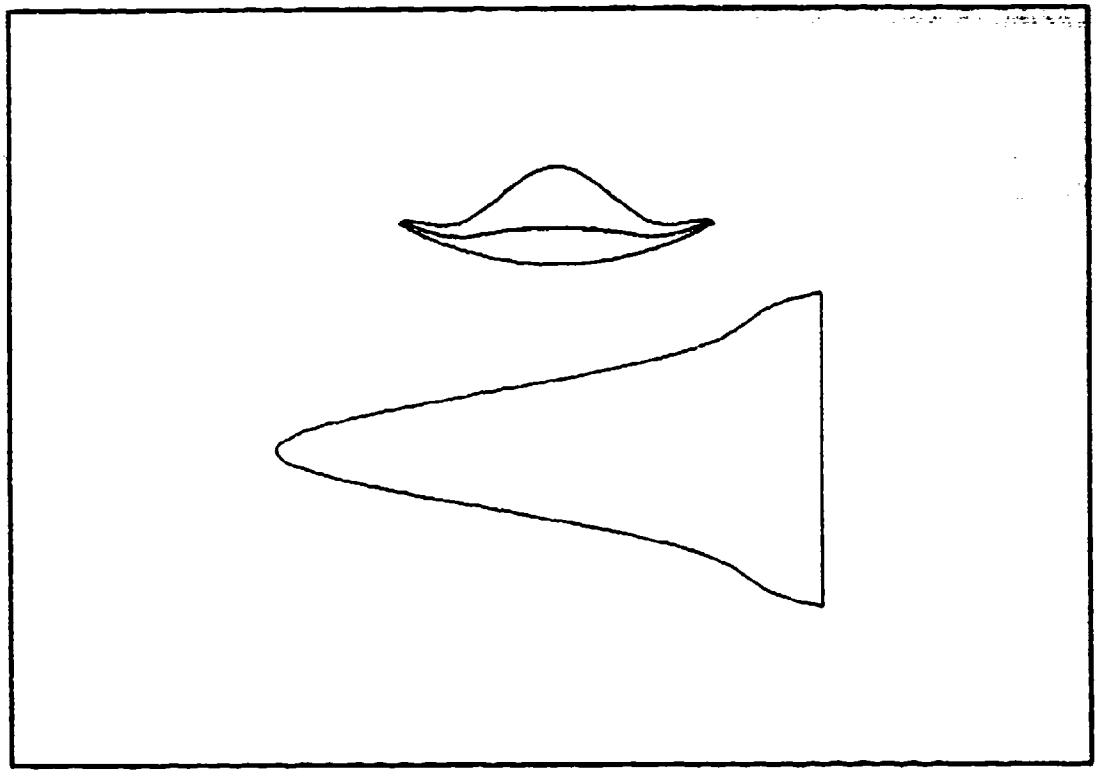

Figure E.19

Table E.19

Phi :30.0	Delta = 8.0	Mach =10.0	Rey = 0.10E+07	Gamma = 1.40
Y = 0.900 + 2.759 Y^2 + -10.000 Y^4 + 11.280 Y^6				
Cftav = 0.001981	CL = 0.040799		CD = 0.000725	
Sw/Sp = 2.156927	V^(2/3)/Sp = 0.173278		(L/D)vis = 4.676111	
Ab/Abi = 0.289528	V/Vi = 0.094622		Sp/Spi = 0.296699	
b/lw = 0.583168	SSD = 0.152450			

APPENDIX F

Presented here are configurations that have the following parameters held fixed:

$$\Phi_1 = 20, \quad \delta = 8, \quad M = 10, \quad Rey = 1X10^6$$

The following parameters are varied:

R_0 from 1.0 to 1.1

b_4 from 8.0 to -8.0

The values of b_2 and b_6 are such that equation 2-i3 and condition (iii) holds.

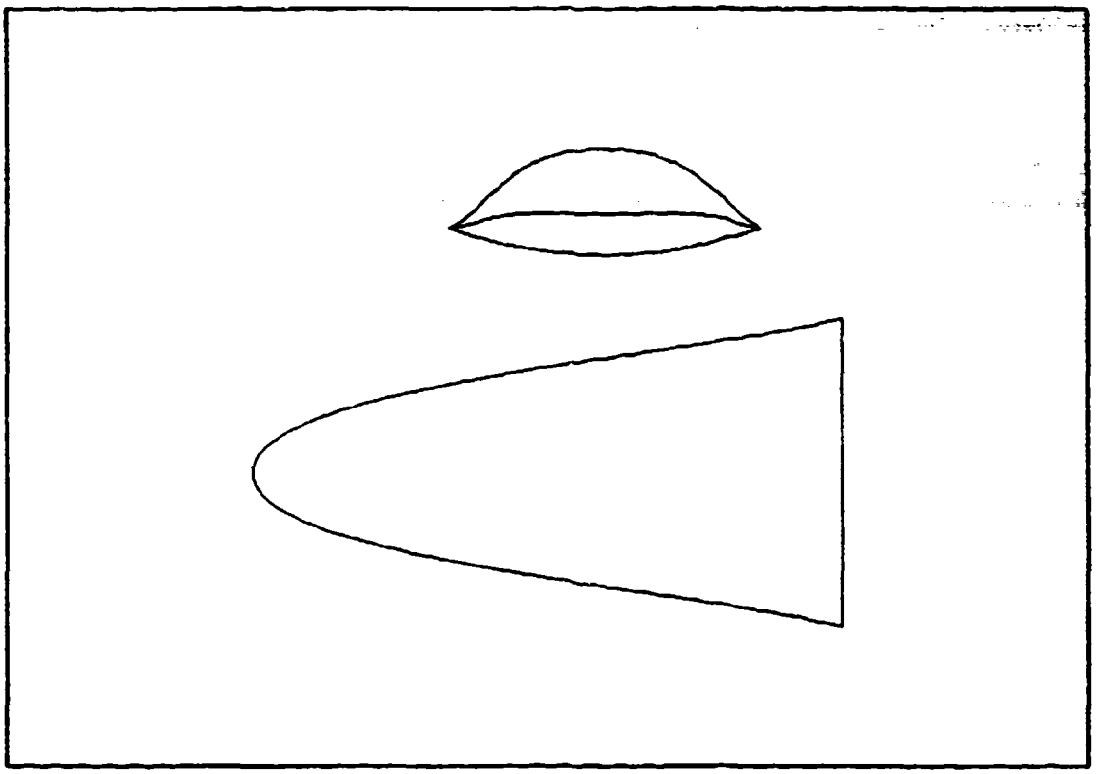

Figure F.1

Table F.1

Phi =20.0	Delta = 8.0	Mach =10.0	Rey = 0.10E+07	Gamma = 1.40
Y = 1.000 + 0.725 Y^2 + 8.000 Y^4 + -29.400 Y^6				
Cftav = 0.001798	CL = 0.040560		CD = 0.008193	
Sw/Sp = 2.116358	V^(2/3)/Sp = 0.176644		(L/D)vic = 4.950312	
Ab/Abi = 0.305388	V/Vi = 0.087251		Sp/Spi = 0.307613	
b/lw = 0.528095	SSD = 0.118747			

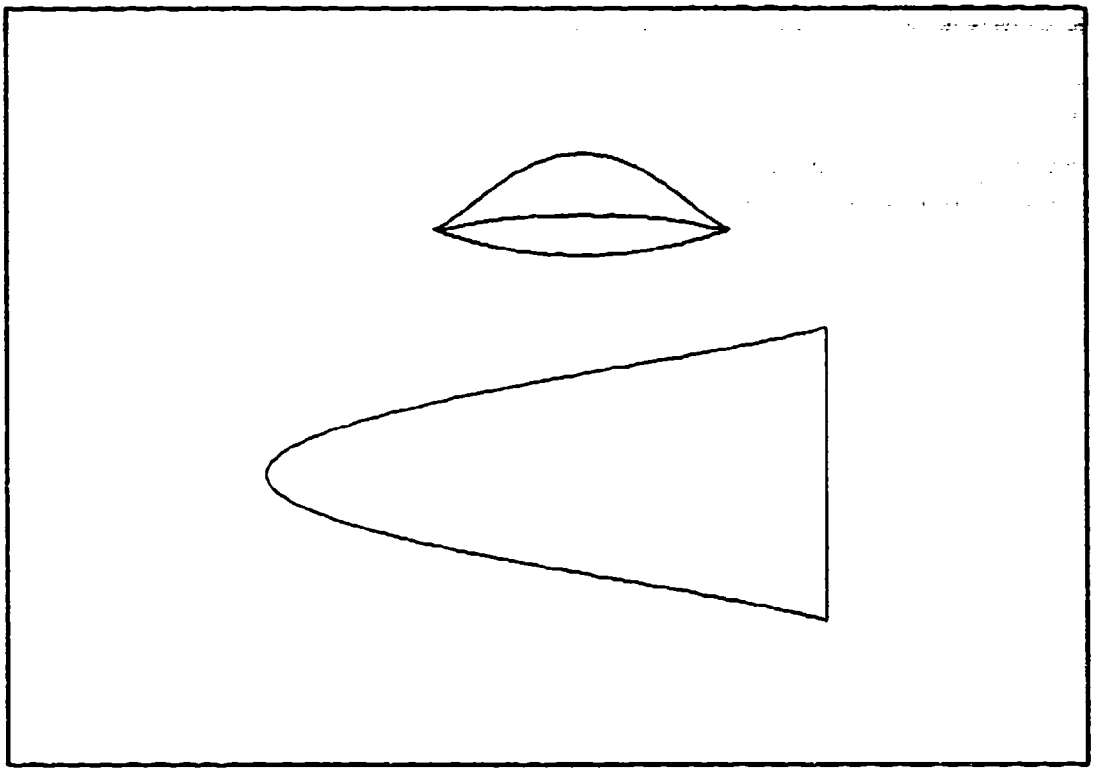

Figure F.2

Table F.2

Phi =20.0	Delta = 8.0	Mach =10.0	Rey = 0.10E+07	Gamma = 1.40
Y = 1.000 + 1.526 Y^2 + 0.000 Y^4 + -9.440 Y^6				
Cftav = 0.001832	CL = 0.040506	CD = 0.008260		
Sw/Sp = 2.118220	V^(2/3)/Sp = 0.175973	(L/D)vis = 4.903740		
Ab/Abi = 0.287061	V/Vi = 0.079159	Sp/Spi = 0.289387		
b/lw = 0.528095	SSD = 0.118747			

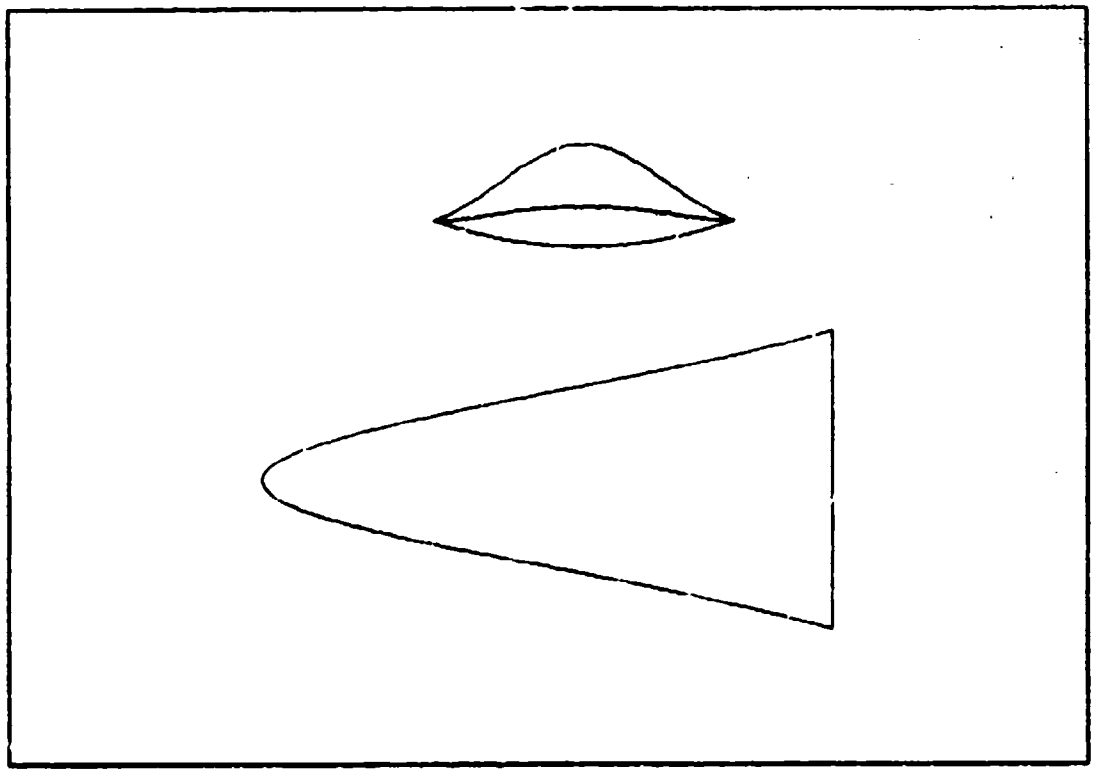

Figure F.3

Table F.3

Phi -20.0	Delta : 8.0	Mach :10.0	Rey . 0.10E+07	Gamma : 1.40
		1 : 1.000 + 2.327 Y^2 + -8.000 Y^4 + 10.530 Y^6		
Cftav : 0.001466		CL : 0.040459	CD : 0.008350	
Sw/Sp : 2.133018		V^(2/3)/Sp : 0.175985	(L/D)vis : 4.845502	
Ab/Ab1 : 0.268757		V/V1 : 0.071670	Sp/ [illegible] : 0.271188	
b/lw : 0.528095		SSD : 0.118747		

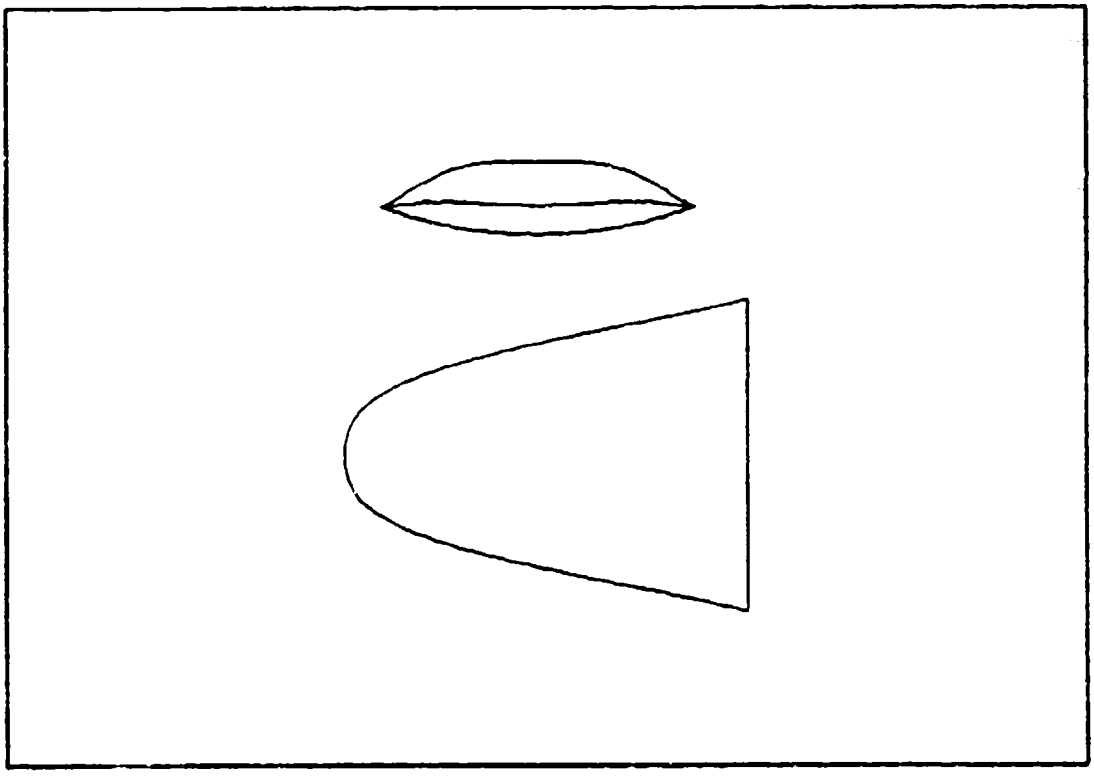

Figure F.4

Table F.4

Phi :20.0	Delta = 8.0	Mach :10.0	Rey = 0.10E+07	Gamma = 1.40
Y = 1.100 + -0.024 Y^2 + 8.000 Y^4 + -23.180 Y^6				
Cftav = 0.001755	CL = 0.040081	CD = 0.007917		
Sw/Sp = 2.040828	V^(2/3)/Sp = 0.154899	(L/D)vis = 5.062539		
Ab/Abi = 0.219841	V/Vi = 0.043740	Sp/Spi = 0.221375		
b/le = 0.781022	SSD = 0.002674			

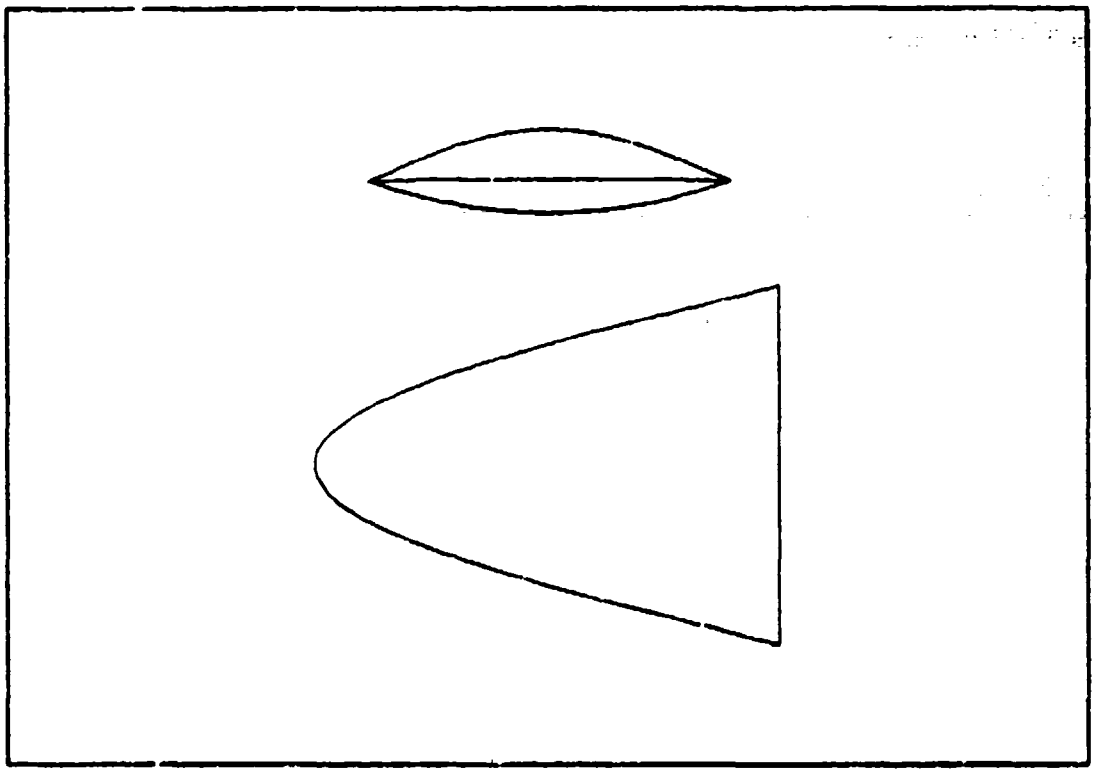

Figure F.5

Table F.5

Phi =20.0	Delta = 8.0	Mach =10.0	Rey = 0.10E+07	Gamma = 1.40
Y = 1.100 + 0.777 Y^2 + 0.000 Y^4 + -3.210 Y^6				
Cftav = 0.001816	CL = 0.040021		CD = 0.066021	
Sw/Sp = 2.035581	V^(2/3)/Sp = 0.153377		(L/D)vis = 4.989471	
Ab/Ab1 = 0.201537	V/V1 = 0.037883		Sp/Sp1 = 0.203138	
b/lw = 0.761022	CBD = 0.002574			

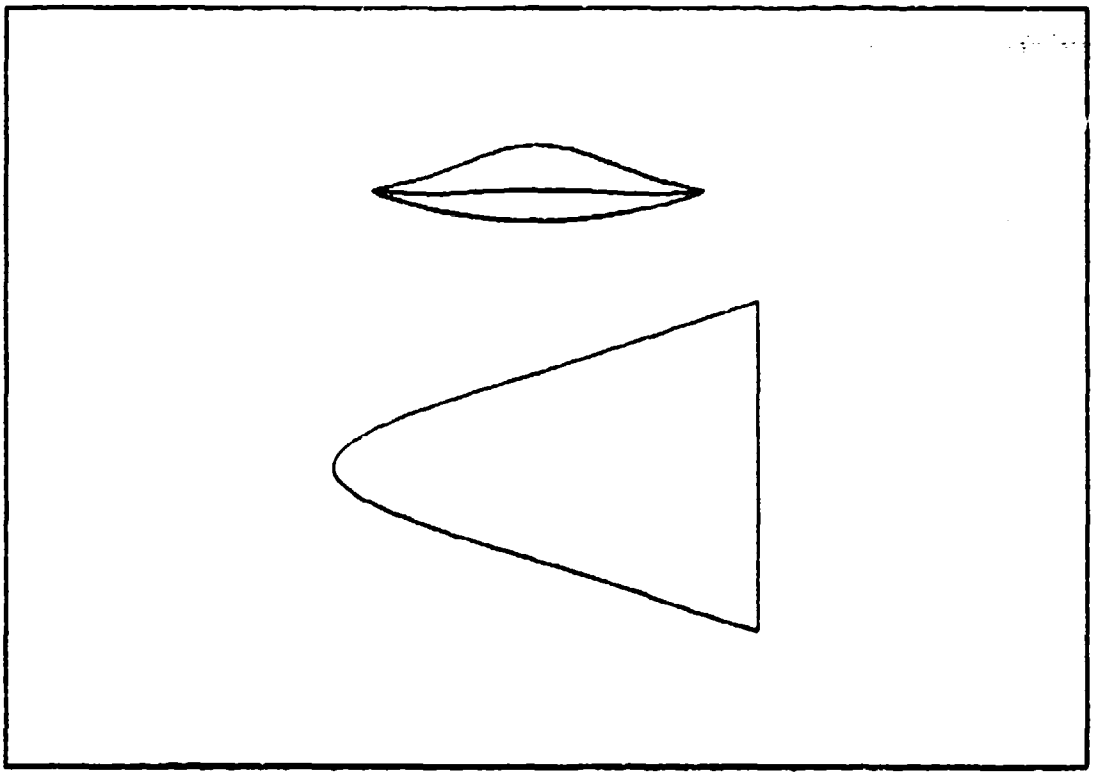

Figure F.6

Table F.6

Phi :20.0	Delta : 8.0	Mach :10.0	Rey : 0.10E+07	Gamma : 1.40
X : 1.100 + 1.579 Y^2 + -8.000 Y^4 + 16.740 Y^6				
Cftav : 0.001879	CL : 0.039971		CD : 0.008157	
Sw/Sp : 2.045084	Y^(2/3)/Sp : 0.152971		(L/D)vis : 4.900140	
Ab/Abi : 0.183187	V/V1 : 0.032752		Sp/Spi : 0.184843	
b/lw : 0.761022	SSD : 0.062574			

APPENDIX G

Presented here are configurations that have the following parameters held fixed:

$$\Phi_1 = 10, \quad \delta = 8, \quad M = 10, \quad Rey = 1X10^6$$

The following parameters are varied:

R_0 from 1.0 to 1.1

b_4 from 120.0 to -120.0

The values of b_2 and b_6 are such that equation 2-13 and condition (iii) holds.

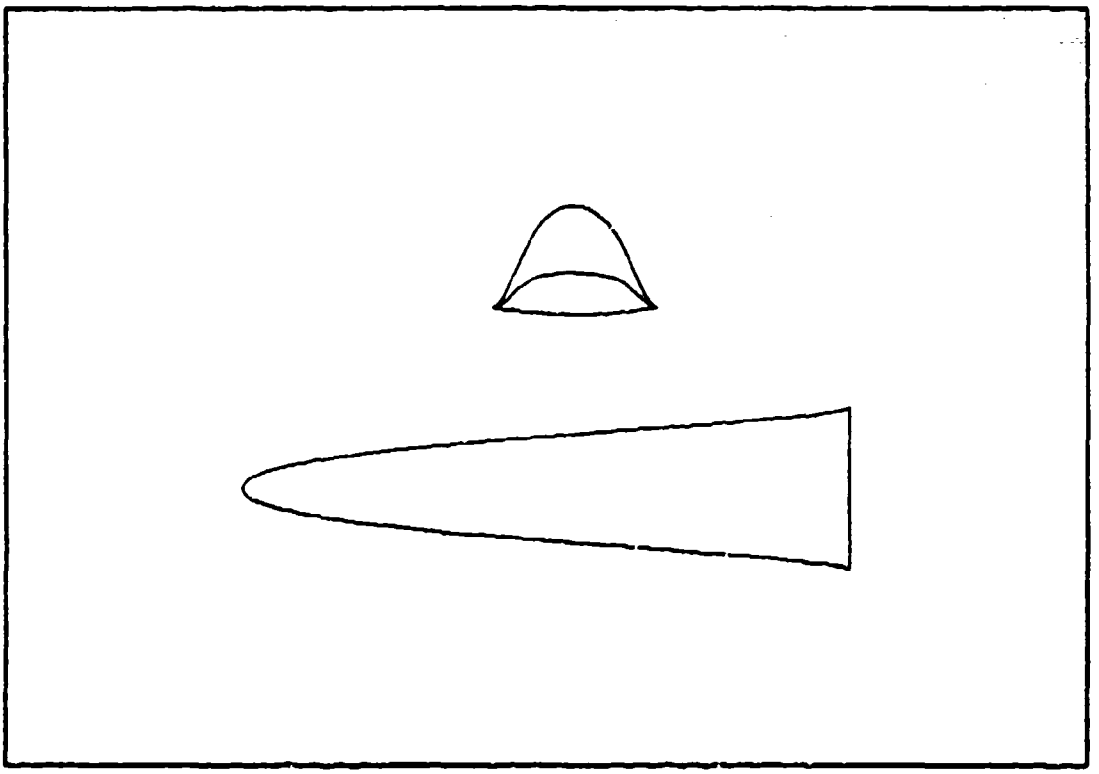

Figure G.1

Table G.1

Phi =10.0	Delta = 8.0	Mach =10.0	Rey = 0.10E+07	Gamma = 1.40
Y = 1.000 + 5.099 Y^2 + 120.000 Y^4 + -2138.0 Y^6				
Cftav = 0.001814	CL = 0.040548		CD = 0.009108	
Sw/Sp = 2.625714	V^(2/3)/Sp = 0.222710		(L/D)vis = 4.452075	
Ab/Abi = 0.292599	V/Vi = 0.063162		Sp/Spi = 0.293198	
b/lw = 0.268121	SSD = 0.118747			

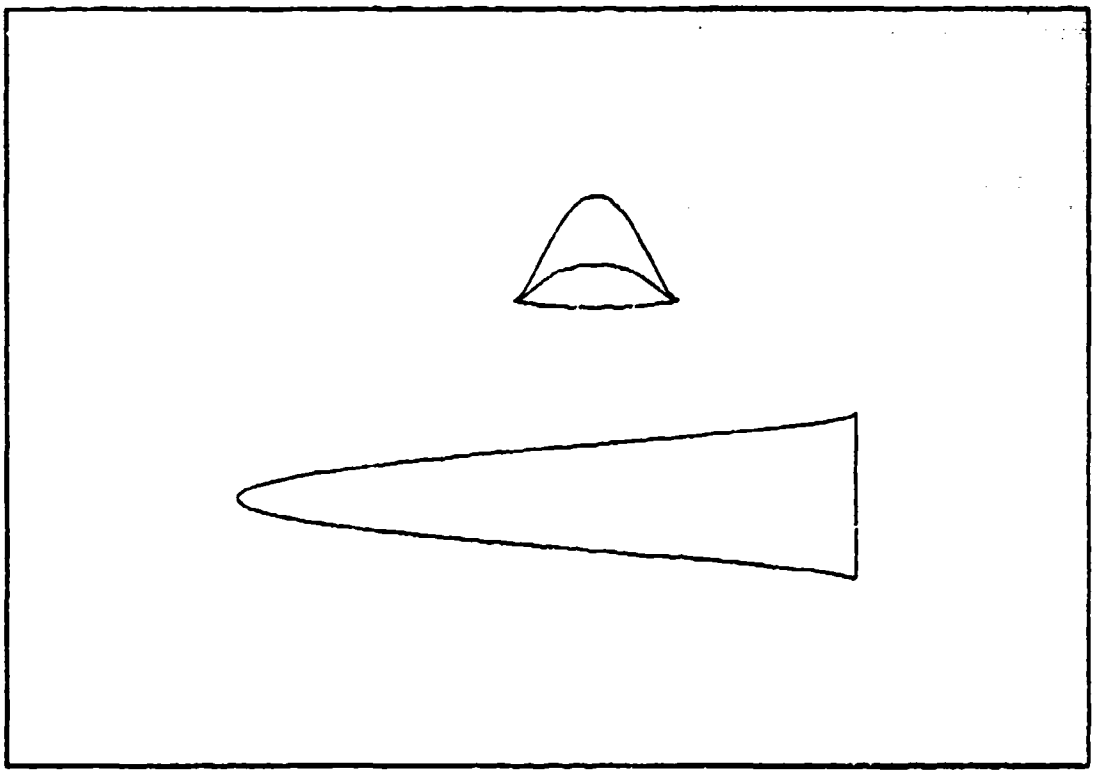

Figure G.2

Table G.2

Phi :10.0	Delta : 8.0	Mach :10.0	Rey : 0.10E+07	Gamma : 1.40
X : 1.000 + 8.200 Y^2 + 0.000 Y^4 + -977.0 Y^6				
Cftav : 0.001331	CL : 0.040500		CD : 0.009214	
Sw/Sp : 2.663484	V^(2/3)/Sp : 0.222803		(L/D)vis : 4.395571	
Ab/Ab1 : 0.274031	V/V1 : 0.075496		Sp/Sp1 : 0.274654	
b/lw : 0.268121	SSD : 0.116747			

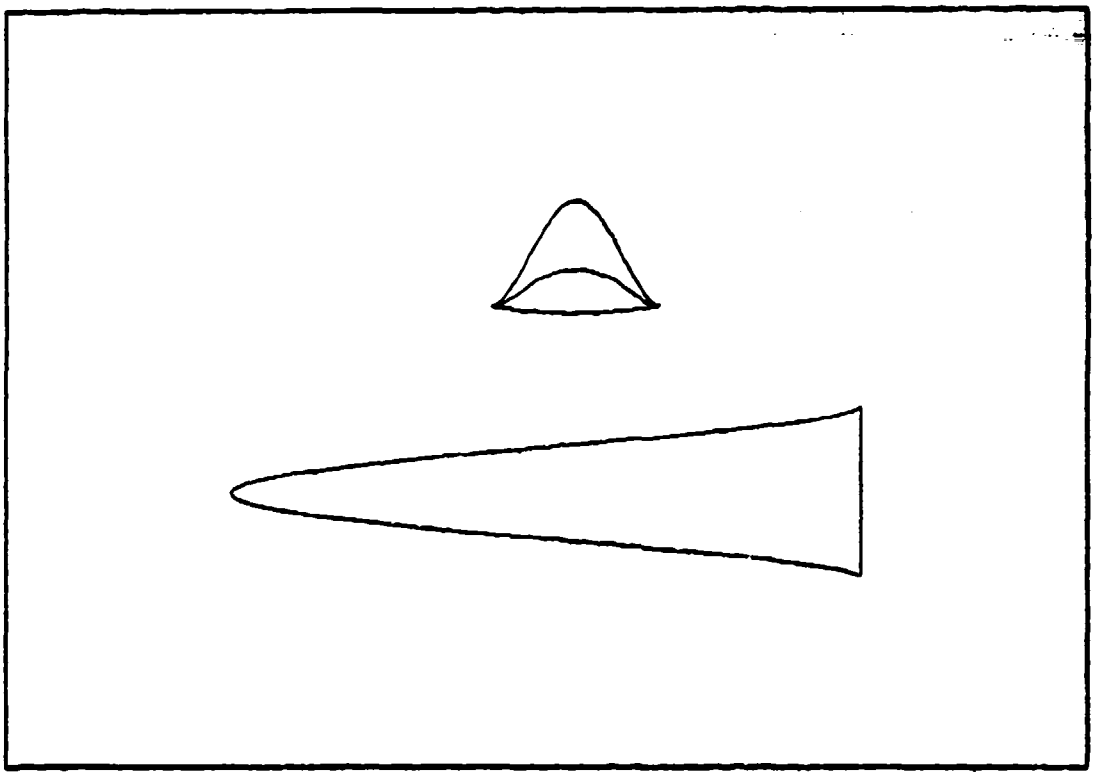

Figure G.3

Table G.3

Phi =10.0	Delta = 8.0	Mach =10.0	Rey = 0.10E+07	Gamma = 1.40
X = 1.000 + 11.309 Y^2 +-120.000 Y^4 + 181.0 Y^6				
Cftav = 0.001844	CL = 0.040462		CD = 0.009387	
Sw/Sp = 2.731035	V^(2/3)/Sp = 0.224272		(L/D)vis = 4.310472	
Ab/Abi = 0.255343	V/Vi = 0.068559		Sp/Spi = 0.255987	
b/lw = 0.260121	SSD = 0.118747			

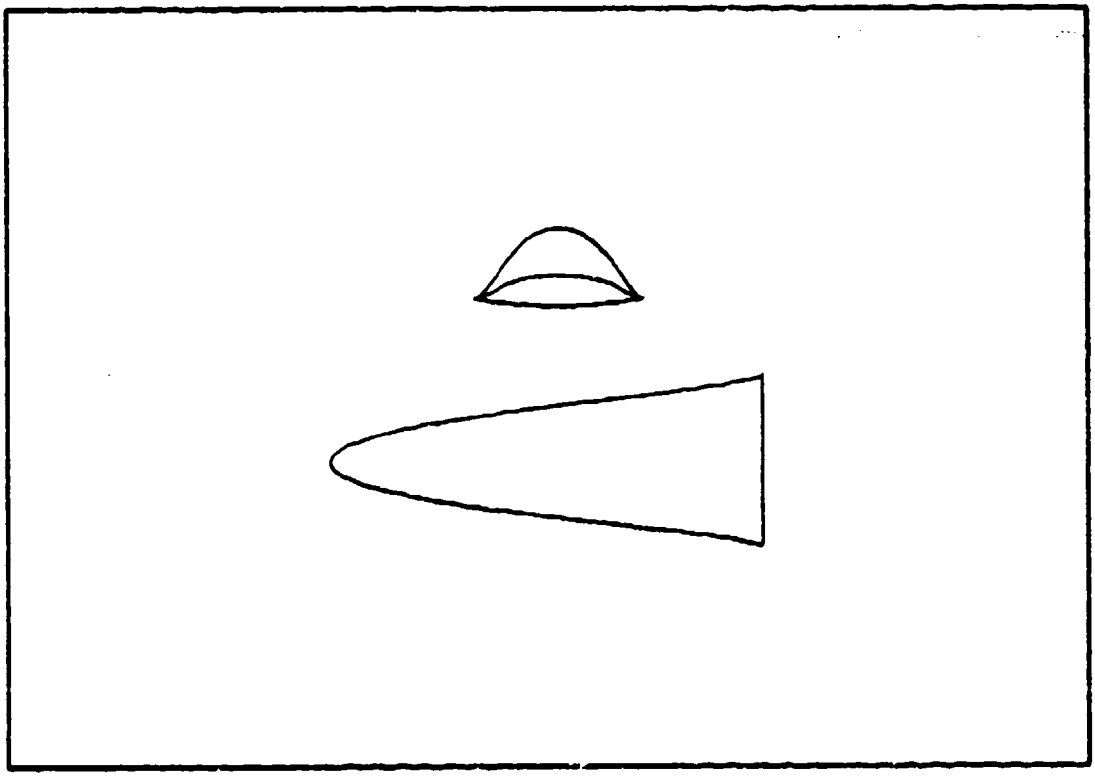

Figure G.4

Table G.4

Phi =10.0	Delta = 8.0	Mach =10.0	Rey = 0.10E+07	Gamma = 1.40
Y = 1.100 + 3.746 T^2 + 60.000 T^4 + -1195.0 T^6				
Cftav = 0.001821	CL = 0.040033		CD = 0.008489	
Sw/Sp = 2.306139	V^(2/3)/Sp = 0.194968		(L/D)vis = 4.715981	
Ab/Abi = 0.196422	V/Vi = 0.037475		Sp/Spi = 0.196855	
b/lw = 0.396535	SSD = 0.082574			

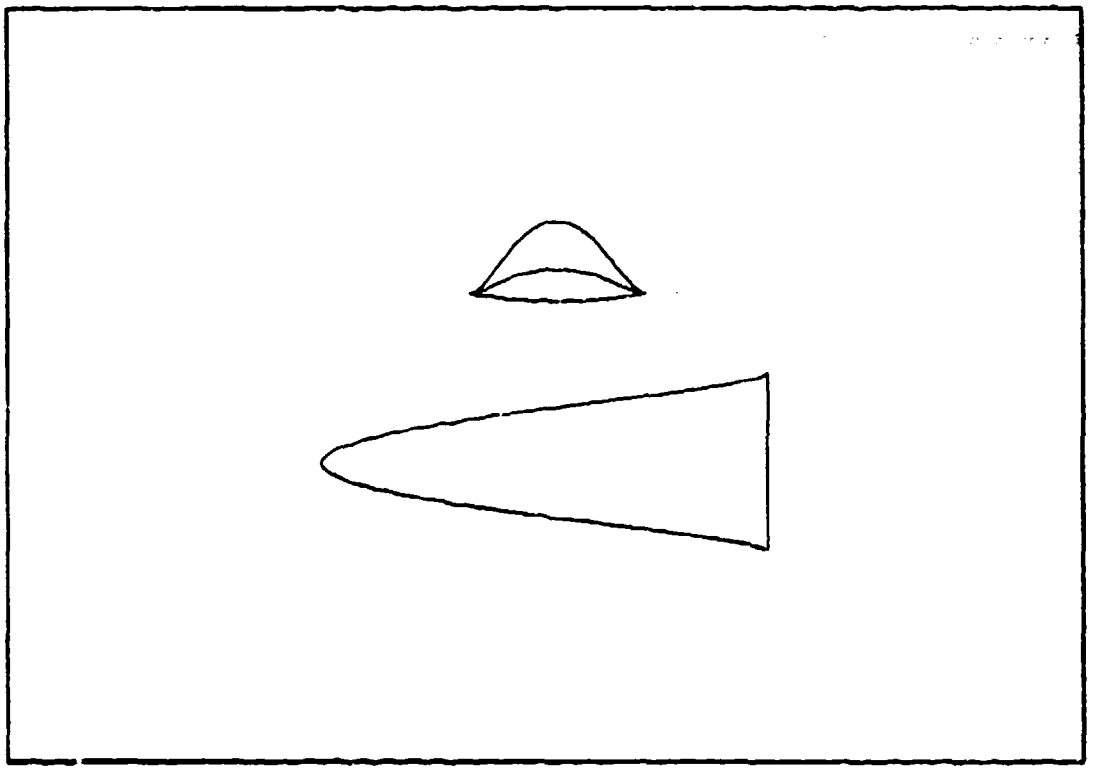

Figure G.5

Table G.5

Phi :10.0	Delta : 8.0	Mach :10.0	Rey : 0.10E+07	Gamma : 1.40
X : 1.100 + 5.295 Y^2 + 0.000 Y^4 + -814.0 Y^6				
Cftav : 0.001841	CL : 0.040009		CD : 0.008556	
Sw/Sp : 2.321569	Y^(2/3)/Sp : 0.195055		(L/D)vis : 4.676066	
Ab/Abi : 0.187158	V/Vi : 0.034888		Sp/Spi : 0.187598	
b/lw : 0.396535	SSD : 0.002574			

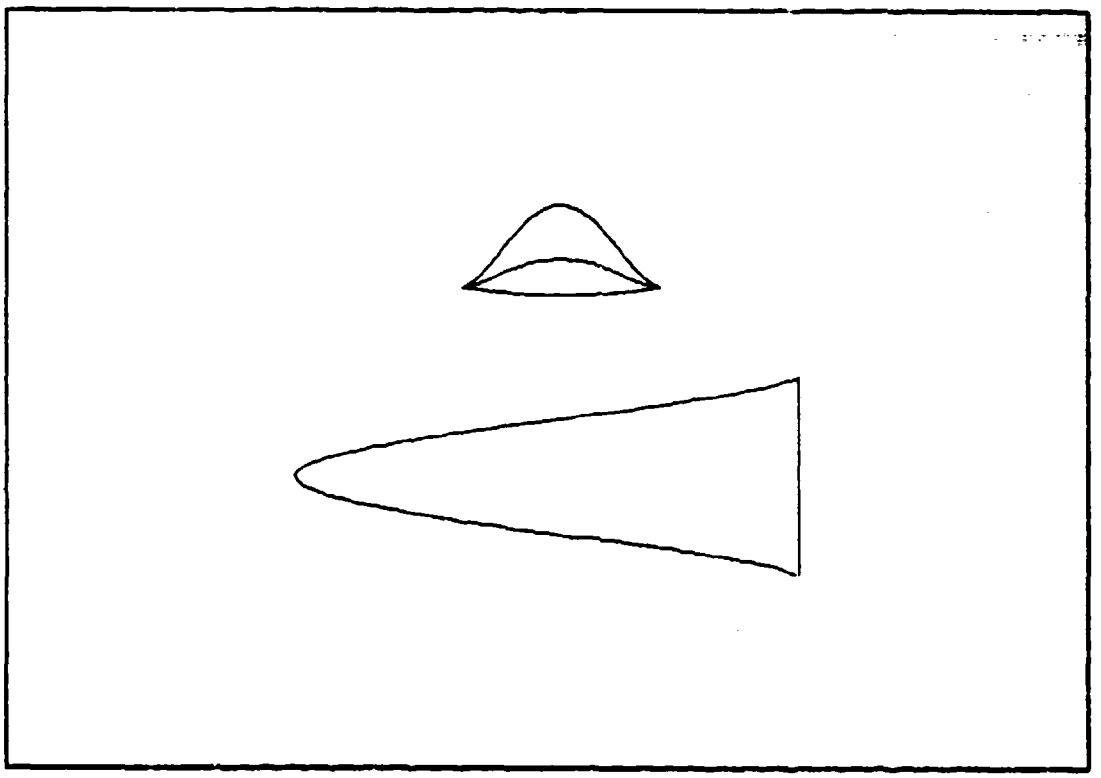

Figure G.6

Table G.6

Phi :10.0	Delta : 8.0	Mach :10.0	Rey : 0.10E+07	Gamma : 1.40
X : 1.100 + 8.845 Y^2 + -60.000 Y^4 + -33.0 Y^6				
Cftav : 0.001859	CL : 0.039989		CD : 0.008639	
Sw/Sp : 2.344983	V^(2/3)/Sp : 0.195659		(L/D)vis : 4.628691	
Ab/Abi : 0.177894	V/Vi : 0.032486		Sp/Spi : 0.176241	
b/lw : 0.396585	SSD : 0.002574			

APPENDIX H

Here in appendix H we show several different configurations in a three-dimensional setting. The configurations shown are repeats of earlier configurations in the above appendices.

These 3-D views are presented so that the reader gets a better perception of the configurations shown and even ones that are shown only in the 2-D views of earlier appendices.

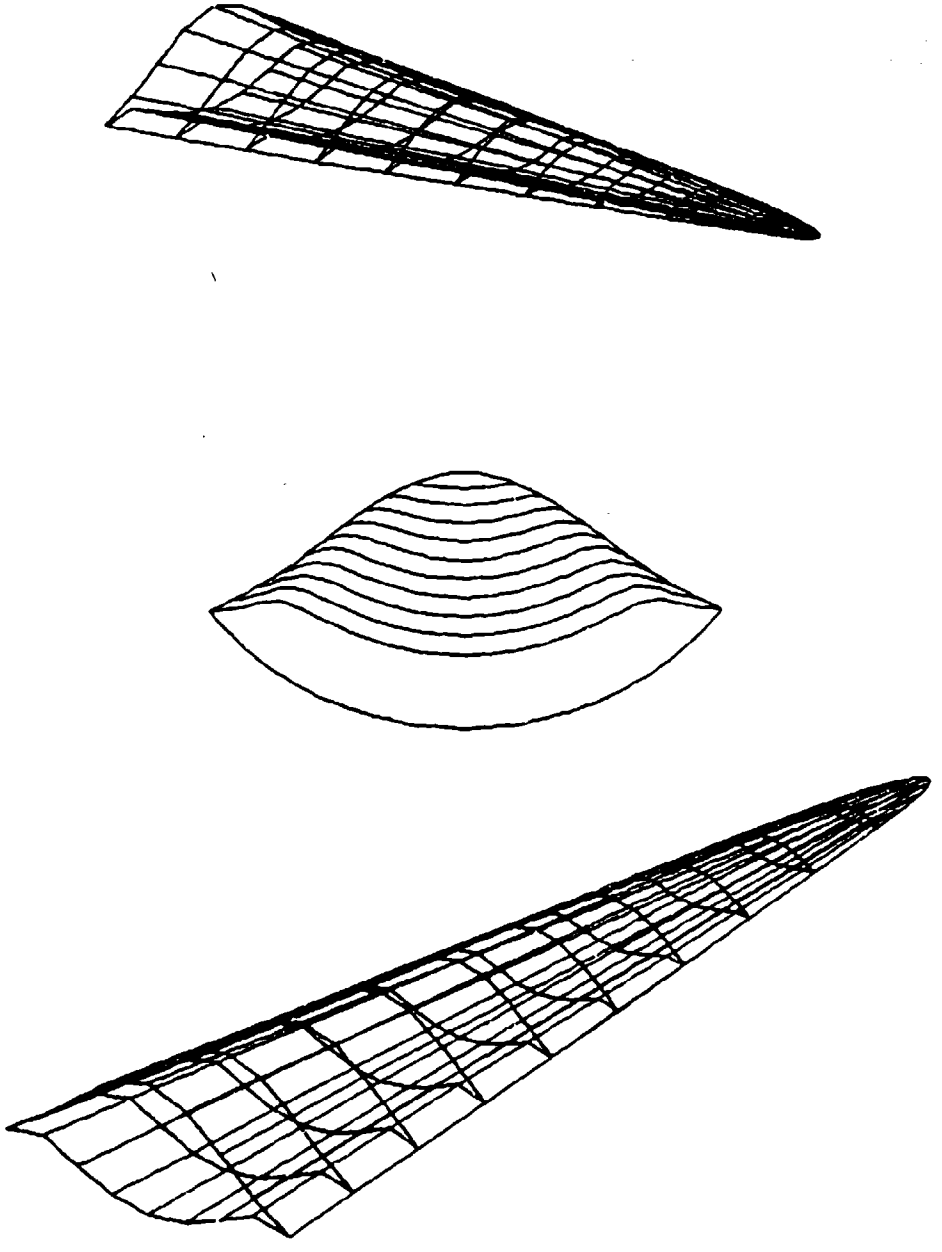

Figure H.1 (C.3)

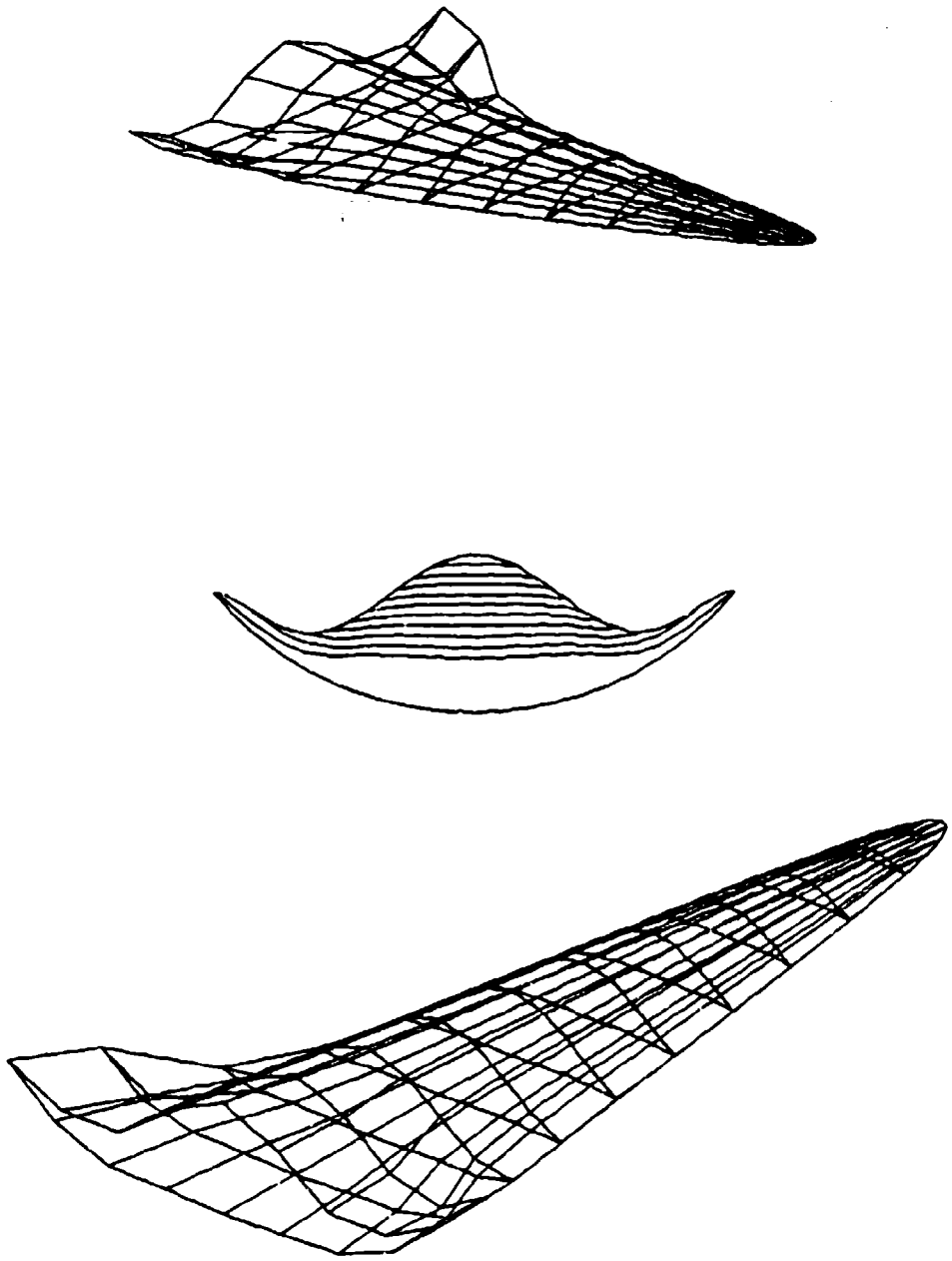

Figure H.2 (C.45)

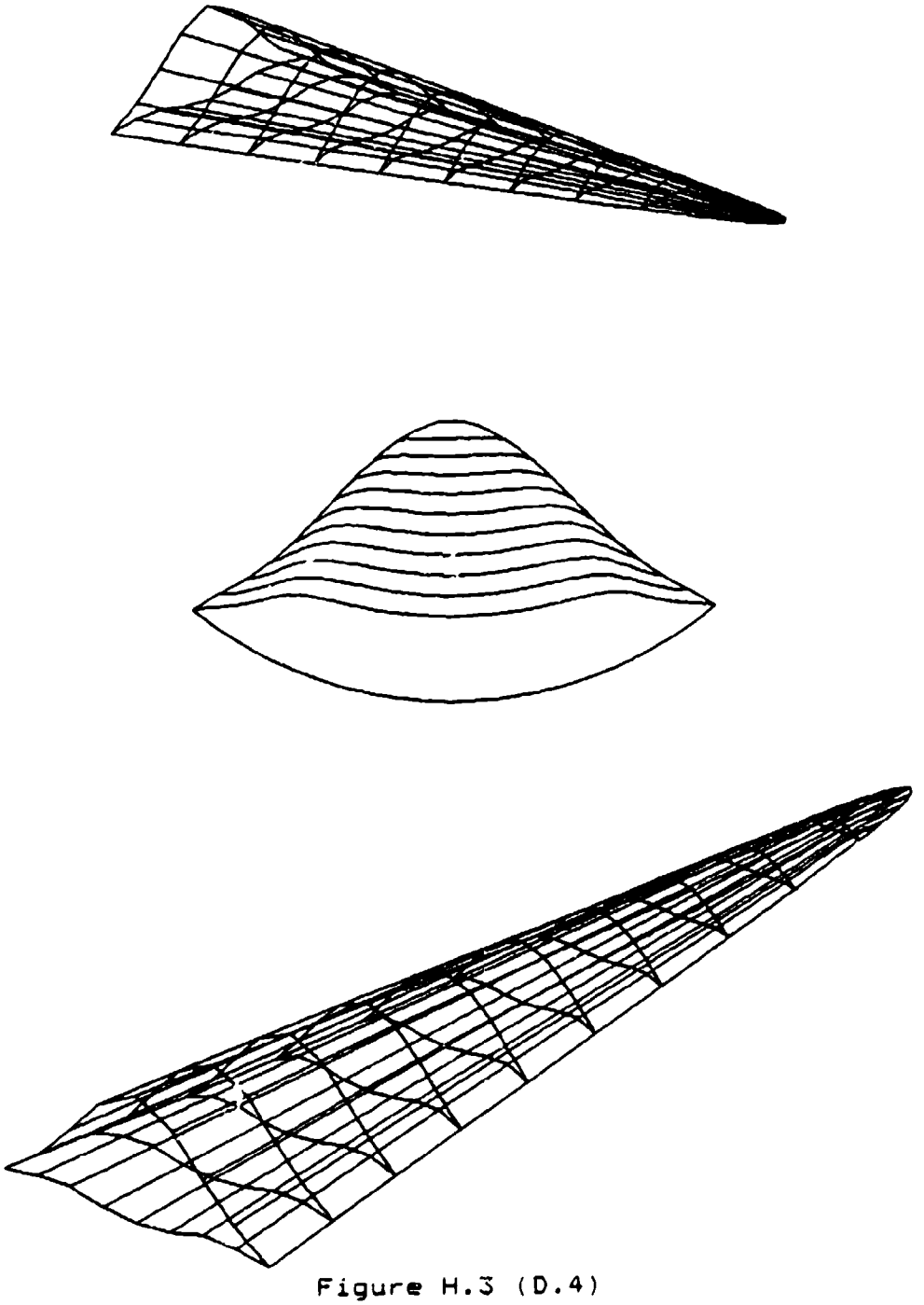

Figure H.3 (D.4)

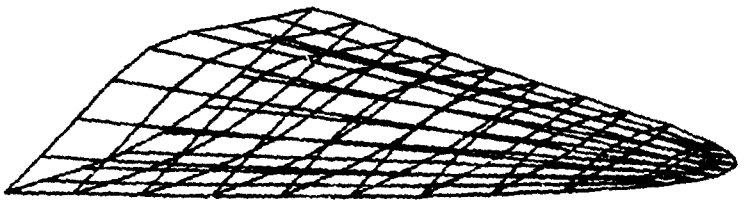

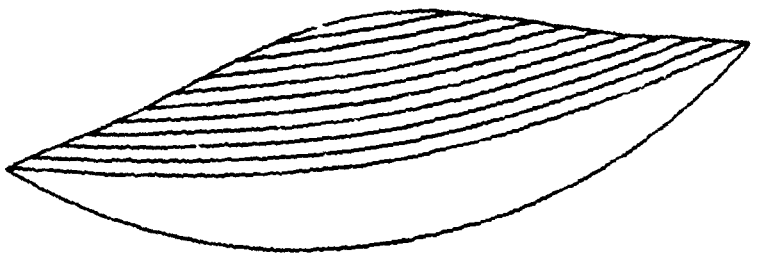

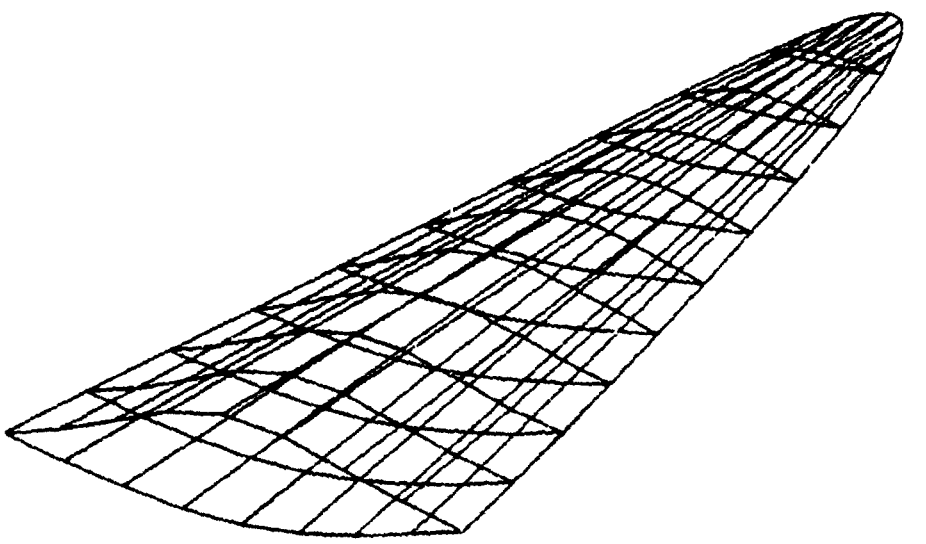

Figure H.4 (D.16)

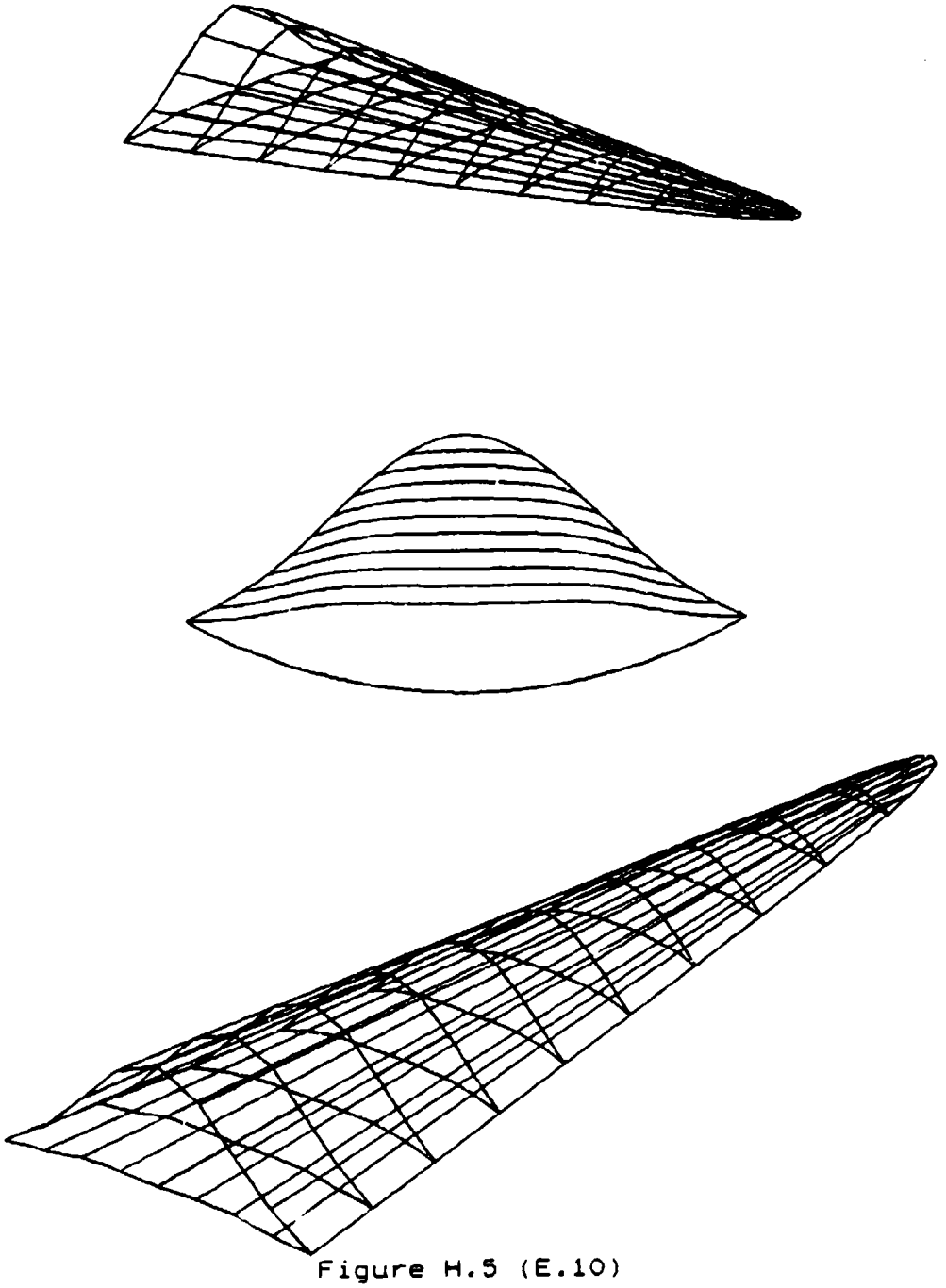

Figure H.5 (E.10)

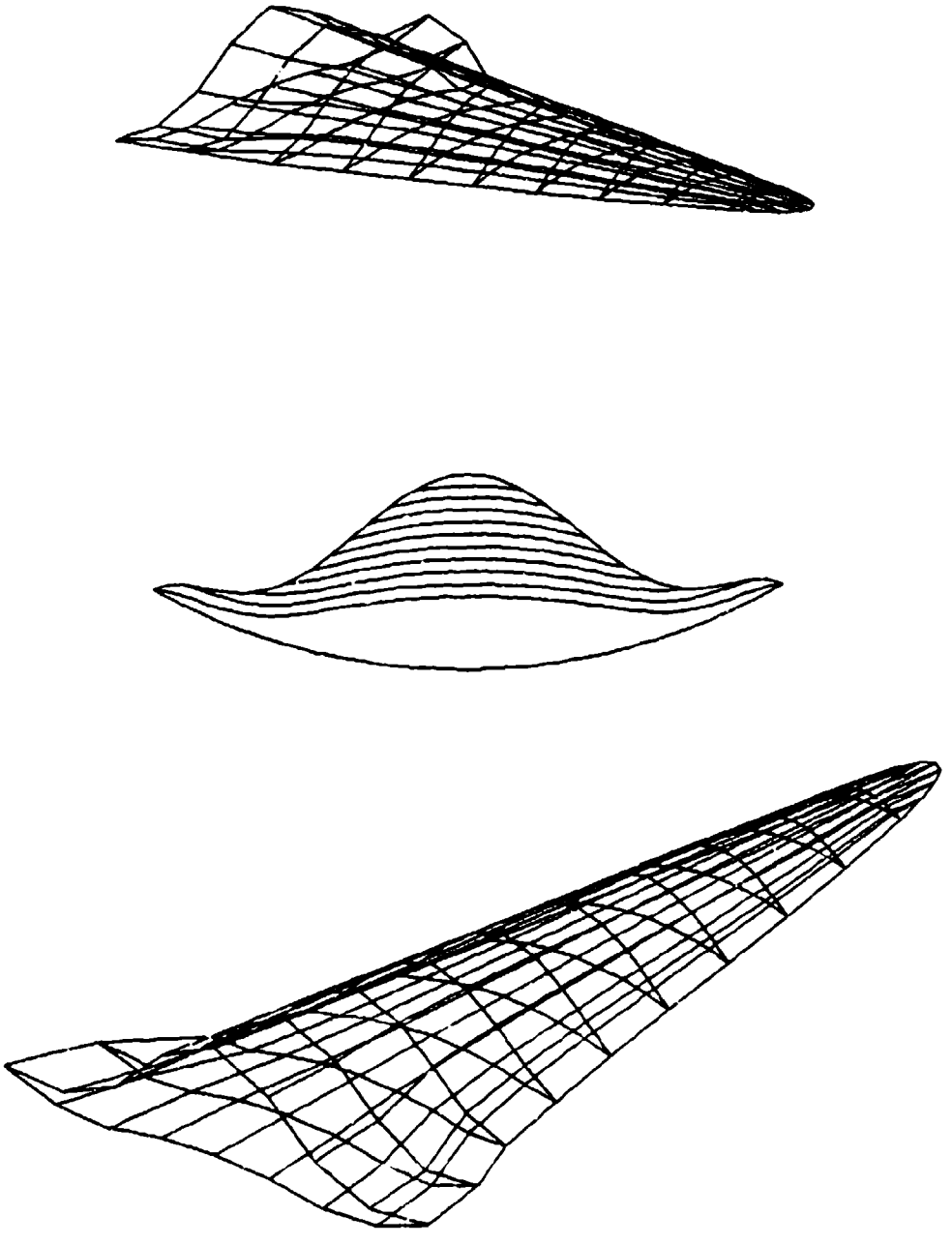

Figure H.6 (E.19)

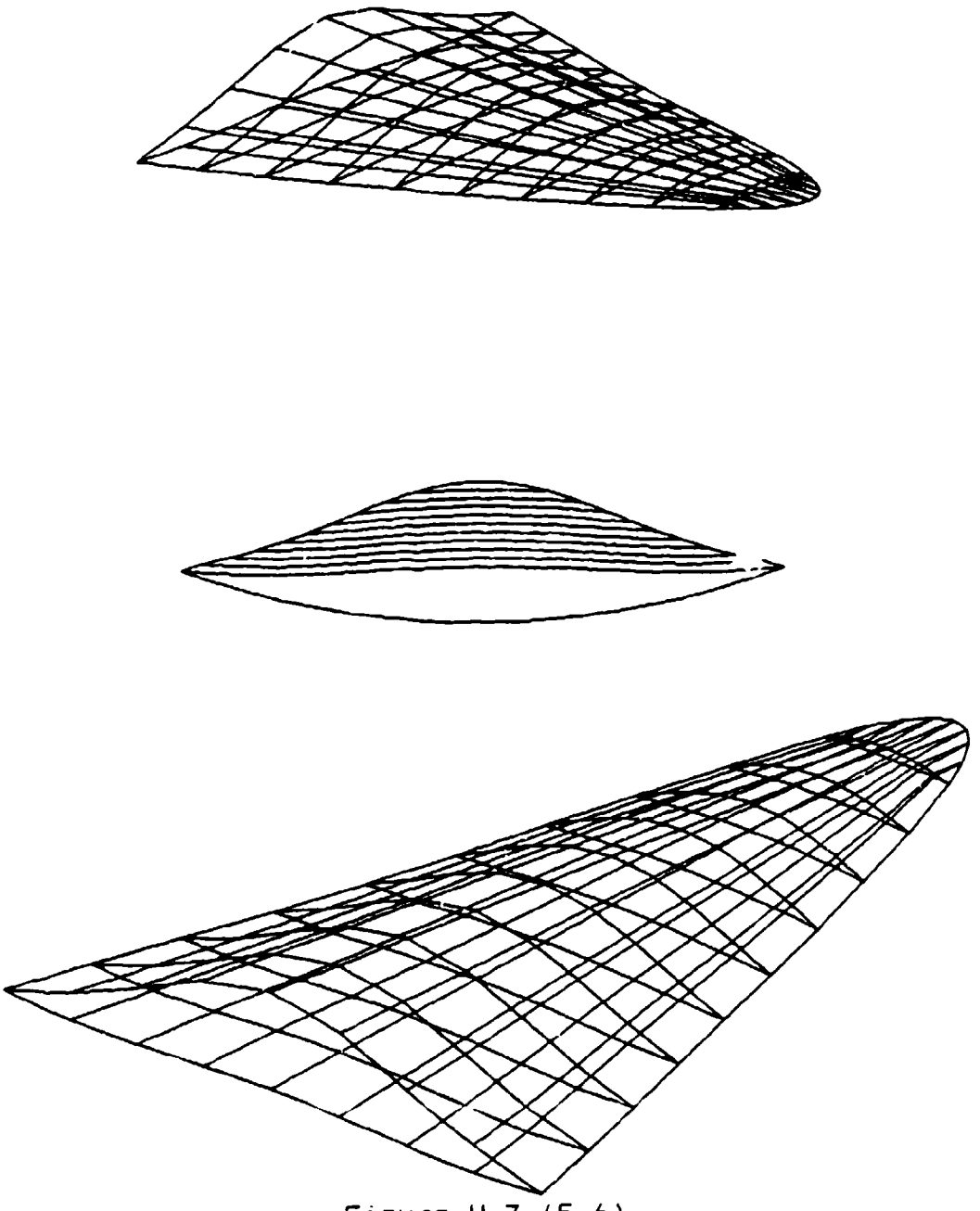

Figure H.7 (F.6)

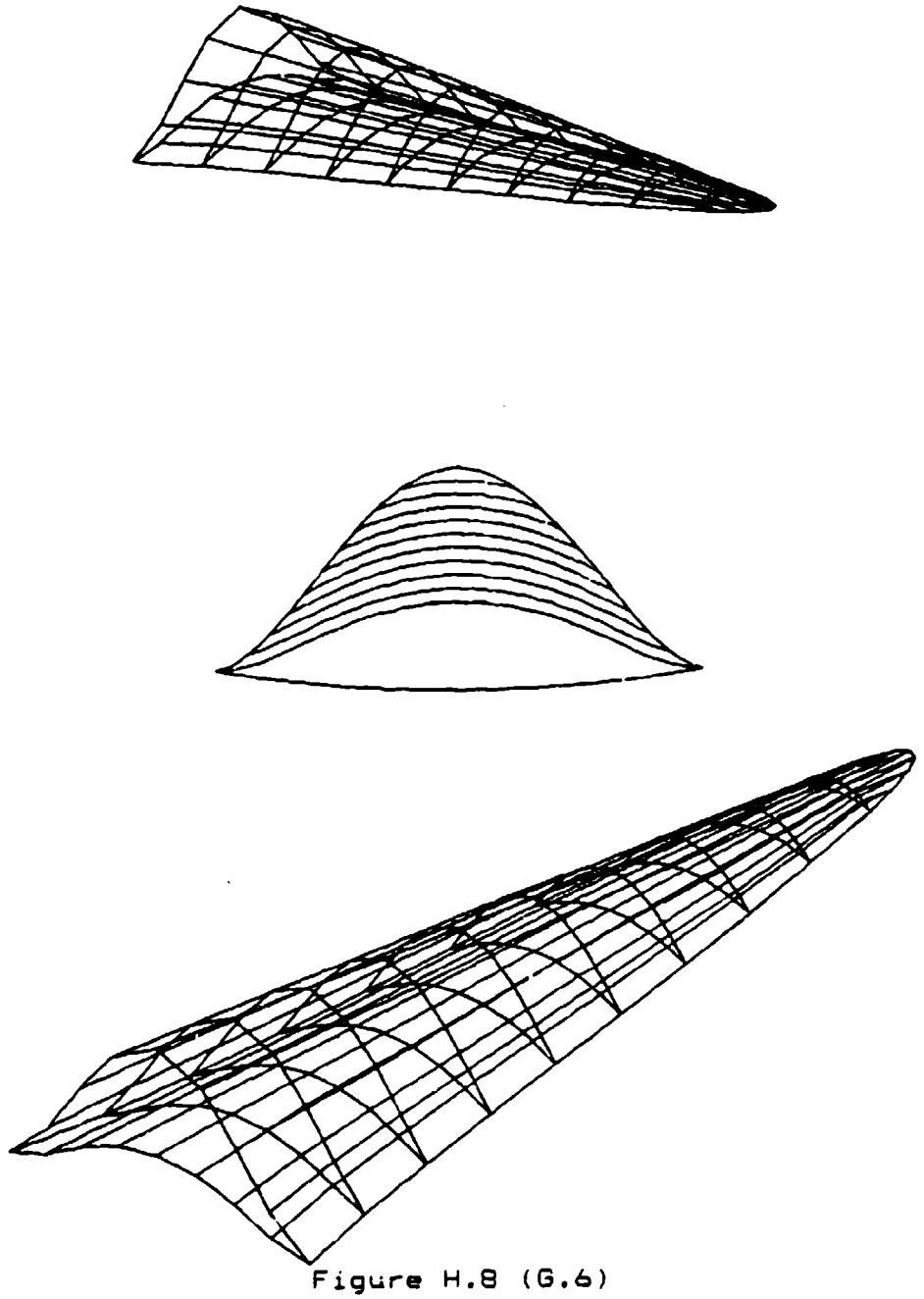

Figure H.8 (G.6)